frontiers | Research Topics

Current trends in muscle diseases and their treatment strategies

Edited by
Shoulong Deng, Jeffrey Allen Towbin and Kunihiro Tsuchida

Published in
Frontiers in Cell and Developmental Biology

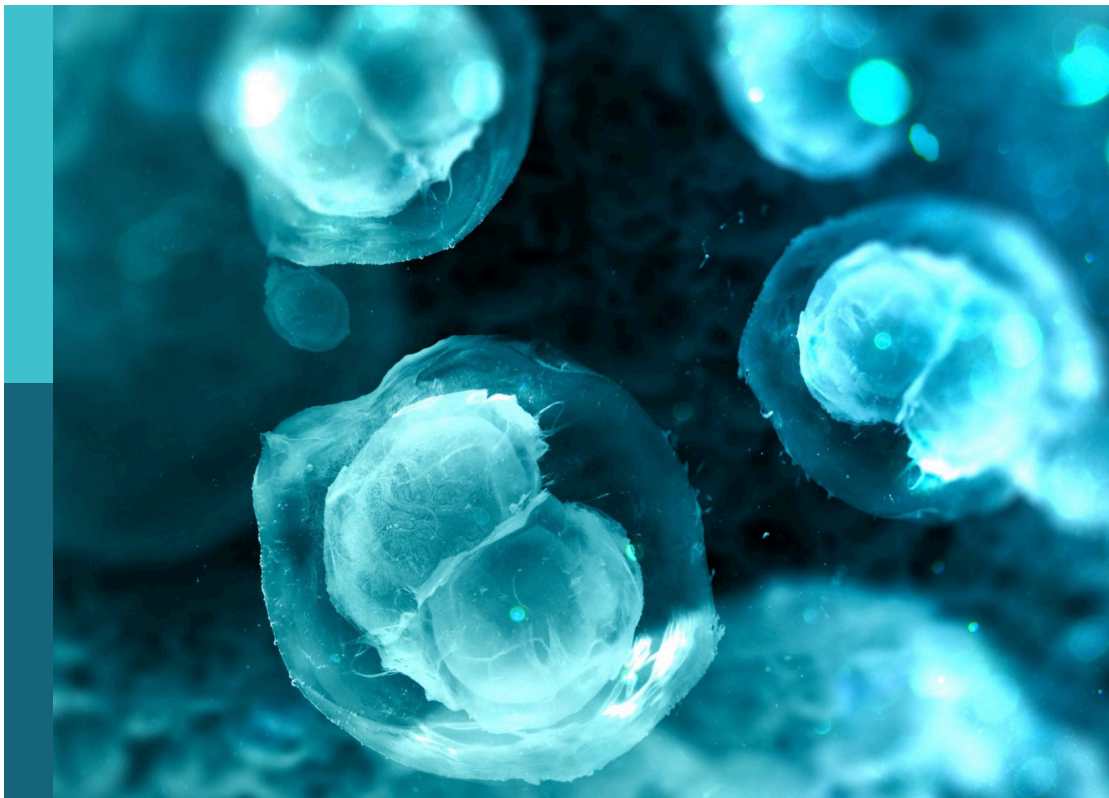

ISSN 1664-8714
ISBN 978-2-8325-6680-0
DOI 10.3389/978-2-8325-6680-0

Generative AI statement
Any alternative text (Alt text) provided alongside figures in the articles in this ebook has been generated by Frontiers with the support of artificial intelligence and reasonable efforts have been made to ensure accuracy, including review by the authors wherever possible. If you identify any issues, please contact us.

About Frontiers

Frontiers is more than just an open access publisher of scholarly articles: it is a pioneering approach to the world of academia, radically improving the way scholarly research is managed. The grand vision of Frontiers is a world where all people have an equal opportunity to seek, share and generate knowledge. Frontiers provides immediate and permanent online open access to all its publications, but this alone is not enough to realize our grand goals.

Frontiers journal series

The Frontiers journal series is a multi-tier and interdisciplinary set of open-access, online journals, promising a paradigm shift from the current review, selection and dissemination processes in academic publishing. All Frontiers journals are driven by researchers for researchers; therefore, they constitute a service to the scholarly community. At the same time, the *Frontiers journal series* operates on a revolutionary invention, the tiered publishing system, initially addressing specific communities of scholars, and gradually climbing up to broader public understanding, thus serving the interests of the lay society, too.

Dedication to quality

Each Frontiers article is a landmark of the highest quality, thanks to genuinely collaborative interactions between authors and review editors, who include some of the world's best academicians. Research must be certified by peers before entering a stream of knowledge that may eventually reach the public - and shape society; therefore, Frontiers only applies the most rigorous and unbiased reviews. Frontiers revolutionizes research publishing by freely delivering the most outstanding research, evaluated with no bias from both the academic and social point of view. By applying the most advanced information technologies, Frontiers is catapulting scholarly publishing into a new generation.

What are Frontiers Research Topics?

Frontiers Research Topics are very popular trademarks of the *Frontiers journals series*: they are collections of at least ten articles, all centered on a particular subject. With their unique mix of varied contributions from Original Research to Review Articles, Frontiers Research Topics unify the most influential researchers, the latest key findings and historical advances in a hot research area.

Find out more on how to host your own Frontiers Research Topic or contribute to one as an author by contacting the Frontiers editorial office: frontiersin.org/about/contact

Current trends in muscle diseases and their treatment strategies

Topic editors

Shoulong Deng — Institute of Laboratory Animal Sciences, Chinese Academy of Medical Sciences and Peking Union Medical College, China

Jeffrey Allen Towbin — Le Bonheur Children's Hospital, United States

Kunihiro Tsuchida — Fujita Health University, Japan

Citation

Deng, S., Towbin, J. A., Tsuchida, K., eds. (2025). *Current trends in muscle diseases and their treatment strategies*. Lausanne: Frontiers Media SA.

doi: 10.3389/978-2-8325-6680-0

Table of contents

frontiers | Frontiers in Cell and Developmental Biology

TYPE Editorial
PUBLISHED 23 July 2025
DOI 10.3389/fcell.2025.1660074

OPEN ACCESS

EDITED BY
Osvaldo Contreras,
Victor Chang Cardiac Research Institute, Australia

REVIEWED BY
Florian Barthelemy,
University of California, Los Angeles, United States

*CORRESPONDENCE
Shoulong Deng,
dengshoulong@cnilas.org

RECEIVED 05 July 2025
ACCEPTED 18 July 2025
PUBLISHED 23 July 2025

CITATION
Guo Z and Deng S (2025) Editorial: Current trends in muscle diseases and their treatment strategies.
Front. Cell Dev. Biol. 13:1660074.
doi: 10.3389/fcell.2025.1660074

Editorial: Current trends in muscle diseases and their treatment strategies

Zihang Guo and Shoulong Deng*

Institute of Laboratory Animal Sciences, Chinese Academy of Medical Sciences and Peking Union Medical College, Beijing, China

KEYWORDS

neuromuscular disorders, muscle diseases, diagnostic techniques, personalized medicine, pig models

Editorial on the Research Topic
Current trends in muscle diseases and their treatment strategies

Muscle diseases encompass a broad spectrum of disorders, including genetic, degenerative and age-associated neuromuscular conditions, all characterized by muscle degeneration, functional impairment and in many cases, premature mortality. These diseases impose significant clinical burdens, with cardiorespiratory failure, fatal motor neuron loss and frailty in aging populations. Advanced diagnostic strategies, ranging from genetic testing and biomarker analysis to advanced imaging techniques have improved early and accurate detection. Meanwhile, therapeutic breakthroughs such as gene therapy and epigenetic modulators are transforming patient care. However, therapeutic development critically depends on translational animal models, particularly porcine models replicating human pathology. This Research Topic tries to present a comprehensive overview of the latest progress in muscle diseases.

Duchenne muscular dystrophy (DMD) is a fatal neuromuscular disease caused by loss-of-function mutations in the X-linked dystrophin gene and characterized by progressive muscle degeneration, loss of ambulation and premature death from cardiac or respiratory failure. Remarkable advancements have been made in both diagnostic methods and targeted therapies for DMD. Current diagnostic approaches combine genetic testing for exon deletion/duplication analysis with ancillary methods which include biomarker such as serum creatine kinase, muscle biopsy for dystrophin analysis and histopathology, advanced imaging techniques (muscle MRI and emerging MSOT), and cardiac monitoring through echocardiography and ECG. These ensure accurate diagnosis and comprehensive disease characterization. Recent breakthroughs in DMD treatment include exon-skipping therapies, gene editing-mediated reading frame restoration, and artificial chromosome transfer. AAV-based micro-dystrophin delivery (Elevidys) partially restores dystrophin expression and slows down disease progression, which is FDA-approved for ambulatory children aged ≥6. Antisense oligonucleotides (e.g., eteplirsen, viltolarsen, golodirsen, casimersen) promote exon

skipping and produce functional truncated-dystrophin, which benefit patients with specific mutations.

Emerging research has expanded to epigenetic modifications. Histone deacetylases (HDACs) have been shown to be hyperactive in patients with DMD and contribute to the pathology, HDAC inhibition has arisen as a potential therapeutic option. The HDAC inhibitor givinostat is the first nonsteroidal treatment approved by FDA for DMD patients ≥6 years old. Aartsma-Rus published a study investigating the multi-targeted mode of givinostat in treating DMD. Givinostat has demonstrated the potential to addresses the pathophysiological cascade of DMD by targeting key pathological events originated by the lack of dystrophin. Preclinical and clinical trials confirmed givinostat works by inhibiting HDACs activity to promote histone acetylation and improve chromatin structure, while significantly slows disease progression by reducing fat infiltration, inflammation and fibrosis, promoting muscle regeneration and improving muscle function with a favorable safety profile. Furthermore, improved anesthesia protocols address perioperative risks. Lian et al. provide a systematic review of the pharmacological interventions for anesthesia and sedation in patients with DMD. They confirmed that patients with DMD are more sensitive to neuromuscular blocking agents (NMBAs), leading to delayed onset time, prolonged recovery time from anesthesia and risks such as malignant hyperpyrexia with volatile anesthetics. Precautions for DMD patients should include quantitative neuromuscular, electrocardiographic monitoring and rapid airway protection throughout anesthesia. Regional anesthesia was deemed relatively safer compared with general anesthesia. This review emphasized avoiding succinylcholine to prevent known anesthetic hazards such as rhabdomyolysis or hypercalcemia and highlighted the efficacy of Dantrolene for reversing malignant hyperpyrexial response to anesthesia.

Porcine DMD models, which replicate the biochemical, clinical, and pathological features of human patients with accelerated disease progression and early cardiac involvement, have been instrumental in evaluating novel diagnostic tools like multispectral optoacoustic tomography (MSOT) for non-invasive disease monitoring and testing therapeutic strategies. Despite challenges like high cost, porcine model of DMD remains invaluable for optimizing therapies and diagnostics and developing personalized care strategies.

Amyotrophic lateral sclerosis (ALS) is an adult-onset neurodegenerative disorder characterized by progressive degeneration of upper and lower motor neurons, leading to muscle weakness and atrophy, dysphagia or respiratory muscle palsy and remains incurable with an average survival of 2–5 years post-diagnosis. Current drugs like riluzole and edaravone offer only modest benefits. ALS is a multifactorial disease, involving oxidative stress, mitochondrial dysfunction, protein misfolding and metabolic disturbances. More than 30 ALS-related genes, including superoxide dismutase 1 (SOD1) gene, have been reported. Diagnosis of ALS relies on clinical assessments and biomarkers, such as elevated TDP-43 levels in peripheral blood mononuclear cells (PBMCs). Therapeutic strategies under investigation include metabolic interventions to restore glucose utilization in skeletal muscle. Fenili et al. provide a review and explore the potential of physical exercise as a co-adjuvant therapy for ALS. While intense exercise may pose risks, moderate and tailored exercise such as swimming have shown neuroprotective effects in animal models by improving glucose metabolism, mitochondrial function, and antioxidant defense. Resistance and endurance training may enhance quality of life and slow down functional decline in human. This review underscores the need for personalized exercise protocols in ALS. Transgenic pig models such as hSOD1G93A and mSOD1-Tg pigs replicate human ALS pathology, including biomarker dynamics and metabolic dysfunction. These models have emerged as transformative tools in testing diagnostics and therapies for ALS to enhance translational relevance.

Sarcopenia, an age-related syndrome characterized by progressive loss of muscle mass, strength, and function, has emerged as a critical health concern. Two representative surveys leveraging China Health and Retirement Longitudinal study (CHARLS) database revealed risk factors and predictive models in vulnerable groups and offered insights for early intervention. Yang et al. proved that sarcopenia mainly affects middle-aged and older Chinese women, closely related to age, waist, education, marriage, area, stroke, physical pain, depression, and region. They offer an effective tool to help clinicians better screen potential female patients. Qiao et al. developed a predictive model for sarcopenia risk in middle-aged and older adults with diabetes mellitus (DM) and validated a strong accuracy. Eight key predictors were identified: age, residence, BMI, diastolic blood pressure, cognitive function, activities of daily living (ADL), peak expiratory flow (PEF), and hemoglobin. This model serves as a practical tool for early identification of high-risk individuals and facilitates timely interventions to mitigate sarcopenia progression in diabetic populations. Zhong et al. employed bioinformatics and systems biology approaches to explore the shared pathogenic mechanisms between COVID-19 and sarcopenia. They identified 66 common differentially expressed genes (DEGs), including 15 hub genes. Enrichment analysis revealed functions and pathways between two diseases. Key regulators like FOXC1 and hsa-mir-155-5p were identified, and immune infiltration analysis highlighted the correlation between hub genes and immune factors. They also proposed potential therapeutic drugs and showed that valinomycin PC3 UP is the best candidate for the treatment of sarcopenia and COVID-19. Finally, they demonstrated ALDH1L2 and KLF5 showed the best diagnostic potential for COVID-19 and sarcopenia. These findings suggest shared pathways in COVID-19 and sarcopenia, offering insights for early diagnosis, effective treatment and targeted therapies.

Beyond above muscle diseases, several other neuromuscular disorders present unique pathological mechanisms and therapeutic challenges. Fibrosarcoma, an aggressive and poorly understood soft tissue sarcoma, poses significant therapeutic challenges. Radzka et al. evaluated the potential role of natural NF-κB inhibitors in fibrosarcoma. The results showed selective cytotoxicity toward cancer cells by inducing apoptosis and indicated that CAPE, biochanin A, and CurE could inhibit actin polymerization and disrupt the cytoskeleton of cancer cells. Cellular stress and vacuolation as well as metabolic changes are more pronounced in cancer cells compared to normal cells. This research supports the effect and safety of these natural compounds with low-toxicity as anticancer agents, particularly in the treatment of fibrosarcoma. Lu et al. provide a review and explore the role of mitochondrial defects in sporadic inclusion body myositis (sIBM), a subtype of idiopathic inflammatory myopathies (IIM) with unique pathological features such as muscle inflammation, rimmed vacuoles, and protein

aggregation within the myofibers. Key mitochondrial abnormalities including large-scale mitochondrial DNA deletion, aberrant protein aggregation, and slowed organelle turnover are more prominent in sIBM than in other types of IIM, indicating that non-immune tissue dysfunction might contribute to the disease's onset as patients with sIBM are refractory to conventional immunosuppressant treatment. They also discuss potential mitochondrial-targeted therapies, such as antioxidants and mitophagy inducers like Urolithin A. Understanding mitochondrial dysfunction in sIBM could pave the way for novel treatments targeting organelle health. Spinal muscular atrophy (SMA) is an autosomal recessive genetic disorder marked by progressive, symmetrical muscle weakness and atrophy. Jieda et al. provide a case report and describe a child with initial limb hypotonia and abnormal signal changes in brain MRI. Genetic testing ultimately confirmed the diagnosis of SMA. This report highlights the rarity of brain MRI abnormalities in SMA and the importance of early intervention, which may aid early diagnosis alongside genetic testing. Pathogenic variations in gene encoding the skeletal muscle ryanodine receptor (RyR1) are associated with malignant hyperthermia (MH) and RYR1-related myopathies (RYR1-RM). R615C porcine model, the first established preclinical model, has been instrumental in understanding pathomechanisms and testing potential therapeutics like dantrolene.

In addition to conventional treatment methods, recent studies demonstrate the successful generation of humanized skeletal muscle in MYF5/MYOD/MYF6-null pig embryos using blastocyst complementation with human induced pluripotent stem cells (hiPSCs). These findings offer potential of producing exogenic tissues for xenotransplantation to address challenges in muscle diseases treatment and highlight the feasibility of interspecies chimeras in regenerative medicine.

In summary, the landscape of muscle disease research is rapidly evolving driven by innovations in diagnostics, targeted therapies, and preclinical models. These advances underscore the importance of multidisciplinary collaboration. While challenges such as therapeutic accessibility and complexity of disease heterogeneity remain, future efforts should focus on personalized interventions, translational research and animal models to bridge the gap between bench and bedside, ultimately offering hope for improved outcomes and enhancing the quality of life for patients worldwide.

Author contributions

ZG: Writing – original draft, Writing – review and editing. SD: Writing – original draft, Writing – review and editing.

Funding

The author(s) declare that no financial support was received for the research and/or publication of this article.

Conflict of interest

The authors declare that the research was conducted in the absence of any commercial or financial relationships that could be construed as a potential conflict of interest.

Generative AI statement

The author(s) declare that no Generative AI was used in the creation of this manuscript.

Publisher's note

frontiers | Frontiers in Cell and Developmental Biology

TYPE Review
PUBLISHED 14 May 2024
DOI 10.3389/fcell.2024.1403463

OPEN ACCESS

EDITED BY
Shoulong Deng,
Chinese Academy of Medical Sciences and Peking Union Medical College, China

REVIEWED BY
François Singh,
University of Iceland, Iceland
Boel De Paepe,
Ghent University, Belgium

*CORRESPONDENCE
Chi Bun Chan,
chancb@hku.hk

RECEIVED 19 March 2024
ACCEPTED 02 May 2024
PUBLISHED 14 May 2024

CITATION
Iu ECY, So H and Chan CB (2024), Mitochondrial defects in sporadic inclusion body myositis—causes and consequences.
Front. Cell Dev. Biol. 12:1403463.
doi: 10.3389/fcell.2024.1403463

Mitochondrial defects in sporadic inclusion body myositis—causes and consequences

Elsie Chit Yu Iu[1], Ho So[2] and Chi Bun Chan[1]*

[1]School of Biological Sciences, The University of Hong Kong, Pokfulam, Hong Kong SAR, China, [2]Department of Medicine and Therapeutics, Faculty of Medicine, The Chinese University of Hong Kong, Shatin, China

Sporadic inclusion body myositis (sIBM) is a distinct subcategory of Idiopathic Inflammatory Myopathies (IIM), characterized by unique pathological features such as muscle inflammation, rimmed vacuoles, and protein aggregation within the myofibers. Although hyperactivation of the immune system is widely believed as the primary cause of IIM, it is debated whether non-immune tissue dysfunction might contribute to the disease's onset as patients with sIBM are refractory to conventional immunosuppressant treatment. Moreover, the findings that mitochondrial dysfunction can elicit non-apoptotic programmed cell death and the subsequent immune response further support this hypothesis. Notably, abnormal mitochondrial structure and activities are more prominent in the muscle of sIBM than in other types of IIM, suggesting the presence of defective mitochondria might represent an overlooked contributor to the disease onset. The large-scale mitochondrial DNA deletion, aberrant protein aggregation, and slowed organelle turnover have provided mechanistic insights into the genesis of impaired mitochondria in sIBM. This article reviews the disease hallmarks of sIBM, the plausible contributors of mitochondrial damage in the sIBM muscle, and the immunological responses associated with mitochondrial perturbations. Additionally, the potential application of mitochondrial-targeted chemicals as a new treatment strategy to sIBM is explored and discussed.

KEYWORDS

mitochondria, myositis, muscle, pathogenesis, pyroptosis, necroptosis

Introduction

Idiopathic inflammatory myopathies (IIM), commonly known as myositis, is a heterogeneous group of muscle diseases with a global prevalence of 2–25 individuals per 100, 000 persons (Khoo et al., 2023). Based on the clinical, serological, and histological examination results, IIM can be classified into 5 major subtypes: dermatomyositis (DM), polymyositis (PM), immune-mediated necrotizing myopathy (IMNM), overlap myositis (OM), and sporadic inclusion body myositis (sIBM). Despite each IIM subtype has distinctive clinical and unique histopathological features, a great majority of IIM patients suffer from muscle weakness with muscle edema, fatty infiltration in muscle fibers, and elevated serum creatine kinase (CK) level (Tsamis et al., 2022). Additionally, most IIM patients demonstrate overactivation of cellular and humoral immunity as revealed by the presence of infiltrating granzyme and perforin-secreting $CD8^+$ cytotoxic T cells and B cells in muscle and autoantibodies in their serum (Goebels et al., 1996; Greenberg et al., 2005; Gunawardena et al., 2009). The involvement of innate immunity in IIM is also

evidenced by the muscle enrichment of dendritic cells and M2 macrophages for tissue repair (Rinnenthal et al., 2014).

Because the muscles of IIM patients exhibit mild-to-severe inflammation phenotypes, most treatments for IIM target the uncontrolled immune response. Glucocorticoids (GC) are the front-line treatment that is widely adopted in PM and DM (Greenberg, 2019). They are often administrated with other immunosuppressants like azathioprine and methotrexate to reduce steroid-related side effects like osteoporosis and cardiovascular diseases (Oddis, 2016). Second-line treatments such as cyclosporine, tacrolimus, and intravenous immunoglobin are used to alleviate the disease symptoms in refractory or severe PM and DM cases (Zeng et al., 2022; Skolka and Naddaf, 2023). Nonetheless, these immunosuppressive agents are not enduringly effective in treating some IIM patients, particularly those with sIBM (Skolka and Naddaf, 2023). A recent study using human sIBM xenografts demonstrated that T cell depletion does not alleviate the muscle degenerative features (Britson et al., 2022), further challenging the pathogenic role of inflammation in the disease. Therefore, it is suspected that the immune response might not be the fundamental cause of muscle damage in sIBM. Because abnormal mitochondrial changes are commonly found in the muscle of sIBM patients, which are more prevalent than other IIM subtypes (Oldfors et al., 2006), impaired mitochondrial function might be an underestimated factor in the pathogenesis of sIBM. Several excellent reviews have discussed how mitochondrial dysfunction may generate muscle weakness in sIBM (De Paepe, 2019; Chapa et al., 2023; Danieli et al., 2023), but the underlying mechanism of mitochondrial defects remains inconclusive. In this article, we review the recent findings of mitochondrial dysfunction in sIBM and discuss their possible linkage with various disease symptoms. We will also discuss some potential mitochondrial-based therapeutic strategies for the treatment of sIBM.

Symptoms, diagnosis, and current treatment of sIBM

sIBM is a male-predominant disease that has a prevalence of 5–71 per million in the whole population (Tsamis et al., 2022). Typically occurring after the age of 50 (Snedden et al., 2022), sIBM is characterized by progressive and asymmetric weakness in the quadriceps and long finger flexors rather than an acute or subacute symmetrical proximal muscle weakness seen in other subtypes of IIM (Zubair et al., 2023). Individuals with sIBM experience a loss of muscle strength at a rate of 3.5%–28% per year (Zubair et al., 2023) and can become wheelchair-bound at a median time of 10.5 years after the disease onset (Skolka and Naddaf, 2023). Respiratory compromise and dysphagia are common risk factors for premature death in sIBM patients, which may account for their slight but significantly shortened lifespan when compared to healthy subjects (Shelly et al., 2021). Recently, an association between sIBM and malignancy has been proposed, although sIBM is not generally regarded as a risk factor for cancer (Damian et al., 2022). Due to the slowly progressive nature of symptom development, there is often a delay of 5–10 years between disease onset and confirmation (Huntley et al., 2019).

The diagnosis of sIBM is typically made in patients having experienced disease symptoms for more than 12 months with onset after 45-year-old, (Greenberg, 2019; Skolka and Naddaf, 2023), and most importantly exhibit histopathological hallmarks in their muscle, including endomysial lymphocyte infiltration, rimmed vacuoles, protein deposition, ragged red fibres, and the presence of cytochrome c oxidase (COX)-negative myofibers (Tanboon et al., 2020). The accumulation of proteins like amyloid beta (Aβ), ubiquitin, phosphor-tau, sequestosome 1 (p62), and TAR DNA binding protein 43 kDa (TDP-43) is also detected in the muscle of some sIBM patients (Skolka and Naddaf, 2023). Autoantibodies against cytosolic 50-nucleotidase (cN-1A), an enzyme highly expressed in the skeletal muscle that catalyses the hydrolysis of adenosine monophosphate (AMP) into adenosine and inorganic phosphate (Salam et al., 2022; Diederichsen et al., 2023) can be found in many sIBM patients but not in any other IIM subtypes (Yamashita et al., 2023), making it an important evidence to the disease diagnosis. Nevertheless, a substantial number of sIBM patients displayed no elevated anti-cN-1A antibody in their circulation, suggesting that the presence of antibody should not be considered a necessary criterion in the disease diagnosis (Mavroudis et al., 2021; Diederichsen et al., 2023). While histological analysis of muscle biopsy remains an essential procedure for sIBM diagnosis (Papadimas et al., 2019; Winkler et al., 2021), other methods such as multi-osmics profiling are being developed to screen for novel biomarkers with 100% sensitivity and specificity (Cantó Santos et al., 2023).

The presence of anti-cN-1A antibodies and the elevated level of inflammatory cytokines like interferon γ (IFN-γ), tumor necrosis factor α (TNF-α), interleukin 7 (IL-7), and interleukin 32 (IL-32) in the serum of sIBM patients indicate that both humoral and cellular immunities are provoked (Tsamis et al., 2022). The hyperactivation of cellular immunity in sIBM is demonstrated by the transformation of $CD4^+$ helper T-cells into $CD28^-$ cytotoxic T-cells and the infiltration of $CD8^+$ T cells in the patient's muscle (Miller et al., 2018). These cytotoxic T-cells might upregulate the muscular expression of major histocompatibility complex I (MHC-I) genes and induce muscle cell death, possibly via perforin-granzymes or Fas ligand-mediated mechanisms (Fyhr and Oldfors, 1998; Snedden et al., 2022). Indeed, immunohistochemical analysis revealed stronger Fas immunoreactivity in the atrophic fibres of sIBM patients than that in other IIM subtypes (De Bleecker et al., 2001). Despite the clear engagement of the immune system in the pathogenesis of sIBM, disease alleviation via immune response inhibition is not satisfactory, as a significant number of patients are irresponsive to the classical immunosuppressive treatment (Askanas and Engel, 2008; Rygiel et al., 2015). For instance, some sIBM patients receiving long-term GC treatment for more than 5 years had a similar number of T-cells-invaded myofibers as those patients without treatment (Pruitt et al., 1996). Muscle atrophy of sIBM patients has also not ceased even though their CK levels have returned to normal after GC treatment (Miller et al., 2018). Moreover, the extent of immune cell infiltration in sIBM patients was found to correlate poorly with the severity of muscle weakness (Lightfoot et al., 2015). Hence, it is argued that prolonged immune system activation in sIBM is secondary to the intrinsic defects in the skeletal muscle.

Presence of abnormal mitochondria in sIBM

Mitochondrial DNA (mtDNA) mutation and deletion

A distinguishing characteristic of sIBM that differentiates it from other IIM subtypes is the presence of ragged red fibers in the patient's muscle (Boncompagni et al., 2012; Tanboon et al., 2020), which appear as red rim in the speckled sarcoplasm after Gomori Trichrome staining. Because ragged red signal is caused by the accumulation of defective mitochondria below the plasma membrane, these unusual histological signals are not exclusive to sIBM but are also seen in the muscle of patients suffering from primary mitochondrial disorders, such as myoclonic epilepsy with ragged red fibers (MERRF) and mitochondrial thymidine kinase (T2K) deficiency (DiMauro et al., 1985; Jou et al., 2022). Indeed, some mitochondria in the muscles of sIBM patients are aberrant in structure and function. In contrast to DM, where single point mutations in mtDNA are frequently detected (Zhao et al., 2022), sIBM muscle features large-scale, single segment deletions (i.e., major rearrangement mutation) in the major arc of mtDNA molecules. It has been reported that 122 deletion breakpoints and 33 different single nucleotide deletions were detected in the mtDNA molecules of sIBM patients (Moslemi et al., 1997), which could lead to the elimination of up to 1/3 of the whole mtDNA. Another study confirmed an average of 67% lower mtDNA copy number in the quadriceps and tibialis anterior muscle of sIBM patients than in healthy subjects (Bhatt et al., 2019). Interestingly, heterogenous mtDNA molecules with differential deletion regions could be detected in a single myofiber (Rygiel et al., 2016), resulting in a high heteroplasmy in the muscle. Moreover, the mtDNA deletion might be present in continuous segments of the same muscle fiber, creating a spatially unique pattern of the mitochondrial protein COX staining within a single myofiber (Oldfors et al., 1995; Horvath et al., 1998).

Biochemical outcomes of mtDNA deletion in sIBM—oxidative phosphorylation (OXPHOS) defects

Because the human mtDNA encodes genes for electron transfer complexes (ETC) subunits, mtDNA deletion might result in the loss of mitochondrial content (Joshi et al., 2014; Catalán-García et al., 2016a; Oikawa et al., 2020; Hedberg-Oldfors et al., 2021). In fact, the severity of mtDNA deletion is highly associated with the number of COX-deficient fibers, which are myofibers that contain abnormally low levels of the mitochondrial complex IV, in the sIBM patients' muscles (Landfeldt et al., 2015). Using single-cell analysis, Rygiel reported that ~85% of COX-deficient cells have major mtDNA deletion and rearrangement (Rygiel et al., 2016). Mitochondrion morphology is also disrupted in the myofiber of sIBM patients, with shortened and enlarged cristae and junction breaks, resulting in a reduced mitochondrial length/width ratio (Oikawa et al., 2020). As COX is an essential component of the ETC for ATP synthesis via OXPHOS, COX deficiency in the myoblasts of sIBM patients leads to a shift in ATP production from OXPHOS to glycolysis (Oikawa et al., 2020), which is a key indicator of mitochondrial dysfunction (Di Leo et al., 2023). The ^{31}P-magnetic resonance spectroscopy assessments revealed that the muscle of sIBM patients has a low ability to synthesize ATP during resting, further supporting the notion of impaired mitochondrial respiration in sIBM (Lodi et al., 1998). A recent study also reported diminished mitochondrial enzymatic activities in cultured sIBM myofibers under low glucose availability, indicating compromised metabolic flexibility (Catalán-García et al., 2020). Consequently, this low mitochondrial activity might significantly impact the overall function of skeletal muscle, causing weakness in contraction strength and endurance (Gonzalez-Chapa et al., 2023).

Potential causes of mtDNA deletion in sIBM—error in mtDNA replication

The occurrence of mtDNA deletion in the muscle of sIBM patients is not limited to a consensus locus within a mtDNA molecule but is present in multiple regions. This suggests that the cause of mtDNA deletion and rearrangement might be more complex than previously assumed. The underlying mechanism that leads to the high frequency of mtDNA deletion in sIBM is still unknown. However, it has been hypothesized that most truncated mtDNA molecules in sIBM muscle are generated from the clonal expansion of a single defective molecular species (Moslemi et al., 1997). It has also been suggested that the mtDNA replication process in sIBM muscle is prone to errors, further contributing to the generation of multiple copies of defective mtDNA (Horvath et al., 1998). The high replication error in sIBM is not caused by any genetic defects in nuclear genes engaged in mitochondrial genome maintenance, as a recent study found no pathogenic variants in nuclear genes that contribute to the high levels of mtDNA deletions in sIBM (Hedberg-Oldfors et al., 2021). Instead, single nucleotide polymorphism of several key genes involved in mtDNA replication and maintenance, including the DNA helicase Twinkle, the DNA polymerase γ (POLG), and ribonucleotide-diphosphate reductase subunit M2B (RRM2B), has been identified in sIBM patients (Lindgren et al., 2015). Nevertheless, the functional consequence of these single mutations has not been elucidated.

Potential causes of mtDNA deletion in sIBM—reactive oxygen species (ROS) accumulation

A possible cause of high mtDNA damage in sIBM muscle is its unique localization and structure. Mitochondria are the organelle that produces ~90% of the total ROS in the cells as the byproducts of, ETC complex I and III (Favaro et al., 2019). These short-lived yet highly reactive molecules are unstable and cause structural damage to mtDNA molecules (Urbina-Varela et al., 2020). The histone-free nature of mtDNA molecules further increases their risk of ROS-induced damage (Taylor and Turnbull, 2005). Histones protect DNA against hydroxyl radical-induced strand breaks, which is a critical defense mechanism against DNA damage (Ljungman and Hanawalt, 1992). Indeed, the high ROS level and mitochondrial

deletion are closely associated with each other in many diseases, such as hepatocellular carcinoma (Moriya et al., 2001) and chronic periodontitis (Canakçi et al., 2006). It is important to note that this "ROS-induced mutation" model can only be valid if the ROS content in the muscle of sIBM patients is higher than that of the healthy subjects. Several studies have demonstrated that ROS level is augmented in the muscles of sIBM. First, myoblasts of sIBM patients displayed a higher ROS concentration when treated with a glutathione synthesis inhibitor (Oikawa et al., 2020). Second, a high level of deglycase DJ-1, an important mitochondrial protective protein against oxidative stress (Taira et al., 2004), has been found in the mitochondria of sIBM muscle (Terracciano et al., 2008), indicating the mitochondria are under high oxidative stress and require stronger protection. In support of this notion, fibroblasts cultured from sIBM patients displayed higher oxidative stress, concomitant with increased antioxidant defense (Cantó-Santos et al., 2023). Furthermore, the protein amount and gene expression of ROS scavengers, Cu, Zn- superoxide dismutase (Cu, Zn-SOD) and manganese superoxide dismutase (Mn-SOD), are augmented in vacuolated myofibers in sIBM (Askanas and Engel, 1998; Tsuruta et al., 2002). However, comparable muscular lipid peroxidation between sIBM patients and healthy subjects was also reported (Catalán-García et al., 2016b), making the ROS hypothesis inconclusive. Instead of having more mutation inducers in the muscle, it is possible that the DNA repair system is blemished in the patient's tissue, hence facilitating the propagation of mutated mtDNA. Because no examination of the activity of DNA repairing machinery, such as apurinic/apyrimidinic endonuclease (APE) or DNA damage-binding protein (DDB) (Jang et al., 2019), in the sIBM sample, has been performed, it remains unknown if the system is involved in the accumulation of truncated mtDNA.

Potential causes of mtDNA deletion in sIBM—β amyloid (Aβ) overproduction

In addition to the occurrence of mtDNA deletion, which resulted in a loss of mitochondria in the muscle (Hedberg-Oldfors et al., 2021), the accumulation of Aβ in the tissue might further impair the function of the existing mitochondria in sIBM. Studies have shown that overproduction of β amyloid precursor protein (APP) in human muscle fibers resulted in decreased COX activity, enlarged mitochondria, and the formation of disrupted cristae that resemble the pathological features of sIBM (Askanas et al., 1996). Abnormal mitochondrial-related functions, including increased rate of ROS production, reduced TCA cycle activities, and a shift of fatty acid-to-glucose utilization, were also seen in the muscle of APP transgenic mice (Boncompagni et al., 2012). It is believed that the mislocation of Aβ to the mitochondrial membrane impedes the function of the mitochondrial transporter, hence hindering the imports of materials that are indispensable for mitochondrial functions (Askanas et al., 1996; Devi et al., 2006). Although this Aβ-mitochondrial interaction, as observed in neuronal tissues, is a logical linkage of Aβ overproduction to the dysregulated mitochondrial function, no colocalization of Aβ and mitochondria in the muscle of sIBM patients has been reported.

Potential causes of mtDNA deletion in sIBM—defective autophagy

It is also possible that the mitochondrial defect in sIBM muscle is attributed to the delayed organelle turnover, which might result in the buildup of dysfunctional mitochondria. The "dysregulated myoproteostasis" model, which covers protein synthesis defect, improper folding, extensive post-translational modification, and impaired degradation of proteins, has been proposed by Askanas et al. to collectively explain the aggregation of abnormal proteins and organelles in sIBM muscle (Askanas et al., 2015). Several studies report that organelle degradation by macroautophagy is compromised in sIBM. First, there is a lack of p62 binding accuracy to LC3 in the patient's muscle, although sIBM muscles contain a higher frequency of LC3-positive autophagosomes, indicating a stop of the autophagy process in its initial stages (Lünemann et al., 2007; Nogalska et al., 2010; Suzuki et al., 2019). Moreover, the activity of lysosomal enzymatic activity cathepsin D and B was lower than the healthy control in the sIBM muscle, which delays the clearance of LC3-associated autophagosomes and the ubiquitinated proteins (Nogalska et al., 2010). Indeed, the muscle biopsies of sIBM patients showed a high density of lipofuscin aggregates, a marker of lysosomal dysfunction (Lu et al., 2020). Nicot et al. (2014) further specified the mechanism by demonstrating that the autophagy cargo receptor NBR1-mediated removal of protein aggregates was inhibited in sIBM. This delayed autophagy provides a logical explanation for the accumulation of p62 and Aβ aggregates in the autophagic vacuoles in sIBM (Güttsches et al., 2017). Furthermore, several genes associated with autophagosome-lysosome processing have been identified as the risk alleles in sIBM (Weihl et al., 2015; Gang et al., 2016; Papadopoulos et al., 2017). Based on these findings, pharmacological inhibition of autophagy by chronic colchicine administration in mice is used as an animal model for sIBM research (Ching et al., 2013). Interestingly, chaperone-mediated autophagy is increased in the muscle of sIBM, as evidenced by elevated levels of lysosomal membrane protein LAMP2A and the chaperone Hsp70 co-aggregates (Cacciottolo et al., 2013). Because chaperone-mediated autophagy mainly targets specific proteins but not large organelles, this escalated chaperone-mediated autophagy might be a compensatory response to abnormal protein aggregation, like p62, in sIBM. Given that the removal of damaged mitochondria is autophagy-dependent, the dysregulated autophagy in sIBM might jeopardize its clearance. Although no comprehensive assessment of mitophagy, the specific pathway of autophagy to induce mitochondria degradation (Lu et al., 2023), has been performed in sIBM muscle, decreased expression of dynamin-related protein 1 (DRP1) has been detected in cultured myoblasts of sIBM patients (Oikawa et al., 2020). DRP1 is a critical factor that promotes the splitting of mitochondria for subsequent degradation (Picca et al., 2023); this low level of DRP1 indirectly supports the hypothesis that the clearance of mitochondria in sIBM muscle might be impaired. Moreover, abnormal accumulation of the mitochondrial fusion marker mitofusin 1 (MFN1) and the mitophagy receptor Bcl-2 adenovirus E1B19 19-kDa interacting protein (BNIP3) was observed in the ragged red fibers of the sIBM patients (Askanas et al., 2015). Because mitofusin accumulation triggers mitochondrial

enlargement, which hinders the sequestration of damaged mitochondria (Joaquim and Escobar-Henriques, 2020), augmented mitofusin content in the sIBM muscle may result in defective clearance of Bnip3-tagged cargos.

Mitochondrial defects and immune response in muscle

Although the invasion of immune cells is commonly observed in all IIM, inflation of highly differentiated $CD8^+CD28^-$ cytotoxic T cells is uniquely present in sIBM (Greenberg and Bourc'his, 2019). It is proposed that autoimmunity is the root cause of sIBM pathogenesis, as genetic mutation of TDP-43 and p62 in myotilinopathies and desminopathies do not result in the formation of protein aggregates (Olivé et al., 2008; Olivé et al., 2009). Moreover, stimulation of cultured muscle cells by inflammatory cytokines, such as IL-1β and IFNγ, or upregulation of much MHC class I alone is sufficient to trigger the formation of protein aggregates and rimmed vacuoles (Fréret et al., 2013; McCord and Day, 2023a; McCord and Day, 2023b). Furthermore, rhabdomyosarcoma cells challenged with the IgG from sIBM patients effectively induced the aggregation of p62 (Tawara et al., 2017). Finally, altering the immune system by virus infection like HIV can produce pathological features of sIBM like p62 aggregates and the formation of rimmed vacuoles in the muscle (Hiniker et al., 2016). While these findings support the causal relationship between autoimmunity and muscle degeneration, mitochondrial defects in the muscle of sIBM might have feed-forward activity to exaggerate tissue inflammation. Supporting this notion, Shelton et al. (2019) found that mutation of the mitochondrial transporter, aspartate glutamate carrier 1 (AGC1), produced a proinflammatory phenotype in the muscle biopsies of dogs. Indeed, recent studies in mitochondrial biology have confirmed that excessive mitochondrial dysfunction can trigger tissue damage and subsequent immune responses via regulated cell death mechanisms.

In principle, damaged mitochondria release their organelle contents, such as mtDNA, cardiolipins, and Ca^{2+}, into the cytosol and the extracellular space (Picca et al., 2023). These mitochondrial-derived damage-associated molecular patterns (DAMPs) are regarded as foreign molecules by the pattern recognition receptors of the immune cells due to the bacterial ancestry of mitochondria. Induction of the innate immune response triggers the activation of pro-inflammatory pathways like toll-like receptor (TLR) signalling (Picca et al., 2023). Indeed, it has been reported that binding of oxidized cardiolipins to TLR4 in the cytosol initiates the NF-κB signalling, leading to increased myostatin (MSTN) expression in the sIBM muscle (Sachdev et al., 2018).

The presence of mtDNA in the cytosol is an intrinsic warning of pathogen infection or cellular dysfunction. These cytosolic mtDNAs are sensed by the cyclic guanosine monophosphate (GMP)-AMP synthase (cGAS) and promote its dimerization, leading to the production of second messenger cyclic GMP-AMP (cGAMP). The binding of cGAMP to the endoplasmic reticulum protein STING (stimulator of interferon genes) induces its translocation to the Golgi apparatus, where it activates the TANK-binding kinase 1 (TBK1) to phosphorylate the transcription factors interferon regulatory factor 1 (IRF1) and the IκB kinase complex. Consequently, transcription of NFκB-targeted genes such as type I interferons will be enhanced, attracting the immune cells to the injured muscle (Zhang et al., 2022). Although no studies have been performed to evaluate the cGAS-STING pathway in the animal models of sIBM or patient samples, the mtDNA-induced cGAS-STING pathway activation is detected in cells when TDP-43 invades mitochondria (Yu et al., 2020). Moreover, a recent report by Irazoki et al. (2023) demonstrated that the release of mtDNA after mitochondrial dysfunction is sufficient to induce sterile inflammation in the skeletal muscle, further supporting the role of cGAS pathway in myositis development.

The release of mtDNA may activate the pyroptotic cell-death pathways via activating another intracellular DNA sensor NLRP (nucleotide-binding oligomerization domain, leucine rich repeat and pyrin domain containing) proteins to form inflammasomes (Marchi et al., 2023) and the subsequent pyroptosis signalling. Inflammasomes are multiprotein complex containing leucine-rich repeated containing proteins (e.g., NLRP2, AIM2, Pyrin), the adapter protein ASC (apoptosis-associated speck-like protein containing a caspase recruitment domain CARD), and pro-caspase 1. Although the molecular details of mtDNA-induced NLRP activation are still unknown, the outcomes of inflammasome formation have been well-defined. Once the caspase 1 in the inflammasome is activated, it cleaves the membrane pore protein Gasdermin D and interleukins (IL-1 and IL-8). Consequently, the membrane permeability is increased, leading to cell swelling, leakage of cellular proteins, and the formation of functional IL-1β and IL-18, all of which are strong inflammation inducers (Sharma and Kanneganti, 2021). A recent study demonstrated that the formation of NLRP3 inflammasome and pyroptosis was upregulated in the muscle fibers of DM and PM (Liu et al., 2021), its activity in sIBM remains to be investigated. Nevertheless, it has been demonstrated that ketogenic diet could alleviate the clinical symptoms of sIBM patients, possibly through suppressing NLRP3 inflammation activation, suggesting that pyroptosis is involved in the pathogenesis of sIBM (Phillips et al., 2020).

Recently, Kamiya et al. (2022) reported that inhibiting the necroptosis signalling effectively ameliorated the invasion of $CD8^+$ cytotoxic T lymphocytes and thus suppressed muscle injury in PM. Necroptosis is a caspase-independent form of programmed cell death that results in membrane rupture, cell swelling, and leakage of DAMPs to promote inflammation (Pasparakis and Vandenabeele, 2015). The canonical necroptosis pathway is typically initiated by the cytokine TNFα in caspase 8-inactive cells. Once TNFα binds to its cognate receptor TNFR1, the receptor forms a complex that contains TNFR1-associated death domain protein (TRADD) and receptor-interacting serine/threonine protein kinase 1 (RIPK1). In certain conditions such as growth factor deprivation, the ligand activated TNFR-TRADD-RIPK1 complex further recruits and activates caspase 8 to cleave the downstream apoptosis executors like BH3-interacting domain death agonist (BID) to induce mitochondrial member depolarization and release of cytochrome c for caspase 3 activation (Luo et al., 1998). In cells with the absence of caspase 8, activation of TNFR1 promotes the heterodimerization of RIPK1 and RIPK3, forming the complex necrosome. Because RIPK3 is a proteolytic substrate of caspase 8, the formation of

necrosome will only be formed in the absence of caspase 8 (Kang et al., 2013). The necrosome further recruits the mixed-lineage kinase domain-like protein (MLKL), which is phosphorylated by RIPK3 to form active oligomers for plasma membrane translocation. Due to its porous nature, the insertion of MLKL oligomers causes leakage of cellular content to the extracellular environment or cell rupture to induce the tethering of immune cells. Interestingly, activation of RIPK1 and RIPK3 triggers mitochondrial dysfunction (Chen et al., 2018) and activates the pyruvate dehydrogenase complex to produce excessive ROS (Yang et al., 2018), respectively. The high ROS feedbacks to the necrosome complex formation, forming a positive feedback loop of the necroptosis pathway to further enhance the necroptosis signalling (Qiu et al., 2018). Peng et al. (2022) reported that the necroptosis machinery is highly expressed in several subtypes of IIM, including DM and IMNM. Moreover, overactivation of the necroptotic pathway is sufficient to cause cell death of healthy muscle cells (Peng et al., 2022). Although high expression of necroptosis inducer TNF-α is detected in the muscle of sIBM patients (Schmidt et al., 2008), the activity of caspase 8 in the muscle has never been studied, making it a mystery if necroptosis is also elevated in sIBM like other IIM subtypes.

Targeting mitochondrial health as a new treatment strategy of sIBM

Due to the immunosuppressant-resistant feature of sIBM, exercise remains the main-stay therapy for sIBM (Koo et al., 2019). In general, endurance exercise is known to benefit skeletal muscle by increasing the disposal of ROS-damaged proteins and the synthesis of new mitochondria to accelerate mitochondrial turnover, thereby maintaining a healthy mitochondria network with boosted OXPHOS capacity (Sorriento et al., 2021). Resistance exercise also enhances the cellular antioxidation capacity by activating FOXO3, a transcription factor that induces the expression of antioxidant enzymes like SOD, to improve muscle function in sIBM (Koo et al., 2019). Interestingly, Coudert et al. (2022) recently reported that testosterone supplementation and exercise training may exert additive effects in improving muscle performance and mitigating the overactivated immunity in sIBM patients. However, performing regular exercise relies heavily on self-motivation and is difficult for cane- or wheelchair-bound patients at the advanced stage of IBM. Therefore, there is an urge to develop agents that recapitulate the benefits of exercise, such as upregulating antioxidant activity, increasing mitochondrial biogenesis, or promoting mitochondrial removal in the muscle. Considering that AMPK activation is a critical event in initiating mitochondrial biogenesis and mitophagy during exercise, AMPK-activating agents are attractive candidates for this purpose. Indeed, the AMP analogue 5-Aminoimidazole-4-carboxamide-1-beta-D-ribofuranosyl 5′-monophosphate (AICAR) downregulated the expression of atrophic marker Atrogin/MAFbx in the gastrocnemius muscle and relieved cancer-induced muscle atrophy in mice (Hall et al., 2018). Another Food and Drug Administration (FDA)-approved AMPK activator, metformin, is found to promote mitophagy in type 2 diabetic patients (Picca et al., 2023). In a cardiovascular disease mouse model, metformin treatment suppressed ROS production in the abnormal heart tissue in an AMPK-dependent manner, which prevented the NLRP3/IL-1β-mediated inflammation and cardiovascular lesions (Marek-Iannucci et al., 2021).

Antioxidant application may be helpful in rescuing cell death in the sIBM muscle by neutralizing ROS into less harmful products (Johnson et al., 2023). For example, the well-known antioxidant polyphenol resveratrol has been shown to suppress myostatin-mediated cell death by activating the NF-κB signalling in cultured sIBM myoblasts (Askanas et al., 2012). The use of mitochondrial-targeted antioxidants like MitoQ and MitoVitE, which are hundred folds more effective in rescuing mitochondrial oxidative stress-induced cell death in human fibroblasts than other non-specific, cellular antioxidants like idebenone and vitamin E (Jauslin et al., 2003), might also alleviate the symptoms of sIBM (Rostamzadeh et al., 2024). Indeed, studies in numerous experimental models have confirmed the protective effect of these mitochondrial-targeted antioxidants in treating ROS-associated diseases like Parkinson's Disease and atherosclerosis (Jiang et al., 2020; Sulaimon et al., 2022), which provide a solid scientific basis to extend their translational potential in ameliorating sIBM. Nevertheless, caution must be exercised when antioxidants are used in the sIBM treatment because exogenous supplementation of NADH and GSH may disrupt the redox balance and impose reductive stress on the cell (Xiao and Loscalzo, 2019). In fact, multiple studies have correlated excessive reductive stress with the development of inflammatory-associated diseases like cardiomyopathy, muscular dystrophy, and Alzheimer's disease (Pérez-Torres et al., 2017).

Target mitophagy, a specific form of autophagy that degrades mitochondria exclusively (Lu et al., 2023), may also be a viable approach to alleviate myopathies associated with excessive oxidative stress (Ito et al., 2022). Traditional mitophagy inducers like oligomycin and carbonyl cyanide m-chlorophenyl hydrazone (CCCP) have been widely adopted in the *in vitro* system but their high toxicity limits their clinical applicability (Lee et al., 2023). Therefore, considerable efforts have been devoted to screen for alternative inducers with low toxicity for clinical applications. In 2021, Luan et al. (2021) reported that Urolithin A (UroA) reversed the declined mitophagy in cultured myoblasts of Duchenne Muscular Dystrophy (DMD) patients and *mdx* mice, which led to a reduction in muscle damage. UroA is a metabolite of microflora produced from the polyphenols ellagic acid and ellagitannins in food (Faitg et al., 2024), which is considered safe for oral consumption in humans as a dietary supplement by the FDA (García-Villalba et al., 2022). In a randomized, double-blinded, placebo-controlled clinical trial, subjects consuming UroA for 4 months exhibited augmented expression of mitophagy markers in their muscle biopsy, which was associated with higher complex I and II-mediated respiration (Faitg et al., 2024). Another clinical trial demonstrated that UroA effectively improved mitochondrial function in the skeletal muscle of the elderly by upregulating mitochondrial gene expression (Andreux et al., 2019). The positive effect of UroA on mitochondrial respiration was also reflected by the 65% higher running capacity in the UroA-administrated Wistar rats (Nat Med, 2016). Mechanically, UroA triggers mitophagy via lowering the mitochondrial membrane potential, as short-term UroA treatment induced membrane depolarization followed by augmented mitophagy marker

10.3389/fcell.2024.1403463

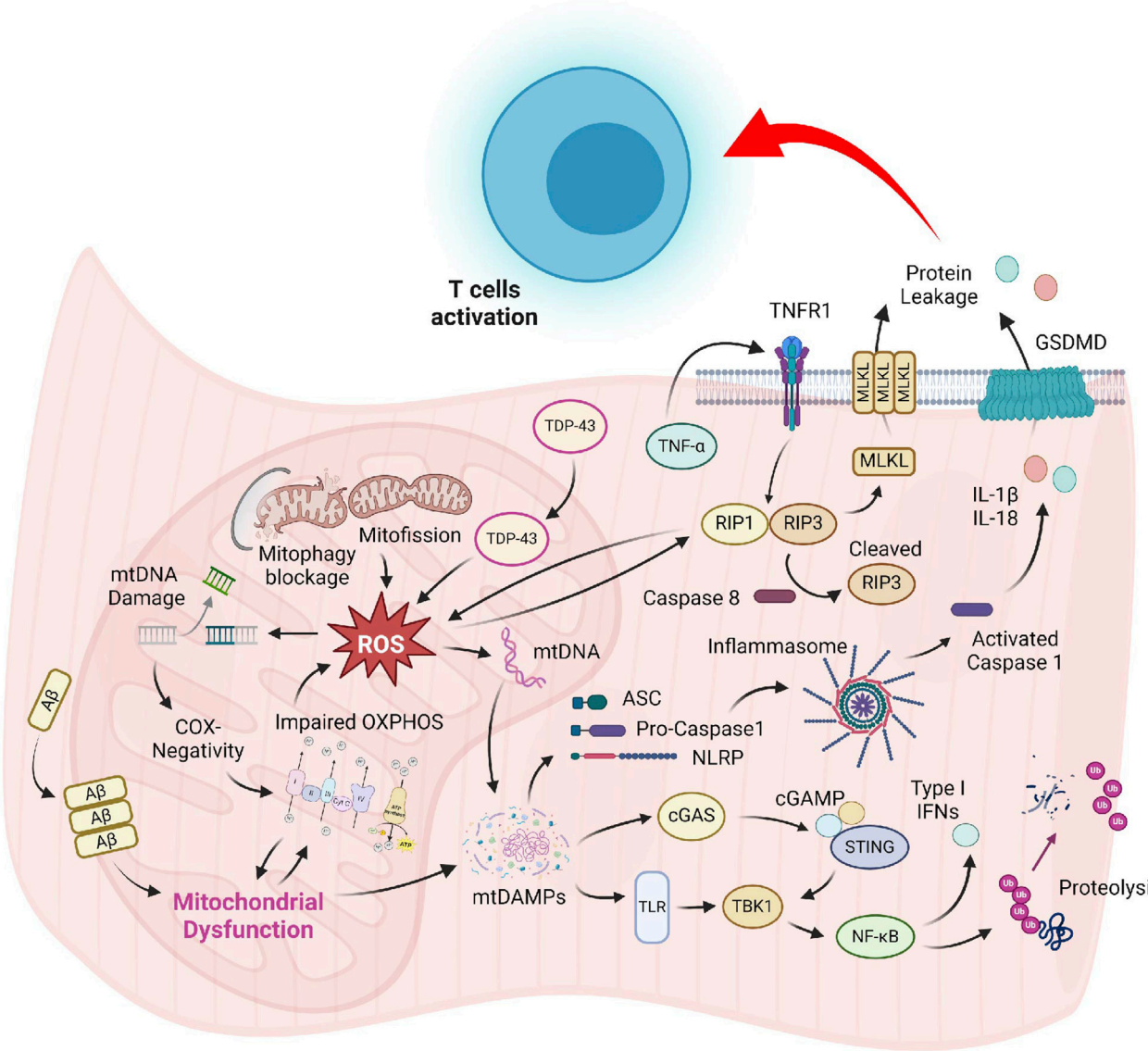

FIGURE 1
Prominent mitochondrial abnormalities in sIBM muscle include COX-negativity, OXPHOS suppression, delayed organelle clearance, and mislocalization of proteins. Augmented ROS produced by the dysfunctional mitochondrial might damage the organelle, resulting in the release of mitochondrial content into the sarcoplasm. These mtDAMPs are strong inducers of the TLR and cGAS-STING pathway, which promote inflammatory cytokines production and muscle breakdown via the NF-κB signaling. Accumulation of mtDAMPs and ROS might also induce the formation of NLRP-mediated inflammasome and TNF-α-triggered necrosome, leading to compromised sarcolemma integrity. Leakage of cellular content generates DAMPs that might serve as activation signals for T-cell recruitment in sIBM.

expression (Ryu et al., 2016). Based on the promising effect of UroA in improving muscle function of age-related atrophic fibers, which share some biochemical characteristics of sIBM myofibers (Romani et al., 2021), it is reasonable to assume that UroA could also be effective in ameliorating mitochondrial defects and reducing muscle damage in sIBM. In supporting the idea that maintaining mitochondria activity is important to sustain the survival of the sIBM muscle cells, Oikawa et al. (2020) reported that mitochonic acid 5 (MA-5), a plant derivative that facilitates mitochondrial activities, such as increasing ATP synthesis, reducing ROS production, and promoting OXPHOS, was effective in protecting the myoblasts of sIBM patients from the buthionine sulfoximine-induced cell death. Presumably, mitochondrial health-improving agents like UroA and MA-5 might represent safe and effective agents for sIBM patients to improve their muscle function.

Conclusion

Although pathological hallmarks of sIBM have been recognized for several decades, the precise molecular mechanism for these cellular abnormalities is still mysterious. Most studies on sIBM pathogenesis are associative in nature, and the lack of mechanistic studies hinders the development of effective treatment, making it still an incurable disease nowadays. The slow progress in the development of new sIBM therapy can be

attributed, in part, to the uncertainty of the sequential relationship between muscle damage and overactivated immune response. Moreover, most studies of sIBM have primarily focused on the detrimental consequence of hyperactive immune cells and protein aggregation on skeletal muscle; the outcomes of other damaged organelles like mitochondria have received little attention. The conventional view of mitochondria solely as ATP-producing powerhouses biased our perception that defective mitochondria in IIM might only result in metabolic deficiency, thus underestimating its functional outcomes. Recent discoveries that highlight mitochondrial defects as inducers of immune response via pyroptosis and necroptosis in many different issues have provided new insights into the pathogenesis of IIM (Figure 1). Hence, it is imperative to recognize the etiological role of mitochondria and developing novel drugs that improve the mitochondrial health as a novel treatment strategy for sIBM.

Author contributions

EI: Writing–original draft, Writing–review and editing. HS: Writing–review and editing. CC: Writing–original draft, Writing–review and editing.

Funding

The author(s) declare that financial support was received for the research, authorship, and/or publication of this article. This work is supported by the HKU Seed Fund for Basic Research to CC and Hong Kong Health and Medical Research Fund (HMRF21222301) to CC and HS.

Conflict of interest

The authors declare that the research was conducted in the absence of any commercial or financial relationships that could be construed as a potential conflict of interest.

Publisher's note

References

Andreux, P. A., Blanco-Bose, W., Ryu, D., Burdet, F., Ibberson, M., Aebischer, P., et al. (2019). The mitophagy activator urolithin A is safe and induces a molecular signature of improved mitochondrial and cellular health in humans. *Nat. Metab.* 1 (6), 595–603. doi:10.1038/s42255-019-0073-4

Askanas, V., and Engel, W. K. (1998). Sporadic inclusion-body myositis and hereditary inclusion-body myopathies: diseases of oxidative stress and aging? *Archives Neurology* 55 (7), 915–920. doi:10.1001/archneur.55.7.915

Askanas, V., and Engel, W. K. (2008). Inclusion-body myositis: muscle-fiber molecular pathology and possible pathogenic significance of its similarity to Alzheimer's and Parkinson's disease brains. *Acta Neuropathol.* 116 (6), 583–595. doi:10.1007/s00401-008-0449-0

Askanas, V., Engel, W. K., and Nogalska, A. (2012). Pathogenic considerations in sporadic inclusion-body myositis, a degenerative muscle disease associated with aging and abnormalities of myoproteostasis. *J. Neuropathol. Exp. Neurol.* 71 (8), 680–693. doi:10.1097/NEN.0b013e31826183c8

Askanas, V., Engel, W. K., and Nogalska, A. (2015). Sporadic inclusion-body myositis: a degenerative muscle disease associated with aging, impaired muscle protein homeostasis and abnormal mitophagy. *Biochim. Biophys. Acta* 1852 (4), 633–643. doi:10.1016/j.bbadis.2014.09.005

Askanas, V., McFerrin, J., Baqué, S., Alvarez, R. B., Sarkozi, E., and Engel, W. K. (1996). Transfer of beta-amyloid precursor protein gene using adenovirus vector causes mitochondrial abnormalities in cultured normal human muscle. *Proc. Natl. Acad. Sci. U. S. A.* 93 (3), 1314–1319. doi:10.1073/pnas.93.3.1314

Bhatt, P. S., Tzoulis, C., Balafkan, N., Miletic, H., Tran, G. T. T., Sanaker, P. S., et al. (2019). Mitochondrial DNA depletion in sporadic inclusion body myositis. *Neuromuscul. Disord.* 29 (3), 242–246. doi:10.1016/j.nmd.2019.02.001

Boncompagni, S., Moussa, C. E., Levy, E., Pezone, M. J., Lopez, J. R., Protasi, F., et al. (2012). Mitochondrial dysfunction in skeletal muscle of amyloid precursor protein-overexpressing mice. *J. Biol. Chem.* 287 (24), 20534–20544. doi:10.1074/jbc.M112.359588

Britson, K. A., Ling, J. P., Braunstein, K. E., Montagne, J. M., Kastenschmidt, J. M., Wilson, A., et al. (2022). Loss of TDP-43 function and rimmed vacuoles persist after T cell depletion in a xenograft model of sporadic inclusion body myositis. *Sci Transl Med.* 14 (628), eabi9196. doi:10.1126/scitranslmed.abi9196

Cacciottolo, M., Nogalska, A., D'Agostino, C., Engel, W. K., and Askanas, V. (2013). Chaperone-mediated autophagy components are upregulated in sporadic inclusion-body myositis muscle fibres. *Neuropathol. Appl. Neurobiol.* 39 (7), 750–761. doi:10.1111/nan.12038

Canakçi, C. F., Tatar, A., Canakçi, V., Cicek, Y., Oztas, S., and Orbak, R. (2006). New evidence of premature oxidative DNA damage: mitochondrial DNA deletion in gingival tissue of patients with periodontitis. *J. Periodontol.* 77 (11), 1894–1900. doi:10.1902/jop.2006.060108

Cantó-Santos, J., Valls-Roca, L., Tobías, E., García-García, F. J., Guitart-Mampel, M., Esteve-Codina, A., et al. (2023). Unravelling inclusion body myositis using a patient-derived fibroblast model. *J. Cachexia Sarcopenia Muscle* 14 (2), 964–977. doi:10.1002/jcsm.13178

Cantó Santos, J., Valls-Roca, L., Tobías, E., Oliva, C., García-García, F., Guitart-Mampel, M., et al. (2023). Integrated multi-omics analysis for inferring molecular players in inclusion body myositis. *Antioxidants* 12, 1639. doi:10.3390/antiox12081639

Catalán-García, M., García-García, F. J., Moreno-Lozano, P. J., Alcarraz-Vizán, G., Tort-Merino, A., Milisenda, J. C., et al. (2020). Mitochondrial dysfunction: a common hallmark underlying comorbidity between sIBM and other degenerative and age-related diseases. *J. Clin. Med.* 9 (5), 1446. doi:10.3390/jcm9051446

Catalán-García, M., Garrabou, G., Morén, C., Guitart-Mampel, M., Gonzalez-Casacuberta, I., Hernando, A., et al. (2016a). BACE-1, PS-1 and sAPPβ levels are increased in plasma from sporadic inclusion body myositis patients: surrogate biomarkers among inflammatory myopathies. *Mol. Med.* 21 (1), 817–823. doi:10.2119/molmed.2015.00168

Catalán-García, M., Garrabou, G., Morén, C., Guitart-Mampel, M., Hernando, A., Díaz-Ramos, À., et al. (2016b). Mitochondrial DNA disturbances and deregulated expression of oxidative phosphorylation and mitochondrial fusion proteins in sporadic inclusion body myositis. *Clin. Sci. (Lond)* 130 (19), 1741–1751. doi:10.1042/cs20160080

Chapa, J., Macêdo, M., Naddaf, E., Saketkoo, L., and Lood, C. (2023). Mitochondrial transfer and implications for muscle function in idiopathic inflammatory myopathies. *Clin. Exp. Rheumatology* 42. doi:10.55563/clinexprheumatol/5lfq5x

Chen, S., Lv, X., Hu, B., Zhao, L., Li, S., Li, Z., et al. (2018). Critical contribution of RIPK1 mediated mitochondrial dysfunction and oxidative stress to compression-induced rat nucleus pulposus cells necroptosis and apoptosis. *Apoptosis* 23 (5-6), 299–313. doi:10.1007/s10495-018-1455-x

Ching, J. K., Ju, J. S., Pittman, S. K., Margeta, M., and Weihl, C. C. (2013). Increased autophagy accelerates colchicine-induced muscle toxicity. *Autophagy* 9 (12), 2115–2125. doi:10.4161/auto.26150

Coudert, J. D., Slater, N., Sooda, A., Beer, K., Lim, E. M., Boyder, C., et al. (2022). Immunoregulatory effects of testosterone supplementation combined with exercise training in men with Inclusion Body Myositis: a double-blind, placebo-controlled, cross-over trial. *Clin. Transl. Immunol.* 11 (9), e1416. doi:10.1002/cti2.1416

Damian, L., Login, C. C., Solomon, C., Belizna, C., Encica, S., Urian, L., et al. (2022). Inclusion body myositis and neoplasia: a narrative review. *Int. J. Mol. Sci.* 23 (13), 7358. doi:10.3390/ijms23137358

Danieli, M. G., Antonelli, E., Piga, M. A., Cozzi, M. F., Allegra, A., and Gangemi, S. (2023). Oxidative stress, mitochondrial dysfunction, and respiratory chain enzyme defects in inflammatory myopathies. *Autoimmun. Rev.* 22 (5), 103308. doi:10.1016/j.autrev.2023.103308

De Bleecker, J. L., Meire, V. I., Van Walleghem, I. E., Groessens, I. M., and Schröder, J. M. (2001). Immunolocalization of FAS and FAS ligand in inflammatory myopathies. *Acta Neuropathol.* 101 (6), 572–578. doi:10.1007/s004010000324

De Paepe, B. (2019). Sporadic inclusion body myositis: an acquired mitochondrial disease with extras. *Biomolecules* 9 (1), 15. doi:10.3390/biom9010015

Devi, L., Prabhu, B. M., Galati, D. F., Avadhani, N. G., and Anandatheerthavarada, H. K. (2006). Accumulation of amyloid precursor protein in the mitochondrial import channels of human Alzheimer's disease brain is associated with mitochondrial dysfunction. *J. Neurosci.* 26 (35), 9057–9068. doi:10.1523/jneurosci.1469-06.2006

Diederichsen, L. P., Iversen, L. V., Nielsen, C. T., Jacobsen, S., Hermansen, M. L., Witting, N., et al. (2023). Myositis-related autoantibody profile and clinical characteristics stratified by anti-cytosolic 5'-nucleotidase 1A status in connective tissue diseases. *Muscle Nerve* 68 (1), 73–80. doi:10.1002/mus.27841

Di Leo, V., Bernardino Gomes, T. M., and Vincent, A. E. (2023). Interactions of mitochondrial and skeletal muscle biology in mitochondrial myopathy. *Biochem. J.* 480 (21), 1767–1789. doi:10.1042/bcj20220233

DiMauro, S., Bonilla, E., Zeviani, M., Nakagawa, M., and DeVivo, D. C. (1985). Mitochondrial myopathies. *Ann. Neurol.* 17 (6), 521–538. doi:10.1002/ana.410170602

Faitg, J., D'Amico, D., Rinsch, C., and Singh, A. (2024). Mitophagy activation by urolithin A to target muscle aging. *Calcif. Tissue Int.* 114 (1), 53–59. doi:10.1007/s00223-023-01145-5

Favaro, G., Romanello, V., Varanita, T., Andrea Desbats, M., Morbidoni, V., Tezze, C., et al. (2019). DRP1-mediated mitochondrial shape controls calcium homeostasis and muscle mass. *Nat. Commun.* 10 (1), 2576. doi:10.1038/s41467-019-10226-9

Fréret, M., Drouot, L., Obry, A., Ahmed-Lacheheb, S., Dauly, C., Adriouch, S., et al. (2013). Overexpression of MHC class I in muscle of lymphocyte-deficient mice causes a severe myopathy with induction of the unfolded protein response. *Am. J. Pathol.* 183 (3), 893–904. doi:10.1016/j.ajpath.2013.06.003

Fyhr, I. M., and Oldfors, A. (1998). Upregulation of Fas/Fas ligand in inclusion body myositis. *Ann. Neurol.* 43 (1), 127–130. doi:10.1002/ana.410430123

Gang, Q., Bettencourt, C., Machado, P. M., Brady, S., Holton, J. L., Pittman, A. M., et al. (2016). Rare variants in SQSTM1 and VCP genes and risk of sporadic inclusion body myositis. *Neurobiol. Aging* 47, 218.e1–218.e9. doi:10.1016/j.neurobiolaging.2016.07.024

García-Villalba, R., Giménez-Bastida, J. A., Cortés-Martín, A., Ávila-Gálvez, M., Tomás-Barberán, F. A., Selma, M. V., et al. (2022). Urolithins: a comprehensive update on their metabolism, bioactivity, and associated gut microbiota. *Mol. Nutr. Food Res.* 66 (21), e2101019. doi:10.1002/mnfr.202101019

Goebels, N., Michaelis, D., Engelhardt, M., Huber, S., Bender, A., Pongratz, D., et al. (1996). Differential expression of perforin in muscle-infiltrating T cells in polymyositis and dermatomyositis. *J. Clin. Investig.* 97 (12), 2905–2910. doi:10.1172/jci118749

Gonzalez-Chapa, J. A., Macêdo, M. B., and Lood, C. (2023). The emerging role of mitochondrial dysfunction in the pathogenesis of idiopathic inflammatory myopathies. *Rambam Maimonides Med. J.* 14 (2), e0006. doi:10.5041/rmmj.10493

Greenberg, M. V. C., and Bourc'his, D. (2019). The diverse roles of DNA methylation in mammalian development and disease. *Nat. Rev. Mol. Cell. Biol.* 20 (10), 590–607. doi:10.1038/s41580-019-0159-6

Greenberg, S. A. (2019). Inclusion body myositis: clinical features and pathogenesis. *Nat. Rev. Rheumatol.* 15 (5), 257–272. doi:10.1038/s41584-019-0186-x

Greenberg, S. A., Bradshaw, E. M., Pinkus, J. L., Pinkus, G. S., Burleson, T., Due, B., et al. (2005). Plasma cells in muscle in inclusion body myositis and polymyositis. *Neurology* 65 (11), 1782–1787. doi:10.1212/01.wnl.0000187124.92826.20

Gunawardena, H., Betteridge, Z. E., and McHugh, N. J. (2009). Myositis-specific autoantibodies: their clinical and pathogenic significance in disease expression. *Rheumatol. Oxf.* 48 (6), 607–612. doi:10.1093/rheumatology/kep078

Güttsches, A. K., Brady, S., Krause, K., Maerkens, A., Uszkoreit, J., Eisenacher, M., et al. (2017). Proteomics of rimmed vacuoles define new risk allele in inclusion body myositis. *Ann. Neurol.* 81 (2), 227–239. doi:10.1002/ana.24847

Hall, D. T., Griss, T., Ma, J. F., Sanchez, B. J., Sadek, J., Tremblay, A. M. K., et al. (2018). The AMPK agonist 5-aminoimidazole-4-carboxamide ribonucleotide (AICAR), but not metformin, prevents inflammation-associated cachectic muscle wasting. *EMBO Mol. Med.* 10 (7), e8307. doi:10.15252/emmm.201708307

Hedberg-Oldfors, C., Lindgren, U., Basu, S., Visuttijai, K., Lindberg, C., Falkenberg, M., et al. (2021). Mitochondrial DNA variants in inclusion body myositis characterized by deep sequencing. *Brain Pathol.* 31 (3), e12931. doi:10.1111/bpa.12931

Hiniker, A., Daniels, B. H., and Margeta, M. (2016). T-cell-mediated inflammatory myopathies in HIV-positive individuals: a histologic study of 19 cases. *J. Neuropathol. Exp. Neurol.* 75 (3), 239–245. doi:10.1093/jnen/nlv023

Horvath, R., Fu, K., Johns, T., Genge, A., Karpati, G., and Shoubridge, E. A. (1998). Characterization of the mitochondrial DNA abnormalities in the skeletal muscle of patients with inclusion body myositis. *J. Neuropathol. Exp. Neurol.* 57 (5), 396–403. doi:10.1097/00005072-199805000-00003

Huntley, M. L., Gao, J., Termsarasab, P., Wang, L., Zeng, S., Thammongkolchai, T., et al. (2019). Association between TDP-43 and mitochondria in inclusion body myositis. *Lab. Investig.* 99 (7), 1041–1048. doi:10.1038/s41374-019-0233-x

Irazoki, A., Gordaliza-Alaguero, I., Frank, E., Giakoumakis, N. N., Seco, J., Palacín, M., et al. (2023). Disruption of mitochondrial dynamics triggers muscle inflammation through interorganellar contacts and mitochondrial DNA mislocation. *Nat. Commun.* 14 (1), 108. doi:10.1038/s41467-022-35732-1

Ito, A., Hashimoto, M., Tanihata, J., Matsubayashi, S., Sasaki, R., Fujimoto, S., et al. (2022). Involvement of Parkin-mediated mitophagy in the pathogenesis of chronic obstructive pulmonary disease-related sarcopenia. *J. Cachexia Sarcopenia Muscle* 13 (3), 1864–1882. doi:10.1002/jcsm.12988

Jang, S., Kumar, N., Beckwitt, E. C., Kong, M., Fouquerel, E., Rapić-Otrin, V., et al. (2019). Damage sensor role of UV-DDB during base excision repair. *Nat. Struct. Mol. Biol.* 26 (8), 695–703. doi:10.1038/s41594-019-0261-7

Jauslin, M. L., Meier, T., Smith, R. A., and Murphy, M. P. (2003). Mitochondria-targeted antioxidants protect Friedreich Ataxia fibroblasts from endogenous oxidative stress more effectively than untargeted antioxidants. *Faseb J.* 17 (13), 1972–1974. doi:10.1096/fj.03-0240fje

Jiang, Q., Yin, J., Chen, J., Ma, X., Wu, M., Liu, G., et al. (2020). Mitochondria-targeted antioxidants: a step towards disease treatment. *Oxid. Med. Cell. Longev.* 2020, 8837893. doi:10.1155/2020/8837893

Joaquim, M., and Escobar-Henriques, M. (2020). Role of mitofusins and mitophagy in life or death decisions. *Front. Cell. Dev. Biol.* 8, 572182. doi:10.3389/fcell.2020.572182

Johnson, G. A., Krishnamoorthy, R. R., and Stankowska, D. L. (2023). Modulating mitochondrial calcium channels (TRPM2/MCU/NCX) as a therapeutic strategy for neurodegenerative disorders. *Front. Neurosci.* 17, 1202167. doi:10.3389/fnins.2023.1202167

Joshi, P. R., Vetterke, M., Hauburger, A., Tacik, P., Stoltenburg, G., and Hanisch, F. (2014). Functional relevance of mitochondrial abnormalities in sporadic inclusion body myositis. *J. Clin. Neurosci.* 21 (11), 1959–1963. doi:10.1016/j.jocn.2014.05.051

Jou, C., Nascimento, A., Codina, A., Montoya, J., López-Gallardo, E., Emperador, S., et al. (2022). Pathological features in paediatric patients with TK2 deficiency. *Int. J. Mol. Sci.* 23 (19), 11002. doi:10.3390/ijms231911002

Kamiya, M., Mizoguchi, F., Kawahata, K., Wang, D., Nishibori, M., Day, J., et al. (2022). Targeting necroptosis in muscle fibers ameliorates inflammatory myopathies. *Nat. Commun.* 13 (1), 166. doi:10.1038/s41467-021-27875-4

Kang, T. B., Yang, S. H., Toth, B., Kovalenko, A., and Wallach, D. (2013). Caspase-8 blocks kinase RIPK3-mediated activation of the NLRP3 inflammasome. *Immunity* 38 (1), 27–40. doi:10.1016/j.immuni.2012.09.015

Khoo, T., Lilleker, J. B., Thong, B. Y., Leclair, V., Lamb, J. A., and Chinoy, H. (2023). Epidemiology of the idiopathic inflammatory myopathies. *Nat. Rev. Rheumatol.* 19 (11), 695–712. doi:10.1038/s41584-023-01033-0

Koo, J. H., Kang, E. B., and Cho, J. Y. (2019). Resistance exercise improves mitochondrial quality control in a rat model of sporadic inclusion body myositis. *Gerontology* 65 (3), 240–252. doi:10.1159/000494723

Landfeldt, E., Lindgren, P., Bell, C. F., Schmitt, C., Guglieri, M., Straub, V., et al. (2015). Compliance to care guidelines for Duchenne muscular dystrophy. *J. Neuromuscul. Dis.* 2 (1), 63–72. doi:10.3233/jnd-140053

Lee, D. Y., Lee, K. M., Um, J. H., Kim, Y. Y., Kim, D. H., and Yun, J. (2023). The natural alkaloid palmatine selectively induces mitophagy and restores mitochondrial function in an alzheimer's disease mouse model. *Int. J. Mol. Sci.* 24 (22), 16542. doi:10.3390/ijms242216542

Lightfoot, A. P., McArdle, A., Jackson, M. J., and Cooper, R. G. (2015). In the idiopathic inflammatory myopathies (IIM), do reactive oxygen species (ROS) contribute to muscle weakness? *Ann. Rheum. Dis.* 74 (7), 1340–1346. doi:10.1136/annrheumdis-2014-207172

Lindgren, U., Roos, S., Hedberg Oldfors, C., Moslemi, A.-R., Lindberg, C., and Oldfors, A. (2015). Mitochondrial pathology in inclusion body myositis. *Neuromuscul. Disord.* 25 (4), 281–288. doi:10.1016/j.nmd.2014.12.010

Liu, D., Xiao, Y., Zhou, B., Gao, S., Li, L., Zhao, L., et al. (2021). PKM2-dependent glycolysis promotes skeletal muscle cell pyroptosis by activating the NLRP3 inflammasome in dermatomyositis/polymyositis. *Rheumatol. Oxf.* 60 (5), 2177–2189. doi:10.1093/rheumatology/keaa473

Ljungman, M., and Hanawalt, P. C. (1992). Efficient protection against oxidative DNA damage in chromatin. *Mol. Carcinog.* 5 (4), 264–269. doi:10.1002/mc.2940050406

Lodi, R., Taylor, D. J., Tabrizi, S. J., Hilton-Jones, D., Squier, M. V., Seller, A., et al. (1998). Normal *in vivo* skeletal muscle oxidative metabolism in sporadic inclusion body myositis assessed by 31P-magnetic resonance spectroscopy. *Brain* 121 (Pt 11), 2119–2126. doi:10.1093/brain/121.11.2119

Lu, J. Q., Monaco, C. M. F., Hawke, T. J., Yan, C., and Tarnopolsky, M. A. (2020). Increased intra-mitochondrial lipofuscin aggregates with spherical dense body formation in mitochondrial myopathy. *J. Neurol. Sci.* 413, 116816. doi:10.1016/j.jns.2020.116816

Lu, Y., Li, Z., Zhang, S., Zhang, T., Liu, Y., and Zhang, L. (2023). Cellular mitophagy: mechanism, roles in diseases and small molecule pharmacological regulation. *Theranostics* 13 (2), 736–766. doi:10.7150/thno.79876

Luan, P., D'Amico, D., Andreux, P. A., Laurila, P. P., Wohlwend, M., Li, H., et al. (2021). Urolithin A improves muscle function by inducing mitophagy in muscular dystrophy. *Sci. Transl. Med.* 13 (588), eabb0319. doi:10.1126/scitranslmed.abb0319

Lünemann, J. D., Schmidt, J., Schmid, D., Barthel, K., Wrede, A., Dalakas, M. C., et al. (2007). Beta-amyloid is a substrate of autophagy in sporadic inclusion body myositis. *Ann. Neurol.* 61 (5), 476–483. doi:10.1002/ana.21115

Luo, X., Budihardjo, I., Zou, H., Slaughter, C., and Wang, X. (1998). Bid, a Bcl2 interacting protein, mediates cytochrome c release from mitochondria in response to activation of cell surface death receptors. *Cell.* 94 (4), 481–490. doi:10.1016/s0092-8674(00)81589-5

Marchi, S., Guilbaud, E., Tait, S. W. G., Yamazaki, T., and Galluzzi, L. (2023). Mitochondrial control of inflammation. *Nat. Rev. Immunol.* 23 (3), 159–173. doi:10.1038/s41577-022-00760-x

Marek-Iannucci, S., Ozdemir, A. B., Moreira, D., Gomez, A. C., Lane, M., Porritt, R. A., et al. (2021). Autophagy-mitophagy induction attenuates cardiovascular inflammation in a murine model of Kawasaki disease vasculitis. *JCI Insight* 6 (18), e151981. doi:10.1172/jci.insight.151981

Mavroudis, I., Knights, M., Petridis, F., Chatzikonstantinou, S., Karantali, E., and Kazis, D. (2021). Diagnostic accuracy of anti-cn1a on the diagnosis of inclusion body myositis. A hierarchical bivariate and bayesian meta-analysis. *J. Clin. Neuromuscul. Dis.* 23 (1), 31–38. doi:10.1097/CND.0000000000000353

McCord, B., and Day, R. M. (2023a). Cytotoxic immune cells do not affect TDP-43 and p62 sarcoplasmic aggregation but influence TDP-43 localisation. *Sci. Rep.* 13 (1), 15935. doi:10.1038/s41598-023-42824-5

McCord, B., and Day, R. M. (2023b). Influence of inflammatory cytokines IL-1β and IFNγ on sarcoplasmic aggregation of p62 and TDP-43 in myotubes. *Mediat. Inflamm.* 2023, 9018470. doi:10.1155/2023/9018470

Miller, F. W., Lamb, J. A., Schmidt, J., and Nagaraju, K. (2018). Risk factors and disease mechanisms in myositis. *Nat. Rev. Rheumatol.* 14 (5), 255–268. doi:10.1038/nrrheum.2018.48

Moriya, K., Nakagawa, K., Santa, T., Shintani, Y., Fujie, H., Miyoshi, H., et al. (2001). Oxidative stress in the absence of inflammation in a mouse model for hepatitis C virus-associated hepatocarcinogenesis. *Cancer Res.* 61 (11), 4365–4370.

Moslemi, A. R., Lindberg, C., and Oldfors, A. (1997). Analysis of multiple mitochondrial DNA deletions in inclusion body myositis. *Hum. Mutat.* 10 (5), 381–386. doi:10.1002/(sici)1098-1004(1997)10:5<381::Aid-humu8>3.0.Co;2-i

Nicot, A. S., Lo Verso, F., Ratti, F., Pilot-Storck, F., Streichenberger, N., Sandri, M., et al. (2014). Phosphorylation of NBR1 by GSK3 modulates protein aggregation. *Autophagy* 10 (6), 1036–1053. doi:10.4161/auto.28479

Nogalska, A., D'Agostino, C., Terracciano, C., Engel, W. K., and Askanas, V. (2010). Impaired autophagy in sporadic inclusion-body myositis and in endoplasmic reticulum stress-provoked cultured human muscle fibers. *Am. J. Pathol.* 177 (3), 1377–1387. doi:10.2353/ajpath.2010.100050

Oddis, C. V. (2016). Update on the pharmacological treatment of adult myositis. *J. Intern. Med.* 280 (1), 63–74. doi:10.1111/joim.12511

Oikawa, Y., Izumi, R., Koide, M., Hagiwara, Y., Kanzaki, M., Suzuki, N., et al. (2020). Mitochondrial dysfunction underlying sporadic inclusion body myositis is ameliorated by the mitochondrial homing drug MA-5. *PLoS One* 15 (12), e0231064. doi:10.1371/journal.pone.0231064

Oldfors, A., Moslemi, A. R., Fyhr, I. M., Holme, E., Larsson, N. G., and Lindberg, C. (1995). Mitochondrial DNA deletions in muscle fibers in inclusion body myositis. *J. Neuropathol. Exp. Neurol.* 54 (4), 581–587. doi:10.1097/00005072-199507000-00012

Oldfors, A., Moslemi, A. R., Jonasson, L., Ohlsson, M., Kollberg, G., and Lindberg, C. (2006). Mitochondrial abnormalities in inclusion-body myositis. *Neurology* 66 (2 Suppl. 1), S49–S55. doi:10.1212/01.wnl.0000192127.63013.8d

Olivé, M., Janué, A., Moreno, D., Gámez, J., Torrejón-Escribano, B., and Ferrer, I. (2009). TAR DNA-Binding protein 43 accumulation in protein aggregate myopathies. *J. Neuropathol. Exp. Neurol.* 68 (3), 262–273. doi:10.1097/NEN.0b013e3181996d8f

Olivé, M., van Leeuwen, F. W., Janué, A., Moreno, D., Torrejón-Escribano, B., and Ferrer, I. (2008). Expression of mutant ubiquitin (UBB+1) and p62 in myotilinopathies and desminopathies. *Neuropathol. Appl. Neurobiol.* 34 (1), 76–87. doi:10.1111/j.1365-2990.2007.00864.x

Papadimas, G. K., Kokkinis, C., Xirou, S., Chrysanthou, M., Kararizou, E., and Papadopoulos, C. (2019). Polymyositis with mitochondrial pathology or atypical form of sporadic inclusion body myositis: case series and review of the literature. *Rheumatol. Int.* 39 (8), 1459–1466. doi:10.1007/s00296-019-04314-8

Papadopoulos, C., Kirchner, P., Bug, M., Grum, D., Koerver, L., Schulze, N., et al. (2017). VCP/p97 cooperates with YOD1, UBXD1 and PLAA to drive clearance of ruptured lysosomes by autophagy. *EMBO J.* 36 (2), 135–150. doi:10.15252/embj.201695148

Pasparakis, M., and Vandenabeele, P. (2015). Necroptosis and its role in inflammation. *Nature* 517 (7534), 311–320. doi:10.1038/nature14191

Peng, Q. L., Zhang, Y. M., Liu, Y. C., Liang, L., Li, W. L., Tian, X. L., et al. (2022). Contribution of necroptosis to myofiber death in idiopathic inflammatory myopathies. *Arthritis Rheumatol.* 74 (6), 1048–1058. doi:10.1002/art.42071

Pérez-Torres, I., Guarner-Lans, V., and Rubio-Ruiz, M. E. (2017). Reductive stress in inflammation-associated diseases and the pro-oxidant effect of antioxidant agents. *Int. J. Mol. Sci.* 18 (10), 2098. doi:10.3390/ijms18102098

Phillips, M. C. L., Murtagh, D. K. J., Ziad, F., Johnston, S. E., and Moon, B. G. (2020). Impact of a ketogenic diet on sporadic inclusion body myositis: a case study. *Front. Neurol.* 11, 582402. doi:10.3389/fneur.2020.582402

Picca, A., Faitg, J., Auwerx, J., Ferrucci, L., and D'Amico, D. (2023). Mitophagy in human health, ageing and disease. *Nat. Metab.* 5 (12), 2047–2061. doi:10.1038/s42255-023-00930-8

Pruitt, J. N., Showalter, C. J., and Engel, A. G. (1996). Sporadic inclusion body myositis: counts of different types of abnormal fibers. *Ann. Neurol.* 39 (1), 139–143. doi:10.1002/ana.410390122

Qiu, X., Zhang, Y., and Han, J. (2018). RIP3 is an upregulator of aerobic metabolism and the enhanced respiration by necrosomal RIP3 feeds back on necrosome to promote necroptosis. *Cell. Death Differ.* 25 (5), 821–824. doi:10.1038/s41418-018-0075-x

Rinnenthal, J. L., Goebel, H. H., Preuße, C., Lebenheim, L., Schumann, M., Moos, V., et al. (2014). Inflammatory myopathy with abundant macrophages (IMAM): the immunology revisited. *Neuromuscul. Disord.* 24 (2), 151–155. doi:10.1016/j.nmd.2013.11.004

Romani, M., Sorrentino, V., Oh, C. M., Li, H., de Lima, T. I., Zhang, H., et al. (2021). NAD(+) boosting reduces age-associated amyloidosis and restores mitochondrial homeostasis in muscle. *Cell. Rep.* 34 (3), 108660. doi:10.1016/j.celrep.2020.108660

Rostamzadeh, F., Najafipour, H., Aminizadeh, S., and Jafari, E. (2024). Therapeutic effects of the combination of moderate-intensity endurance training and MitoQ supplementation in rats with isoproterenol-induced myocardial injury: the role of mitochondrial fusion, fission, and mitophagy. *Biomed. Pharmacother.* 170, 116020. doi:10.1016/j.biopha.2023.116020

Rygiel, K. A., Miller, J., Grady, J. P., Rocha, M. C., Taylor, R. W., and Turnbull, D. M. (2015). Mitochondrial and inflammatory changes in sporadic inclusion body myositis. *Neuropathol. Appl. Neurobiol.* 41 (3), 288–303. doi:10.1111/nan.12149

Rygiel, K. A., Tuppen, H. A., Grady, J. P., Vincent, A., Blakely, E. L., Reeve, A. K., et al. (2016). Complex mitochondrial DNA rearrangements in individual cells from patients with sporadic inclusion body myositis. *Nucleic Acids Res.* 44 (11), 5313–5329. doi:10.1093/nar/gkw382

Ryu, D., Mouchiroud, L., Andreux, P. A., Katsyuba, E., Moullan, N., Nicolet-Dit-Félix, A. A., et al. (2016). Urolithin A induces mitophagy and prolongs lifespan in *C. elegans* and increases muscle function in rodents. *Nat. Med.* 22 (8), 879–888. doi:10.1038/nm.4132

Sachdev, R., Kappes-Horn, K., Paulsen, L., Duernberger, Y., Pleschka, C., Denner, P., et al. (2018). Endoplasmic reticulum stress induces myostatin high molecular weight aggregates and impairs mature myostatin secretion. *Mol. Neurobiol.* 55 (11), 8355–8373. doi:10.1007/s12035-018-0997-9

Salam, S., Dimachkie, M. M., Hanna, M. G., and Machado, P. M. (2022). Diagnostic and prognostic value of anti-cN1A antibodies in inclusion body myositis. *Clin. Exp. Rheumatol.* 40 (2), 384–393. doi:10.55563/clinexprheumatol/r625rm

Schmidt, J., Barthel, K., Wrede, A., Salajegheh, M., Bähr, M., and Dalakas, M. C. (2008). Interrelation of inflammation and APP in sIBM: IL-1 beta induces accumulation of beta-amyloid in skeletal muscle. *Brain* 131 (Pt 5), 1228–1240. doi:10.1093/brain/awn053

Sharma, B. R., and Kanneganti, T. D. (2021). NLRP3 inflammasome in cancer and metabolic diseases. *Nat. Immunol.* 22 (5), 550–559. doi:10.1038/s41590-021-00886-5

Shelly, S., Mielke, M. M., Mandrekar, J., Milone, M., Ernste, F. C., Naddaf, E., et al. (2021). Epidemiology and natural history of inclusion body myositis: a 40-year population-based study. *Neurology* 96 (21), e2653–e2661. doi:10.1212/wnl.0000000000012004

Shelton, G. D., Minor, K. M., Li, K., Naviaux, J. C., Monk, J., Wang, L., et al. (2019). A mutation in the mitochondrial aspartate/glutamate carrier leads to a more oxidizing intramitochondrial environment and an inflammatory myopathy in Dutch shepherd dogs. *J. Neuromuscul. Dis.* 6 (4), 485–501. doi:10.3233/jnd-190421

Skolka, M. P., and Naddaf, E. (2023). Exploring challenges in the management and treatment of inclusion body myositis. *Curr. Opin. Rheumatol.* 35 (6), 404–413. doi:10.1097/bor.0000000000000958

Snedden, A. M., Kellett, K. A. B., Lilleker, J. B., Hooper, N. M., and Chinoy, H. (2022). The role of protein aggregation in the pathogenesis of inclusion body myositis. *Clin. Exp. Rheumatol.* 40 (2), 414–424. doi:10.55563/clinexprheumatol/pp0oso

Sorriento, D., Di Vaia, E., and Iaccarino, G. (2021). Physical exercise: a novel tool to protect mitochondrial health. *Front. Physiol.* 12, 660068. doi:10.3389/fphys.2021.660068

Sulaimon, L. A., Afolabi, L. O., Adisa, R. A., Ayankojo, A. G., Afolabi, M. O., Adewolu, A. M., et al. (2022). Pharmacological significance of MitoQ in ameliorating mitochondria-related diseases. *Adv. Redox Res.* 5, 100037. doi:10.1016/j.arres.2022.100037

Suzuki, N., Mori-Yoshimura, M., Yamashita, S., Nakano, S., Murata, K. Y., Mori, M., et al. (2019). The updated retrospective questionnaire study of sporadic inclusion body myositis in Japan. *Orphanet J. Rare Dis.* 14 (1), 155. doi:10.1186/s13023-019-1122-5

Taira, T., Saito, Y., Niki, T., Iguchi-Ariga, S. M., Takahashi, K., and Ariga, H. (2004). DJ-1 has a role in antioxidative stress to prevent cell death. *EMBO Rep.* 5 (2), 213–218. doi:10.1038/sj.embor.7400074

Tanboon, J., Uruha, A., Stenzel, W., and Nishino, I. (2020). Where are we moving in the classification of idiopathic inflammatory myopathies? *Curr. Opin. Neurol.* 33 (5), 590–603. doi:10.1097/wco.0000000000000855

Tawara, N., Yamashita, S., Zhang, X., Korogi, M., Zhang, Z., Doki, T., et al. (2017). Pathomechanisms of anti-cytosolic 5'-nucleotidase 1A autoantibodies in sporadic inclusion body myositis. *Ann. Neurol.* 81 (4), 512–525. doi:10.1002/ana.24919

Taylor, R. W., and Turnbull, D. M. (2005). Mitochondrial DNA mutations in human disease. *Nat. Rev. Genet.* 6 (5), 389–402. doi:10.1038/nrg1606

Terracciano, C., Nogalska, A., Engel, W. K., Wojcik, S., and Askanas, V. (2008). In inclusion-body myositis muscle fibers Parkinson-associated DJ-1 is increased and oxidized. *Free Radic. Biol. Med.* 45 (6), 773–779. doi:10.1016/j.freeradbiomed.2008.05.030

Tsamis, K. I., Boutsoras, C., Kaltsonoudis, E., Pelechas, E., Nikas, I. P., Simos, Y. V., et al. (2022). Clinical features and diagnostic tools in idiopathic inflammatory myopathies. *Crit. Rev. Clin. Lab. Sci.* 59 (4), 219–240. doi:10.1080/10408363.2021.2000584

Tsuruta, Y., Furuta, A., Taniguchi, N., Yamada, T., Kira, J., and Iwaki, T. (2002). Increased expression of manganese superoxide dismutase is associated with that of nitrotyrosine in myopathies with rimmed vacuoles. *Acta Neuropathol.* 103 (1), 59–65. doi:10.1007/s004010100428

Urbina-Varela, R., Castillo, N., Videla, L. A., and Del Campo, A. (2020). Impact of mitophagy and mitochondrial unfolded protein response as new adaptive mechanisms underlying old pathologies: sarcopenia and non-alcoholic fatty liver disease. *Int. J. Mol. Sci.* 21 (20), 7704. doi:10.3390/ijms21207704

Weihl, C. C., Baloh, R. H., Lee, Y., Chou, T. F., Pittman, S. K., Lopate, G., et al. (2015). Targeted sequencing and identification of genetic variants in sporadic inclusion body myositis. *Neuromuscul. Disord.* 25 (4), 289–296. doi:10.1016/j.nmd.2014.12.009

Winkler, M., von Landenberg, C., Kappes-Horn, K., Neudecker, S., Kornblum, C., and Reimann, J. (2021). Diagnosis and clinical development of sporadic inclusion body myositis and polymyositis with mitochondrial pathology: a single-center retrospective analysis. *J. Neuropathol. Exp. Neurol.* 80 (11), 1060–1067–1067. doi:10.1093/jnen/nlab101

Xiao, W., and Loscalzo, J. (2019). Metabolic responses to reductive stress. *Antioxidants Redox Signal.* 32 (18), 1330–1347. doi:10.1089/ars.2019.7803

Yamashita, S., Tawara, N., Zhang, Z., Nakane, S., Sugie, K., Suzuki, N., et al. (2023). Pathogenic role of anti-cN1A autoantibodies in sporadic inclusion body myositis. *J. Neurol. Neurosurg. Psychiatry* 94 (12), 1018–1024. doi:10.1136/jnnp-2023-331474

Yang, Z., Wang, Y., Zhang, Y., He, X., Zhong, C. Q., Ni, H., et al. (2018). RIP3 targets pyruvate dehydrogenase complex to increase aerobic respiration in TNF-induced necroptosis. *Nat. Cell. Biol.* 20 (2), 186–197. doi:10.1038/s41556-017-0022-y

Yu, C. H., Davidson, S., Harapas, C. R., Hilton, J. B., Mlodzianoski, M. J., Laohamonthonkul, P., et al. (2020). TDP-43 triggers mitochondrial DNA release via mPTP to activate cGAS/STING in ALS. *Cell.* 183 (3), 636–649. doi:10.1016/j.cell.2020.09.020

Zeng, R., Glaubitz, S., and Schmidt, J. (2022). Antibody therapies in autoimmune inflammatory myopathies: promising treatment options. *Neurotherapeutics* 19 (3), 911–921. doi:10.1007/s13311-022-01220-z

Zhang, Z., Zhou, H., Ouyang, X., Dong, Y., Sarapultsev, A., Luo, S., et al. (2022). Multifaceted functions of STING in human health and disease: from molecular mechanism to targeted strategy. *Signal Transduct. Target Ther.* 7 (1), 394. doi:10.1038/s41392-022-01252-z

Zhao, Y., Peng, C., Lai, R., Zhang, J., Zhang, X., and Guo, Z. (2022). The SNPs of mitochondrial DNA displacement loop region and mitochondrial DNA copy number associated with risk of polymyositis and dermatomyositis. *Sci. Rep.* 12 (1), 5903. doi:10.1038/s41598-022-09943-x

Zubair, A. S., Salam, S., Dimachkie, M. M., Machado, P. M., and Roy, B. (2023). Imaging biomarkers in the idiopathic inflammatory myopathies. *Front. Neurol.* 14, 1146015. doi:10.3389/fneur.2023.1146015

frontiers | Frontiers in Medicine

TYPE Original Research
PUBLISHED 24 June 2024
DOI 10.3389/fmed.2024.1378846

OPEN ACCESS

EDITED BY
Shoulong Deng,
Chinese Academy of Medical Sciences and Peking Union Medical College, China

REVIEWED BY
Mingming Chen,
Zhejiang University, China
Artem Kasianov,
Russian Academy of Sciences, Russia
Nima Gharahdaghi,
University of Oxford, United Kingdom

*CORRESPONDENCE
Zhong Li
✉ lzlizhong199403@163.com
Yanshi Liu
✉ liuyanshi_1990@163.com

†These authors have contributed equally to this work

RECEIVED 30 January 2024
ACCEPTED 13 June 2024
PUBLISHED 24 June 2024

CITATION
Zhong J, Yuan H, Yang J, Du Y, Li Z, Liu X, Yang H, Wang Z, Wang Z, Jiang L, Ren Z, Li H, Li Z and Liu Y (2024) Bioinformatics and system biology approach to identify potential common pathogenesis for COVID-19 infection and sarcopenia. *Front. Med.* 11:1378846. doi: 10.3389/fmed.2024.1378846

Bioinformatics and system biology approach to identify potential common pathogenesis for COVID-19 infection and sarcopenia

Jun Zhong[1†], Hui Yuan[1†], Jinghong Yang[1], Yimin Du[1], Zheng Li[2], Xu Liu[1], Haibo Yang[1], Zhaojun Wang[1], Zi Wang[1], Lujun Jiang[1], Zhiqiang Ren[1], Hongliang Li[1], Zhong Li[2]* and Yanshi Liu[2]*

[1]School of Clinical Medicine, Southwest Medical University, Luzhou, Sichuan, China, [2]Department of Orthopedics, Affiliated Hospital of Southwest Medical University, Luzhou, Sichuan, China

Sarcopenia is a condition characterized by age-related loss of muscle mass and strength. Increasing evidence suggests that patients with sarcopenia have higher rates of coronavirus 2019 (COVID-19) infection and poorer post-infection outcomes. However, the exact mechanism and connections between the two is unknown. In this study, we used high-throughput data from the GEO database for sarcopenia (GSE111016) and COVID-19 (GSE171110) to identify common differentially expressed genes (DEGs). We conducted GO and KEGG pathway analyses, as well as PPI network analysis on these DEGs. Using seven algorithms from the Cytoscape plug-in cytoHubba, we identified 15 common hub genes. Further analyses included enrichment, PPI interaction, TF-gene and miRNA-gene regulatory networks, gene-disease associations, and drug prediction. Additionally, we evaluated immune cell infiltration with CIBERSORT and assessed the diagnostic accuracy of hub genes for sarcopenia and COVID-19 using ROC curves. In total, we identified 66 DEGs (34 up-regulated and 32 down-regulated) and 15 hub genes associated with sarcopenia and COVID-19. GO and KEGG analyses revealed functions and pathways between the two diseases. TF-genes and TF-miRNA regulatory network suggest that FOXOC1 and hsa-mir-155-5p may be identified as key regulators, while gene-disease analysis showed strong correlations with hub genes in schizophrenia and bipolar disorder. Immune infiltration showed a correlation between the degree of immune infiltration and the level of infiltration of different immune cell subpopulations of hub genes in different datasets. The ROC curves for ALDH1L2 and KLF5 genes demonstrated their potential as diagnostic markers for both sarcopenia and COVID-19. This study suggests that sarcopenia and COVID-19 may share pathogenic pathways, and these pathways and hub genes offer new targets and strategies for early diagnosis, effective treatment, and tailored therapies for sarcopenia patients with COVID-19.

KEYWORDS

sarcopenia, COVID-19, bioinformatics, pathogenesis, biomarkers

Introduction

Sarcopenia is a progressive and systemic disease of extreme skeletal muscle dysfunction (1) characterized by reduced muscle mass/quantity and muscle strength that is observed in both physiological and pathological processes (2, 3). According to the most recent guidelines from the European Working Group on Sarcopenia in the Elderly (EWGSOP), the primary diagnostic criteria for sarcopenia have shifted to include diminished muscle strength and function, rather than solely the loss of muscle mass. Additionally, impaired physical performance is now recognized as a key marker of advanced sarcopenia (4, 5). Studies have shown that sarcopenia occurs with age and the effects of many long-term conditions (2, 5), and is associated with decreased mobility, increased morbidity and increased mortality (6). Currently, sarcopenia affects over 50 million people and this number is expected to reach 500 million by 2050 (7, 8). Sarcopenia is estimated to affect 10–16% of older adults worldwide (9). One study reported that the prevalence of sarcopenia patients (EWGSOP definition) ranged from 8 to 36% in those aged <60 years and from 10 to 27% in those aged ≥60 years (10). The pathogenesis of sarcopenia is complex, with high morbidity and mortality, and it is currently believed that the pathogenesis of sarcopenia may be related to factors such as reduced satellite cell numbers and aging (11, 12), mitochondrial dysfunction (13), loss of motor neurons, decreased activity of neuromuscular junctions (14), endocrine alterations (15), and weight loss with decreased appetite (16), or a combination of these factors (17).

COVID-19 is a multi-organ infectious disease caused by Severe Acute Respiratory Syndrome Coronavirus 2 (SARSCoV-2), particularly severe pneumonia and acute respiratory distress syndrome (18). As of September 7, 2023, the World Health Organization reported 770,437,327 confirmed cases, including 6,956,900 deaths.[1] COVID-19 can pose a serious health burden individuals, especially the elderly and those with underlying medical conditions such as advanced age (19), chronic kidney disease, diabetes mellitus, hypertension (20), and cancer (21, 22) are risk factors that have been widely documented to be responsible for COVID-19 infections and deaths. COVID-19 is characterized by severe inflammation and a highly muscle catabolic state, which affects the body's metabolic stress and profound changes in body composition. Researchers have attempted to prevent and treat COVID-19 by investigating drugs and developing vaccines, but its intervention in adverse body states (e.g., sarcopenia) may facilitate the treatment of COVID-19 (23, 24).

A study indicated that patients with sarcopenia experienced a higher prevalence of infection and poorer prognosis during the COVID-19 pandemic (23). Patients with sarcopenia have impaired immune cells (e.g., peripheral monocytes, neutrophils, and natural killer lymphocytes) (25), which result in the production of aberrant myofactors such as IL-6, IL-7, IL-15, or LIF (26), which ultimately lead to muscle catabolism and immune senescence (24, 25). However, the onset and progression of sarcopenia is accelerated during COVID-19 infection due to increased muscle atrophy and inhibition of muscle synthesis caused by severe inflammatory response and metabolic stress (27), decreased physical activity and inadequate nutrient intake (28). Hospitalization, protein deficiency, and corticosteroid therapy during COVID-19 infection have been reported in several studies that often lead to the rapid progression of sarcopenia in patients with severe COVID-19 infection (29, 30). Skeletal muscle regulates immune system function through myokine signaling and expression of immunoregulatory surface molecules. Immune cells in turn severely affect muscle mass and function (25). This indicates that the interaction between sarcopenia and COVID-19 may be bidirectional, potentially creating a vicious cycle.

An increasing number of studies indicate a strong relationship between sarcopenia and COVID-19 infection; however, the mechanisms have not been fully elucidated. This study utilizes bioinformatics, R software, and several large databases to analyze the common DEGs and hub genes of sarcopenia and COVID-19 in terms of expression differences, functional enrichment, regulatory networks, disease drug prediction, and immune infiltration. This analysis will help further understand the potential co-pathogenesis of sarcopenia and COVID-19 and to screen for biomarkers and drug candidates.

Materials and methods

Data collection

RNA-seq data for patients with sarcopenia (GSE111016) and COVID-19 infections (GSE171110) were obtained from the GEO database.[2] GEO is one of the largest public database that includes microarray data and high-throughput gene expression data submitted by research institutions around the world (31). Both datasets used the GPL 16791 (Illumina NextSeq 500) high-throughput sequencing platform to extract RNA sequences. The GSE111016 dataset includes 20 muscle biopsies from healthy testers and 20 muscle biopsies from patients with sarcopenia (32). The GSE171110 dataset includes 44 COVID- 19 patients and 10 healthy donors with whole blood gene expression profiling data (33).

Identification of common DEGs between sarcopenia and COVID-19

The "limma" package (version 4.3.1) of the R software (version 4.3.1) was used to select DEGs between COVID-19 and non-COVID-19 and between sarcopenia and non-sarcopenia. Because of the differences in sample size and data quality, different difference multiples criteria were selected to ensure statistical significance and biological relevance of the results. In the sarcopenia dataset, genes with $p < 0.05$ and a fold change >1.2 were identified as DEGs; for COVID-19, genes with $p < 0.05$ and a fold change >2 were identified as DEGs. In the sarcopenia dataset, the DEG of $\log_2$FC<−0.263 was considered down-regulated, whereas $\log_2$FC>0.263 was considered up-regulated. For COVID-19, the DEG of $\log_2$FC<−1 was considered

1 https://covid19.who.int/

2 https://www.ncbi.nlm.nih.gov/geo/

down-regulated, whereas $\log_2$FC>1 was considered up-regulated. The "Pheatmap" (version 1.0.12), "EnhancedVolcano" and "ggplot2" packages of the R software were applied to generate the heatmaps and volcano maps. Common DEGs for GSE111016 and GSE171110 were then obtained using the online VENN analysis tool.[3]

Enrichment analysis of gene ontology and pathways

EnrichrR[4] is a comprehensive resource for analyzing gene sets generated from genome-wide experiments, containing a total of 180,184 annotated gene sets from 102 gene set libraries (34). GO and pathway enrichment analyses were performed using EnrichR online tools [the Kyoto Encyclopedia of Genes and Genomes (KEGG)] to specify shared functions and pathways between sarcopenia and COVID-19. The GO terminology consists of three categories: biological process (BP), cellular component (CC), and molecular function (MF). A p-values <0.05 was considered significantly enriched.

PPI network construction

STRING[5] (version 12.0) is a database for studying protein–protein association networks, with an expanded information coverage of more than 12,535 species, 59.3 million proteins, and 20 billion interactions, integrating experimental interaction evidence and computational interaction prediction information, with the goal of realizing a comprehensive and objective global network (35). We performed PPI network analysis of the common DEG using the STRING database to construct differentially expressed and potential interactions of genes with interaction scores >0.15. The protein–protein interaction networks constructed in the String database were then imported into Cytoscape (version: 3.9.1) software for visualization (36, 37).

Identification and analysis of hub genes

In a PPI consisting of nodes, edges and their connections, the most entangled nodes were considered hub gene. Cytohubba[6] is a novel plugin for Cytoscape that provides 11 topological analysis methods to rank nodes in a network (38). We applied seven algorithms (Closeness, MCC, Degree, MNC, Radality, Stress and EPC) to finally intersect them to select hub gene.

GeneMANIA[7] is a flexible and user-friendly website that uses large amounts of genomics and proteomics data to generate hypotheses about gene function, analyze gene lists and prioritize genes for functional analysis (39). We used it to construct co-expression networks of identified central genes.

Construction of TF-gene and miRNA-gene regulatory network

TFs are proteins that control the transcription of DNA into RNA by attaching to specific DNA sequences. miRNAs are mainly involved in the regulation of protein expression by binding to target sites on mRNA transcripts and inhibiting their translation, making them essential for regulating biomolecules (40, 41). We visualized the co-regulatory network of hub genes through the NetworkAnalyst platform, which has been widely used as a bioinformatics tool (42). We used NetworkAnalyst to extract microRNAs interacting with hub genes from the miRTarBase database (43) and construct a DEG-microRNA (miRNA) interaction network, and then localized TFs binding to hub genes through the JASPAR database (44) and constructed a DEG-transcription factor interaction network. We performed GRN analysis using hub-DEG to reveal transcription elements and miRNAs that regulate DEG at the post-transcriptional level.

Gene-disease association analysis

DisGeNET is a comprehensive knowledge management platform that integrates and normalizes data on disease-associated genes and variants from multiple sources, including the scientific literature, and can be used to study the molecular basis of specific human diseases and their complications, to analyze the characterization of disease genes and to validate the performance of computationally predicted disease genes (45). It currently covers more than 24,000 diseases and traits, 17,000 genes and 117,000 genomic variants (46). We examined gene-disease relationships using the DisGeNET database through NetworkAnalyst to reveal diseases and their complications associated with central genes.

Correlation analysis of hub gene expression with immune infiltration

To explore the immune infiltration of multiple immune cells including T cells, B cells, NK cells, monocytes, macrophages, neutrophils, and dendritic cells in GSE111016 and GSE171110 peripheral blood (47), single-sample gene set enrichment analysis (ssGSEA) (48) of 28 immune gene sets was performed using the "GSVA" R package, assessing the immunological characteristics of the samples. The Vioplot and pheatmap R packages were used for visualization. Finally, the Pearson correlation coefficient determined the correlation between hub genes and different immune infiltrating cells, visualized through the ggplot2 package.

Target drugs analysis

The DSigDB database is a new gene set resource that links drugs/compounds to their target genes. It currently has 22,527 gene sets

3 http://jvenn.toulouse.inra.fr/app/example.html
4 https://maayanlab.cloud/Enrichr/
5 http://string-db.org
6 http://apps.cytoscape.org/apps/cytohubba
7 https://genemania.org

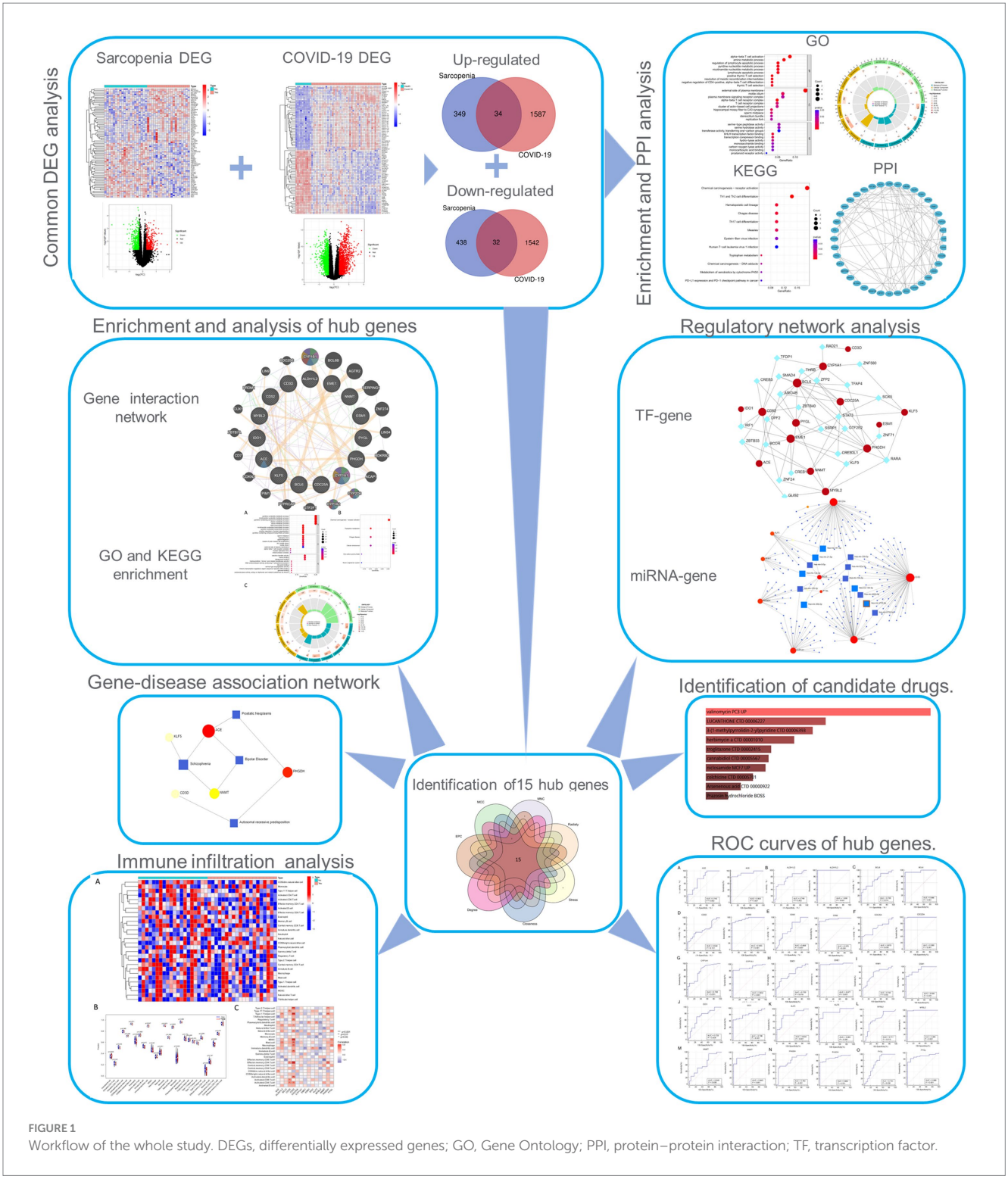

FIGURE 1
Workflow of the whole study. DEGs, differentially expressed genes; GO, Gene Ontology; PPI, protein–protein interaction; TF, transcription factor.

consisting of 17,389 unique compounds, covering 19,531 genes (49). We detected 15 drug molecules identified based on hub genes from the DSigDB database on the Enrichr[8] platform. These drugs represent possible common drugs used for sarcopenia and COVID-19.

ROC curves of hub genes

The receiver operating characteristic (ROC) curve is a useful tool for evaluating classifiers in biomedical and bioinformatics applications. In

8 https://amp.Pharm.mssm.Edu/Enrichr./

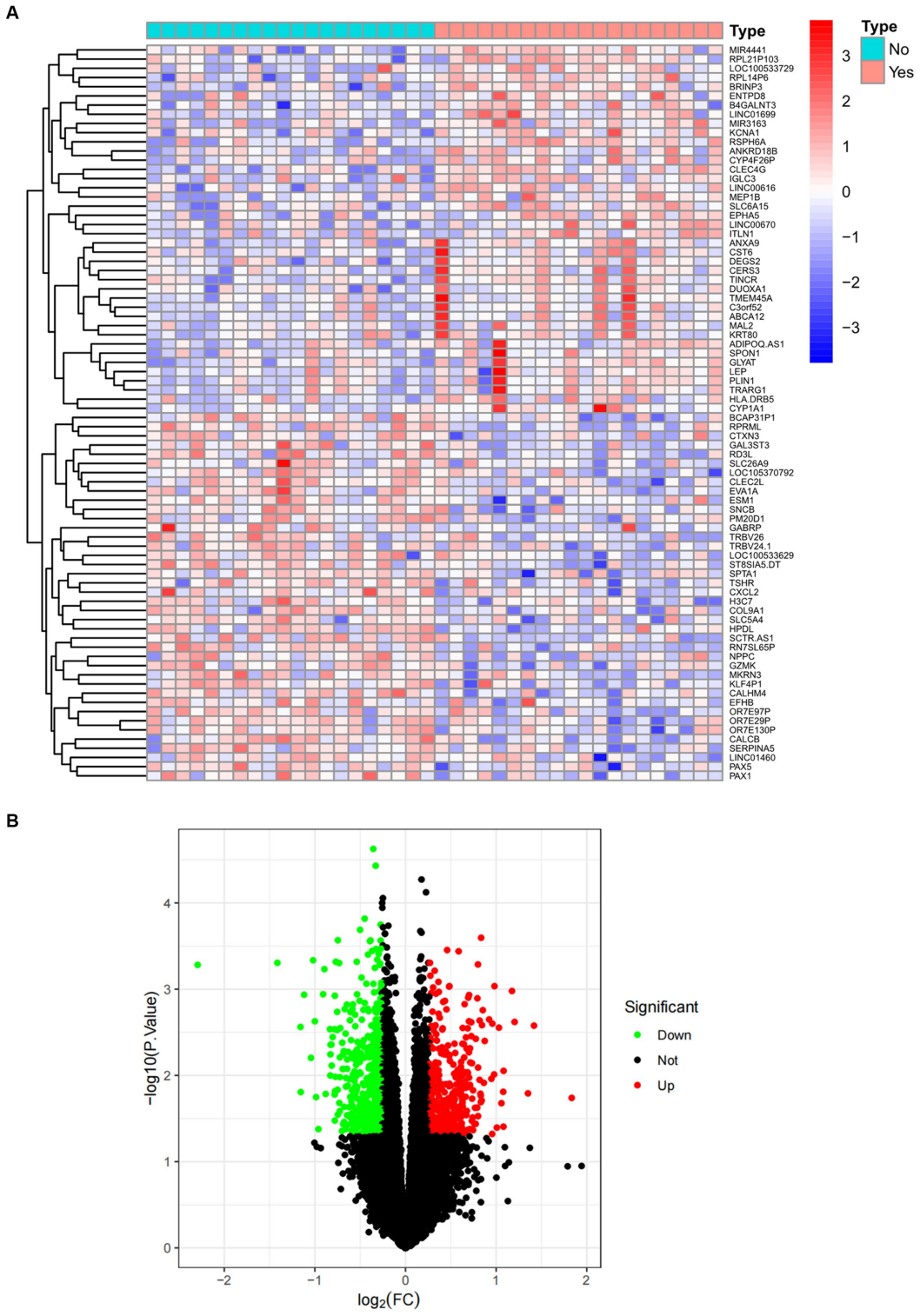

FIGURE 2
Expression characteristics of DEG in sarcopenia. **(A)** Heat map and **(B)** volcano plot present the DEGs identified between sarcopenia patients and normal controls ($|log_2FC|>0.263$ defined as the screening criterion to obtain DEGs in sarcopenia). Blue color indicates low expression values and red color indicates high expression values.

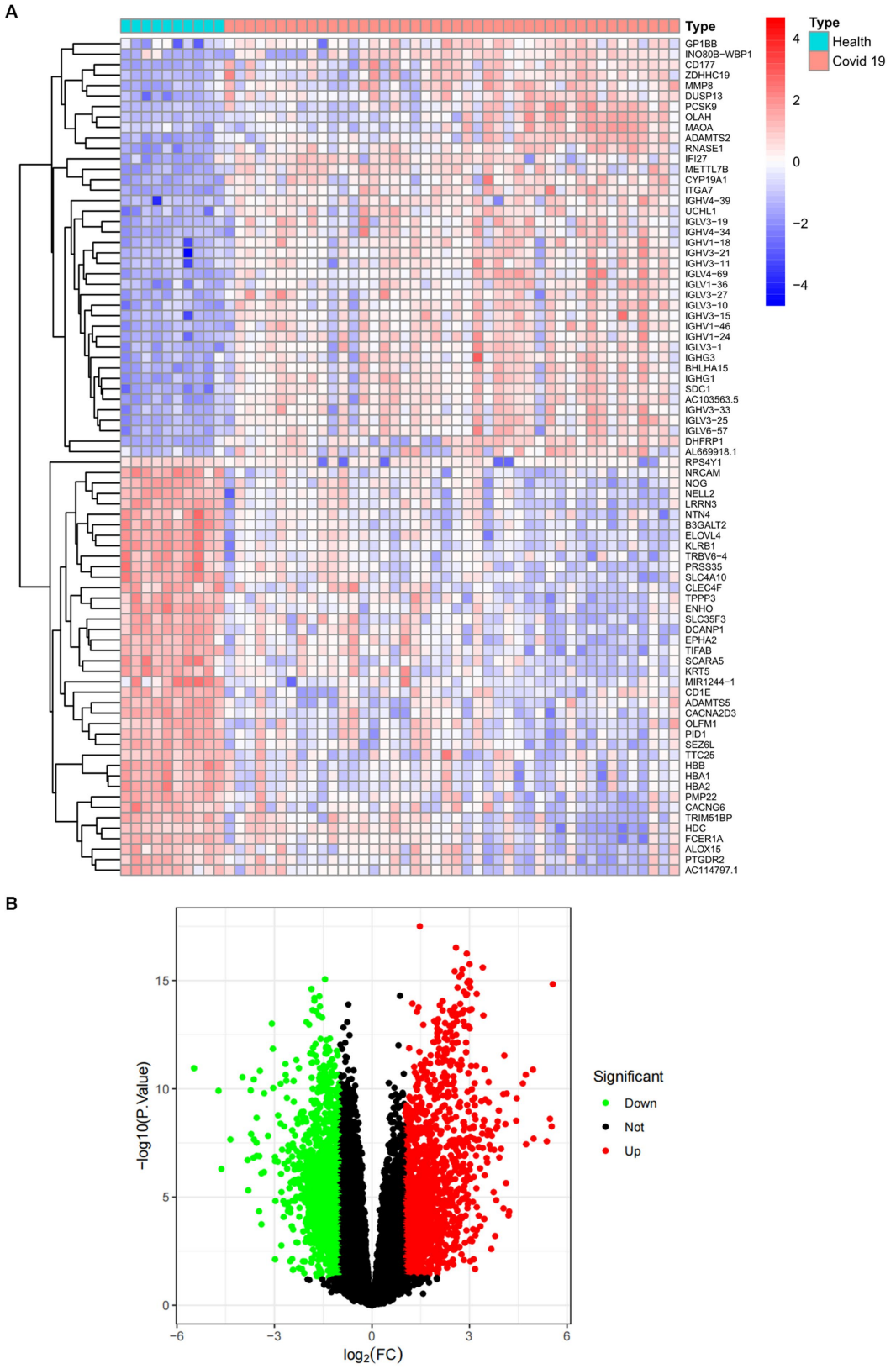

FIGURE 3
Expression characteristics of DEGs in COVID-19 patients. **(A)** Heat map and **(B)** volcano plot present the DEGs identified between COVID-19 patients and normal controls ($|\log_2 FC|>1.0$ is defined as a screening criterion to obtain a DEG for COVID-19). Blue indicates a low expression value and red indicates high expression value.

this study, R was established by "pROC" based on the expression profile data of hub genes (50). The area under the ROC curve (AUC) was used to evaluate the diagnostic value of candidate hub genes separately.

Results

Identification of DEGs and shared genes between sarcopenia and diabetes

The overall flowchart of this study is shown in Figure 1A. A total of 853 differential genes (DEGs) were identified based on the sarcopenia dataset GSE111016 using the limma R software package, of which 383 were upregulated and 470 were downregulated. The heatmap plot shows the identified DEGs (Figure 2A), and the heat map shows the distribution of the top 25 DEGs for up- and down-regulation in sarcopenia patients and non-sarcopenia patients, respectively (Figure 2B). In addition, a total of 3,195 DEGs were obtained from the COVID-19 dataset GSE171110, of which 1,621 genes were up-regulated and 1,574 genes were down-regulated. The top 25 DEG heat maps of up- and down-regulation and the volcano map of DEG are shown in Figures 3A,B. The intersection of DEGs from the GSE111016 and GSE171110 datasets was visualized by a Wayne's diagram. In total, 34 common up-regulated DEGs and 32 common down-regulated DEGs are shown (Figures 4A,B).

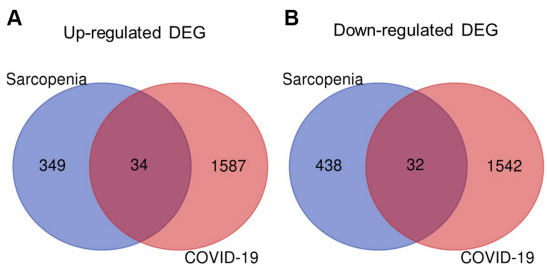

FIGURE 4
Identification of shared DEGs between sarcopenia and COVID-19. Venn diagram showing two datasets owning **(A)** 34 common up-regulated DEGs and **(B)** 32 common down-regulated DEGs.

Gene ontology and pathway enrichment analysis

Enrichment analysis aids in further understanding the biological functions of genes shared between COVID-19 and sarcopenia patients. By analyzing Gene Ontology (GO) and the Kyoto Encyclopedia of Genes and Genomes (KEGG), we predicted the functions of DEGs and their common differential genes in COVID-19 and sarcopenia. GO analysis predicted gene functions in three categories: biological processes, cellular components, and molecular functions. Results indicated that key biological processes include alpha-beta T cell activation, amine metabolic processes, and the regulation of lymphocyte apoptotic processes. Primary cellular components involved are the alpha-beta T cell receptor complex, the external side of the plasma membrane, and the hippocampal mossy fiber to CA3 synapse. Predominant molecular functions include binding of bHLH transcription factors, transcription corepressor binding, and hydro-lyase activity (Figure 5; Supplementary Figure S2).

The enrichment pathways of common DEGs between COVID-19 and sarcopenia were collected from the KEGG database and visualized in Figure 6. KEGG enrichment analysis showed that common genes were mostly enriched in the Th1 and Th2 cell differentiation, chemical carcinogenesis – receptor activation, and hematopoietic cell lineage pathways (Figure 6).

PPI network analysis

We utilized the STRING database to construct a Protein–Protein Interaction (PPI) network analysis of the shared genes, aiming to

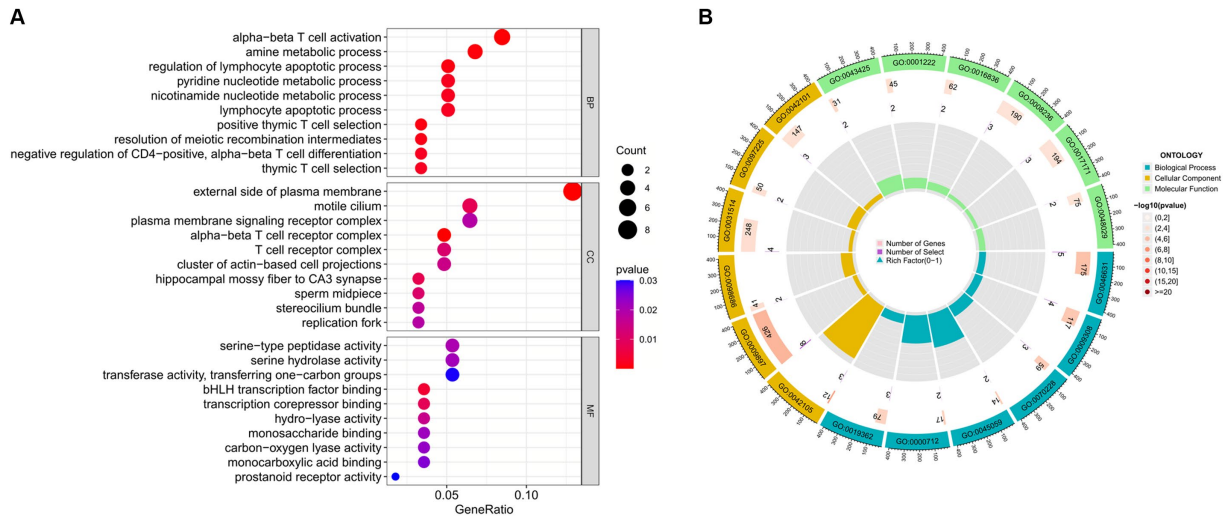

FIGURE 5
GO functional enrichment analysis of common genes between sarcopenia and COVID-19. **(A)** Bubble plot showing enriched GO terms. **(B)** Circle plots showing enriched GO terms. Results are shown by –log 10 (*p*-value).

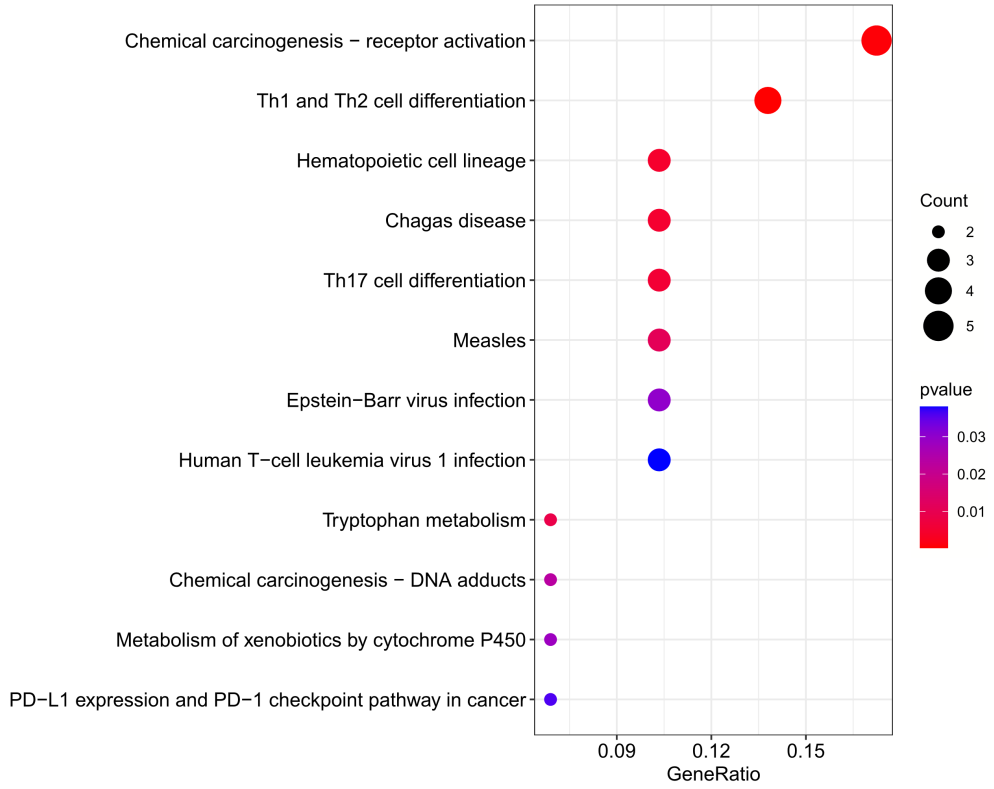

FIGURE 6
Functional enrichment analysis of the common gene KEGG between sarcopenia and COVID-19. Results are shown as −log 10 (*p* value).

predict interactions and adhesion pathways among common DEGs. The network was then imported into Cytoscape for visualization to explore their potential interactions. As expected (Supplementary Figure S3), the PPI network of shared DEGs comprises 40 nodes and 82 edges, and it was subsequently used in subsequent steps for identifying hub genes and detecting drug molecules for both COVID-19 and sarcopenia.

Identification of hub genes

From the PPI network in CytoHubba, a plugin for Cytoscape software, we selected the top 23 hub genes using seven algorithms. Through intersection using a Venn diagram, we ultimately identified 15 common hub genes, including ACE, ALDH1L, CYP1A1, PYGL, KLF5, NNMT, PHGDH, IDO1, EME1, CD52, MYBL2, CDC25A, BCL6, CD3D, and ESM1 (Figure 7). These hub genes may be potential biomarkers and common molecular mechanisms of pathogenesis in patients with sarcopenia and COVID-19, which may guide new therapeutic strategies for disease research.

Functional enrichment analysis of hub genes

Based on GeneMANIA database, we constructed an interaction network of common hub genes and their related genes to decipher the biological functions and predictive values of these hub genes, with Co-expression of 65.97%, Co-localization of 19.71%, Predicted of 12.57%, and Genetic Interactions was 1.75%. The GeneMANIA results also indicated that the functions of common hub genes and their related genes (CYP1B1, BCL6B, AGTR2, SERPING1, ZNF274 LIN54, BDKRB2, ACAP1, CYP2D6, etc.) were mainly related to the metabolic process of retinoids, steroid hydroxylase activity, protol metabolic processes, hormone metabolic processes, long-chain fatty acid metabolic processes, cytokinetic hormone metabolic processes, and monooxygenase activity (Figure 8).

To further explore the biological functions and signaling pathways associated with the hub genes involved in sarcopenia and COVID-19, we performed gene ontology (GO) and Kyoto Encyclopedia of Genes and Genomes (KEGG) analyses. GO analysis predicted the functional roles of the genes in terms of biological processes, cellular components and molecular functions, and the results showed (Figures 9A,C) that hub genes were enriched in several biological processes (BP), including pyridine nucleotide metabolism, nicotinamide nucleotide metabolism, pyridine compounds metabolism, vitamins metabolism, amine metabolism, and NAD biosynthesis; with regard to cellular component (CC), hub genes are mainly associated with sperm midpiece, replication fork, sperm flagellum, actin-based cell protrusion, active cilia, and T cell receptor complex. In MF it mainly includes electron transfer activity, heme binding, tetrapyrrole binding, hydroxymethyl-formyl- and related transferase activity, DNA endonuclease activity and bile acid binding. As shown in Figures 6, 9B KEGG pathways were significantly associated with sarcopenia and COVID-19 common

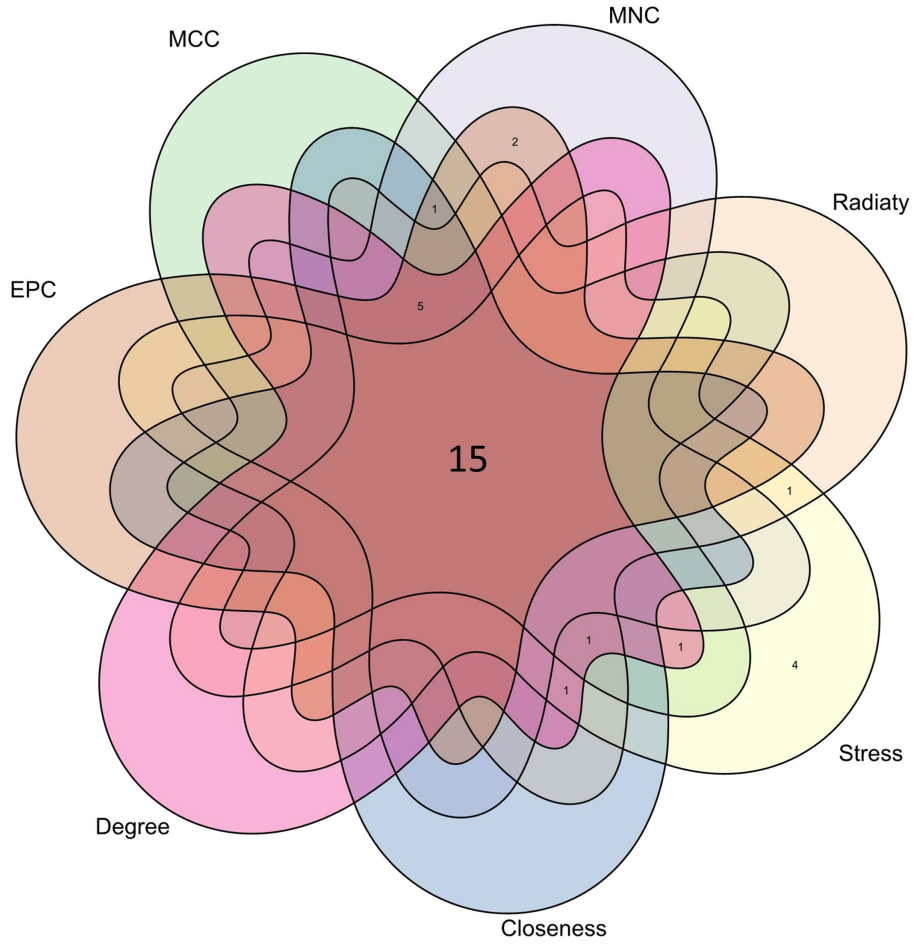

FIGURE 7
The Venn diagram shows that 7 algorithms screen out 15 overlapping hub genes.

hub genes: chemical oncogenic-receptor activation of tryptophan metabolism, Chagas disease, cellular senescence, One carbon pool by folate, and renin-angiotensin system.

Determination of regulatory signatures

The NetworkAnalyst network tool was used to predict and generate TF and miRNAs separately for 15 hub genes, and to construct TF-gene and miRNA-gene interaction network. The TF-gene network (Figure 10) contained 63 nodes, 140 edges and 15 genes. Among them, BCL6, ACE and EME1 genes were regulated by 17, 16 and 14 TF genes, respectively, and the transcription factor FOXC1 was closely associated with 10 genes (CYP1A1, KLF5, NNMT, PHGDH, EME1, CD52, CDC25A, BCL6, CD3D, ESM1), and these transcription factors may be important molecules that regulate the expression levels of related genes at the same time.

Finally, we explored the upstream miRNAs that may regulate the expression levels of these genes and constructed the regulatory network of these 15 genes and all miRNAs (Figure 11), with a total of 231 nodes, 242 edges and 12 genes. The results showed that the miRNA (hsa-mir-155-5p) was associated with four genes (CYP1A1, PHGDH, BCL6, PYGL) at the same time, while has-mir-21-5p, has-mir-92a-3p and has-mir-10a-5p were associated with three genes at the same time. In the future, we can intervene in the expression of these upstream to affect their downstream genes to further study and control the disease progression.

Identification of disease association

In some cases, different diseases can be linked or related, such as when they share one or more similar genes. Therapeutic design strategies for diseases open the door to revealing the relationship between genes and diseases. Through Networkanalyst's analysis of gene-disease associations, we found that schizophrenia, bipolar disorder, prostate tumors, and autosomal recessive susceptibility were most associated with our hub genes. The gene-disease associations are shown in Figure 12.

Immune cell infiltration and correlation analysis

To explore the relationship between the immune system and the co-occurrence of sarcopenia and COVID-19, immune infiltration

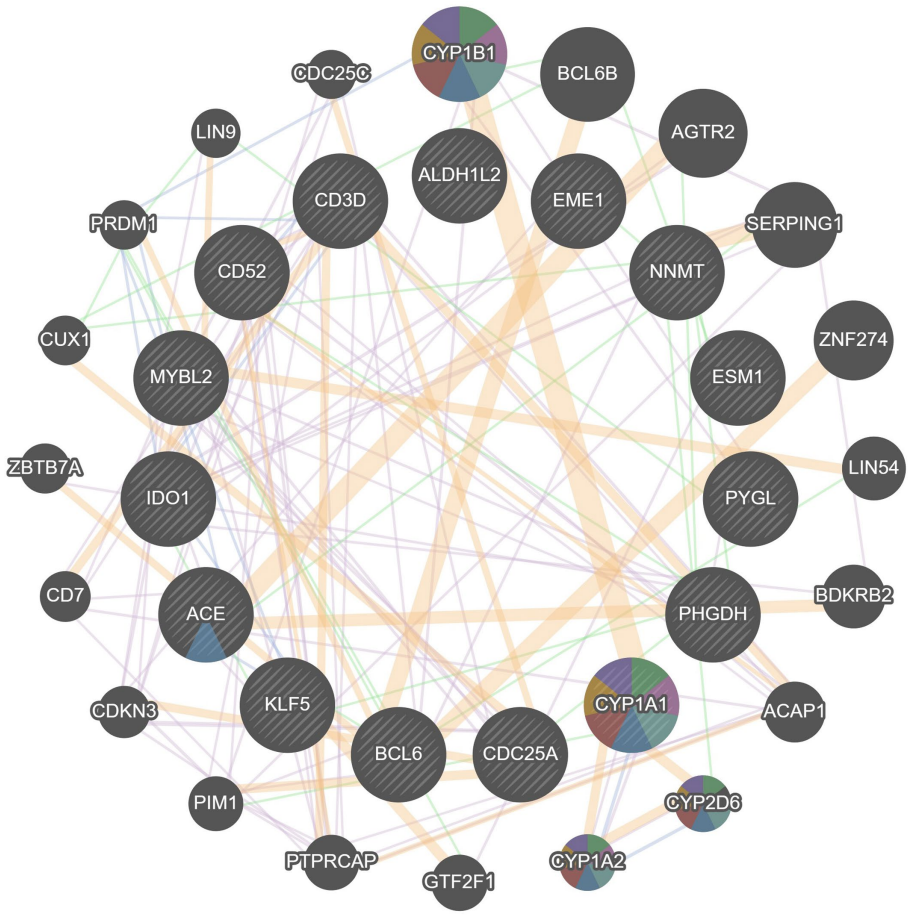

FIGURE 8
Analyze hub genes and their co-expressed genes by GeneMANIA.

analysis was performed on the sarcopenia and COVID-19 datasets. Figures A and B show the degree of infiltration of different immune cells in the sarcopenia dataset. The relationship between common key genes and immune cells was analyzed and visualized in Figure 13C. The sarcopenia group had lower expression scores of Activated.CD8.T.cell ($p = 0.018$) and Type.17.T.helper.cell ($p = 0.015$) compared to healthy controls, however, the proportion of other immune cell subsets did not differ significantly between the two groups. Subsequently, we evaluated the correlation between the expression of common hub genes and the level of infiltration of different cell subpopulations, and showed that CD52 had a strong positive correlation with Type.2.T.helper.cell, Type.1.T.helper.cell, MDSC, and Effector.memory.CD4.T.cell cells ($p < 0.0001$), whereas PHGDH had a strong correlation with Effector.memory.CD4.T.cell and Type.1.T.helper.cell cells ($p < 0.001$). In contrast, MYBL2 was negatively correlated with Plasmacytoid.dendritic.cell, Monocyte and Immature.dendritic.cell ($p < 0.01$). Similarly, the immunoinfiltration results of the COVID-19 dataset are shown in Supplementary Figure S1.

Identification of candidate drugs

Ten potential therapeutic small molecule drugs were identified using Enrichr based on transcriptional characterization of the DSigDB database, which represent possible common drugs used for sarcopenia and COVID-19. The results of potential small molecules were generated based on their *p*-values to indicate the proximity between the small molecule and the gene. Figure 14 show the top 10 enriched drugs (valinomycin PC3 UP, LUCANTHONE CTD 00006227, 3-(1-methylpyrrolidin-2-yl) pyridine CTD 00006393, herbimycin a CTD 00001010, troglitazone CTD 00002415, cannabidiol CTD 00005567, niclosamide MCF7 UP, colchicine CTD 00005701, Arsenenous acid CTD 00000922, Prazosin hydrochloride BOSS).

ROC curves of hub genes

ROC curves were plotted to assess the diagnostic efficacy of 15 key genes (Figure 15). ACE (AUC: 0.923), CYP1A1 (AUC: 0.902), EME1 (AUC: 0.977), CD52 (AUC: 0.970), MYBL2 (AUC: 0.995), CDC25A (AUC: 0.998), BCL6 (AUC: 0.966) and CD3D (AUC: 0.955) showed relatively good diagnostic efficiency in distinguishing COVID-19 patients from healthy controls. While in the sarcopenia dataset, ACE (AUC: 0.742), ALDH1L2 (AUC: 0.748), CYP1A1 (AUC: 0.765), PYGL (AUC: 0.73), KLF5 (AUC: 0.803), PHGDH (AUC: 0.76), IDO1 (AUC: 0.72), EME1 (AUC: 0.703), MYBL2 (AUC: 0.711), BCL6 (AUC: 0.705), and ESM1 (AUC: 0.746) demonstrated better diagnostic performance for distinguishing sarcopenia from healthy individuals.

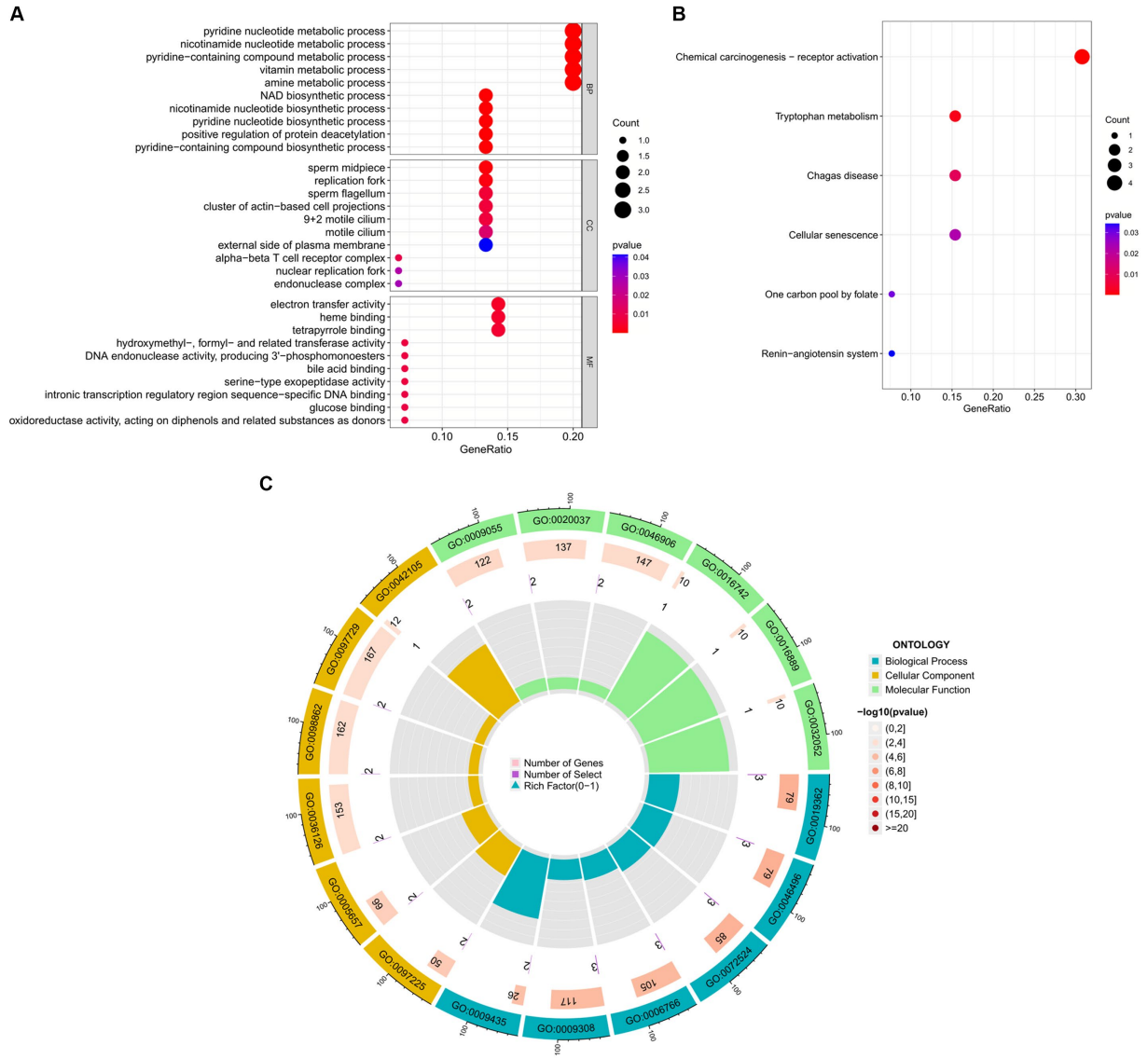

FIGURE 9
Functional enrichment analysis of Hub gene. **(A)** Bubble plot of gene ontology (GO) enrichment analysis of the Hub gene, including biological process (BP), cellular component (CC), and molecular function (MF). **(B)** Bubble plot of enrichment analysis of hub genes by the Kyoto Encyclopedia of Genes and Genomics (KEGG). **(C)** Circle plot of GO enrichment analysis.

Specifically, ALDH1L2 (AUC: 1) showed the best diagnostic efficiency for differentiation in the COVID-19 dataset, whereas KLF5 (AUC: 0.803) demonstrated the best discriminatory ability in the sarcopenia dataset.

Discussion

There is evidence that patients with sarcopenia have a higher prevalence and worse prognosis after COVID-19 infection (23). COVID-19 infection can cause pathologic changes in multiple organs, including the musculoskeletal system (51), which may be associated with certain mechanisms of inflammation, immune response, and metabolic stress (52). Therefore, we sought to explore the common functions and pathways between COVID-19 and sarcopenia and to determine the interrelationship between COVID-19 and sarcopenaia. In this study, 66 common DEGs and 15 key genes (ACE, ALDH1L, CYP1A1, PYGL, KLF5, NNMT, PHGDH, IDO1, EME1, CD52, MYBL2, CDC25A, BCL6, CD3D, and ESM1) have been identified.

Four of these genes (ACE, KLF5, IDO1, and CDC25A) have been reported to be associated with the pathological mechanisms of COVID-19 and sarcopenia. Angiotensin-converting enzyme (ACE) is a chloride- and zinc-dependent peptidyl-carboxypeptidase that hydrolyzes AngI (angiotensin I) to AngII and serves as a biologically active component of the renin-angiotensin system (RAS) and the kinin-releasing enzyme-kinin system (KKS) (53, 54). ACE has been a drug target for screening against cardiovascular diseases such as hypertension and heart failure (55), and inhibition of ACE activity can prevents mitochondrial decline, improves endothelial function and muscle metabolism, and thus plays an important role in water-electrolyte homeostasis, blood pressure regulation, cardiovascular system development and vascular remodeling (53, 56). Meanwhile, it

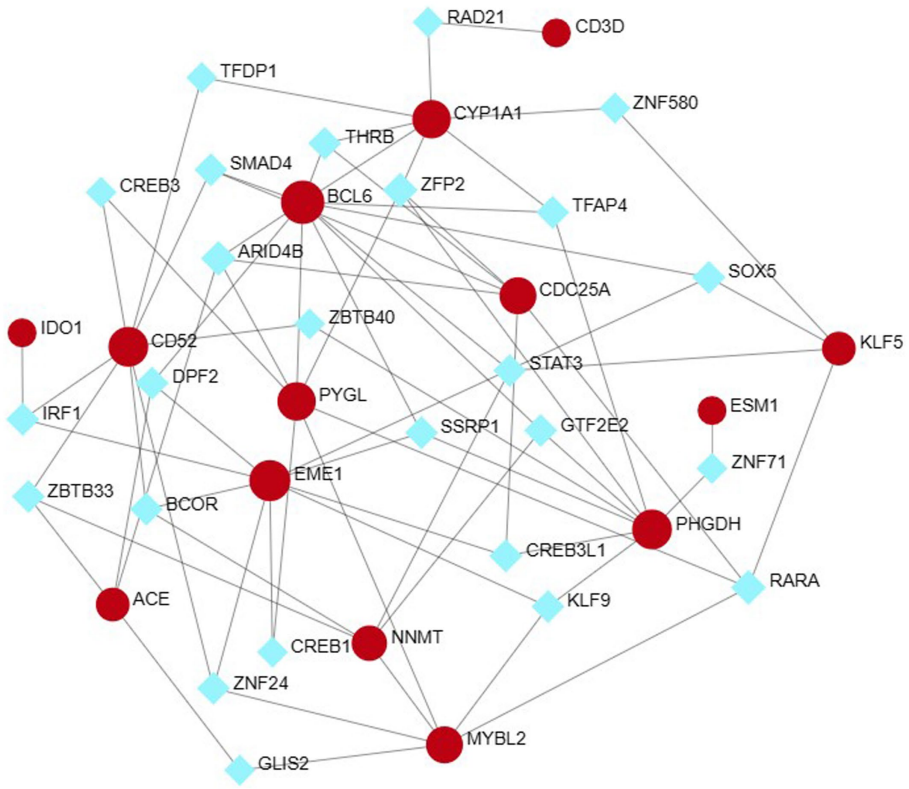

FIGURE 10
Hub-TF gene regulatory interaction network. Square nodes represent TF and round nodes represent genes.

has been reported that SARS-CoV-2 virus has a strong affinity for angiotensin-converting enzyme-2 (ACE2) receptor (57). The coronavirus type 2 spiking proteins bind to cells via angiotensin-converting enzyme 2 (ACE2) receptors, leading to fusion of the viral envelope with the cell membrane and allowing viral genetic material to enter the cell where ACE2 receptors are prevalent throughout the body, leading to a wide range of tissue damage (58). KLF5 is a key zinc finger transcriptional regulator mediating muscle atrophy and is upregulated in atrophied myotubes (59, 60). It can play a key role in the development of muscle atrophy *in vitro* and *in vivo* by controlling lipid metabolism in mature skeletal muscle (61) and regulating muscle differentiation in adult myoblasts (62). It has been reported that KLF5 can also physically interacts with the transcription factor Foxo1 and cooperates with it to control the transcription of Fbxo32 (63). IDO1 (indoleamine-2,3-dioxygenase) is a cofactor-binding, redox-sensitive protein that converts tryptophan to kynurenine (Kyn) (64). Some studies have reported that inflammatory cytokines such as interferon-gamma induce IDO1 production, which leads to catabolism to produce kynurenine. Kyn levels increase with age, which can lead to muscle atrophy and bone marrow stem cells aging, and are closely associated with diseases such as sarcopenia and osteoporosis (65). Meanwhile, IDO1, as an immunomodulatory enzyme that enhances cellular immune escape, has also been significantly associated with inflammatory neointima formation (66). Coronaviruses (CoV) can activate AhR and establish infection through the IDO1-kynurenine-AhR signaling pathway (67). Recent histologic studies have shown that indoleamine 2,3-dioxygenase (IDO) is differentially expressed in the pulmonary vasculature in patients with COVID-19, and that IDO1 is predominantly present in lung tissues of patients with early/mild pneumonitis and those suffering from prolonged pneumonia (68). CDC25A (Cell Division Cycle-25A) plays a crucial role in the cell cycle and apoptosis by dephosphorylating its substrates (69). mRNA expression of CDC25A has been reported to be down-regulated in aging skeletal muscle (70) and up-regulated in COVID-19 (71). In COVID-19, CDC25A has been found to be closely associated with immune cell infiltration such as plasma cells, macrophages, T cells, dendritic cells and NK cells, and plays an important role in disease progression as a biomarker for COVID-19 diagnosis (71, 72). It has been demonstrated that MYBL2 and BCL6 are significantly upregulated in SARS-CoV-2 infected patients (73, 74). CYP1A1 is a key enzyme mediating the metabolism of broad-spectrum xenobiotics and endogenous elements, and is expressed predominantly in the peripheral airway epithelium (75). CYP1A1 has been extensively studied in pneumonia, and an association between CYP1A1 polymorphisms and the risk of pneumonia has been reported (76). The role of the remaining eight key genes (ALDH1L, EME1, PYGL, NNMT, PHGDH, CD52, CD3D, and ESM1) in COVID-19 and sarcopenia has been less studied, emphasizing their importance in future research.

In our study, GO enrichment analysis revealed that these hub genes are mainly associated with biological processes involved in energy and nucleotide metabolism. This is consistent with earlier studies that dysfunctional mitochondria play a key role in the progression of sarcopenia (77), associated with decreased respiration and increased oxidative stress (78). KEGG analysis suggests that chemical oncogenic-receptor activation and tryptophan metabolic

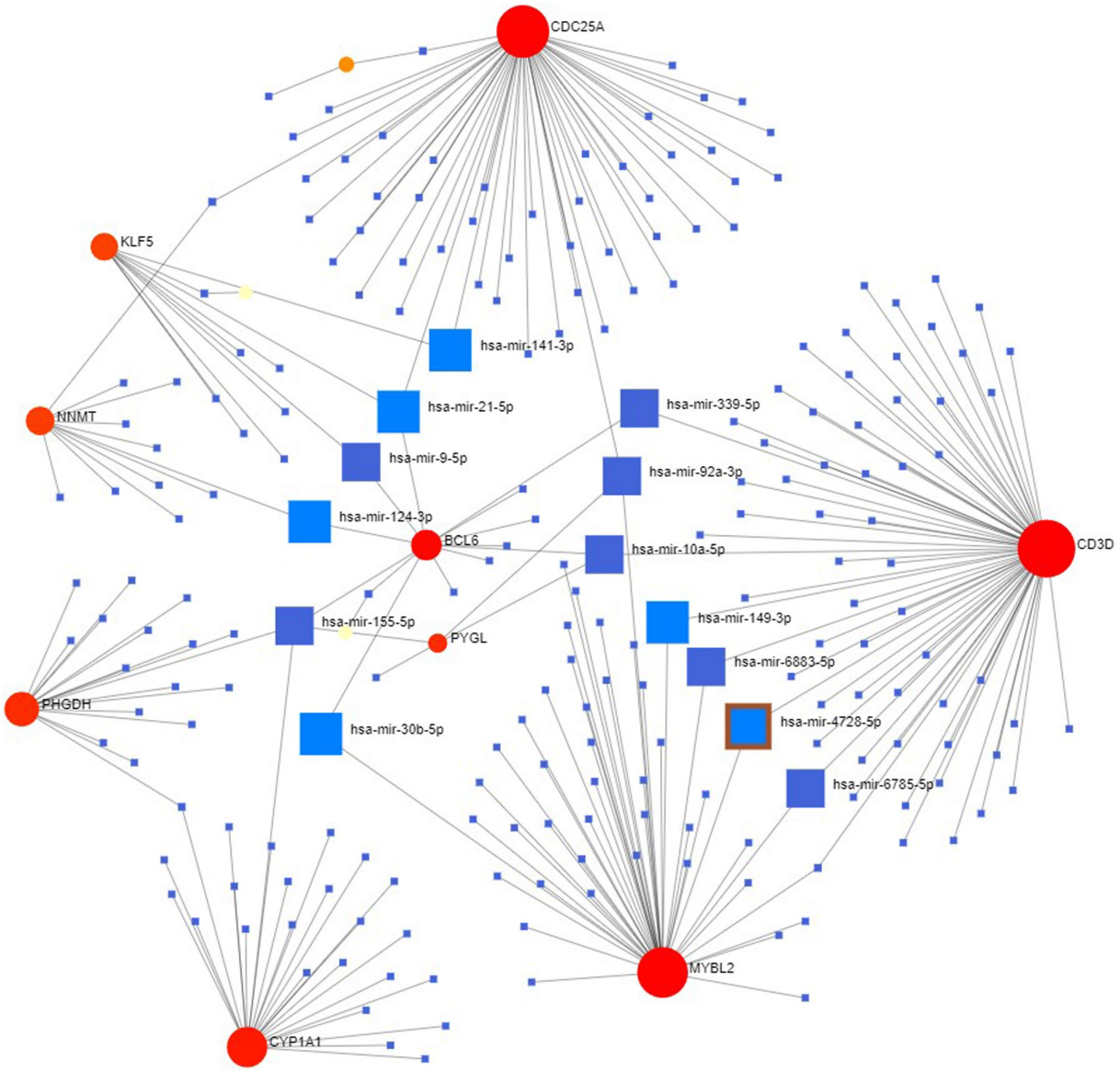

FIGURE 11
miRNA-hub gene regulatory interaction network. Square nodes represent miRNAs and round nodes represent genes.

signaling pathways are common pathogenic mechanisms in COVID-19 and sarcopenia. Tryptophan uses two metabolic pathways in humans, kynurenine and serotonin, and the imbalance in the synthesis of itself and its metabolites can lead to the occurrence of various neuropsychiatric disorders (79). In our study, disease-gene association analysis confirmed that these 15 hub genes were most associated with schizophrenia, bipolar disorder, prostate tumors, and autosomal recessive susceptibility. This finding is consistent with previous evidence that dementia and depression have been significantly associated with sarcopenia (80).

TFs and miRNAs regulate gene expression in transcription and post-transcription, respectively, and the results suggest that the transcription factor FOXC1 and miRNA (hsa-mir-155-5p) may be common molecules that simultaneously regulate the expression of these hub genes. FOXC1 is an important member of the FOX family of transcription factors, and several studies have reported that it is an important TF for COVID-19 (81, 82). And microRNA-155-5p is significantly upregulated in the acute phase of COVID-19, which promotes its immune-inflammatory response (83, 84), thus establishing its association with disease prognosis and playing an important role as a useful biomarker for monitoring and diagnosing COVID-19 disease (85). It suggests that in the future, we can intervene in its expression to regulate the gene and further study and control the disease.

In this study, we further analyzed the infiltration of immune cells in different diseases and the correlation between hub genes and immune factors. The results revealed that the sarcopenia group had lower expression scores of Activated.CD8.T.cells ($p = 0.018$) and Type.17.T.helper.cells ($p = 0.015$) compared with the healthy controls group. CD52 had a strong positive correlation ($p < 0.0001$) with Type.2.T.helper.cells, Type.1.T.helper. Cells and MDSC cells, whereas MYBL2 was negatively correlated with Plasmacytoid.dendritic.cell, Monocyte and Immature.dendritic.cell ($p < 0.01$). It was previously

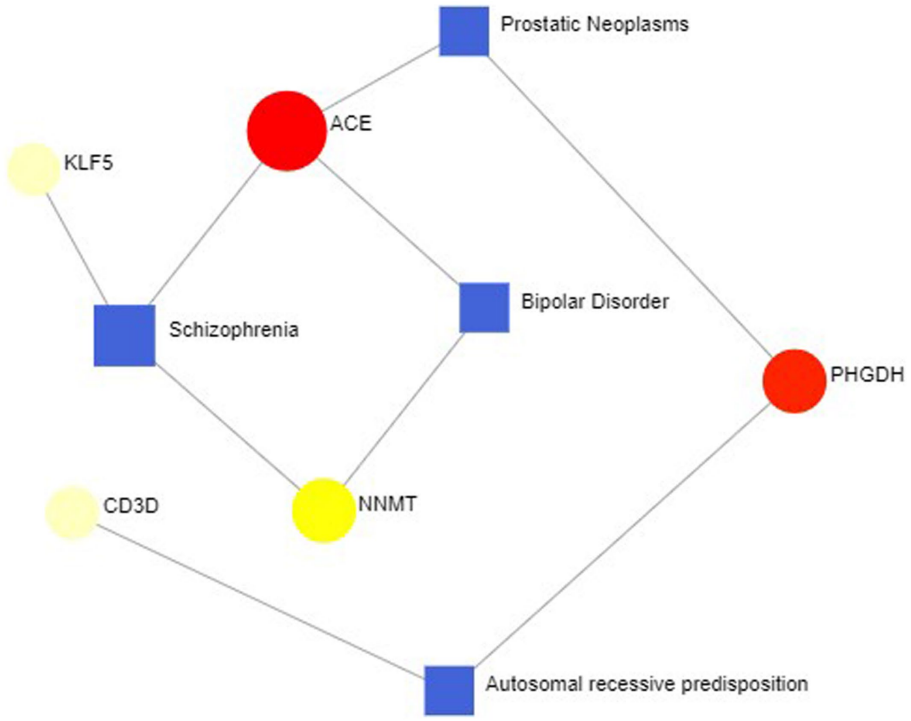

FIGURE 12
Gene-disease association network represent diseases associated with hub genes. Square nodes represent diseases, and round nodes represent genes.

proposed that the immune system regulates muscle regeneration and growth and plays an important role in the progression of sarcopenia (86). These immune cells, including lymphocytes, macrophages, neutrophils and other immune cells, work together to alter the condition of muscle fibers, leading to loss of muscle strength and muscle mass (87). It has also been found that aging of the immune system leads to a reduction in muscle stem cell populations, promoting their transition to a fibrotic phenotype, which regulates sarcopenia (88). This suggests the importance of different levels of immune cell infiltration for COVID-19 and sarcopenia. Several chemical agents and drugs have been used as potential therapeutic targets against COVID-19 or sarcopenia. However, to date, no drugs have been identified to treat individuals with both COVID-19 and sarcopenia. In our study, we explored 10 drugs that could be used as possible targets. The results showed that valinomycin PC3 UP is the best candidate for the treatment of sarcopenia and COVID-19.

Although some previous studies have reported the relationship between COVID-19 or sarcopenia and the hub gene, but the common molecular mechanisms between the two have not been explored by bioinformatics approaches. In this study, we explored and identified the common DEG and hub genes of COVID-19 and sarcopenia for the first time, which may help to further elucidate the common pathogenesis of both. However, there are some limitations of our study. First, the data were downloaded from public databases, and the amount of data and information was limited and unbalanced. In addition, even though differential and enrichment analyses were performed for sarcopenia and COVID-19, key genes driving disease progression may still be missed. Finally, the pathological causal mechanism of diseases caused by HUB gene and immune infiltration require external experiments to further validate our findings.

Overall, we explored the link between sarcopenia and COVID-19 using transcriptomic data analysis, further identified the common DEG and hub genes for sarcopenia and COVID-19, and performed several bioinformatics analyses based on them. It was found sarcopenia and COVID-19 share some common pathogenic mechanisms, which may be mediated by specific key genes. This study provides new biological targets and ideas for further investigation of molecular mechanisms, search for new drugs, and early diagnosis and effective treatment for patients with sarcopenia and COVID-19. However, the biological significance of these results needs to be further explored through *in vitro* and *in vivo* experiments.

Data availability statement

Publicly available datasets were analyzed in this study. This data can be found at: https://www.ncbi.nlm.nih.gov/geo/, GSE111016 and GSE171110.

Author contributions

JZ: Conceptualization, Data curation, Formal analysis, Funding acquisition, Investigation, Methodology, Project administration, Resources, Software, Supervision, Validation, Visualization, Writing – original draft, Writing – review & editing. HuY: Conceptualization, Data curation, Formal analysis, Funding acquisition, Investigation, Methodology, Project administration, Resources, Software, Supervision, Validation, Visualization, Writing – original draft, Writing – review & editing. JY:

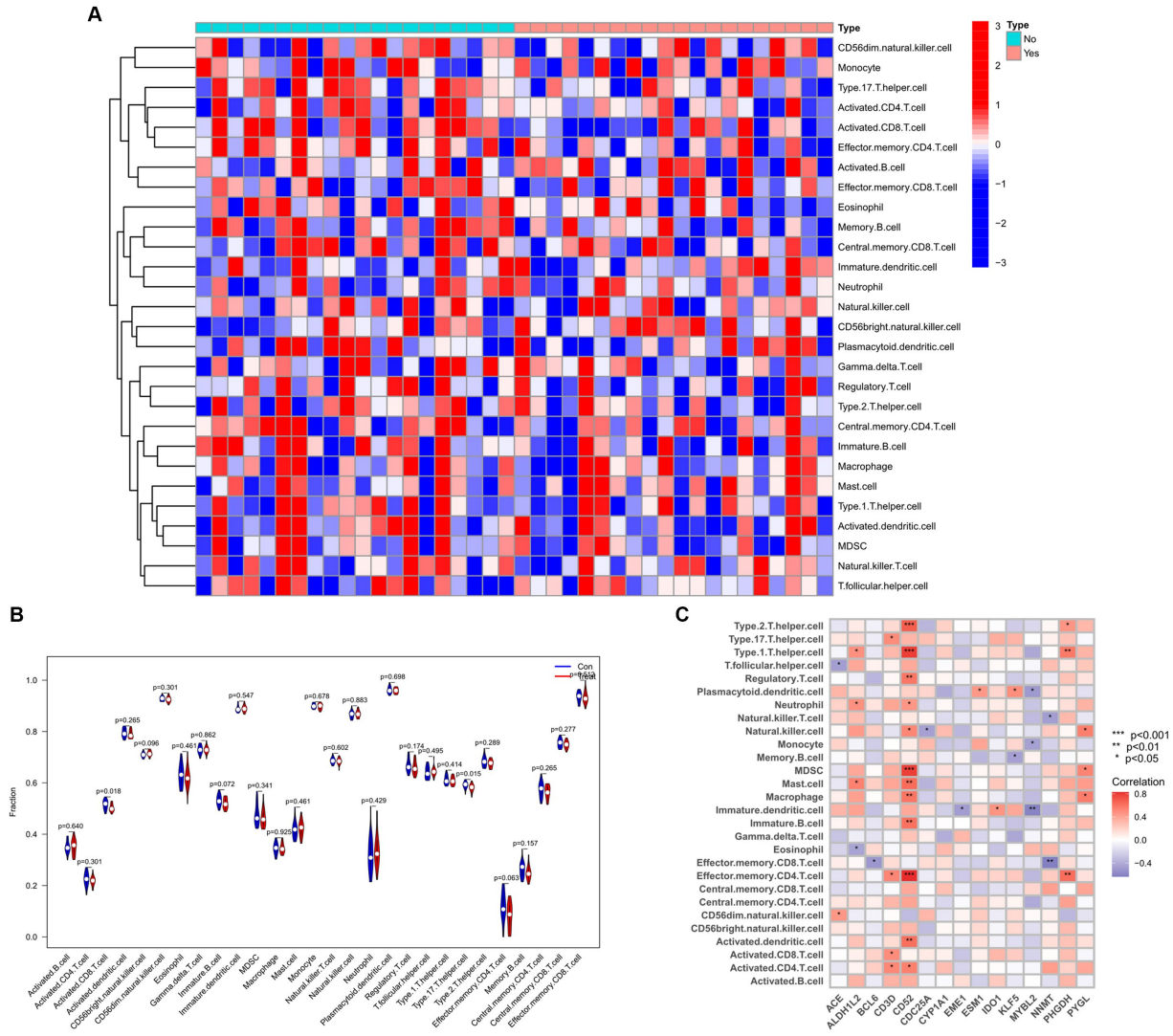

FIGURE 13
Infiltration analysis and correlation analysis of immune cells in the sarcopenia group and healthy controls group. **(A)** Heat map of immune cell subsets in the sarcopenia dataset. **(B)** Violin diagram of immune cell subsets in the sarcopenia dataset. **(C)** Correlation of immune cell subsets with common key genes. $p < 0.05$ indicates statistical difference.

Conceptualization, Data curation, Formal analysis, Funding acquisition, Investigation, Methodology, Project administration, Resources, Software, Supervision, Validation, Visualization, Writing – original draft, Writing – review & editing. YD: Conceptualization, Data curation, Formal analysis, Investigation, Methodology, Project administration, Validation, Writing – original draft. ZheL: Conceptualization, Data curation, Formal analysis, Methodology, Project administration, Resources, Supervision, Validation, Visualization, Writing – review & editing. XL: Conceptualization, Data curation, Formal analysis, Methodology, Project administration, Validation, Writing – original draft. HaY: Data curation, Formal analysis, Methodology, Project administration, Supervision, Validation, Writing – original draft. ZhW: Conceptualization, Data curation, Investigation, Methodology, Writing – original draft. ZiW: Conceptualization, Data curation, Investigation, Methodology, Writing – original draft. LJ: Conceptualization, Data curation, Software, Supervision, Writing – original draft. ZR: Conceptualization, Data curation, Formal analysis, Investigation, Writing – original draft. HL: Data curation, Methodology, Project administration, Resources, Writing – original draft. ZhoL: Conceptualization, Data curation, Formal analysis, Funding acquisition, Investigation, Methodology, Project administration, Resources, Software, Supervision, Validation, Visualization, Writing – review & editing. YL: Conceptualization, Data curation, Formal analysis, Funding acquisition, Investigation, Methodology, Project administration, Resources, Software, Supervision, Validation, Visualization, Writing – review & editing.

Funding

The author(s) declare that financial support was received for the research, authorship, and/or publication of this article. This research

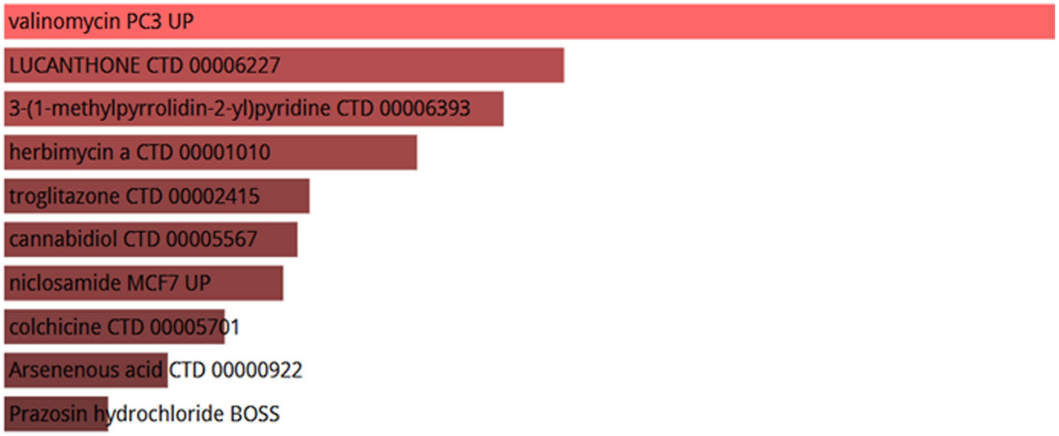

FIGURE 14
List of top 10 drugs recommended for COVID-19 and sarcopenia patients.

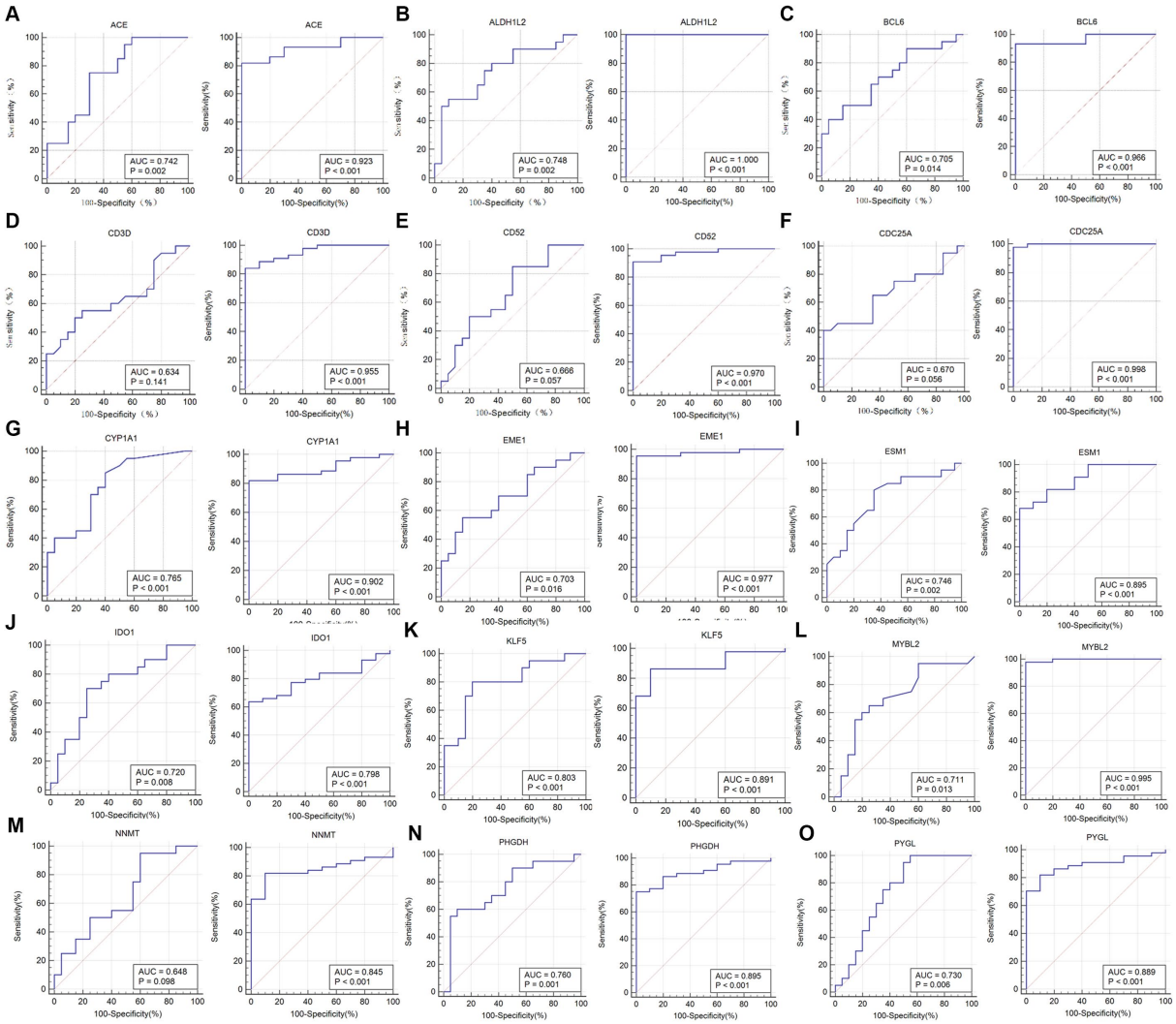

FIGURE 15
Validation of the common hub gene for diagnosis in the sarcopenia (GSE111016) dataset and the COVID-19 infected patient (GSE171110) dataset. **(A)** ACE, **(B)** ALDHIL2, **(C)** BCL6, **(D)** CD3D, **(E)** CD52, **(F)** CDC25A, **(G)** CYP1A1, **(H)** EME1, **(I)** ESM1, **(J)** IDO1, **(K)** KLF5, **(L)** MYBL2, **(M)** NNMT, **(N)** PHGDH, and **(O)** PYGL.

was funded by the Key Research and Development Program of Sichuan Province, grant number 2023YFO0009.

Acknowledgments

We thank the researchers who made their datasets publicly available.

Conflict of interest

The authors declare that the research was conducted in the absence of any commercial or financial relationships that could be construed as a potential conflict of interest.

Publisher's note

Supplementary material

The Supplementary material for this article can be found online at: https://www.frontiersin.org/articles/10.3389/fmed.2024.1378846/full#supplementary-material

References

1. Cruz-Jentoft AJ. Sarcopenia, the last organ insufficiency. *European Geriatric Med*. (2016) 7:195–6. doi: 10.1016/j.eurger.2016.01.003

2. Cruz-Jentoft AJ, Sayer AA. Sarcopenia. *Lancet*. (2019) 393:2636–46. doi: 10.1016/s0140-6736(19)31138-9

3. Damluji AA, Alfaraidhy M, AlHajri N, Rohant NN, Kumar M, Al Malouf C, et al. Sarcopenia and cardiovascular diseases. *Circulation*. (2023) 147:1534–53. doi: 10.1161/CIRCULATIONAHA.123.064071

4. Cruz-Jentoft AJ, Bahat G, Bauer J, Boirie Y, Bruyère O, Cederholm T, et al. Sarcopenia: revised European consensus on definition and diagnosis. *Age Ageing*. (2019) 48:16–31. doi: 10.1093/ageing/afy169

5. Sayer AA, Cruz-Jentoft A. Sarcopenia definition, diagnosis and treatment: consensus is growing. *Age Ageing*. (2022) 51:10. doi: 10.1093/ageing/afac220

6. Rosenberg IH. Sarcopenia: origins and clinical relevance. *J Nutr*. (1997) 127:990S–1S. doi: 10.1093/jn/127.5.990S

7. Dhillon RJS, Hasni S. Pathogenesis and Management of Sarcopenia. *Clin Geriatr Med*. (2017) 33:17–26. doi: 10.1016/j.cger.2016.08.002

8. Chen LK, Liu LK, Woo J, Assantachai P, Auyeung TW, Bahyah KS, et al. Sarcopenia in Asia: consensus report of the Asian working Group for Sarcopenia. *J Am Med Dir Assoc*. (2014) 15:95–101. doi: 10.1016/j.jamda.2013.11.025

9. Yuan S, Larsson SC. Epidemiology of sarcopenia: prevalence, risk factors, and consequences. *Metabolism*. (2023) 144:155533. doi: 10.1016/j.metabol.2023.155533

10. Petermann-Rocha F, Balntzi V, Gray SR, Lara J, Ho FK, Pell JP, et al. Global prevalence of sarcopenia and severe sarcopenia: a systematic review and meta-analysis. *J Cachexia Sarcopenia Muscle*. (2021) 13:86–99. doi: 10.1002/jcsm.12783

11. Verdijk LB, Snijders T, Drost M, Delhaas T, Kadi F, van Loon LJC. Satellite cells in human skeletal muscle; from birth to old age. *Age*. (2013) 36:545–57. doi: 10.1007/s11357-013-9583-2

12. Ciciliot S, Rossi AC, Dyar KA, Blaauw B, Schiaffino S. Muscle type and fiber type specificity in muscle wasting. *Int J Biochem Cell Biol*. (2013) 45:2191–9. doi: 10.1016/j.biocel.2013.05.016

13. Ferri E, Marzetti E, Calvani R, Picca A, Cesari M, Arosio B. Role of age-related mitochondrial dysfunction in sarcopenia. *Int J Mol Sci*. (2020) 21:15. doi: 10.3390/ijms21155236

14. Manini TM, Hong SL, Clark BC. Aging and muscle. *Curr Opin Clin Nutr Metab Care*. (2013) 16:21–6. doi: 10.1097/MCO.0b013e32835b5880

15. Fielding RA, Vellas B, Evans WJ, Bhasin S, Morley JE, Newman AB, et al. Sarcopenia: an undiagnosed condition in older adults. Current consensus definition: prevalence, etiology, and consequences. International working group on sarcopenia. *J Am Med Dir Assoc*. (2011) 12:249–56. doi: 10.1016/j.jamda.2011.01.003

16. Hunter GR, Singh H, Carter SJ, Bryan DR, Fisher G. Sarcopenia and its implications for metabolic health. *J Obes*. (2019) 2019:1–10. doi: 10.1155/2019/8031705

17. Chen L-K, Woo J, Assantachai P, Auyeung TW, Chou MY, Iijima K, et al. Asian working Group for Sarcopenia: 2019 consensus update on sarcopenia diagnosis and treatment. *J Am Med Dir Assoc*. (2020) 21:300–7.e2. doi: 10.1016/j.jamda.2019.12.012

18. Rothan HA, Byrareddy SN. The epidemiology and pathogenesis of coronavirus disease (COVID-19) outbreak. *J Autoimmun*. (2020) 109:102433. doi: 10.1016/j.jaut.2020.102433

19. Zhou F, Yu T, du R, Fan G, Liu Y, Liu Z, et al. Clinical course and risk factors for mortality of adult inpatients with COVID-19 in Wuhan, China: a retrospective cohort study. *Lancet*. (2020) 395:1054–62. doi: 10.1016/s0140-6736(20)30566-3

20. de Lusignan S, Dorward J, Correa A, Jones N, Akinyemi O, Amirthalingam G, et al. Risk factors for SARS-CoV-2 among patients in the Oxford Royal College of general practitioners research and surveillance Centre primary care network: a cross-sectional study. *Lancet Infect Dis*. (2020) 20:1034–42. doi: 10.1016/s1473-3099(20)30371-6

21. Bailey C, Black JRM, Swanton C. Cancer research: the lessons to learn from COVID-19. *Cancer Discov*. (2020) 10:1263–6. doi: 10.1158/2159-8290.Cd-20-0823

22. Jordan RE, Adab P. Who is most likely to be infected with SARS-CoV-2? *Lancet Infect Dis*. (2020) 20:995–6. doi: 10.1016/s1473-3099(20)30395-9

23. Wang P-y, Li Y, Wang Q. Sarcopenia: an underlying treatment target during the COVID-19 pandemic. *Nutrition*. (2021) 84:111104. doi: 10.1016/j.nut.2020.111104

24. Meftahi GH, Jangravi Z, Sahraei H, Bahari Z. The possible pathophysiology mechanism of cytokine storm in elderly adults with COVID-19 infection: the contribution of "inflame-aging". *Inflamm Res*. (2020) 69:825–39. doi: 10.1007/s00011-020-01372-8

25. Nelke C, Dziewas R, Minnerup J, Meuth SG, Ruck T. Skeletal muscle as potential central link between sarcopenia and immune senescence. *EBioMedicine*. (2019) 49:381–8. doi: 10.1016/j.ebiom.2019.10.034

26. Giudice J, Taylor JM. Muscle as a paracrine and endocrine organ. *Curr Opin Pharmacol*. (2017) 34:49–55. doi: 10.1016/j.coph.2017.05.005

27. Bano G, Trevisan C, Carraro S, Solmi M, Luchini C, Stubbs B, et al. Inflammation and sarcopenia: a systematic review and meta-analysis. *Maturitas*. (2017) 96:10–5. doi: 10.1016/j.maturitas.2016.11.006

28. Akseer N, Kandru G, Keats EC, Bhutta ZA. COVID-19 pandemic and mitigation strategies: implications for maternal and child health and nutrition. *Am J Clin Nutr*. (2020) 112:251–6. doi: 10.1093/ajcn/nqaa171

29. Jackson TA, Wilson D, Masud T, Greig C, Welch C. COVID-19 and acute sarcopenia. *Aging Dis*. (2020) 11:1345–51. doi: 10.14336/ad.2020.1014

30. Raveendran AV, Misra A. Post COVID-19 syndrome ("long COVID") and diabetes: challenges in diagnosis and management. *Diabetes Metab Syndr Clin Res Rev*. (2021) 15:102235. doi: 10.1016/j.dsx.2021.102235

31. Patra BG, Maroufy V, Soltanalizadeh B, Deng N, Zheng WJ, Roberts K, et al. A content-based literature recommendation system for datasets to improve data reusability – a case study on gene expression omnibus (GEO) datasets. *J Biomed Inform*. (2020) 104:103399. doi: 10.1016/j.jbi.2020.103399

32. Migliavacca E, Tay SKH, Patel HP, Sonntag T, Civiletto G, McFarlane C, et al. Mitochondrial oxidative capacity and NAD+ biosynthesis are reduced in human sarcopenia across ethnicities. *Nat Commun*. (2019) 10:5808. doi: 10.1038/s41467-019-13694-1

33. Lévy Y, Wiedemann A, Hejblum BP, Durand M, Lefebvre C, Surénaud M, et al. CD177, a specific marker of neutrophil activation, is associated with coronavirus disease 2019 severity and death. *iScience*. (2021) 24:102711. doi: 10.1016/j.isci.2021.102711

34. Kuleshov MV, Jones MR, Rouillard AD, Fernandez NF, Duan Q, Wang Z, et al. Enrichr: a comprehensive gene set enrichment analysis web server 2016 update. *Nucleic Acids Res*. (2016) 44:W90–7. doi: 10.1093/nar/gkw377

35. Szklarczyk D, Kirsch R, Koutrouli M, Nastou K, Mehryary F, Hachilif R, et al. The STRING database in 2023: protein–protein association networks and functional enrichment analyses for any sequenced genome of interest. *Nucleic Acids Res*. (2023) 51:D638–46. doi: 10.1093/nar/gkac1000

36. Doncheva NT, Morris JH, Gorodkin J, Jensen LJ. Cytoscape StringApp: network analysis and visualization of proteomics data. *J Proteome Res*. (2018) 18:623–32. doi: 10.1021/acs.jproteome.8b00702

37. Shannon P, Markiel A, Ozier O, Baliga NS, Wang JT, Ramage D, et al. Cytoscape: a software environment for integrated models of biomolecular interaction networks. *Genome Res*. (2003) 13:2498–504. doi: 10.1101/gr.1239303

38. Chin C-H, Chen S-H, Wu H-H, Ho C-W, Ko M-T, Lin C-Y. cytoHubba: identifying hub objects and sub-networks from complex interactome. *BMC Syst Biol*. (2014) 8:S11. doi: 10.1186/1752-0509-8-S4-S11

39. Franz M, Rodriguez H, Lopes C, Zuberi K, Montojo J, Bader GD, et al. GeneMANIA update 2018. *Nucleic Acids Res*. (2018) 46:W60–4. doi: 10.1093/nar/gky311

40. Cai Y, Yu X, Hu S, Yu J. A brief review on the mechanisms of miRNA regulation. *Genomics Proteomics Bioinformatics*. (2009) 7:147–54. doi: 10.1016/s1672-0229(08)60044-3

41. Lambert SA, Jolma A, Campitelli LF, das PK, Yin Y, Albu M, et al. The human transcription factors. *Cell*. (2018) 172:650–65. doi: 10.1016/j.cell.2018.01.029

42. Zhou G, Soufan O, Ewald J, Hancock REW, Basu N, Xia J. NetworkAnalyst 3.0: a visual analytics platform for comprehensive gene expression profiling and meta-analysis. *Nucleic Acids Res*. (2019) 47:W234–41. doi: 10.1093/nar/gkz240

43. Huang H-Y, Lin Y-C-D, Li J, Huang KY, Shrestha S, Hong HC, et al. miRTarBase 2020: updates to the experimentally validated microRNA–target interaction database. *Nucleic Acids Res*. (2019) 48:D148–54. doi: 10.1093/nar/gkz896

44. Castro-Mondragon JA, Riudavets-Puig R, Rauluseviciute I, Berhanu Lemma R, Turchi L, Blanc-Mathieu R, et al. JASPAR 2022: the 9th release of the open-access database of transcription factor binding profiles. *Nucleic Acids Res*. (2022) 50:D165–73. doi: 10.1093/nar/gkab1113

45. Piñero J, Bravo À, Queralt-Rosinach N, Gutiérrez-Sacristán A, Deu-Pons J, Centeno E, et al. DisGeNET: a comprehensive platform integrating information on human disease-associated genes and variants. *Nucleic Acids Res*. (2017) 45:D833–9. doi: 10.1093/nar/gkw943

46. Piñero J, Ramírez-Anguita JM, Saüch-Pitarch J, Ronzano F, Centeno E, Sanz F, et al. The DisGeNET knowledge platform for disease genomics: 2019 update. *Nucleic Acids Res*. (2019) 48:D845–55. doi: 10.1093/nar/gkz1021

47. Subramanian A, Tamayo P, Mootha VK, Mukherjee S, Ebert BL, Gillette MA, et al. Gene set enrichment analysis: a knowledge-based approach for interpreting genome-wide expression profiles. *Proc Natl Acad Sci USA*. (2005) 102:15545–50. doi: 10.1073/pnas.0506580102

48. Chen Y, Feng Y, Yan F, Zhao Y, Zhao H, Guo Y. A novel immune-related gene signature to identify the tumor microenvironment and Prognose disease among patients with Oral squamous cell carcinoma patients using ssGSEA: a bioinformatics and biological validation study. *Front Immunol*. (2022) 13:922195. doi: 10.3389/fimmu.2022.922195

49. Yoo M, Shin J, Kim J, Ryall KA, Lee K, Lee S, et al. DSigDB: drug signatures database for gene set analysis. *Bioinformatics*. (2015) 31:3069–71. doi: 10.1093/bioinformatics/btv313

50. Robin X, Turck N, Hainard A, Tiberti N, Lisacek F, Sanchez JC, et al. pROC: an open-source package for R and S+ to analyze and compare ROC curves. *BMC Bioinformatics*. (2011) 12:77. doi: 10.1186/1471-2105-12-77

51. Veronesi F, Contartese D, Martini L, Visani A, Fini M. Speculation on the pathophysiology of musculoskeletal injury with COVID-19 infection. *Front Med*. (2022) 9:930789. doi: 10.3389/fmed.2022.930789

52. Lauwers M, Au M, Yuan S, Wen C. COVID-19 in joint ageing and osteoarthritis: current status and perspectives. *Int J Mol Sci*. (2022) 23:2. doi: 10.3390/ijms23020720

53. Khurana V, Goswami B. Angiotensin converting enzyme (ACE). *Clin Chim Acta*. (2022) 524:113–22. doi: 10.1016/j.cca.2021.10.029

54. Zhao Y. Structure and function of angiotensin converting enzyme and its inhibitors. *Chin J Biotechnol*. (2008) 24:171–6. doi: 10.1016/s1872-2075(08)60007-2

55. Pitt B. ACE inhibitors in heart failure: prospects and limitations. *Cardiovasc Drugs Ther*. (1997) 11:285–90. doi: 10.1023/a:1007795915009

56. Sumukadas D, Struthers AD, McMurdo MET. Sarcopenia – a potential target for angiotensin-converting enzyme inhibition? *Gerontology*. (2006) 52:237–42. doi: 10.1159/000093656

57. Aladag E, Tas Z, Ozdemir BS, Akbaba TH, Akpınar MG, Goker H, et al. Human ace D/I polymorphism could affect the Clinicobiological course of COVID-19. Journal of the renin-angiotensin-aldosterone. *System*. (2021) 2021:1–7. doi: 10.1155/2021/5509280

58. Kai H, Kai M. Interactions of coronaviruses with ACE2, angiotensin II, and RAS inhibitors—lessons from available evidence and insights into COVID-19. *Hypertens Res*. (2020) 43:648–54. doi: 10.1038/s41440-020-0455-8

59. McConnell BB, Yang VW. Mammalian Krüppel-like factors in health and diseases. *Physiol Rev*. (2010) 90:1337–81. doi: 10.1152/physrev.00058.2009

60. Prosdocimo DA, Sabeh MK, Jain MK. Kruppel-like factors in muscle health and disease. *Trends Cardiovasc Med*. (2015) 25:278–87. doi: 10.1016/j.tcm.2014.11.006

61. Oishi Y, Manabe I, Tobe K, Ohsugi M, Kubota T, Fujiu K, et al. SUMOylation of Krüppel-like transcription factor 5 acts as a molecular switch in transcriptional programs of lipid metabolism involving PPAR-δ. *Nat Med*. (2008) 14:656–66. doi: 10.1038/nm1756

62. Hayashi S, Manabe I, Suzuki Y, Relaix F, Oishi Y. Klf5 regulates muscle differentiation by directly targeting muscle-specific genes in cooperation with MyoD in mice. *eLife*. (2016) 5:17462. doi: 10.7554/eLife.17462

63. Liu L, Koike H, Ono T, Hayashi S, Kudo F, Kaneda A, et al. Identification of a KLF5-dependent program and drug development for skeletal muscle atrophy. *Proc Natl Acad Sci*. (2021) 118:35. doi: 10.1073/pnas.2102895118

64. Hennes E, Lampe P, Dötsch L, Bruning N, Pulvermacher LM, Sievers S, et al. Cell-based identification of new IDO1 modulator Chemotypes. *Angew Chem Int Ed*. (2021) 60:9869–74. doi: 10.1002/anie.202016004

65. Sultana S, Elengickal A, Bensreti H, de Chantemèle EB, McGee-Lawrence ME, Hamrick MW. The kynurenine pathway in HIV, frailty and inflammaging. *Front Immunol*. (2023) 14:1244622. doi: 10.3389/fimmu.2023.1244622

66. Mondal A, Smith C, DuHadaway JB, Sutanto-Ward E, Prendergast GC, Bravo-Nuevo A, et al. IDO1 is an integral mediator of inflammatory neovascularization. *EBioMedicine*. (2016) 14:74–82. doi: 10.1016/j.ebiom.2016.11.013

67. Turski WA, Wnorowski A, Turski GN, Turski CA, Turski L. AhR and IDO1 in pathogenesis of Covid-19 and the "systemic AhR activation syndrome:" a translational review and therapeutic perspectives. *Restor Neurol Neurosci*. (2020) 38:343–54. doi: 10.3233/rnn-201042

68. Chilosi M, Doglioni C, Ravaglia C, Martignoni G, Salvagno GL, Pizzolo G, et al. Unbalanced IDO1/IDO2 endothelial expression and skewed Keynurenine pathway in the pathogenesis of COVID-19 and post-COVID-19 pneumonia. *Biomedicines*. (2022) 10:6. doi: 10.3390/biomedicines10061332

69. Boutros R, Lobjois V, Ducommun B. CDC25 phosphatases in cancer cells: key players? Good targets? *Nat Rev Cancer*. (2007) 7:495–507. doi: 10.1038/nrc2169

70. Drummond MJ, McCarthy JJ, Sinha M, Spratt HM, Volpi E, Esser KA, et al. Aging and microRNA expression in human skeletal muscle: a microarray and bioinformatics analysis. *Physiol Genomics*. (2011) 43:595–603. doi: 10.1152/physiolgenomics.00148.2010

71. Chen Z-j, Xiao J, Chen H-h. Identification of key genes related to immune cells in patients with COVID-19 via integrated bioinformatics-based analysis. *Biochem Genet*. (2023) 61:2650–71. doi: 10.1007/s10528-023-10400-1

72. Sagulkoo P, Chuntakaruk H, Rungrotmongkol T, Suratanee A, Plaimas K. Multi-level biological network analysis and drug repurposing based on leukocyte transcriptomics in severe COVID-19: in silico systems biology to precision medicine. *J Personal Med*. (2022) 12:7. doi: 10.3390/jpm12071030

73. Khalid Z, Huan M, Sohail Raza M, Abbas M, Naz Z, Kombe Kombe AJ, et al. Identification of novel therapeutic candidates against SARS-CoV-2 infections: an application of RNA sequencing toward mRNA based Nanotherapeutics. *Front Microbiol*. (2022) 13:901848. doi: 10.3389/fmicb.2022.901848

74. Nain Z, Rana HK, Liò P, Islam SMS, Summers MA, Moni MA. Pathogenetic profiling of COVID-19 and SARS-like viruses. *Brief Bioinform*. (2021) 22:1175–96. doi: 10.1093/bib/bbaa173

75. Guin D, Yadav S, Singh P, Singh P, Thakran S, Kukal S, et al. Human genetic factors associated with pneumonia risk, a cue for COVID-19 susceptibility. *Infect Genet Evol*. (2022) 102:105299. doi: 10.1016/j.meegid.2022.105299

76. Zhao J, Zhang W, Shen L, Yang X, Liu Y, Gai Z. Association of the ACE, GSTM1, IL-6, NOS3, and CYP1A1 polymorphisms with susceptibility of *mycoplasma pneumoniae* pneumonia in Chinese children. *Medicine*. (2017) 96:e6642. doi: 10.1097/md.0000000000006642

77. Hoogkamer W. Mitochondria initiate and regulate sarcopenia. *Exerc Sport Sci Rev*. (2017) 45:34–40. doi: 10.1249/jes.0000000000000094

78. López-Otín C, Blasco MA, Partridge L, Serrano M, Kroemer G. Hallmarks of aging: an expanding universe. *Cell*. (2023) 186:243–78. doi: 10.1016/j.cell.2022.11.001

79. Davidson M, Rashidi N, Nurgali K, Apostolopoulos V. The role of tryptophan metabolites in neuropsychiatric disorders. *Int J Mol Sci*. (2022) 23:17. doi: 10.3390/ijms23179968

80. Mogi M, Endo T, Akai K, Kitahara S, Abe T, Takeda M, et al. An association analysis between hypertension, dementia, and depression and the phases of pre-sarcopenia to sarcopenia: a cross-sectional analysis. *PLoS One*. (2021) 16:e0252784. doi: 10.1371/journal.pone.0252784

81. Islam T, Rahman MR, Aydin B, Beklen H, Arga KY, Shahjaman M. Integrative transcriptomics analysis of lung epithelial cells and identification of repurposable drug candidates for COVID-19. *Eur J Pharmacol*. (2020) 887:173594. doi: 10.1016/j.ejphar.2020.173594

82. Li P, Li T, Zhang Z, Dai X, Zeng B, Li Z, et al. Bioinformatics and system biology approach to identify the influences among COVID-19, ARDS and sepsis. *Front Immunol*. (2023) 14:1152186. doi: 10.3389/fimmu.2023.1152186

83. Gaytán-Pacheco N, Ibáñez-Salazar A, Herrera-van Oostdam AS, Oropeza-Valdez JJ, Magaña-Aquino M, Adrián López J, et al. miR-146a, miR-221, and miR-155 are involved in inflammatory immune response in severe COVID-19 patients. *Diagnostics*. (2022) 13:1. doi: 10.3390/diagnostics13010133

84. Gedikbasi A, Adas G, Isiksacan N, Kart Yasar K, Canbolat Unlu E, Yilmaz R, et al. The effect of host miRNAs on prognosis in COVID-19: miRNA-155 may promote

severity via targeting suppressor of cytokine signaling 1 (SOCS1) gene. *Genes*. (2022) 13:7. doi: 10.3390/genes13071146

85. Li X, Wang Y, Zhou Q, Pan J, Xu J. Potential predictive value of miR-125b-5p, miR-155-5p and their target genes in the course of COVID-19. *Infect Drug Resist*. (2022) 15:4079–91. doi: 10.2147/idr.S372420

86. Tidball JG. Regulation of muscle growth and regeneration by the immune system. *Nat Rev Immunol*. (2017) 17:165–78. doi: 10.1038/nri.2016.150

87. Zhang X, Li H, He M, Wang J, Wu Y, Li Y. Immune system and sarcopenia: presented relationship and future perspective. *Exp Gerontol*. (2022) 164:111823. doi: 10.1016/j.exger.2022.111823

88. Wang Y, Wehling-Henricks M, Welc SS, Fisher AL, Zuo Q, Tidball JG. Aging of the immune system causes reductions in muscle stem cell populations, promotes their shift to a fibrogenic phenotype, and modulates sarcopenia. *FASEB J*. (2018) 33:1415–27. doi: 10.1096/fj.201800973R

frontiers | Frontiers in Cell and Developmental Biology

TYPE Review
PUBLISHED 02 August 2024
DOI 10.3389/fcell.2024.1421566

OPEN ACCESS

EDITED BY
Kunihiro Tsuchida,
Fujita Health University, Japan

REVIEWED BY
Agnese De Mario,
University of Padua, Italy
Ramona Meanti,
University of Milano Bicocca, Italy

*CORRESPONDENCE
Maria Paola Paronetto,
mariapaola.paronetto@uniroma4.it

RECEIVED 22 April 2024
ACCEPTED 25 June 2024
PUBLISHED 02 August 2024

CITATION
Fenili G, Scaricamazza S, Ferri A, Valle C and Paronetto MP (2024), Physical exercise in amyotrophic lateral sclerosis: a potential co-adjuvant therapeutic option to counteract disease progression.
Front. Cell Dev. Biol. 12:1421566.
doi: 10.3389/fcell.2024.1421566

Physical exercise in amyotrophic lateral sclerosis: a potential co-adjuvant therapeutic option to counteract disease progression

Gianmarco Fenili[1,2], Silvia Scaricamazza[3,4], Alberto Ferri[3,4], Cristiana Valle[3,4] and Maria Paola Paronetto[1,2]*

[1]Department of Movement, Human and Health Sciences, University of Rome "Foro Italico", Rome, Italy, [2]Laboratory of Molecular and Cellular Neurobiology, Fondazione Santa Lucia IRCCS, Rome, Italy, [3]Laboratory of Metabolomics, Fondazione Santa Lucia IRCCS, Rome, Italy, [4]Institute of Translational Pharmacology (IFT), Consiglio Nazionale Delle Ricerche (CNR), Rome, Italy

Amyotrophic lateral sclerosis (ALS) is a fatal disorder characterized by the selective degeneration of upper and lower motor neurons, leading to progressive muscle weakness and atrophy. The mean survival time is two to five years. Although the hunt for drugs has greatly advanced over the past decade, no cure is available for ALS yet. The role of intense physical activity in the etiology of ALS has been debated for several decades without reaching a clear conclusion. The benefits of organized physical activity on fitness and mental health have been widely described. Indeed, by acting on specific mechanisms, physical activity can influence the physiology of several chronic conditions. It was shown to improve skeletal muscle metabolism and regeneration, neurogenesis, mitochondrial biogenesis, and antioxidant defense. Interestingly, all these pathways are involved in ALS pathology. This review will provide a broad overview of the effect of different exercise protocols on the onset and progression of ALS, both in humans and in animal models. Furthermore, we will discuss challenges and opportunities to exploit physiological responses of imposed exercise training for therapeutic purposes.

KEYWORDS

ALS, physical activity, muscle atrophy, neurodegenerative disease, exercise

1 Introduction

Amyotrophic lateral sclerosis (ALS) is a fatal disorder characterized by the selective degeneration of upper motor neurons in the primary motor cortex and lower motor neurons in the brainstem and spinal cord, leading to progressive muscle weakness and atrophy (Masrori and Van Damme, 2020). Overall survival varies from a few months to decades, but on average death occurs between 2.5 and 5 years from the diagnosis (Cozzolino et al., 2008), usually for respiratory failure (Masrori and Van Damme, 2020).

ALS can be classified in two different forms depending on the region of the primary degeneration: bulbar or spinal. The spinal form (two-thirds of the cases) affects the muscles of the limbs and the trunk, and causes muscular weakness and atrophy, cramps and fasciculations. The bulbar form (one-third of the cases) affects at first the muscle of the lips, tongue and throat, and results in dysarthria and dysphagia (Hulisz, 2018). Approximately, 90% of ALS cases are sporadic (sALS), while 10% are familial (fALS). Particularly, pathogenic variants in superoxide dismutase 1 (SOD1), TAR DNA-binding protein

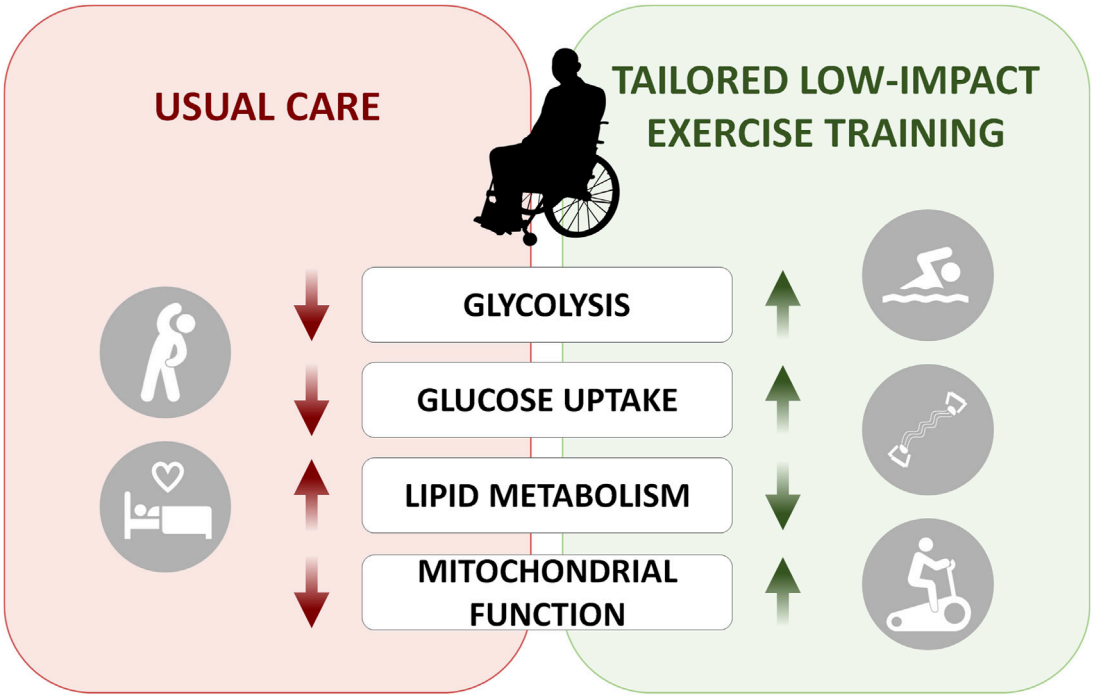

GRAPHICAL ABSTRACT
Energy metabolism is dysregulated in ALS patients. On the left panel, metabolic processes shown to be affected in ALS patients can be partially rescued with tailored low-impact exercise training protocols.

(*TARDBP*), fused in sarcoma (*FUS*) and chromosome 9 open reading frame 72 (*C9orf72*) genes, account for approximately 60% of the familial cases and about 10% of sporadic ALS (Akçimen et al., 2023). SOD1 is an intracellular antioxidant enzyme which protects cells by regulating basal levels of reactive oxygen species (ROS) arising from mitochondrial and cytosolic superoxide ions (Trist et al., 2021). To date, over 140 distinct *SOD1* mutations have been identified, but the precise mechanisms underlying the effect of *SOD1* mutants on mitochondrial metabolism remain unclear. Nevertheless, ALS is considered a multifactorial disease, due to a combination of risk-genotypes that interact with environmental factors, impacting and accelerating the neurodegenerative cascade (Al-Chalabi and Hardiman, 2013).

Although numerous preclinical and clinical trials have been performed, a cure for ALS does not exist yet. Indeed, since 1941, more than 60 compounds, with different mechanisms of action, have been evaluated in clinical trials for ALS treatment (Petrov et al., 2017), but only four of them have been approved by FDA for clinical use: riluzole (Rilutek, Tiglutik, Exservan), edaravone (Radicava), tofersen (Qalsody), and AMX0035 (Relyvrio), which was removed from the market in april 2024 due to negative topline data (NCT03127514). The "usual care" for ALS patients consists of treatments that slow the progression of the disease: to date, riluzole is the only treatment that has been shown to prolong survival in ALS (Bensimon et al., 1994), offered to all patients as early as possible (Miller and Appel, 2017).

Several studies documented higher incidence and lower age onset of ALS in high profile athletes, leading to the hypothesis that strenuous, repetitive exercise may represent an environmental risk factor to develop the disease (Chio et al., 2009). To date, the role of regular exercise and fitness in the pathogenesis and treatment of ALS is still controversial. ALS is commonly known as Lou Gehrig's disease, from a famous professional baseball player who was afflicted by this devastating neurodegenerative disorder during the late 1930s. Several studies have suggested that people with active lifestyle and reduced body fat have increased risk to develop ALS (Scarmeas et al., 2002), supporting the hypothesis that heavy exercise could represent a suspected risk factor for ALS. Consistently, frequent, and strenuous physical activity seems to increase the penetrance of ALS, particularly those patients with a predisposing genotypic background as *C9ORF72* expansion have a higher risk to develop exercise-aggravated disease. (Julian et al., 2021).

The role of intense physical activity in the etiology of ALS has been debated for several decades (Harwood et al., 2009), without reaching a clear conclusion. Most athletes and physically active individuals do not develop ALS. Instead, regular physical activity has been associated with increased quality of life and has shown neuroprotective properties, ameliorating neurological impairment in different neurodegenerative processes, even hindering age-related neuronal loss. Physical activity can also enhance neurogenesis, implementing neuronal plasticity (Radak et al., 2016).

A deeper understanding of the potential interaction between genetic and environmental factors would be instrumental to deepen this debate, and for the development of preventive strategies for patients and their family members. Recent reviews have tried to answer this question, to understand whether physical activity could be considered a factor in the etiology of ALS (Chapman et al., 2023). On the other hand, considering that physical activity is able to induce cellular adaptations in the brain, spinal cord, and skeletal

muscles that could counteract the oxidative stress complication of ALS, it is conceivable that exercise could be beneficial for ALS patients (Elbasiouny and Schuster, 2011; Kincaid and Bossy-Wetzel, 2013).

Physical activity represents one of the most commonly prescribed therapies, either in terms of prevention or as non-pharmacological adjunctive treatment for several chronic conditions (Vina et al., 2012). Regular moderate-intensity training reduces oxidative stress (Radak et al., 2008a; Radak et al., 2008b), decreases levels of inflammatory markers in elderly (Sellami et al., 2021), helps to preserve cardiovascular fitness and brain function (Hotta et al., 2017), and protects individuals from the negative effects of stress on cell aging (Rebelo-Marques et al., 2018). In skeletal muscle, it attenuates mitochondrial deficits, thus improving muscle function (Wyckelsma et al., 2017). However, strenuous exercise training generates high levels of reactive oxygen species (ROS) known to cause oxidative stress and activate pathogenic pathways, thus accelerating the aging process (Sahl et al., 2017). In ALS, mitochondrial dysfunction and oxidative stress are tightly dependent on each other and represent the basis of the redox dysregulation, which contributes, at least in part, to death of motor neurons. Mitochondria are the main site of production of ROS; hence, impairment of mitochondrial function, as in ALS, increases the oxidative stress (Carrì et al., 2015). However, exercise ROS production could also represent a potentially harmful stressor able to promote adaptive changes, enabling to tolerate subsequent stress. According to the mitohormesis, in response to ROS perturbation the mitochondria can initiate and transduce a signal transduction pathway coordinating a transcriptional response which results in both mitochondrial and non-mitochondrial adaptations, and maintains cellular homeostasis (Merry and Ristow, 2016).

An additional layer of complexity is given by the impact of ALS on energy metabolism. Indeed, altered metabolic homeostasis represents an early event in ALS, documented both in patients and in mouse models of ALS, with weight loss and reduced fat mass, altered glucose and lipid handling, and increased resting energy expenditure (Dupuis et al., 2004; Dupuis et al., 2011; Scaricamazza et al., 2020; Steyn et al., 2020). Notably, these metabolic alterations also affect the neurodegenerative process: as a result, increased dietary lipid content offers neuroprotection and extends survival in mouse models of ALS (Dupuis et al., 2004; Dupuis et al., 2011), whereas restricting calorie intake exacerbates motor symptoms (Pedersen and Mattson, 1999; Fergani et al., 2007). Affected skeletal muscles decrease using glucose as a source of energy but use lipids instead and this chronic pathologic alteration is exacerbated with disease progression (Steyn et al., 2020). The switch toward lipid use in glycolytic muscle precedes neuromuscular junction denervation in mouse models (Dupuis et al., 2009; Palamiuc et al., 2015). Remarkably, administration of dichloroacetate (DCA), a halogenated organic acid that inhibits the activity of PDK and facilitates the entry of pyruvate into the Krebs cycle and the oxidation of glucose, is sufficient to force metabolism toward glucose oxidation, reverting metabolic imbalance (Palamiuc et al., 2015).

Given these reported findings, specific physical exercises are expected to differentially shift the muscular energy metabolism either toward an oxidative pattern, lipidic, in case of low-intensity exercise, or toward a glycolytic metabolism, in case of high-intensity exercise (Romijn et al., 1993; van Loon et al., 2001).

Herein, we review and discuss the effect of exercise training on the onset and progression of ALS, both in humans and in animal models, with particular emphasis on novel therapeutic options intended to take advantage of the physiological response to exercise, suggesting the possible set up of personalized therapies.

2 Physical activity and exercise training in ALS

"Physical activity" and "exercise" describe different concepts, often confused with one another. Physical activity is defined as any body movement produced by skeletal muscles that require energy and can be categorized into occupational, sports, conditioning, household, or other activities. "Exercise" represents a subset of physical activity that is planned, structured, and repetitive and has, as final or intermediate objective, the improvement or maintenance of physical fitness, physical performance, or health (Caspersen et al., 1985).

The molecular basis of responses to acute and chronic exercise training have been extensively studied both in humans and in mice affected by ALS. While some researchers have found that exercise may improve the quality of life of patients, other studies have shown that exercise may paradoxically impair their neuromuscular function (Angelini and Siciliano, 2021). For sure, exercise training can offer physiological and psychological benefits for patients with ALS, particularly during the early stages of the disease (Lunetta et al., 2016). One important effect of physical activity, besides its positive impact on mental and behavior status, is that exercise improves metabolism in skeletal muscle by enhancing both glucose metabolism and mitochondrial biogenesis, which, in turn, strengthens the antioxidative defense.

So, what is the main difference between the exercise protocols administrated?

Resistance exercise entails repetition of dynamic muscle-shortening (concentric) and muscle-lengthening (eccentric) contractions against external load (performed with the help of weight machines or resistance bands). It improves muscle strength and force, helps maintaining skeletal muscle function, minimizes the risk of disability, also favoring muscle hypertrophy (Smith et al., 2023).

Endurance exercise (or aerobic exercise) is associated with training-induced improvements in maximal oxygen consumption (VO_{2MAX}). This exercise type is divided according to intensity: low (<50%), moderate (~50%–79%) or high intensities (≥80%) of VO_{2MAX} (Smith et al., 2023).

3 Exercise training protocols in mouse models of ALS

To elucidate whether physical exercise displays a positive or negative effect on ALS onset and progression, different training protocols have been administrated in animal models of ALS, summarized in Table 1. Particularly, transgenic mice that express G93A mutant *SOD1* ($SOD1^{G93A}$) human gene have been generated

TABLE 1 Training protocols in mouse models of ALS. Specific protocols, outcomes and Reference of the studies are indicated.

Training protocol	Outcomes	Ref. Study
Running-based training protocol in ALS mice (Treadmill)		
Treadmill running at 17 m/min for 30 min, 5 days/week	Increased survival in males and females	Kirkinezos et al. (2003)
Treadmill running at 16 m/min for 45 min, 5 days/week	Delayed onset of disease in female Decreased survival in males	Veldink et al. (2003)
Treadmill running at 20 m/min for 45 min, 5 days/week +/- nandrolone	No changes on the onset of disease Increased motor neuron counts after PA	Kassa et al. (2017)
Moderate intensity: treadmill running at 10 m/min, for 30 min, 3 days/week	Delayed onset of Motor neuron deficit	Carreras et al. (2010)
High intensity: treadmill running at 20 m/min, for 60 min, 5 days/week	Hastened onset Motor neuron density Decreased survival	Carreras et al. (2010)
Running in a speed-regulated treadmill (max. 13 m/min), for 30 min, 5 days/week	No changes in the Onset of disease No changes in Survival	Deforges et al. (2009)
Running in a speed-regulated treadmill (from 10 m/min to max. 22 m/min), increasing from 15 to 60 min, 5 days/week	Anticipated onset Decreased survival	Scaricamazza et al. (2024)
Running-based training protocol in ALS mice (wheels)		
2 h daily exposure to running wheels	Increased Survival	Kaspar et al. (2005)
6 h daily exposure to running wheels	Increased Motor performance Increased Survival	Kaspar et al. (2005)
12 h daily exposure to running wheels	Increased Motor performance Increased Survival	Kaspar et al. (2005)
10 h daily exposure to running wheels: 40 × 10 min of running, 5 min rest	No changes in the Onset of disease No changes in Motor performance Increased Survival	Liebetanz et al. (2004)
multiple exercise sessions at asymptomatic and pre-symptomatic stages in an automated home-cage running-wheel system for 3 months	Anticipated onset Decreased survival	Golini et al. (2023)
Swimming-based training protocol in ALS mice		
Swimming (max. 5 L/min), for 30 min, 5 days/week	Delayed Onset of disease Increased Survival Increased Motor performance	Deforges et al. (2009)
Swimming (max. 5 L/min), for 30 min, 5 days/week	Increased Glucose tolerance Increased Plasma lactate Increased GLUT4 expression Increased Lipid synthesis	Desseille et al. (2017)
Swimming (max. 5 L/min), for 30 min, 5 days/week	Increased Motor performance Decreased Mitochondrial dysfunction Increased malate synthase activity	Flis et al. (2019)
Swimming (max. 5 L/min), for 30 min, 5 days/week	Increased GPx activity	Dzik et al. (2021)

(Ripps et al., 1995) and extensively used for this purpose. *SOD1*^{G93A} mice develop progressive lower motor neuron weakness and increased oxidative stress and reproduce the clinical and pathological hallmarks of ALS (Ripps et al., 1995). Furthermore, the *Sod1*^{G86R} mouse models were developed, which express the missense mutation Gly86 to Arg of the murine SOD1 enzyme (Ripps et al., 1995), reported in the corresponding amino acid residue (position 85) of some fALS patients (Deng et al., 1993; Rosen et al., 1993).

In mice, three commonly used protocols for exercise training have been developed: swimming, voluntary wheel running, and "forced" wheel or treadmill running. Treadmill running and wheel running induce adaptations in mice associated with endurance exercise training (Kemi et al., 1985; Waters et al., 2004; Massett and Berk, 2005). However, while with the treadmill running protocol the total amount of work performed can be precisely established through the selection of exercise testing and training parameters, the voluntary wheel running does not offer this advantage. Unlike for humans, there are no well-accepted standards for exercise training paradigms or levels of activity required for optimal changes in exercise capacity or other training adaptations (Fuller and Thyfault, 1985). Unlike treadmill exercise, voluntary wheel-running enables mice to run freely and at a lower intensity. Although this practice may cause individual differences among mice in the amount of exercise they get, the mice do not experience much stress.

Swimming-based training protocol display changes in skeletal muscle energetic metabolism of *SOD1*^{G93A} mice, shifting energetic fuels to the anaerobic glycolytic pathway, as detailed below.

Notably, mouse strain, sex, and age have been reported to influence exercise training responses. For example, male mice had significantly greater biochemical adaptations to exercise training than female mice (Massett and Berk, 2005). Moreover, the adaptation to exercise training strictly depends on factors such as training load, duration, and frequency.

The first studies investigating the role of physical exercise on ALS onset and progression demonstrated a beneficial effect achieved by an endurance training protocol in *SOD1*^{G93A} mice (Kirkinezos et al., 2003). In particular, Kirkinezos and colleagues performed a treadmill protocol with a 5 days per week exercise regimen of 30 min at 17 m/min, showing a significant increase in the life span of both male and female *SOD1*^{G93A} mice (Kirkinezos et al., 2003). Conversely, Veldink and colleagues found a positive neuroprotective effect of their treadmill protocol only for female *SOD1*^{G93A} mice. In detail, the endurance exercise training, consisting of 45 min per day, 5 days per week at 16 m/min, was able to delay the onset of the disease in female but not in male *SOD1*^{G93A} mice, that showed instead a hastened death (Veldink et al., 2003). In either case, the authors highlighted the potential role of sex hormones as a possible explanation for their gender-specific response to exercise. A similar protocol showed no impact on disease onset, whereas a beneficial effect on survival of motoneurons was demonstrated (Kassa et al., 2017). In this latter study the use of anabolic steroids, still debated in epidemiological studies on patients and murine models of ALS, was also assessed. The authors showed that nandrolone treatment markedly enhanced motoneuron loss; its detrimental effect was reverted by the combination with exercise, suggesting a potential neuroprotective effect of physical exercise (Kassa et al., 2017).

Carreras and colleagues found that moderate exercise (30 min of exercise per day, 3 days a week at 10 m/min) was able to delay the onset of motor deficit by over a week in *SOD1*^{G93A} mice, whereas high intensity exercise (60 min of exercise per day, 5 days per week at 20 m/min) slightly but significantly hastened the onset of motor performance deficits (Carreras et al., 2010). More recently, Scaricamazza and colleagues demonstrated that intense endurance exercise exerted a detrimental effect on *SOD1*^{G93A} mice (Scaricamazza et al., 2024). Particularly, starting the training far from the onset, they demonstrated that intense endurance exercise was able to bring the onset of the disease forward and to worsens the progression of symptoms by hastening the motor-skill impairment and accelerating the denervation process and the motor neuron death. These data suggest that intense endurance exercise could represent a risk factor in ALS (Scaricamazza et al., 2024).

Running wheels protocols provided more positive results than treadmill protocols, as mentioned above. Mice with the opportunity to exercise with wheels voluntarily choose to do so; even those with debilitating conditions, such as symptomatic *SOD1*^{G93A} mice, exhibit a strong motivation to use an exercise wheel. Hence, different enrichment strategies, including running wheels, affect disease progression and may have implications for experimental outcomes (Sorrells et al., 2009). A short 2-h exposure to the running wheels showed a significant 7-day extension in median survival compared with non-running animals (Kaspar et al., 2005), whereas 6–12-h exposure to the running wheels provided significant benefits to motor functions (Kaspar et al., 2005). Even vigorous training protocols, as achieved by chronic exposure to motor-driven running wheels, did not negatively impact disease onset in *SOD1*^{G93A} mice, but increased survival of 1 week (Liebetanz et al., 2004). Interestingly, exercise training was shown to exert a remarkable synergistic effect with insulin-like growth factor-1 administration, promoting motor neuron survival, attenuating astrogliosis, improving motor function, and extending survival (Kaspar et al., 2005).

Notably, the administration of multiple exercise sessions at an early pre-symptomatic disease stage through a running wheels system to *SOD1*^{G93A} mice expressing low copy of mutant *SOD1*, significantly worsened disease course predating the symptoms onset (Golini et al., 2023). This latter evidence allows to hypothesize a negative impact of intense physical exercise, if administered at a very early age.

By comparing running-to swimming-based exercise protocols, Deforges and colleagues demonstrated that, in *SOD1*^{G93A} mice, a swimming-based training protocol was able to sustain the motor function limiting astrogliosis and hypertrophic processes, with a remarkable increase in the life span by about 25 days (Deforges et al., 2009). The magnitude of this beneficial effect is one of the highest among those induced by any therapeutic strategy in ALS. Unlike running, swimming significantly delayed spinal motoneuron death and, more specifically, the motoneurons of large soma area. Analysis of the muscular phenotype revealed a swimming-induced relative maintenance of the fast phenotype in fast-twitch muscles (Desseille et al., 2017). Moreover, high intensity swimming exercise significantly improved glucose metabolism, which is strongly impaired in *SOD1*^{G93A} mice, as well as in ALS patients. These swimming-induced benefits were associated with changes in skeletal muscle energetic metabolism, leading to energetic fuel shifts toward glucose re-use and fat deposition. In particular, the increase in GLUT4 expression induced by swimming was instrumental to switch energetic fuel, feeding the glycolytic pathway.

Thus, if running-based trainings showed to reinforce the oxidative pathway contributing to the neurodegenerative process, swimming-based training worked as modulator of skeletal muscle energy metabolism, with concomitant improvement of skeletal muscle function. Notably, swim training significantly decreased the reduction in muscle strength clearly visible at the symptomatic stage of ALS (Flis et al., 2018). Swim-training is characterized by non-weight bearing exercises that minimize damage to muscle fibers, reducing oxidative stress, and improving muscle energy metabolism at the terminal stage of the disease (Flis et al., 2018). As discussed above, energy metabolism dysfunction is a characteristic sign of ALS disease and defects in skeletal muscle energy metabolism deeply contribute to disease progression (Dupuis et al., 2011). However, Flis and colleagues report that after swim training the electron transport chain did not change between wild type and *SOD1*^{G93A} mice, in contrast significant changes were observed in citrate synthase, malate dehydrogenase, and cytochrome c oxidase (Flis et al., 2019). In ALS skeletal muscles, the increase in the activity of malate dehydrogenase and cytochrome C is accompanied by a decrease in citrate synthase activity, activating a compensatory mechanism to maintain the production of oxalacetate in the muscles, and thus the

TABLE 2 Training protocols performed in ALS patients. Specific protocols, outcomes and reference of the studies are indicated.

Training protocol	Outcomes	Ref. Study
Resistance training		
Resistance exercises to upper extremities (2 sets × 10 reps, 5 min rest), 6 days/week, for 75 days	Beneficial effect	Bohannon (1983)
Resistance training and stretching for the trunk muscles, upper and lower limbs, 6 days/week, for 6 months	Beneficial effect; higher respiratory function	Kitano et al. (2018)
Shoulder, elbow, hip, knee flexion; elbow, knee extension; grip; increase intensity, 3 days/week for 6 months	Beneficial effect	Clawson et al. (2018)
Moderate-load and moderate-intensity resistance exercise program to upper and lower extremities, 3 days/week, for 6 months	Beneficial effect	Bello-Haas et al. (2007)
Active exercises against gravity in six muscle groups in the upper and lower limbs (3 sets × 3 reps each muscle group) performed daily for 2 weeks each month, for 6 months	No significative effect	Lunetta et al. (2016)
Passive exercises consisting of 20 min of 20 flexion–extension movements per minute in the upper and lower limbs, daily for 2 weeks/month, for 6 months	No significative effect	Lunetta et al. (2016)
Passive, active and cycle ergometer exercises, strictly supervised; 2/week, for 6 months	No effect on survival, reduced motor deterioration	Lunetta et al. (2016)
Resistance exercises targeting both upper and lower body (2 sets × 5 reps at 6RM), 2–3 days/week, for 12 weeks	Negative effect	Jensen et al. (2017)
Endurance training		
Endurance exercises to whole body, against modest loads, lasted 15 min twice daily, for 12 months	Beneficial effects	Drory et al. (2001)
Walking on a weight-supported treadmill for 30 min (6 sets × 5 min, 5 min rest), 3 days/week, for 8 weeks	Beneficial effect	Sanjak et al. (2010)
10 min of upper limb exercise followed by 10 min lower limb exercise using a minicycle, 40%–70% of target HR or 13–15 in Borg scale, 3 days/week for 6 months	Beneficial effect	Clawson et al. (2018)
Aerobic exercise therapy in cycle ergometer; 50 min, 3 sessions a week, for 16 weeks	No significant effect	van Groenestijn et al. (2019)
Reclining stepped aerobic exercise of moderate intensity. 70 steps/minute; 40 min, 3 sessions a week, for 4 weeks	No significant effect	Sivaramakrishnan and Madhavan (2019)
Ramp treadmill protocol. (exercise performed with the assistance of the ventilator Bipap STD®), for 12 months	Beneficial effects	Pinto et al. (1999)
Moderate aerobic exercise on a treadmill with non-invasive ventilation and body weight supporting system, 2 days/week, for 6 months	Beneficial effect	Braga et al. (2018)
Combined endurance and resistance training		
Moderate/high intensity strength and endurance exercises; 30 min, 7 sessions a week, for 2 weeks	No significative differences	Kato et al. (2018)
Submaximal aerobic exercise 65% HR and 80% strength RM; 50 min, 7 sessions a week, for 5 weeks	Beneficial effect	Merico et al. (2018)
Moderate/high intensity aerobic and strength exercise; 50 min, 3 sessions a week, for 12 weeks	Beneficial effect	Ferri et al. (2019)
High frequency aerobic and resistance training (5/week) vs aerobic exercise, low frequency (2/week); 45 min, for 10 weeks	No significative differences	Zucchi et al. (2019)

Krebs cycle. Administration of the swimming protocol was able to significantly increase the citrate synthase activity while reducing the malate dehydrogenase activity, thus maintaining ATP production capacity by mitochondria (Flis et al., 2019). In this way, swimming-training resulted neuroprotective and delayed muscle wasting, as demonstrated by the grip strength test (Flis et al., 2019). Moreover, the activation of the BDNF/TrkB neurotrophic signaling, which retrogradely modulate neurotransmission and protect neuromuscular junctions and motoneurons (Just-Borràs et al., 2020), together with the increased glutathione peroxidase activity (Dzik et al., 2021), could contribute, at least in part, to the beneficial effect of the swimming training protocol.

4 Exercise training protocols in ALS patients

In patients with ALS, various training protocols have been proposed to evaluate their potential beneficial effects. These protocols are summarized in Table 2. However, it is noteworthy

that these studies are constrained by the significant intrinsic heterogeneity among ALS patients. Furthermore, it is important to acknowledge that epidemiological studies conducted in this patient population frequently rely on retrospective investigations, which may introduce biases and potentially result in an overestimation or underestimation of activity levels.

The first exercise protocol on ALS patients was performed by Bohannon and colleagues (Bohannon, 1983); they reported an increase in static strength in the muscles of upper extremities, suggesting a beneficial effect of resistance training. These results were confirmed by Kitano (Kitano et al., 2018), showing that resistance and stretching exercise are safe and feasible for patients at early stage of ALS, especially in respiratory function. In 2017, Clawson and colleagues (Clawson et al., 2018) demonstrated that resistance training ameliorated patient function more than standard care (Bello-Haas et al., 2007). By comparing individuals who received 'standard care' with a group who underwent a strictly monitored exercise program (SMEP), it was shown that the SMEP group obtained beneficial effects from the training protocol (Lunetta et al., 2016). In particular, the SMEP group was further divided into three subgroups: one performing an active exercise program plus cycloergometer activity, a second subgroup performing only active exercise, and a third subgroup performing passive exercises. At a single 180-day endpoint of the study, a difference in the ALSFRS-R was observed between those who underwent the SMEP and those who received 'standard care', but not at earlier time-points. Although no effect on survival was demonstrated, the obtained results suggest that a strictly monitored exercise program may significantly reduce motor deterioration in ALS patients (Lunetta et al., 2016). The only study with negative results reported that did not attenuate disease progression with possible negative effects on skeletal muscle (observed by functionality, voluntary muscle activation and cross-sectional area), with loss of muscle strength and power (Jensen et al., 2017).

Collectively these studies indicate that resistance training increases muscle strength, power, and force. Although these parameters are fundamental to ameliorate the lifestyle, they do not reduce the disease progression.

In 2001, Drory and colleagues performed a comparison between a daily endurance exercise program and usual daily care (Drory et al., 2001). They noticed that a tailorized, moderate range of motion training displays a beneficial effect on muscle endurance and a mild, temporary positive effect on the motor deficit, disability, fatigue, and health-related quality of life (Sanjak et al., 2010). Endurance training was also shown to display an improvement in work capacity and gait function in ALS patients dependent on walking aids devices (Sanjak et al., 2010). The comparison of endurance exercise to SROM (Stretching/Range of Motion) revealed that this latter appeared safe and well tolerated, whereas endurance training appeared too vigorous and had lower overall compliance (Clawson et al., 2018). Van Groenestijn and colleagues (van Groenestijn et al., 2019) proposed for the first-time aerobic exercise therapy (AET). Due to the small number of patients who completed the exercise protocol, they concluded that AET should not be included in usual care therapy. As specified in the United Kingdom clinical guidelines for motor neuron disease, the "usual care" comprises medications and treatments such as non-invasive ventilation, physiotherapy and gastrostomy, and access to other hospital-based and community-based services, including equipment and adaptations, orthotics, respiratory, gastroenterology, clinical psychology, neuropsychology, and counselling, as well as social care services. Even if a stepping exercise was well tolerated by all study participants, no significant improvements in clinical parameters were documented (Sivaramakrishnan and Madhavan, 2019).

In general, the beneficial effects of endurance exercise appear enhanced using non-invasive ventilation.

To maximize the beneficial effects of exercise therapy, a few clinical trials have included a combination of aerobic and resistance training protocols. However, they did not show differences in comparison to usual care (Kato et al., 2018; Merico et al., 2018; Ferri et al., 2019; Zucchi et al., 2019).

5 Exercise impact on skeletal muscle metabolism

Physical exercise impacts on specific energy fuels depending on the intensity and duration. An acute bout of exercise leads to the activation of signaling pathways driving short-term and long-term systemic adaptations. As first, breakdown of ATP and phosphocreatine, provides a substantial quantity of high-energy phosphate in a remarkably short time, typically within milliseconds. If the physical activity last up to 1 min, also anaerobic glycolysis is used for energy production, giving rise to lactate by lactate-dehydrogenase (LDH). Glycolysis rate-limiting enzyme phosphofructokinase (PFK) activation is promoted by the increase of glucose cytoplasmatic concentration. Eventually, for exercise longer than 1 min, oxidative phosphorylation is the major ATP-generating pathway. Increased metabolic demands are accomplished through mechanisms that are mostly mediated by the sympathetic nervous system, such as lipolysis, mobilization of hepatic glycogen stores, that favor the increase in available glucose and free fatty acids for the exercising skeletal muscles (Hawley et al., 2014). Chronic aerobic exercise upregulates oxidative metabolism in a time-dependent manner, immediately reverted to baseline following abstinence from exercise. Indeed, skeletal muscles undergo multiple adaptive mechanisms, including increased mitochondrial biogenesis, expression of fatty acid transporters, activity of oxidative enzymes and of those involved in the electron transport chain in the mitochondria, contributing to skeletal muscle hypertrophy (Hawley et al., 2014).

Changes in mitochondrial bioenergetics might underlie defects in exercise capacity of ALS muscles. As anticipated above, a switch from glucose to lipid metabolism occurs early in the disease process and prior to any detectable motor and clinical symptoms in animal models (Scaricamazza et al., 2020). Thus, the decreased capacity to tolerate acute physical exercise that solicits anaerobic metabolism in muscle occurs before muscle weakness or denervation (Palamiuc et al., 2015; Scaricamazza et al., 2020). This low resistance to intense exercise seems in contrast with the enhanced endurance capacity observed during acute aerobic exercise. This observation suggests that ALS mice acquire new properties in muscle fibers that enhance global aerobic capacity and promote endurance ability (Pradat et al., 2010; Palamiuc et al., 2015).

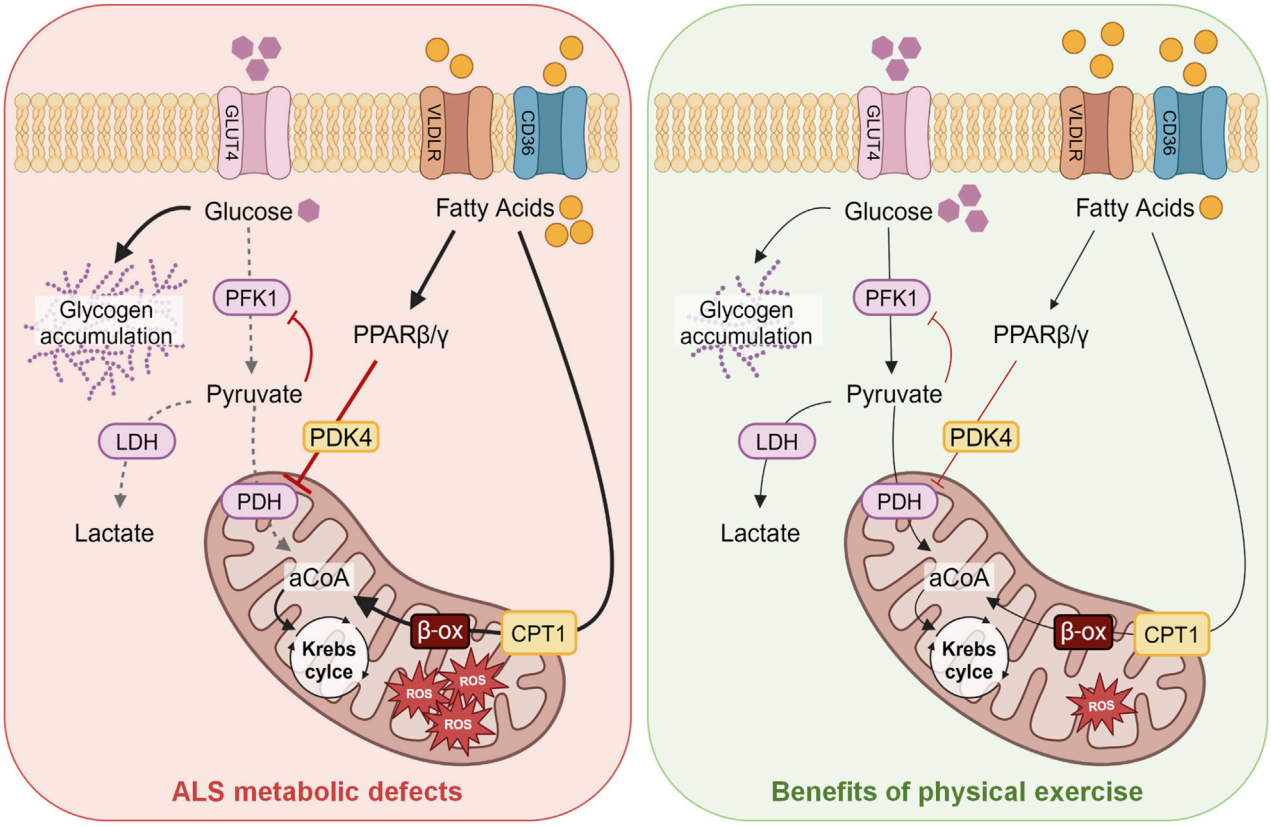

FIGURE 1
Schematic model of the energetic metabolism of ALS skeletal muscles and their changes induced by swimming-training. The main alterations in ALS skeletal muscles observed in the glycolytic and lipidic metabolism are shown on the left (red panel), whereas the improvements in energetic fuels induced by exercise protocols, particularly swimming, are schematized on the right (green panel). Abbreviations: GLUT4, glucose transporter 4; PFK1, phosphofructokinase 1; LDH, lactate dehydrogenase; PDH, pyruvate dehydrogenase; VLDLR, very-low-density lipoprotein receptor; PPAR β/γ, peroxisome proliferator-activated receptor; PDK4, pyruvate dehydrogenase lipoamide kinase isozyme 4; CPT1, carnitine palmitoyltransferase 1; aCoA, acetyl coenzyme A; ROS, reactive oxygen species; ALS, amyotrophic lateral sclerosis.

Endurance exercise is supported by slow-twitch oxidative type I fibers, while intense exercise is supported by fast-twitch glycolytic type IIb fibers (Bassel-Duby and Olson, 2006). Remarkably, a switch in fiber type, from glycolytic to oxidative, has been described in ALS patients (Telerman-Toppet and Coërs, 1978) as well as and in mice (Deforges et al., 2009), thus explaining the different exercise capacity. The increase in endurance capacity in ALS mice might underlie a profound alteration of fuel preference in muscle fibers, paralleling altered glucose metabolism. The rate-limiting enzyme of the glycolysis is represented by the phosphofructokinase-1 (PFK1), whose inhibition leads to an increase in glycogen synthase activity and glycogen accumulation in skeletal muscle, which is in fact a characteristic of a muscle subjected to endurance training (Vestergaard, 1999), but also a characteristic of ALS mice (Palamiuc et al., 2015) (Figure 1, left panel). At symptomatic stages of disease in ALS mouse models, a fiber type switching toward more oxidative metabolism (Deforges et al., 2009) is paralleled by the increased expression of genes encoding enzymes involved in lipid metabolism (Dupuis et al., 2004; Fergani et al., 2007), which may support lipid mobilization and uptake. This can lead to increased β-oxidation by-products, thus activating the pyruvate dehydrogenase lipoamide kinase isozyme 4 (PDK4) and inhibiting pyruvate dehydrogenase (PDH) activity (Denton et al., 1975). In line with this observation, PDK4 is strongly induced in ALS mouse models and patients (Palamiuc et al., 2015). PDK4 phosphorylates PDH and inhibits the entry of pyruvate into the Krebs cycle, thus hampering glucose oxidation (Denton et al., 1975). Increased β-oxidation of fatty acids leads to the generation of lipid by-products that contribute to ROS production (Aon et al., 2014). At later stages of the disease, reduced activities of both PFK1 and glycogen synthase, together with an increase in the glycogen stores and reduced levels of pyruvate, give evidence of the inhibition of the glycolytic pathway (Figure 1, left panel). In contrast, the lipid pathway is stimulated (Dupuis et al., 2004), as documented by the increased lipid clearance in ALS mice (Fergani et al., 2007) and patients (Pradat et al., 2010).

The upregulation of the muscle-specific peroxisome proliferator-activated receptor β/δ (PPARβ/δ) could explain the shift from fast-twitch to slow-twitch fibers (Wang et al., 2004). PPARβ/δ acts as a metabolic regulator in several tissues; its activation, as upon physical exercise or long-term fasting, promotes fatty acid oxidation in skeletal muscle and induces a switch toward type I muscle fibers, resembling the fiber type transition induced by endurance training (Wang et al., 2004). Activation of PPARβ/δ enhances mitochondrial capacity and fat

oxidation in the skeletal muscle (Figure 1). Thus, the metabolic imbalance in muscle fibers of ALS mice and patients represents an early event; glycolytic muscle fibers become progressively unable to use glucose as an energy substrate, switching to lipid use to maintain energy supply, as reported by Steyn and colleagues that described a decreased metabolic flexibility in muscle fibers obtained from ALS patients (Steyn et al., 2020). In particular, the authors observed an increased propensity to use lipids with respect to glucose as energy source in skeletal muscle of ALS patients. The restoration of metabolic equilibrium in glycolytic muscle fibers induced by exercise, particularly swimming endurance training, could protect muscle mitochondria and hamper oxidative stress, also preventing denervation and atrophy. Remarkably, physical exercise, particularly swimming, can lead to increased glucose uptake also by upregulating GLUT4 expression, thus contributing to improve glycolysis, as revealed by the enhanced lactate production (Desseille et al., 2017). This suggests that pyruvate is used to enhance the anaerobic glycolytic pathway in ALS muscles. Therefore, a tailored physical exercise could help in restoring the correct glucose uptake by skeletal muscle, decreasing insulin or glucose resistance observed in both mouse models and patients (Dobrowolny et al., 2018; Scaricamazza et al., 2020). The use of glucose instead of fatty acids might decrease mitochondrial overwhelming with a positive impact on oxidative stress. Conversely, reinforcing the oxidative pathway by running-based training seems to contribute to altering energetic metabolism in ALS muscle and to favor the neurodegenerative process.

6 Concluding remarks

ALS is a complex neurodegenerative disease where several pathological mechanisms contribute to the selective death of motor neurons, including glutamate excitotoxicity, protein aggregation, oxidative stress, neuroinflammation and dysregulation of energy metabolism (Tefera et al., 2021). In particular, overproduction of ROS overwhelms the protective defense mechanism of cells, in particular, thus contributing to neurodegenerative diseases, including ALS. These events, in turn, can cause mitochondrial dysfunction and excitotoxicity. Direct consequences of the redox imbalance are lipid peroxidation, oxidation of proteins, DNA damage, and interference of ROS with signal transduction pathways. These consequences become even more harmful when associated with inherited genetic variations. Therefore, therapeutic strategies should aim at reducing free-radical formation, and at improving clearance. On the other hand, cellular adaptations to redox imbalance can get cells used to low doses of ROS, thus buffering cellular response and contributing to mitigate direct consequences of ROS interference. In fact, beyond inducing oxidative stress, ROS play a crucial role in maintaining cellular function. In the skeletal muscle, exercise-induced ROS can promote adaptive changes, including enhanced protein synthesis, activation of insulin signaling, mitochondrial biogenesis, regulation of muscle development, gene expression, and positive modulation of antioxidants (Ristow et al., 2009). Hence, repeated exposure to sublethal stress, such as during exercise training, can enhance stress resistance and ultimately increase survival rates due to the hormesis process (Merry and Ristow, 2016). To this regard, the intake of vitamins C and E is sufficient to reduce the positive effects of exercise via ROS-related induction of PPARγ, PGC1α, and PGC1β, as well as the ROS-detoxifying enzymes, indicating that the removal of ROS can reduce, or even inhibit, the health benefits of exercise (Ristow et al., 2009). These reported findings highlight the role of ROS as signaling molecules in promoting skeletal muscle health during exercise.

Several exercise protocols have been tested in ALS patients and mouse models of the disease. Besides the neuroprotective effects exerted by any physical activity, swimmimg-based protocols displayed the most positive outcomes in mice. Particularly, swimming-based protocol resulted in a remarkable increase in the lifespan and neuroprotection, associated with changes in skeletal muscle energetic metabolism, leading to energetic fuel shifts toward glucose (Deforges et al., 2009). Although swimming is suggested as an advantageous type of exercise in many neurological disorders (Ayán and Cancela, 2012), its beneficial role has not yet been experimentally validated in ALS patients.

Overall, endurance training with a supplemental support such as ventilation or weight support seems to have positive effects on respiratory capacity, functionality, and physical performance in ALS patients, but further studies investigating the therapeutic benefits of exercise with a larger number of participants are needed to confirm these findings.

Future work should also consider the interaction of exercise with the full spectrum of genetic changes linked to ALS, both in humans and in mice. To date, however, small sample sizes, non-representative control populations, heterogeneous disease-stage of patients, have strongly affected the interpretation of results. Thus, while promising, more pre-clinical and clinical studies are needed to elucidate the role of exercise training in ALS patients.

In conclusion, disturbances in energetic metabolism are clearly linked to the selective vulnerability of motor neurons, thus, a therapeutic strategy tackling energy metabolism through tailored exercise protocols in ALS patients may pave the ground for future combined therapeutic interventions.

Author contributions

GF: Investigation, Writing–original draft. SS: Writing–original draft, Investigation. AF: Writing–original draft, Funding acquisition, Project administration, Writing–review and editing. CV: Writing–original draft, Writing–review and editing, Project administration. MP: Project administration, Writing–original draft, Writing–review and editing, Conceptualization, Funding acquisition, Supervision.

Funding

The author(s) declare that financial support was received for the research, authorship, and/or publication of this article. This work was supported by grants from the Associazione Italiana Ricerca sul

Cancro (AIRC) IG21877 (to MPP), from "CNR IFT DBA.AD005.225 - NUTRAGE-FOE2021" (to AF), and Italian Ministry of Health RF-2019-12369105 to AF, and from Ministry of Health "Ricerca Corrente" to Fondazione Santa Lucia. GF was supported by a PhD Scholarship funded by EU-PNRR-Ministerial Decree 351 2022-Next Generation EU.

Conflict of interest

The authors declare that the research was conducted in the absence of any commercial or financial relationships that could be construed as a potential conflict of interest.

The author(s) declared that they were an editorial board member of Frontiers, at the time of submission. This had no impact on the peer review process and the final decision.

Publisher's note

References

Akçimen, F., Lopez, E. R., Landers, A., Nath, A., Chiò, A., Chia, R., et al. (2023). Amyotrophic lateral sclerosis: translating genetic discoveries into therapies. *Nat. Rev. Genet.* 24, 642–658.

Al-Chalabi, A., and Hardiman, O. (2013). The epidemiology of ALS: a conspiracy of genes, environment and time. *Nat. Rev. Neurol.* 9, 617–628. doi:10.1038/nrneurol.2013.203

Angelini, C., and Siciliano, G. (2021). An updated review on the role of prescribed exercise in the management of Amyotrophic lateral sclerosis. *Expert Rev. Neurother.* 21, 871–879. doi:10.1080/14737175.2021.1951706

Aon, M. A., Bhatt, N., and Cortassa, S. C. (2014). Mitochondrial and cellular mechanisms for managing lipid excess. *Front. Physiol.* 5, 282. doi:10.3389/fphys.2014.00282

Ayán, C., and Cancela, J. (2012). Feasibility of 2 different water-based exercise training programs in patients with Parkinson's disease: a pilot study. *Arch. Phys. Med. Rehabil.* 93, 1709–1714. doi:10.1016/j.apmr.2012.03.029

Bassel-Duby, R., and Olson, E. N. (2006). Signaling pathways in skeletal muscle remodeling. *Annu. Rev. Biochem.* 75, 19–37. doi:10.1146/annurev.biochem.75.103004.142622

Bello-Haas, V. D., Florence, J. M., Kloos, A. D., Scheirbecker, J., Lopate, G., Hayes, S. M., et al. (2007). A randomized controlled trial of resistance exercise in individuals with ALS. *Neurology* 68, 2003–2007. doi:10.1212/01.wnl.0000264418.92308.a4

Bensimon, G., Lacomblez, L., and Meininger, V. (1994). A controlled trial of riluzole in amyotrophic lateral sclerosis. ALS/Riluzole Study Group. *N. Engl. J. Med.* 330, 585–591. doi:10.1056/NEJM199403033300901

Bohannon, R. W. (1983). Results of resistance exercise on a patient with amyotrophic lateral sclerosis. A case report. *Phys. Ther.* 63, 965–968. doi:10.1093/ptj/63.6.965

Braga, A. C .M., Pinto, A., Pinto, S., and de Carvalho, M. (2018). The role of moderate aerobic exercise as determined by cardiopulmonary exercise testing in ALS. *Neurol. Res. Int.* 8218697. doi:10.1155/2018/8218697

Carreras, I., Yuruker, S., Aytan, N., Hossain, L., Choi, J. K., Jenkins, B. G., et al. (2010). Moderate exercise delays the motor performance decline in a transgenic model of ALS. *Brain Res.* 1313, 192–201. doi:10.1016/j.brainres.2009.11.051

Carrì, M. T., Valle, C., Bozzo, F., and Cozzolino, M. (2015). Oxidative stress and mitochondrial damage: importance in non-SOD1 ALS. *Front. Cell Neurosci.* 9, 41. doi:10.3389/fncel.2015.00041

Caspersen, C. J., Powell, K. E., and Christenson, G. M. (1985). Physical activity, exercise, and physical fitness: definitions and distinctions for health-related research. *Public Health Rep.* 100, 126–131.

Chapman, L., Cooper-Knock, J., and Shaw, P. J. (2023). Physical activity as an exogenous risk factor for amyotrophic lateral sclerosis: a review of the evidence. *Brain* 146, 1745–1757. doi:10.1093/brain/awac470

Chio, A., Calvo, A., Dossena, M., Ghiglione, P., Mutani, R., and Mora, G. (2009). ALS in Italian professional soccer players: the risk is still present and could be soccer-specific. *Amyotroph. Lateral Scler.* 10, 205–209. doi:10.1080/17482960902721634

Clawson, L. L., Cudkowicz, M., Krivickas, L., Brooks, B. R., Sanjak, M., Allred, P., et al. (2018). A randomized controlled trial of resistance and endurance exercise in amyotrophic lateral sclerosis. *Amyotroph. Lateral Scler. Front. Degener.* 19, 250–258. doi:10.1080/21678421.2017.1404108

Cozzolino, M., Ferri, A., and Carrì, M. T. (2008). Amyotrophic lateral sclerosis: from current developments in the laboratory to clinical implications. *Antioxid. Redox Signal* 10, 405–443. doi:10.1089/ars.2007.1760

Deforges, S., Branchu, J., Biondi, O., Grondard, C., Pariset, C., Lécolle, S., et al. (2009). Motoneuron survival is promoted by specific exercise in a mouse model of amyotrophic lateral sclerosis. *J. Physiol.* 587, 3561–3572. doi:10.1113/jphysiol.2009.169748

Deng, H. X., Hentati, A., Tainer, J. A., Iqbal, Z., Cayabyab, A., Hung, W. Y., et al. (1993). Amyotrophic lateral sclerosis and structural defects in Cu,Zn superoxide dismutase. *Science* 261, 1047–1051. doi:10.1126/science.8351519

Denton, R. M., Randle, P. J., Bridges, B. J., Cooper, R. H., Kerbey, A. L., Pask, H. T., et al. (1975). Regulation of mammalian pyruvate dehydrogenase. *Mol. Cell Biochem.* 9, 27–53. doi:10.1007/BF01731731

Desseille, C., Deforges, S., Biondi, O., Houdebine, L., D'amico, D., Lamazière, A., et al. (2017). Specific physical exercise improves energetic metabolism in the skeletal muscle of amyotrophic-lateral- sclerosis mice. *Front. Mol. Neurosci.* 10, 332. doi:10.3389/fnmol.2017.00332

Dobrowolny, G., Lepore, E., Martini, M., Barberi, L., Nunn, A., Scicchitano, B. M., et al. (2018). Metabolic changes associated with muscle expression of SOD1G93A. *Front. Physiol.* 9, 831. doi:10.3389/fphys.2018.00831

Drory, V. E., Goltsman, E., Reznik, J. G., Mosek, A., and Korczyn, A. D. (2001). The value of muscle exercise in patients with amyotrophic lateral sclerosis. *J. Neurol. Sci.* 191, 133–137. doi:10.1016/s0022-510x(01)00610-4

Dupuis, L., Gonzalez de Aguilar, J. L., Echaniz-Laguna, A., Eschbach, J., Rene, F., Oudart, H., et al. (2009). Muscle mitochondrial uncoupling dismantles neuromuscular junction and triggers distal degeneration of motor neurons. *PLoS One* 4, e5390. doi:10.1371/journal.pone.0005390

Dupuis, L., Oudart, H., René, F., Gonzalez de Aguilar, J. L., and Loeffler, J. P. (2004). Evidence for defective energy homeostasis in amyotrophic lateral sclerosis: benefit of a high-energy diet in a transgenic mouse model. *Proc. Natl. Acad. Sci. U. S. A.* 101, 11159–11164. doi:10.1073/pnas.0402026101

Dupuis, L., Pradat, P. F., Ludolph, A. C., and Loeffler, J. P. (2011). Energy metabolism in amyotrophic lateral sclerosis. *Lancet Neurol.* 10, 75–82. doi:10.1016/S1474-4422(10)70224-6

Dzik, K. P., Flis, D. J., Bytowska, Z. K., Karnia, M. J., Ziolkowski, W., and Kaczor, J. J. (2021). Swim training ameliorates hyperlocomotion of ALS mice and increases glutathione peroxidase activity in the spinal cord. *Int. J. Mol. Sci.* 22, 11614. doi:10.3390/ijms222111614

Elbasiouny, S. M., and Schuster, J. E. (2011). The effect of training on motoneuron survival in amyotrophic lateral sclerosis: which motoneuron type is saved? *Front. Physiol.* 2, 18. doi:10.3389/fphys.2011.00018

Fergani, A., Oudart, H., Gonzalez De Aguilar, J. L., Fricker, B., René, F., Hocquette, J. F., et al. (2007). Increased peripheral lipid clearance in an animal model of amyotrophic lateral sclerosis. *J. Lipid Res.* 48, 1571–1580. doi:10.1194/jlr.M700017-JLR200

Ferri, A., Lanfranconi, F., Corna, G., Bonazzi, R., Marchese, S., Magnoni, A., et al. (2019). Tailored exercise training counteracts muscle disuse and attenuates reductions in physical function in individuals with amyotrophic lateral sclerosis. *Front. Physiol.* 10, 1537. doi:10.3389/fphys.2019.01537

Flis, D. J., Dzik, K., Kaczor, J. J., Cieminski, K., Halon-Golabek, M., Antosiewicz, J., et al. (2019). Swim training modulates mouse skeletal muscle energy metabolism and ameliorates reduction in grip strength in a mouse model of amyotrophic lateral sclerosis. *Int. J. Mol. Sci.* 20, 233. doi:10.3390/ijms20020233

Flis, D. J., Dzik, K., Kaczor, J. J., Halon-Golabek, M., Antosiewicz, J., Wieckowski, M. R., et al. (2018). Swim training modulates skeletal muscle energy metabolism, oxidative stress, and mitochondrial cholesterol content in amyotrophic lateral sclerosis mice. *Oxid. Med. Cell Longev.* 2018, 5940748. doi:10.1155/2018/5940748

Fuller, K. N. Z., and Thyfault, J. P. (1985). Barriers in translating preclinical rodent exercise metabolism findings to human health. *J. Appl. Physiol.* 130, 182–192. doi:10.1152/japplphysiol.00683.2020

Golini, E., Marinelli, S., Pisu, S., De Angelis, F., Vacca, V., Rava, A., et al. (2023). Wheel running adversely affects disease onset and neuromuscular interplay in amyotrophic lateral sclerosis slow progression mouse model. *Curr. Neurovasc Res.* 20, 362–376. doi:10.2174/1567202620666230823095922

Harwood, C. A., McDermott, C. J., and Shaw, P. J. (2009). Physical activity as an exogenous risk factor in motor neuron disease (MND): a review of the evidence. *Amyotroph. Lateral Scler.* 10, 191–204. doi:10.1080/17482960802549739

Hawley, J. A., Hargreaves, M., Joyner, M. J., and Zierath, J. R. (2014). Integrative biology of exercise. *Cell* 159, 738–749. doi:10.1016/j.cell.2014.10.029

Hotta, K., Chen, B., Behnke, B. J., Ghosh, P., Stabley, J. N., Bramy, J. A., et al. (2017). Exercise training reverses age-induced diastolic dysfunction and restores coronary microvascular function. *J. Physiol.* 595, 3703–3719. doi:10.1113/JP274172

Hulisz, D. (2018). Amyotrophic lateral sclerosis: disease state overview. *Am. J. Manag. Care* 24, S320–S326.

Jensen, L., Djurtoft, J. B., Bech, R. D., Nielsen, J. L., Jørgensen, L. H., Schrøder, H. D., et al. (2017). Influence of resistance training on neuromuscular function and physical capacity in ALS patients. *J. Neurodegener. Dis.* 2017, 1436519. doi:10.1155/2017/1436519

Julian, T. H., Glascow, N., Barry, A. D. F., Moll, T., Harvey, C., Klimentidis, Y. C., et al. (2021). Physical exercise is a risk factor for amyotrophic lateral sclerosis: convergent evidence from Mendelian randomisation, transcriptomics and risk genotypes. *EBioMedicine* 68, 103397. doi:10.1016/j.ebiom.2021.103397

Just-Borràs, L., Hurtado, E., Cilleros-Mañé, V., Biondi, O., Charbonnier, F., Tomàs, M., et al. (2020). Running and swimming prevent the deregulation of the BDNF/TrkB neurotrophic signalling at the neuromuscular junction in mice with amyotrophic lateral sclerosis. *Cell Mol. Life Sci.* 77, 3027–3040. doi:10.1007/s00018-019-03337-5

Kaspar, B. K., Frost, L. M., Christian, L., Umapathi, P., and Gage, F. H. (2005). Synergy of insulin-like growth factor-1 and exercise in amyotrophic lateral sclerosis. *Ann. Neurol.* 57, 649–655. doi:10.1002/ana.20451

Kassa, R. M., Bonafede, R., Boschi, F., Bentivoglio, M., and Mariotti, R. (2017). Effect of physical exercise and anabolic steroid treatment on spinal motoneurons and surrounding glia of wild-type and ALS mice. *Brain Res.* 1657, 269–278. doi:10.1016/j.brainres.2016.12.029

Kato, N., Hashida, G., and Konaka, K. (2018). Effect of muscle strengthening exercise and time since onset in patients with amyotrophic lateral sclerosis: a 2-patient case series study. *Med. Baltim.* 97, e11145. doi:10.1097/MD.0000000000011145

Kemi, O. J., Loennechen, J. P., Wisløff, U., and Ellingsen, Ø. (1985). Intensity-controlled treadmill running in mice: cardiac and skeletal muscle hypertrophy. *J. Appl. Physiol.* 93, 1301–1309. doi:10.1152/japplphysiol.00231.2002

Kincaid, B., and Bossy-Wetzel, E. (2013). Forever young: SIRT3 a shield against mitochondrial meltdown, aging, and neurodegeneration. *Front. Aging Neurosci.* 5, 48. doi:10.3389/fnagi.2013.00048

Kirkinezos, I. G., Hernandez, D., Bradley, W. G., and Moraes, C. T. (2003). Regular exercise is beneficial to a mouse model of amyotrophic lateral sclerosis. *Ann. Neurol.* 53, 804–807. doi:10.1002/ana.10597

Kitano, K., Asakawa, T., Kamide, N., Yorimoto, K., Yoneda, M., Kikuchi, Y., et al. (2018). Effectiveness of home-based exercises without supervision by physical therapists for patients with early-stage amyotrophic lateral sclerosis: a pilot study. *Arch. Phys. Med. Rehabil.* 99, 2114–2117. doi:10.1016/j.apmr.2018.02.015

Liebetanz, D., Hagemann, K., von Lewinski, F., Kahler, E., and Paulus, W. (2004). Extensive exercise is not harmful in amyotrophic lateral sclerosis. *Eur. J. Neurosci.* 20, 3115–3120. doi:10.1111/j.1460-9568.2004.03769.x

Lunetta, C., Lizio, A., Sansone, V. A., Cellotto, N. M., Maestri, E., Bettinelli, M., et al. (2016). Strictly monitored exercise programs reduce motor deterioration in ALS: preliminary results of a randomized controlled trial. *J. Neurol.* 263, 52–60. doi:10.1007/s00415-015-7924-z

Masrori, P., and Van Damme, P. (2020). Amyotrophic lateral sclerosis: a clinical review. *Eur. J. Neurol.* 27, 1918–1929. doi:10.1111/ene.14393

Massett, M. P., and Berk, B. C. (2005). Strain-dependent differences in responses to exercise training in inbred and hybrid mice. *Am. J. Physiol. Regul. Integr. Comp. Physiol.* 288, R1006–R1013. doi:10.1152/ajpregu.00476.2004

Merico, A., Cavinato, M., Gregorio, C., Lacatena, A., Gioia, E., Piccione, F., et al. (2018). Effects of combined endurance and resistance training in Amyotrophic Lateral Sclerosis: a pilot, randomized, controlled study. *Eur. J. Transl. Myol.* 28, 7278. doi:10.4081/ejtm.2018.7278

Merry, T. L., and Ristow, M. (2016). Mitohormesis in exercise training. *Free Radic. Biol. Med.* 98, 123–130. doi:10.1016/j.freeradbiomed.2015.11.032

Miller, R. G., and Appel, S. H. (2017). Introduction to supplement: the current status of treatment for ALS. *Amyotroph. Lateral Scler. Front. Degener.* 18, 1–4. doi:10.1080/21678421.2017.1361447

Palamiuc, L., Schlagowski, A., Ngo, S. T., Vernay, A., Dirrig-Grosch, S., Henriques, A., et al. (2015). A metabolic switch toward lipid use in glycolytic muscle is an early pathologic event in a mouse model of amyotrophic lateral sclerosis. *EMBO Mol. Med.* 7, 526–546. doi:10.15252/emmm.201404433

Pedersen, W. A., and Mattson, M. P. (1999). No benefit of dietary restriction on disease onset or progression in amyotrophic lateral sclerosis Cu/Zn-superoxide dismutase mutant mice. *Brain Res.* 833, 117–120. doi:10.1016/s0006-8993(99)01471-7

Petrov, D., Mansfield, C., Moussy, A., and Hermine, O. (2017). ALS clinical trials review: 20 Years of failure. Are we any closer to registering a new treatment? *Front. Aging Neurosci.* 9, 68. doi:10.3389/fnagi.2017.00068

Pinto, A. C., Alves, M., Nogueira, A., Evangelista, T., Carvalho, J., Coelho, A., et al. (1999). Can amyotrophic lateral sclerosis patients with respiratory insufficiency exercise? *J. Neurol. Sci.* 169, 69–75. doi:10.1016/s0022-510x(99)00218-x

Pradat, P. F., Bruneteau, G., Gordon, P. H., Dupuis, L., Bonnefont-Rousselot, D., Simon, D., et al. (2010). Impaired glucose tolerance in patients with amyotrophic lateral sclerosis. *Amyotroph. Lateral Scler.* 11, 166–171. doi:10.3109/17482960902822960

Radak, Z., Chung, H. Y., and Goto, S. (2008b). Systemic adaptation to oxidative challenge induced by regular exercise. *Free Radic. Biol. Med.* 44, 153–159. doi:10.1016/j.freeradbiomed.2007.01.029

Radak, Z., Chung, H. Y., Koltai, E., Taylor, A. W., and Goto, S. (2008a). Exercise, oxidative stress and hormesis. *Ageing Res. Rev.* 7, 34–42. doi:10.1016/j.arr.2007.04.004

Radak, Z., Suzuki, K., Higuchi, M., Balogh, L., Boldogh, I., and Koltai, E. (2016). Physical exercise, reactive oxygen species and neuroprotection. *Free Radic. Biol. Med.* 98, 187–196. doi:10.1016/j.freeradbiomed.2016.01.024

Rebelo-Marques, A., De Sousa Lages, A., Andrade, R., Ribeiro, C. F., Mota-Pinto, A., Carrilho, F., et al. (2018). Aging hallmarks: the benefits of physical exercise. *Front. Endocrinol. (Lausanne)* 9, 258. doi:10.3389/fendo.2018.00258

Ripps, M. E., Huntley, G. W., Hof, P. R., Morrison, J. H., and Gordon, J. W. (1995). Transgenic mice expressing an altered murine superoxide dismutase gene provide an animal model of amyotrophic lateral sclerosis. *Proc. Natl. Acad. Sci. U. S. A.* 92, 689–693. doi:10.1073/pnas.92.3.689

Ristow, M., Zarse, K., Oberbach, A., Klöting, N., Birringer, M., Kiehntopf, M., et al. (2009). Antioxidants prevent health-promoting effects of physical exercise in humans. *Proc. Natl. Acad. Sci. U. S. A.* 106, 8665–8670. doi:10.1073/pnas.0903485106

Romijn, J. A., Coyle, E. F., Sidossis, L. S., Gastaldelli, A., Horowitz, J. F., Endert, E., et al. (1993). Regulation of endogenous fat and carbohydrate metabolism in relation to exercise intensity and duration. *Am. J. Physiol.* 265, E380–E391. doi:10.1152/ajpendo.1993.265.3.E380

Rosen, D. R., Siddique, T., Patterson, D., Figlewicz, D. A., Sapp, P., Hentati, A., et al. (1993). Mutations in Cu/Zn superoxide dismutase gene are associated with familial amyotrophic lateral sclerosis. *Nature* 362, 59–62. doi:10.1038/362059a0

Sahl, R. E., Andersen, P. R., Gronbaek, K., Morville, T. H., Rosenkilde, M., Rasmusen, H. K., et al. (2017). Repeated excessive exercise attenuates the anti-inflammatory effects of exercise in older men. *Front. Physiol.* 8, 407. doi:10.3389/fphys.2017.00407

Sanjak, M., Bravver, E., Bockenek, W. L., Norton, H. J., and Brooks, B. R. (2010). Supported treadmill ambulation for amyotrophic lateral sclerosis: a pilot study. *Arch. Phys. Med. Rehabil.* 91, 1920–1929. doi:10.1016/j.apmr.2010.08.009

Scaricamazza, S., Nesci, V., Salvatori, I., Fenili, G., Rosina, M., Gloriani, M., et al. (2024). Endurance exercise has a negative impact on the onset of SOD1-G93A ALS in female mice and affects the entire skeletal muscle-motor neuron axis. *Front. Pharmacol.* 15, 1360099. doi:10.3389/fphar.2024.1360099

Scaricamazza, S., Salvatori, I., Giacovazzo, G., Loeffler, J. P., Renè, F., Rosina, M., et al. (2020). Skeletal-muscle metabolic reprogramming in ALS-sod1g93a mice predates disease onset and is A promising therapeutic target. *iScience* 23, 101087. doi:10.1016/j.isci.2020.101087

Scarmeas, N., Shih, T., Stern, Y., Ottman, R., and Rowland, L. P. (2002). Premorbid weight, body mass, and varsity athletics in ALS. *Neurology* 59, 773–775. doi:10.1212/wnl.59.5.773

Sellami, M., Bragazzi, N. L., Aboghaba, B., and Elrayess, M. A. (2021). The impact of acute and chronic exercise on immunoglobulins and cytokines in elderly: insights from a critical review of the literature. *Front. Immunol.* 12, 631873. doi:10.3389/fimmu.2021.631873

Sivaramakrishnan, A., and Madhavan, S. (2019). Recumbent stepping aerobic exercise in amyotrophic lateral sclerosis: a pilot study. *Neurol. Sci.* 40, 971–978. doi:10.1007/s10072-019-03736-3

Smith, J. A. B., Murach, K. A., Dyar, K. A., and Zierath, J. R. (2023). Exercise metabolism and adaptation in skeletal muscle. *Nat. Rev. Mol. Cell Biol.* 24, 607–632. doi:10.1038/s41580-023-00606-x

Sorrells, A. D., Corcoran-Gomez, K., Eckert, K. A., Fahey, A. G., Hoots, B. L., Charleston, L. B., et al. (2009). Effects of environmental enrichment on the amyotrophic lateral sclerosis mouse model. *Lab. Anim.* 43, 182–190. doi:10.1258/la.2008.005090

Steyn, F. J., Li, R., Kirk, S. E., Tefera, T. W., Xie, T. Y., Tracey, T. J., et al. (2020). Altered skeletal muscle glucose-fatty acid flux in amyotrophic lateral sclerosis. *Brain Commun.* 2, fcaa154. doi:10.1093/braincomms/fcaa154

Tefera, T. W., Steyn, F. J., Ngo, S. T., and Borges, K. (2021). CNS glucose metabolism in Amyotrophic Lateral Sclerosis: a therapeutic target?. *Cell Biosci.* 11, 14.

Telerman-Toppet, N., and Coërs, C. (1978). Motor innervation and fiber type pattern in amyotrophic lateral sclerosis and in Charcot-Marie-Tooth disease. *Muscle Nerve* 1, 133–139. doi:10.1002/mus.880010205

Trist, B. G., Hilton, J. B., Hare, D. J., Crouch, P. J., and Double, K. L. (2021). Superoxide dismutase 1 in health and disease: how a frontline antioxidant becomes neurotoxic. *Angew. Chem. Int. Ed. Engl.* 60, 9215–9246. doi:10.1002/anie.202000451

van Groenestijn, A. C., Schröder, C. D., van Eijk, R. P. A., Veldink, J. H., Kruitwagen-van Reenen, E. T., Groothuis, J. T., et al. (2019). Aerobic exercise therapy in ambulatory patients with ALS: a randomized controlled trial. *Neurorehabil Neural Repair* 33, 153–164. doi:10.1177/1545968319826051

van Loon, L. J., Greenhaff, P. L., Constantin-Teodosiu, D., Saris, W. H., and Wagenmakers, A. J. (2001). The effects of increasing exercise intensity on muscle fuel utilisation in humans. *J. Physiol.* 536, 295–304. doi:10.1111/j.1469-7793.2001.00295.x

Veldink, J. H., Bär, P. R., Joosten, E. A., Otten, M., Wokke, J. H., and van den Berg, L. H. (2003). Sexual differences in onset of disease and response to exercise in a transgenic model of ALS. *Neuromuscul. Disord.* 13, 737–743. doi:10.1016/s0960-8966(03)00104-4

Vestergaard, H. (1999). Studies of gene expression and activity of hexokinase, phosphofructokinase and glycogen synthase in human skeletal muscle in states of altered insulin-stimulated glucose metabolism. *Dan. Med. Bull.* 46, 13–34.

Vina, J., Sanchis-Gomar, F., Martinez-Bello, V., and Gomez-Cabrera, M. C. (2012). Exercise acts as a drug; the pharmacological benefits of exercise. *Br. J. Pharmacol.* 167, 1–12. doi:10.1111/j.1476-5381.2012.01970.x

Wang, Y. X., Zhang, C. L., Yu, R. T., Cho, H. K., Nelson, M. C., Bayuga-Ocampo, C. R., et al. (2004). Regulation of muscle fiber type and running endurance by PPARdelta. *PLoS Biol.* 2, e294. doi:10.1371/journal.pbio.0020294

Waters, R. E., Rotevatn, S., Li, P., Annex, B. H., and Yan, Z. (2004). Voluntary running induces fiber type-specific angiogenesis in mouse skeletal muscle. *Am. J. Physiol. Cell Physiol.* 287, C1342–C1348. doi:10.1152/ajpcell.00247.2004

Wyckelsma, V. L., Levinger, I., McKenna, M. J., Formosa, L. E., Ryan, M. T., Petersen, A. C., et al. (2017). Preservation of skeletal muscle mitochondrial content in older adults: relationship between mitochondria, fibre type and high-intensity exercise training. *J. Physiol.* 595, 3345–3359. doi:10.1113/JP273950

Zucchi, E., Vinceti, M., Malagoli, C., Fini, N., Gessani, A., Fasano, A., et al. (2019). High-frequency motor rehabilitation in amyotrophic lateral sclerosis: a randomized clinical trial. *Ann. Clin. Transl. Neurol.* 6, 893–901. doi:10.1002/acn3.765

frontiers | Frontiers in Cell and Developmental Biology

TYPE Original Research
PUBLISHED 23 December 2024
DOI 10.3389/fcell.2024.1476007

OPEN ACCESS

EDITED BY
Shoulong Deng,
Chinese Academy of Medical Sciences and Peking Union Medical College, China

REVIEWED BY
Asuncion Romero-Molina,
Consultant, Spain
Rahul Kumar,
Roswell Park Comprehensive Cancer Center, United States

*CORRESPONDENCE
Julita Kulbacka,
julita.kulbacka@umw.edu.pl

RECEIVED 04 August 2024
ACCEPTED 06 December 2024
PUBLISHED 23 December 2024

CITATION
Radzka J, Gizak A, Drąg-Zalesińska M, Haczkiewicz-Leśniak K, Kulus M, Szewczyk A, Szlasa W, Podhorska-Okołów M and Kulbacka J (2024) Efficacy of natural NF-κB inhibitors in the treatment of fibrosarcoma: an in vitro model study.
Front. Cell Dev. Biol. 12:1476007.
doi: 10.3389/fcell.2024.1476007

Efficacy of natural NF-κB inhibitors in the treatment of fibrosarcoma: an in vitro model study

Justyna Radzka[1], Agnieszka Gizak[1], Małgorzata Drąg-Zalesińska[2], Katarzyna Haczkiewicz-Leśniak[3], Michał Kulus[3], Anna Szewczyk[4,5], Wojciech Szlasa[4], Marzenna Podhorska-Okołów[3] and Julita Kulbacka[4,5]*

[1]Department of Molecular Physiology and Neurobiology, Faculty of Biology, University of Wroclaw, Wroclaw, Poland, [2]Division of Histology and Embryology, Department of Human Morphology and Embryology, Faculty of Medicine, Wroclaw Medical University, Wroclaw, Poland, [3]Division of Ultrastructure Research, Department of Human Morphology and Embryology, Wroclaw Medical University, Wroclaw, Poland, [4]Department of Molecular and Cellular Biology, Faculty of Pharmacy, Wroclaw Medical University, Wroclaw, Poland, [5]Department of Immunology and Bioelectrochemistry, State Research Institute Centre for Innovative Medicine, Vilnius, Lithuania

Introduction: NF-κB plays a pivotal role in the progression of cancers, including myosarcomas such as fibrosarcoma. Plants possess considerable potential for the provision of chemotherapeutic effects against cancer. The present study assessed, among others, the cytotoxicity, migration capacity and DNA damage induced by several natural compounds (berberine, curcumin, biochanin A, cucurbitacin E (CurE) and phenethyl caffeic acid (CAPE)) in cancer cells (WEHI-164) and normal muscle cells (L6).

Methods: IC50 parameter was determined for all substances after 24-hour incubation. Molecular docking studies were performed to assess compound binding to cytoskeletal proteins. Neutral comet assay and immunocytochemical analysis were used to assess the intensity of apoptosis, and transmission electron microscopy was employed to validate these results at the ultrastructural level.

Results and Discussion: The results showed that the tested compounds had a significantly increased cytotoxic effect on cancer cells compared to normal cells. Furthermore, molecular docking studies indicated that CAPE, biochanin A, and CurE could inhibit actin polymerization, suggesting their potential role in disrupting the cytoskeleton of cancer cells. Increased expression of caspase-3 and PARP-1 in WEHI-164 cells after treatment indicated the induction of apoptosis. Transmission electron microscopy confirmed the presence of cellular stress and vacuolation in cells treated with these compounds, with more pronounced effects observed in cancer cells compared to normal cells. The results indicate that natural NF-κB inhibitors may be capable of selectively targeting cancer cells, reducing their viability and inducing apoptosis while sparing normal cells. This selectivity is of great importance for the development of safer anticancer therapies. The results of this research support the hypothesis that these natural compounds may be effective anticancer agents, particularly in the treatment of fibrosarcoma. Further, in

vivo studies and clinical trials are required to gain a full understanding of their mechanisms of action and potential synergies with existing chemotherapeutic agents.

KEYWORDS

muscle cancer, berberine, cucurbitacin E (CurE), curcumin, biochanin A, caffeic acid phenethyl ester (CAPE)

1 Introduction

Cancer is currently a significant public health issue, ranking among the leading causes of death worldwide. Approximately 70% of cancer-related deaths occur in developing nations. According to estimates by the International Agency for Research on Cancer (IARC), the annual number of new cancer cases is projected to increase to around 21.7 million by 2030, with deaths reaching 13 million (Dalton et al., 2019). Among the various strategies for cancer treatment, chemotherapy is widely recognized as one of the most commonly used methods to prevent and treat cancer. However, current chemotherapeutic drugs have significant side effects and can lead to acquired drug resistance (Srivastava et al., 2016). Therefore, it is imperative to identify new, effective, and less toxic therapeutic agents for the treatment of cancer. Plants possess considerable potential for the provision of chemotherapeutic effects against cancer. Over 60% of anti-cancer drugs have been derived from natural sources, including plants, microorganisms, and marine organisms (Dey et al., 2019). The research presented in this work makes use of a number of substances derived from natural sources. Biochanin A (5,7-dihydroxy-4′-methoxyisoflavone) is an isoflavone that can be found, among others, in red clover (*Trifolium pratense* L.) (Yu et al., 2019). Biochanin A has been demonstrated to inhibit epithelial-mesenchymal transition and to reduce the proliferation rate of lung cancer cells. This is achieved by activating the Bcl-2 and caspase-3 pathways, in addition to regulating the expression of cell cycle-related proteins (Y. Li et al., 2018). The polyphenol compound curcumin, derived from the spice turmeric (*Curcuma longa*), has been demonstrated to inhibit the nuclear factor kappa-light-chain-enhancer of activated B cells (NF-κB) signalling pathway in a range of cancer types, including rhabdomyosarcoma. As a naturally occurring chemotherapeutic agent, curcumin has the potential to prevent and slow the progression of carcinogenesis. Additionally, it exhibits antioxidant and anti-inflammatory properties. The inhibition of factors responsible for cell proliferation and the inhibition of apoptosis, such as COX-2, AP-1, and NF-κB, is likely to occur as a result of the prevention of IκB phosphorylation by curcumin (Radzka et al., 2023). Berberine is a compound belonging to the isoquinoline alkaloid group that occurs naturally in a number of plant species, including those belonging to the Annonaceae, Berberidaceae, and Menispermaceae genera (Neag et al., 2018). Berberine exerts its effect by inhibiting the phosphorylation of the nuclear factor IκBα, which is responsible for activating NF-κB. Furthermore, evidence indicates that berberine treatment impairs the phosphorylation of the NF-κB subunit transcription factor p65. Berberine has been demonstrated to possess anti-cancer properties, whereby it downregulates caspase-1/IL-1β and also inhibits the cell cycle at the G1 phase in RMS cells (Jin et al., 2017). Caffeic acid phenethyl ester (CAPE) is a component identified in propolis. A substantial body of scientific literature attests to the antioxidant, anti-inflammatory, and cytotoxic effects of CAPE on cancer cells. It has been demonstrated that CAPE can inhibit NF-κB signaling by preventing the activation of upstream kinases, including IκB kinase (IKK) and TGF-β-activated kinase (TAK1), which are involved in the activation of the NF-κB pathway (Wang et al., 2010). Furthermore, evidence indicates that caffeic acid can inhibit the nuclear translocation of NF-κB and its binding to DNA, which are crucial steps in the transcriptional activation of NF-κB target genes (Abdel-Latif et al., 2005). Cucurbitacin E (CurE) is a triterpenoid compound that has been identified in a number of different plant species, including bitter melon (*Momordica charantia*) and cucumber (*Cucumis sativus*) (Chanda et al., 2020). This compound has been shown to modulate NF-κB signaling by inhibiting its activation and nuclear translocation (Qiao et al., 2013). Cucurbitacin E has been demonstrated to inhibit TNF-α-induced phosphorylation of inflammatory cytokines by modulating the NF-κB pathway. Additionally, cucurbitacin E inhibits the PI3K/Akt/mTOR pathway and the epithelial-mesenchymal transition (EMT) in osteosarcoma cells (Jia et al., 2015).

The NF-κB factor has been identified as the regulator of genes involved in tumour promotion, including those related to cell proliferation, angiogenesis, and adhesion. Furthermore, the activation of NF-κB has been demonstrated to influence the production of prostaglandins through the COX2 protein, which is overexpressed in a number of different types of cancer (Colotta et al., 2009). In neoplastic tissues, where elevated levels of the NF-κB factor are observed, there is an accumulation of pro-inflammatory cytokines, which contribute to the creation of a pro-neoplastic environment. Prolonged inflammation results in genomic instability and the emergence of genetic mutations that promote the formation and development of tumours (Elinav et al., 2013). Fibrosarcoma, an aggressive and poorly understood form of soft tissue sarcoma, poses significant therapeutic challenges, and recent evidence suggests that the NF-κB pathway may play a key role in its progression or angiogenesis (46). In this study, we demonstrated the effects of naturally occurring NF-κB inhibitors on fibrosarcoma cells, a cancer type where NF-κB's role has not been extensively characterised in the context of these specific inhibitors. Although previous studies have investigated the activity of these compounds in various cancer models, their effects on fibrosarcoma remain underexplored, representing an important area of investigation. Fibrosarcoma is a particularly aggressive form of soft tissue sarcoma with a paucity of efficacious therapeutic options. Emerging evidence suggests that the NF-κB pathway plays a crucial role in its progression. By targeting NF-κB in fibrosarcoma, our objective is to provide new insights into potential therapeutic approaches for this malignancy. Apoptotic genes, including FLICE

inhibitory protein, survivin, XIAP, c-IAP1/2 inhibitor, and the Bcl-2 family of proteins, are overexpressed in numerous types of cancer cells. The NF-κB factor induces this overexpression. It is therefore postulated that NF-κB plays a role in the regulation of anti-apoptotic mechanisms in the context of tumour formation (Kucharczak et al., 2003). A study of human prostate cancer cells (PC-3M cell line) has demonstrated that NF-κB plays a role in angiogenesis, invasion, and metastasis by regulating vascular endothelial growth factor (VEGF) and matrix metalloproteinases (MMP) (Huang et al., 2001). It has been demonstrated that the NF-κB factor exerts an influence on the resistance of cells to a range of chemotherapeutic agents. NF-κB plays a role in regulating the expression of the mdr1 gene, which is responsible for producing P-glycoprotein (P-gp). P-glycoprotein is a plasma membrane-associated multidrug transporter that affects the efflux of chemotherapy drugs, thereby contributing to treatment resistance (Wang et al., 2015). It has been demonstrated that NF-κB inhibits P-glycoprotein expression and may reactivate chemosensitivity. The involvement of the NF-κB factor in the degradation of muscle proteins has been demonstrated by research using cell cultures and in in vivo studies on laboratory animals (Wyke et al., 2004). In the study conducted by Moore–Carrasco et al., rats with hepatocellular carcinoma (AH-130 cell line) were treated with an NF-κB inhibitor (SP100030) and an activator protein-1 (AP-1) activator. The treatment was found to be effective in addressing skeletal muscle atrophy (Moore-Carrasco et al., 2007). Muscle wasting is a common occurrence in individuals of advanced age and those suffering from pathological conditions such as cancer. A study using a murine model indicated that the levels of NF-κB were elevated in the skeletal muscle tissues of animals with Lewis Lung Cancer (LLC). The study demonstrated that the transgenic overexpression of the super-repressor mutant protein IκBα (IκBαSR) resulted in a significant reduction in skeletal muscle and body weight loss in mice with LLC, which was achieved by inhibiting NF-κB activity (Cai et al., 2004). Recently, there has been a surge in interest in fructose 1,6-bisphosphatase (FBP) in the scientific community. This is a consequence of research which has demonstrated that FBP not only regulates the synthesis of glucose and glycogen from carbohydrate precursors, but also impacts (in a non-catalytic manner) a variety of cellular processes thanks to interactions with numerous proteins, e.g., mitochondrial VDAC, ANT, and ATP synthase, CAMK2, and transcription factors HIF1α and NF-κB. As a result of these interactions, FBP exerts influence over a number of cellular processes, including cell cycle-related events, mitochondrial biogenesis and membrane polarization, microtubule stability, glycolytic enzyme expression, synaptic plasticity, and even the progression of cancer (Gizak et al., 2012; Pirog et al., 2014). Mammalian tissues exhibit two distinct isoenzymes of fructose 1,6-bisphosphatase: liver FBP (FBP1) and muscle FBP (FBP2). The physiological function of FBP2 is modulated not only by its cellular expression levels but also by its oligomeric state. The dimeric form of FBP2 is associated with mitochondria, where it confers protection against cellular stress, while the tetrameric form is localized within the cell nucleus (Wiśniewski et al., 2017). FBP exerts negative effects on cell growth, and inhibits the progression of gastric cancer (Li et al., 2013). A study conducted in 2016 assessed the transcriptional levels of FBP1 and FBP2, revealing that elevated levels of FBP1 mRNA were associated with a favorable prognosis in gastric cancer. Subsequent verification of FBP1 protein expression confirmed that its overexpression correlated with improved clinical outcomes in patients with gastric cancer following surgical resection. Functional analyses further demonstrated that FBP1 expression significantly inhibited the proliferation and invasion of gastric cancer cells (Li et al., 2016). Additionally, FBP2 has been demonstrated to impede the progression of sarcomas by inhibiting mitochondrial biogenesis. It has been demonstrated that FBP2 impedes the progression of sarcoma by hindering mitochondrial biogenesis. Soft tissue sarcomas (STS) constitute a heterogeneous group of neoplasms that originate from connective tissues. Despite the considerable genetic heterogeneity observed among these tumours, an aberrant glucose metabolism is a common feature, although the underlying mechanism remains elusive. As was reported, FBP2 is absent in numerous STS subtypes, and reintroduction of FBP2 has been observed to significantly slow the growth of sarcomas. The researchers identified two distinct tumour-suppressing roles for FBP2 based on its location within the cell. Cytosolic FBP2 was observed to decrease glucose breakdown through its enzymatic function, while nuclear FBP2 was found to suppress a crucial factor involved in mitochondrial formation and function. The two roles of FBP2 result in a reduction in the energy supply to the cancer cells, which provides an explanation for the frequent loss of FBP2 in STS and its potential as a therapeutic target (Huangyang et al., 2020). In 2022, studies demonstrated that the chemically induced tetramerization of FBP2, resulting in a reduction of FBP2-mitochondria interactions, was associated with a range of changes in HL-1 cells. These included a decrease in mitochondrial membrane potential, disruption of the tubulin network and tubulin-mitochondria interactions, a marked reduction in mitochondrial membrane potential, and an increase in the speed and extent of mitophagy (Pietras et al., 2022). Furthermore, motor proteins, such as myosin, utilize ATP to generate force and facilitate movement along these actin filaments. This movement is essential for a number of cellular activities, including cell motility and structural integrity (Masters et al., 2017). The particular actions of myosins in relation to actin serve to illustrate their function in the organisation of the cytoskeleton and in the performance of cellular processes. Myosins, driven by the hydrolysis of ATP, interact with actin filaments, enabling their movement. This process is crucial for a range of cellular activities, including migration, division, and maintaining cellular shape (Nambiar et al., 2010). Recent research indicates that FBP2 is present in mitochondria under specific circumstances, where it interacts with a range of mitochondrial proteins. This mitochondrial localization is significant as it may affect processes such as fusion and fission, which are vital for maintaining the functionality and structural integrity of mitochondria. One investigation demonstrated that FBP2 interacts with proteins such as Voltage-Dependent Anion Channels (VDAC), Adenine Nucleotide Translocator (ANT), and elements of the mitochondrial ATP synthase complex. These interactions have the potential to influence mitochondrial membrane potential and regulate mitochondrial biogenesis. The presence of FBP2 in the mitochondria might also be involved in managing the mitochondrial response to stress, as well as processes such as mitochondrial trafficking and mitophagy (Collins, 2004). Furthermore, mitochondrial dynamics, which encompass the processes of fusion and fission, are vital for preserving mitochondrial structure, distribution, and functionality within cells. Fusion serves as a quality control mechanism, whereby the contents of partially damaged mitochondria are mixed. In contrast, fission is

essential for the removal of damaged mitochondrial components and the distribution of mitochondria during cell division. The involvement of FBP2 in these processes indicates that it may have a broader role in cellular homeostasis and the response to metabolic changes (Reynolds, 1963). The results of our studies presented here support the hypothesis that natural compounds acting as NF-κB inhibitors may be effective anticancer agents, particularly in the treatment of fibrosarcoma.

2 Materials and methods

2.1 Cell cultures

Two cell lines were used in in vitro studies: WEHI-164 - fibrosarcoma cells isolated from mice and L6 – myogenic cell line isolated from skeletal muscles of rat (ATCC®, LGC Standards, Teddington, UK). The WEHI-164 cells were grown in RPMI culture medium supplemented with 10% fetal bovine serum (FBS, HyClone, Logan, UT, USA) and 1% penicillin/streptomycin (Sigma-Aldrich, Merck-Millipore, Poznań, Poland). The L6 cells were grown in DMEM culture medium (Dulbecco's Modified Eagle's Medium, Sigma-Aldrich, Merck-Millipore, Poznan, Poland) with 10% fetal bovine serum (FBS, HyClone, Logan, UT, USA), 1% penicillin/streptomycin (Sigma-Aldrich, Merck-Millipore, Poznan, Poland) and 1% L–glutamine (ThermoFisher, Alab, Poland). Cell culture of both types of cell lines was carried out at 37°C and 5% CO_2. Both cell lines were negative for *mycoplasma* (MycoBlue *Mycoplasma* Detector, Vazyme Biotech, China). Cell passages were carried out 2–3 times a week when confluency was about 80%–90%. Cells were then removed from the flasks by trypsinization (trypsin 0.25% and EDTA 0.02%; IITD, Wroclaw, Poland) and washed with DPBS buffer (Sigma-Aldrich, Merck-Millipore, Poznan, Poland).

2.2 Preparation of drug solutions

CurE (number CAS 18444-66-1), biochanin A (number CAS 207-744-7), CAPE (number CAS 104594-70-9), curcumin (number CAS 458-37-7) and berberine (number CAS 633-65-8) were obtained from Sigma-Aldrich (Merck-Millipore, Poznan, Poland). All reagents were dissolved according to the manufacturer's protocols. DMSO was used as a solvent. Then, immediately before the tests, the substances were diluted in DMEM/RPMI to obtain the concentrations necessary for assays. CurE was diluted to concentrations of 5; 3;2.5; 2;1; 0.5 μM. Biochanin A was diluted to concentrations of 30; 20; 10; 5;2; 0.5 μM. CAPE was diluted to concentrations of 50; 25; 15; 10; 5;1 μM. Curcumin and berberine were diluted to concentrations of 50; 25; 20; 15; 10; and 5 μM. DMEM/RPMI without drugs was used as a control.

2.3 MTT viability assay

Briefly, WEHI-164 and L6 cells were plated in 96-well microculture plates at $1x10^4$ cells/well and incubated with berberine, curcumin, biochanin A, CAPE, and CurE at the indicated concentrations and periods. The culture medium was then removed from each well and 100 μL/well of MTT reagent [3-(4,5-dimethylthiazol-2-yl)-2,5-diphenyltetrazolium bromide] (Sigma-Aldrich, USA) was added, and the cells were incubated for 2 h at 37°C. After incubation, acidified isopropanol (100 PL, 0.04 M HCl in 99.9% isopropanol) was added to dissolve the formed formazan crystals. The samples were completely dissolved using the pipette mixing technique. The absorbance value was measured at 570 nm using a GloMax® Discover multimode microplate reader (Promega, Madison, WI, USA). The IC_{50} values were calculated using Quest Graph™ IC_{50} Calculator (AAT Bioquest, Inc, Sunnyvale, CA, USA). IC_{50} was determined with a non-linear model. The experiments were carried out in five replicates. The results are expressed as the percentage of viable cells relative to untreated control cells.

2.4 Molecular docking

Molecular simulation of CurE, biochanin A and CAPE docking to cytoskeletal proteins: tubulin (PDB: 1TUB) and actin (PDB: 1J6Z). Crystal structures of monomeric actin (PDB:1J6Z) and polymeric actin were obtained from the Protein Data Base (PDB) for the studies. Small molecule compounds were generated using Avogadro Software. Before simulations and screening, both structures were prepared using LigPrep and Protein Prepare. Analysis of the results was performed using Meastro and Canvas Software. The Glide Extra Precision (XP) docking was performed prior to the MM-GBSA calculations. All the data from the *in silico* experiments has been collected and analysed.

2.5 Neutral comet assay (NCA)

Detection of DNA fragmentation associated with apoptosis or the intermediate damage neutral comet assay method described by Collins was used (Collins, 2004). Briefly, after exposure to the examined compounds, WEHI-164/L6 cells (10^4 cells/well) were subjected to a trypsinization process. In the next step, $1x10^5$/ml cells were washed with PBS chilled to 4°C, mixed with low-temperature melting agarose at a ratio of 1:10, and spread on a slide glass. Slides were submerged in precooled lysis buffer (2.5 M NaCl, 100 mM EDTA, pH 10, 10 mM Tris base, and 1% Triton X-100) at 4°C for 1 h. After lysis and rinsing, slides were equilibrated in TBE solution (40 mM Tris/boric acid, 2 mM EDTA, pH 8.3) and electrophoresed at 1.0 V/cm for 20 min and then silver staining was performed. For scoring the comet pattern, 100-200 nuclei were counted from each slide. The ranking of apoptotic comets was performed using the method developed by Collins (Collins, 2004).

2.6 Confocal microscopy studies

WEHI-164 and L6 cells were seeded on the microscopic cover slides, placed in a 6-well plate (Sarstedt, Germany) and incubated overnight for adhesion. The cells were then incubated for 24 h with one of the cytotoxic substances: biochanin A (5 μM), CAPE (25 μM), CurE (2.5 μM), curcumin (20 μM) and berberine (50 μM). Untreated cells were used as a control. Cells were fixed with 4%

paraformaldehyde (PFA) in phosphate-buffered saline (PBS), permeabilized with 0.5% Triton X-100 in PBS (v/v) for 5 min, and blocked with 1% Bovine Serum Albumin (BSA) in PBS for 45 min at room temperature. All washing steps were performed using PBS. The following primary antibody was used: muscle FBPase (mouse, SC390209) antibody at a dilution of 1:250 in PBS. The following secondary antibodies were used: AlexaFluor488 (A11029) antibody at a dilution of 1:200 in PBS. Incubation with primary antibodies was conducted for 120 min and for 1 h with secondary antibodies at room temperature. For the imaging (Zeiss Axio Observer 7 SP stand for LSM 980) confocal laser scanning microscopes was used.

2.7 Immunocytochemical staining

WEHI-164 and L6 cells were seeded on 8-well slides (Thermo Scientific) and incubated overnight for adhesion. The cells were then incubated for 24 h with cytotoxic substances: biochanin A (5 μM), CAPE (25 μM), CurE (2.5 μM), curcumin (20 μM) or berberine (50 μM). Untreated cells were used as a control. The apoptotic activity was assessed by immunocytochemical determination of anti-caspase-3 (C8487) (Sigma-Aldrich, Merck-Millipore, Poznan, Poland) and PARP-1 (SC-74470) (Santa Cruz, USA Biotechnology), and antibodies were diluted in PBS (CAS-3 1:800; PARP-1 1:500). Then, the samples were fixed in 4% formalin, and antibodies were applied for 24 h at 4°C. Then, the slides were washed 3 × 5 min in PBS with Triton. Subsequently, the slides are incubated for 1 h with ImmPRESS Reagent Peroxidase Universal (Anti-mouse/rabbit Ig) (Vector Laboratories, Newark, USA). The slides were rinsed again in PBS for 5 min. Thereafter, the DAB + chromogen diluted in DAB + Substrate Buffer was added for 5 min (incubation in the darkness) and rinsed in distilled water for 10 min. Then, hematoxylin was used to counterstain nuclei (1 min). In the following steps, dehydration was performed by increasing the concentration of ethanol and xylene and mounted in DPX Mounting Medium (Fluka, Germany). The upright microscope (Olympus BX51, Shinjuku, Tokio, Japan) was used to examine the immunocytochemical reaction. Stained cell numbers were evaluated by counting 100 cells in 3 randomly selected fields. The results were judged to be positive if staining was observed in more than 5% of the cells. The intensity of immunohistochemical staining was evaluated as follows: (−) negative, (no reaction), (+)weak, (++) moderate, and (+++) strong.

2.8 Transmission electron microscope (TEM)

Ultrastructural analysis of L6 and WEHI-164 cell lines was performed. The cells were incubated for 24 h with cytotoxic substances: biochanin A (5 μM), CAPE (25 μM), CurE (2.5 μM), curcumin (20 μM) or berberine (50 μM). Untreated cells were used as a control. The cells were then fixed for 30 min in 2.5% (vol/vol) glutaraldehyde and 0.1M phosphate buffer (pH 7.4). After post-fixation in 1% (wt/vol) osmium tetroxide, cells were dehydrated through a graded series of acetone and embedded in Epon (Sigma Aldrich, St. Louis, MI, USA). The Epon blocks were cut on Reichert Ultracut E. Ultrathin sections were, contrasted with uranyl acetate and lead citrate according to the standard method (Kong et al., 2009) and examined with a Talos L120C (ThermoFisher).

2.9 Immunofluorescent studies

WEHI-164 and L6 cells were seeded on the cover microscopic slide, placed in a 6-well plate (Sarstedt, Germany), and incubated overnight for adhesion. The cells were then incubated for 24 h with cytotoxic substances: biochanin A (5 μM), CAPE (25 μM), CurE (2.5 μM), curcumin (20 μM) or berberine (50 μM). Untreated cells were used as a control. Cells were fixed with 4% paraformaldehyde (PFA) in phosphate-buffered saline (PBS) and permeabilized with 0.5% Triton X-100 in PBS (v/v) for 5 min. Following, the incubation with FBS was performed for 1 h at 37°C and 5% CO_2. Next, the cells were washed with Triton-X100. The following primary antibodies were used: Anti-beta tubulin (rabbit, AB108342) antibody at a dilution 1:300 and Zyxin (mouse, MAB6977) antibody at a dilution of 1:300 in PBS. The following secondary antibodies were used: Anti-Mouse AlexFluor488 (AB150113) antibody at a dilution of 1:200 and AlexaFluor594 (A11012) antibody at a dilution of 1:200 in PBS. Primary antibody was added for 1-h incubation at 37°C and 5% CO_2. Following, the cells were washed with PBS and the secondary antibody was added for 1-h incubation at room temperature in the dark. In the end, the samples were washed with PBS. For the nuclei visualization and cell mounting Fluoroshield™ (Sigma-Aldrich, St. Louis, MI, USA) with DAPI (4,6-diamidino-2-phenylindole) was applied. In the end, the samples were washed with PBS. The samples were observed on the Olympus IX53 microscope (40x, Olympus, Tokyo, Japan) after blue, red, and green laser excitations (depending on the fluorophore).

2.10 BCAA–Glo Assay

To measure changes in branched chain amino acids (leucine, isoleucine, valine), L6 and WEHI-164 cells were seeded in 96-well luminescent plates at 25,000 cells/well. Cells were then treated with berberine (50 μM), curcumin (20 μM), biochanin A (5 μM), CAPE (25 μM), or CurE (2.5 μM) for 24 h. The experiment was performed using BCAA-Glo Assay (JE9300, Promega, Madison, WI, USA). Following the completion of the compound treatment, the medium was removed and discarded, and the cells were washed three times with 200 μL of cold PBS. A volume of 25 μL of PBS was then added to the cells that had been washed. A negative control, comprising PBS without cells, was included to ascertain the background of the assay. A volume of 12.5 μL of 0.6N HCl was then added. The mixture was then combined by agitation of the plate for a period of 5 minutes. A volume of 12.5 μL of neutralisation buffer was then added. The mixture was then agitated for 1 minute. A volume of 50 μL of BCAA detection reagent, comprising reductase, NAD, leucine dehydrogenase, reductase substrate and luciferin detection solution, was then added. The solution was then incubated at room temperature for 1 hour. The luminescence value was measured using a GloMax® Discover multimode microplate reader (Promega, Madison, WI, USA). The experiments were carried out in five replicates.

2.11 Glycogen levels detection by luminescent assay

To perform the glycogen sensing measurement, L6 and WEHI-164 cells were seeded in 96-well luminescent plates at 25,000 cells/well. Cells were then treated with berberine (50 μM), curcumin (20 μM), biochanin A (5 μM), CAPE (25 μM), or CurE (2.5 μM) for 24 h. The experiment was performed using Glycogen-Glo Assay (J5051, Promega, Madison, WI, USA). Following the completion of the compound treatment, the medium was removed and discarded, and the cells were washed three times with 200 μL of cold PBS. A volume of 30 μL of PBS was then added to the washed cells. A solution of 0.3 N HCl was then added to the cells in order to lyse them. The contents of the plate were mixed by agitation for a period of 5 minutes. A further 15 μL of Tris buffer (pH 8.0) was then added. The contents of the plate should be mixed by shaking for 1 minute. Twenty-5 μL of each sample, the positive control (glycogen standards in the same buffer as the samples) and the negative control (buffer only) were transferred to a well of a 96-well plate. A volume of 25 μL of the glucoamylase digestion solution, comprising glucoamylase and glucoamylase buffer, was added to each well. The samples were then incubated for 1 hour at room temperature. A volume of 50 μL of the glucose detection reagent, comprising reductase, NAD, reductase substrate, glucose dehydrogenase, and the luciferin detection solution, was added to each well. The plate was mixed by agitation for a period of 1 minute, after which it was incubated for 90 min at room temperature. The luminescence value was determined using a GloMax® Discover multimode microplate reader (Promega, Madison, WI, USA). The experiments were conducted in five replicates. The signal-to-noise ratio (S/N) was calculated by dividing net luminescence (mean luminescence for the sample minus mean luminescence for the negative controls) by the standard deviation of the negative control.

2.12 Wound healing assay

Cells from the L6 and WEHI-164 lines were cultured in 96-well plates (8×10^4) for 24 h until they formed a confluent layer. A scratch was made with a sterile 200 μL pipette tip across the cell monolayer. The medium was removed and the cells were washed twice with DPBS to remove contaminants from the separated cells. Then the DPBS was removed and 200 ul of substances were added to each well in the following concentrations: biochanin A (5 μM), CAPE (25 μM), CurE (2.5 μM), curcumin (20 μM) and berberine (50 μM). Untreated cells were used as a control. Photos were taken every 12 h to assess the crack closure until a monolayer of cells was obtained again. Cell cultures were observed and photographed under the CKX41 Olympus microscope (Tokyo, Japan). Software ImageJ (LOCI, University of Wisconsin) was used to quantify the areas of the closing gap.

2.13 Statistical analysis

The experiments were performed in 3 replicates. The statistical analysis was performed using the GraphPad Prism 8 (GraphPad Software Inc, San Diego, CA, USA). Data are expressed as mean ± SD (standard deviation) of the mean and were analysed by two-way ANOVA (analysis of variance), with $p < 0.05$ being considered statistically significant.

3 Results

3.1 Cytotoxicity of the examined substances and IC_{50} determination

MTT assay assessed the cytotoxicity of the biochanin A, CAPE, CurE, curcumin and berberine. Figure 1 shows the response of L6 cells to 24 h and 48 h incubation with the analyzed substances. Incubation with berberine (e) and CurE (d) did not significantly change the mitochondrial activity of L6 cells compared to the untreated control group. In the case of incubation of L6 cells with biochanin A (c) it was observed that the cytotoxic effect increased with increasing concentration of the substance, both in the case of 24 h and 48 h incubation. At the highest concentration of 30 μM, cell survival after 24 h of incubation was ~30% and after 48 h–18%. Incubation of cells with curcumin (a) showed an enhanced cytotoxic effect with prolonged incubation time (48 h). After exposure of cells to CAPE (b), the strongest cytotoxic effect was observed at a concentration of 1 μM (48 h). Then, with increasing CAPE concentration and prolonged incubation (48 h), cell survival increased, which can be possibly induced by the decay of CAPE in cells.

Figure 2 shows the response of WEHI-164 cells to 24 h and 48 h incubation with the analyzed substances. Control represents the viability of untreated cells. WEHI-164 cells showed increased sensitivity to all of the tested substances. In the case of incubation with berberine (e), the strongest cytotoxic effect was obtained after 48 h of incubation at a concentration of 10 μM, where the percentage of cell survival was ~33%. There was a clear decrease in the mitochondrial activity of cells incubated with biochanin A (c) at a concentration of 10 μM–30 μM and was ~17%–9% (24 h). When incubated with CurE (d) and curcumin (a), cell survival decreased significantly with prolonged incubation and increasing concentration. All analysed substances had a stronger effect on cancer cells from the WEHI-164 line than on normal muscle cells from the L6 line. Table 1 presents the IC_{50} values calculated for biochanin A, curcumin, berberine, CAPE and CurE.

3.2 Apoptosis evaluation

The apoptotic cell death was detected by neutral comet assay. The obtained results are demonstrated in Figures 3 and 4. Apoptotic cells in the L6 line were observed after 24 h of incubation with curcumin (12.5%) and CurE (1%) (a). No cell death was observed after exposure to the remaining substances. After 48 h of incubation of the L6 cells, apoptosis was observed in the case of incubation with curcumin (15.8%), CAPE (13.3%), biochanin A (3.6%) and CurE (2.5%) (c). In the case of WEHI-164 cells, apoptotic cells were observed after 24 h of incubation with CAPE (3.5%) and berberine (2.5%) (b). After 48 h of incubation of the WEHI-164 cells, apoptosis was observed after incubation with CAPE (12.7%), curcumin (4.4%),

10.3389/fcell.2024.1476007

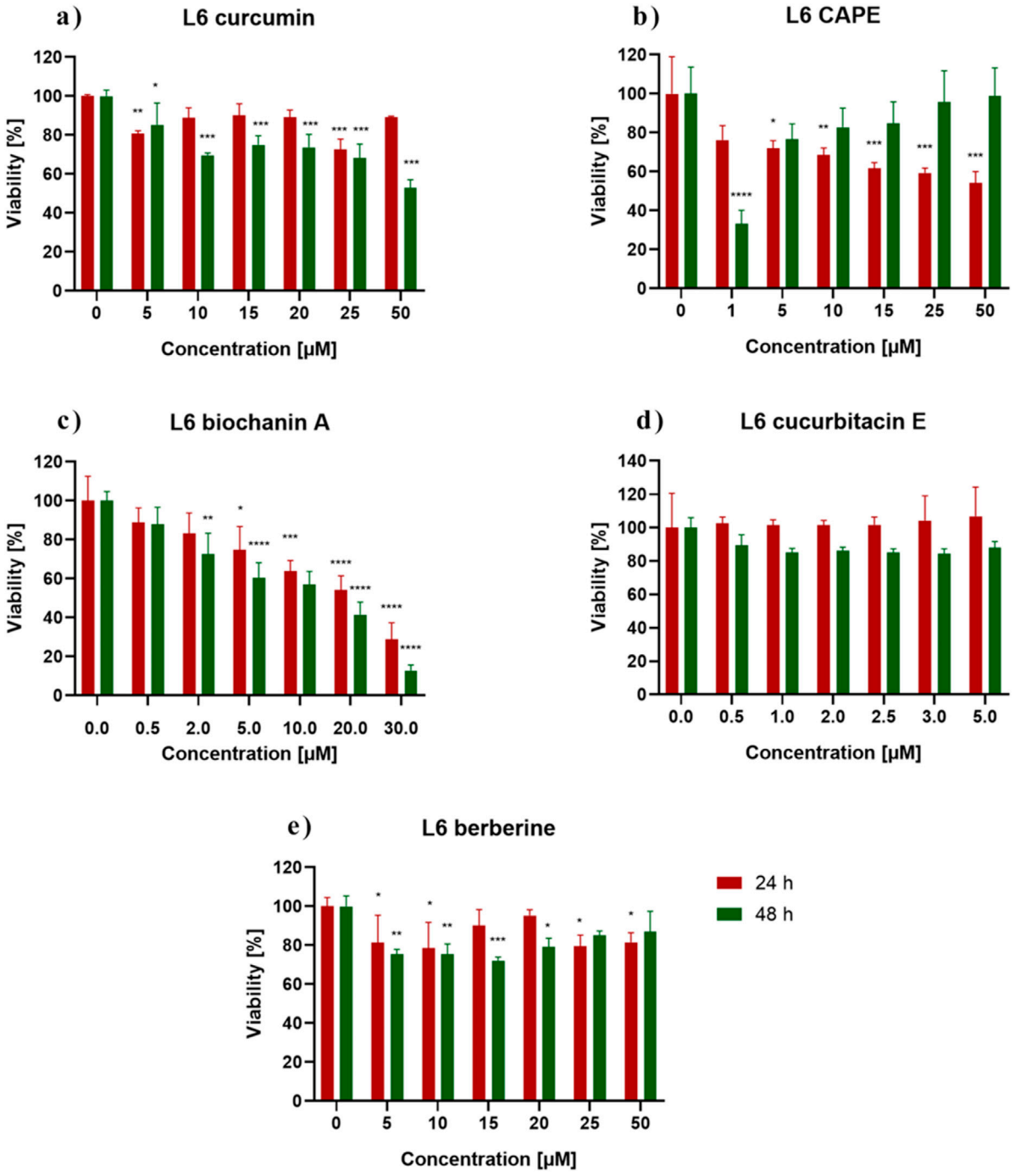

FIGURE 1
L6 cells viability measured by the MTT assay after 24 h and 48 h incubation with **(A)** berberine, **(B)** biochanin A, **(C)** CurE, **(D)** curcumin, **(E)** CAPE. Notes: (mean ± SD) N = 3, *$p < 0.05$, **$p < 0.01$, ***$p < 0.005$.

CurE (3.1%), biochanin A (2.2%) and berberine (1.6%) (d). There was a significant difference in the number of cells indirectly damaged after an extended (48 h) incubation time with the analysed substances. In the case of L6 cells, the highest percentage of damaged cells was observed following incubation with berberine (53%), while in the case of WEHI-164 cells, the highest percentage of damaged cells was observed following incubation with biochanin A (89.5%).

3.3 Immunocytochemical evaluation of PARP-1 and caspase-3

Immunocytochemical staining of PARP-1 and caspase-3 in L6 and WEHI-164 cells treated with biochanin A (5 μM), CAPE (25 μM), CurE (2.5 μM), curcumin (20 μM) or berberine (50 μM) was performed (Figures 5 and 6). PARP-1 is cleaved by caspase-3 during apoptosis, which leads to its inactivation (Wiśniewski et al.,

10.3389/fcell.2024.1476007

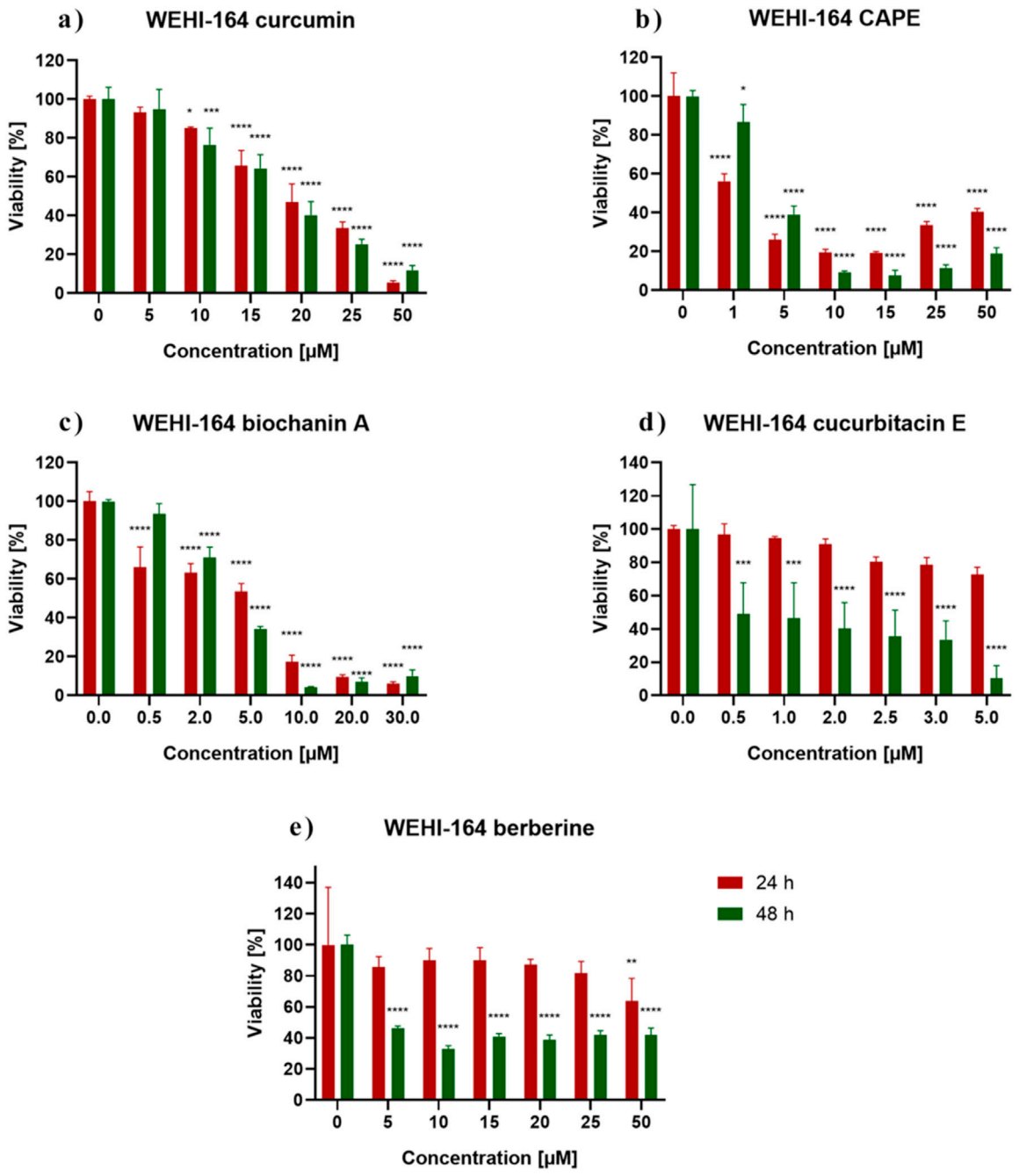

FIGURE 2
WEHI-164 cells viability measured by the MTT assay after 24 h and 48 h incubation with **(A)** berberine, **(B)** biochanin A, **(C)** CurE, **(D)** curcumin, **(E)** CAPE. Notes: (mean ± SD) N = 3, *$p < 0.05$, **$p < 0.01$, ***$p < 0.005$

TABLE 1 IC50 values for the tested compounds determined after 24 h treatment of L6 and WEHI-164 cells.

Cell line/substance	Biochanin A	CAPE	CurE	Berberine	Curcumin
L6	5.903 [μM]	13.694 [μM]	10.38 [μM]	12.075 [μM]	29.305 [μM]
WEHI-164	6.395 [μM]	7.018 [μM]	66.476 [μM]	27.043 [μM]	14.049 [μM]

Based on the results presented above, low-toxic concentrations were selected for further experiment: biochanin A (5 μM), curcumin (20 μM), berberine (50 μM), CAPE (25 μM) and CurE (2.5 μM).

10.3389/fcell.2024.1476007

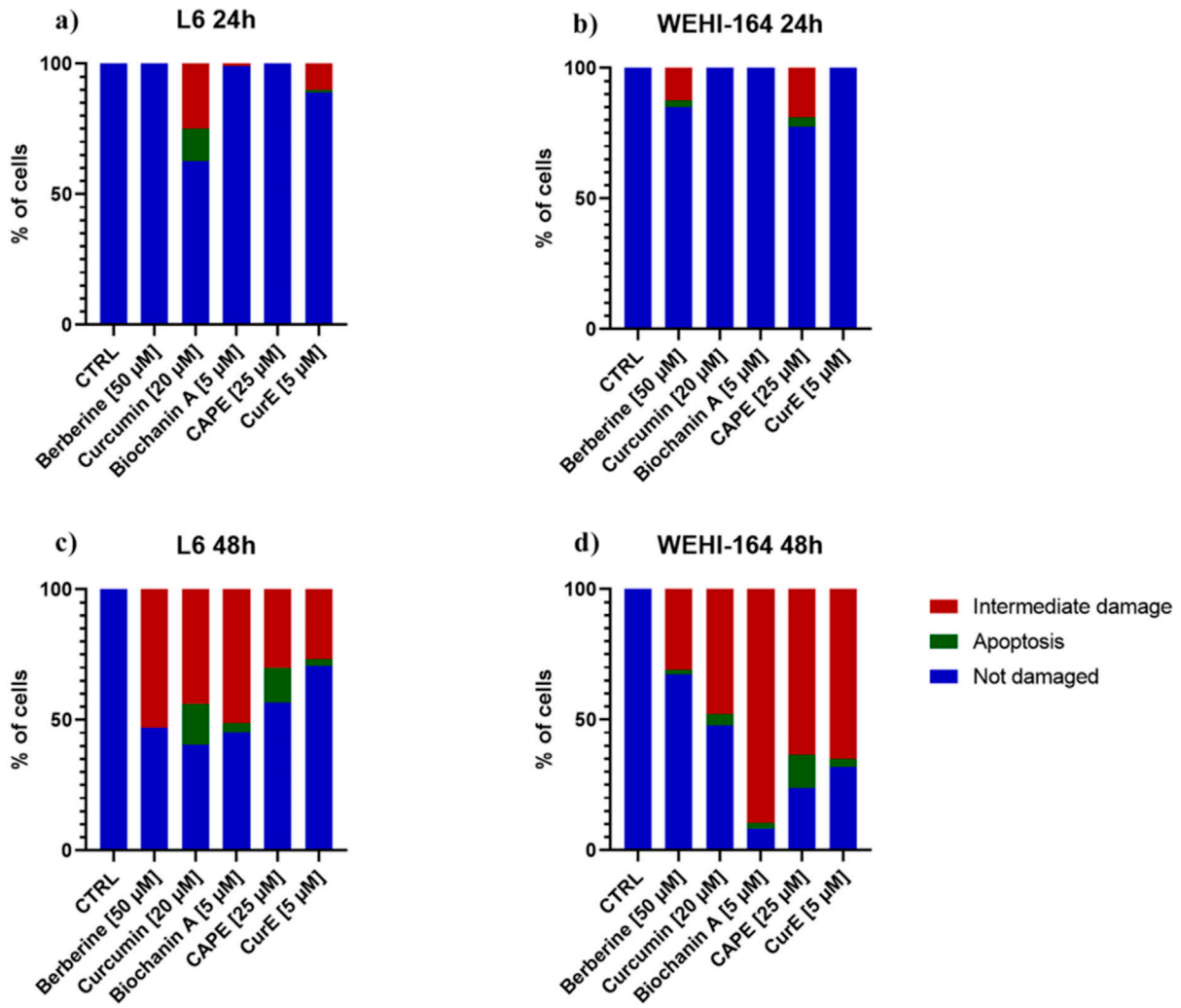

FIGURE 3
The neutral comet assay was performed on L6 and WEHI-164 cells after 24 h **(A, B)** and 48 h **(C, D)** of incubation with berberine, biochanin A, CurE, curcumin or CAPE.

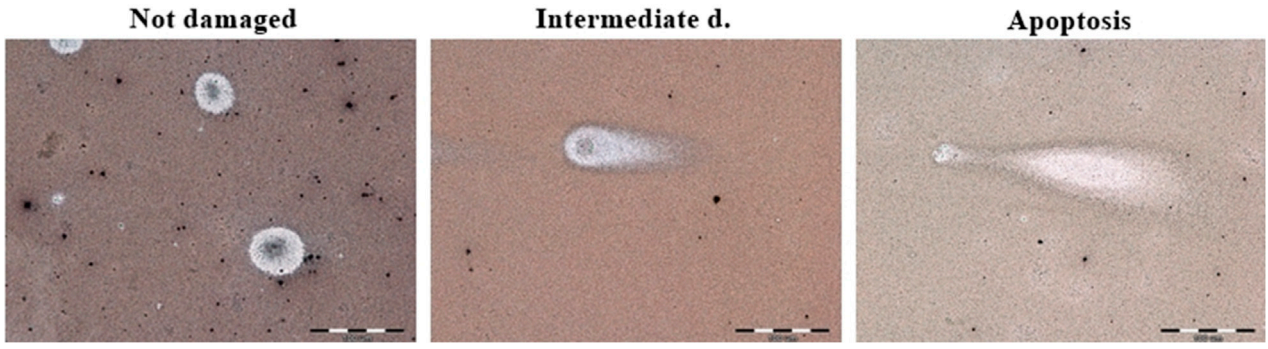

FIGURE 4
Example micrographs of assessed comets in not damaged, intermediately damaged and apoptotic states. Magnification ×600.

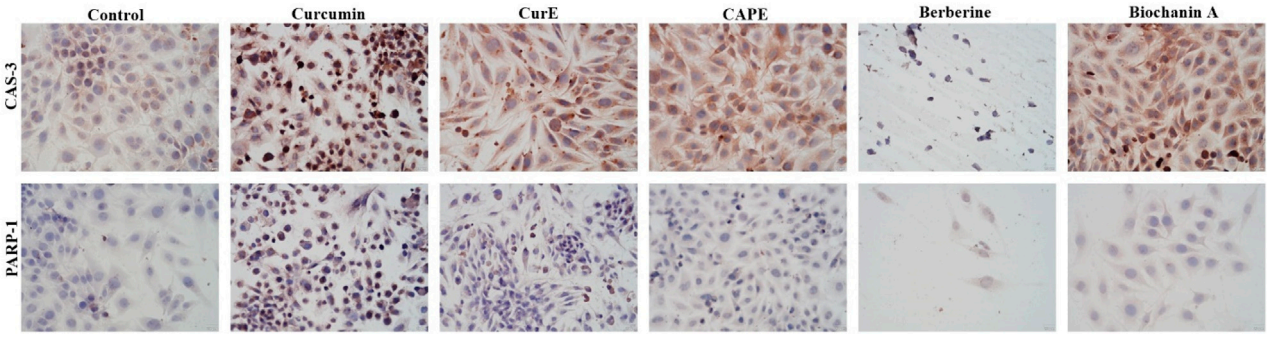

FIGURE 5
Caspase-3 and PARP-1 expression in L6 cells after 24 h incubation with curcumin, CurE, CAPE, berberine and biochanin A.

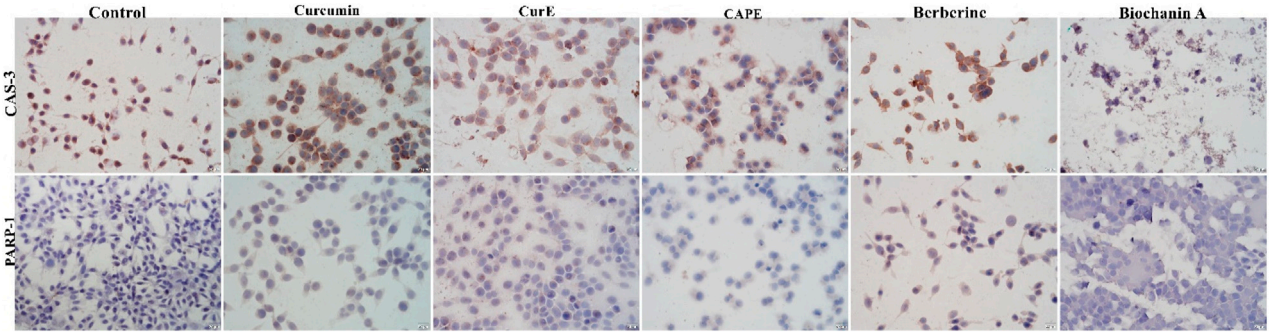

FIGURE 6
Caspase-3 and PARP-1 expression in WEHI-164 cells after 24 h incubation with curcumin, CurE, CAPE, berberine and biochanin A 1.3. Molecular Docking.

TABLE 2 Evaluation of immunocytochemical reaction with anti-PARP-1 and anti-caspase 3 antibodies in L6 and WEHI-164 cells, after exposition to biochanin A (5 μM), CAPE (25 μM), CurE (2.5 μM), curcumin (20 μM) and berberine (50 μM) for 24 h

Compound	WEHI-164 cell line		L6 cell line	
	PARP-1	Caspase-3	PARP-1	Caspase-3
Control cells	<5%	40%, +	20%, +	<5%
Biochanin A [5 μM]	40%, +	95%, +++	15%, +	45%, +
CAPE [25 μM]	50%, +	95%, +++	10%, +	80%, ++
CurE [2.5 μM]	50%, +	85%, ++	15%, +	90%, ++
Curcumin [20 μM]	95%, +++	95%, +++	20%, +	80%, ++
Berberine [50 μM]	<5%	<5%	15%, +	45%, ++

2017), (Li et al., 2013). The results of immunocytochemical analyses of the apoptotic proteins are presented in Table 2. PARP-1 overexpression was observed in L6 cells after exposure to each compound in ca. 10%–15% of cells similarly to control cells. Caspase-3 expression was observed in ~<5% of untreated L6 cells. In the case of incubation with biochanin A and berberine, the expression level of caspase-3 was increased in 45% of cells, and in other cases in 80%–90% of cells. PARP-1 overexpression was observed in WEHI-164 cells at a low level, i.e., in less than 5% of cells after berberine treatment and in untreated cells. After the exposure to biochanin A, CAPE and CurE, PARP-1 expression was increased in 40%–50% cells. The highest level of PARP-1 95% of cells, was noted after incubation with curcumin. Interestingly, in the case of control WEHI-164 cells caspase-3 expression was observed in 40% of cells, and after incubation with biochanin A, CAPE, CurE and curcumin it was detected in 85%–95% of cells. Only after the treatment with berberine, expression of caspase-3 was observed in less than 5% of cells.

10.3389/fcell.2024.1476007

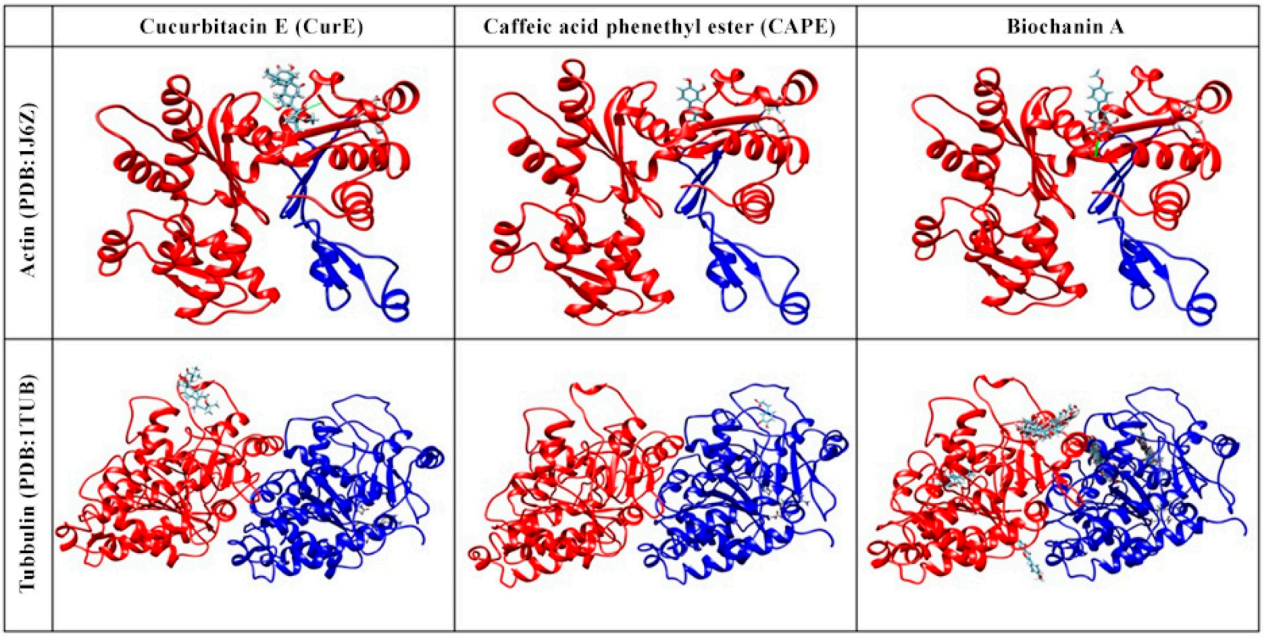

FIGURE 7
Molecular docking of actin (PDB:1J6Z) and tubulin (PDB:1TUB) with CAPE, biochanin A and CurE.

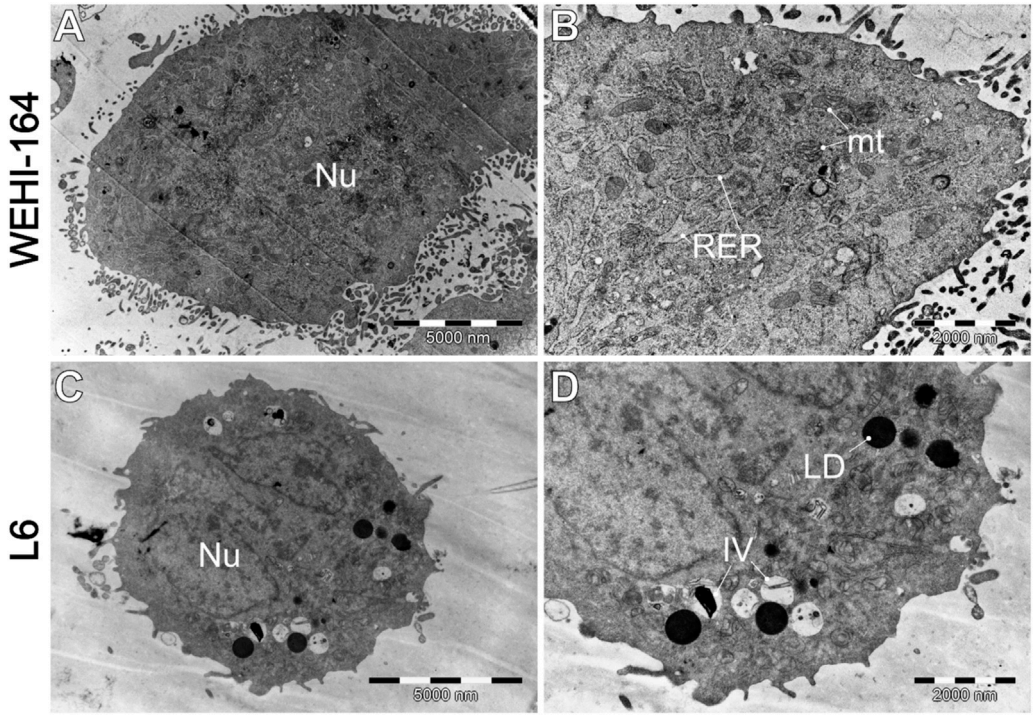

FIGURE 8
Morphology of untreated cells, where **(A, B)** WEHI-164, and **(C, D)** L6 cells. IV–intracellular vesicles; LD–lipid droplets; mt–mitochondria; Nu–cell nucleus; RER–rough endoplasmic reticulum.

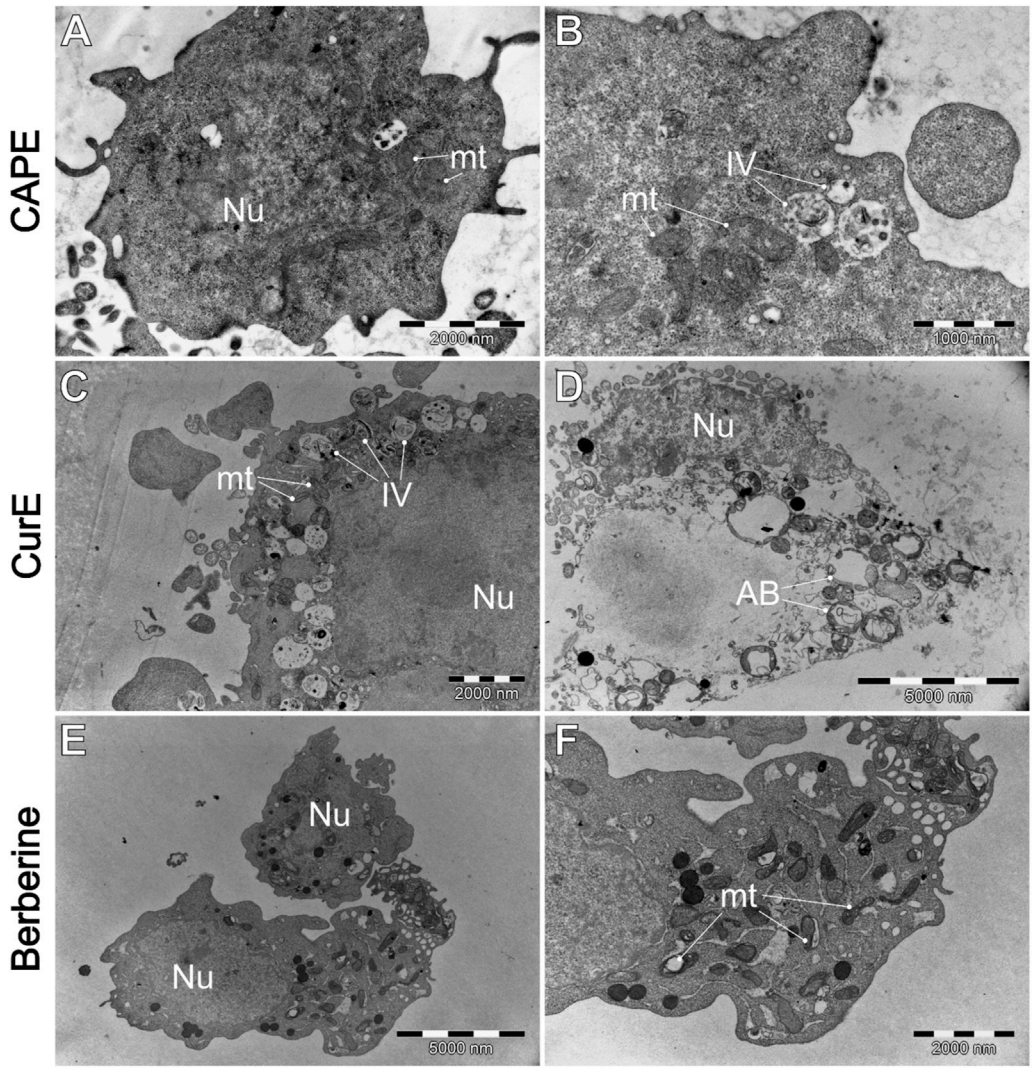

FIGURE 9
WEHI-164 cells' morphology after the exposure to **(A, B)** CAPE (25 μM), **(C, D)** CurE (5 μM), **(E, F)** berberine (50 μM). AB–apoptotic bodies; IV–intracellular vesicles; mt–mitochondria; Nu–cell nucleus.

3.4 Molecular Docking

The obtained results indicate that CAPE, biochanin A and CurE showed anticancer activity (Figure 7). The compounds are also NF-κB and cell cycle inhibitors and therefore should be considered in the treatment of muscle cancers. According to molecular docking, the most likely binding site corresponds to the Taxotere (TMR) binding site (Dey et al., 2019). TMR is an agent that inhibitors actin polymerization, thus the same site of CAPE and biochanin A binding may indicate that the substances will extend similar effect on actin and tubulin.

Berberine does not act specifically on actin or tubulin but interacts with intracellular kinases (AMP-activated kinases). This is an important distinction because the results of molecular docking of berberine to actin and tubulin would not reflect the actual mechanism of action of this compound (Alakurtti et al., 2006).

Curcumin, the active component of turmeric, is known for its potential anti-cancer, anti-inflammatory, and antioxidant properties. However, its interactions with tubulin and actin, key cytoskeletal proteins, have not been extensively studied. This is due to the high binding specificity required by these proteins, which may not be achieved by curcumin's broad spectrum of activity. Additionally, the dynamic nature of the cytoskeleton makes experimental confirmation of these interactions challenging. Focusing solely on docking with tubulin and actin may not fully reflect curcumin's anti-cancer mechanism, considering its interactions with multiple signalling pathways and molecular targets. These factors limit the attractiveness of curcumin as a targeted therapeutic agent for cytoskeletal protein interactions.

In addition to NF-κB, we included tubulin as a secondary target in our molecular docking studies. Tubulin was selected due to its well-established role in cancer cell division and its relevance as a therapeutic target. Inhibiting tubulin can disrupt the mitotic process, which may enhance the anti-proliferative effects of NF-κB inhibition. Although this dual-target approach provides a promising strategy for cancer treatment, it should be noted that

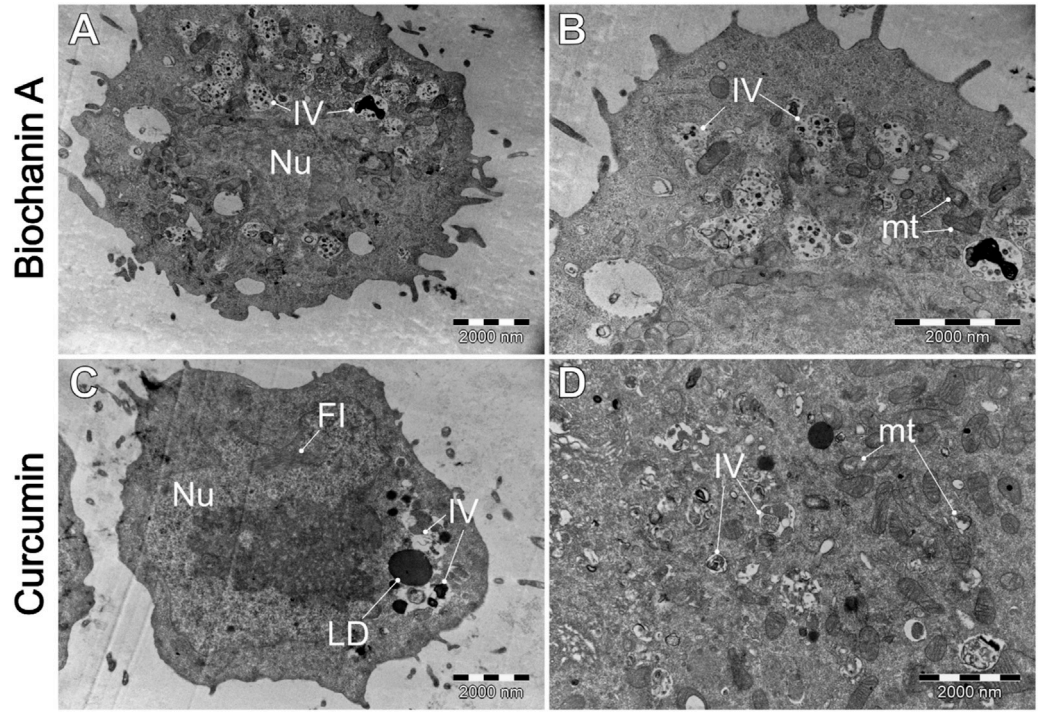

FIGURE 10
A comparative analysis of the morphological characteristics of WEHI-164 cells treated with **(A, B)** biochanin A (5 μM) and **(C, D)** curcumin (20 μM). IV–intracellular vesicles; LD–lipid droplets; mt–mitochondria; Nu–cell nucleus.

molecular docking, while useful for predicting potential binding interactions, offers only preliminary insights.

3.5 Alternations in cell ultrastructure–TEM study

Transmission electron microscopy (TEM) was employed to investigate the ultrastructural effects of biochanin A, curcumin, and berberine on sarcoma (WEHI-164) and normal muscle (L6) cells. This analysis aimed to elucidate the cellular stress mechanisms and morphological changes induced by these natural compounds, providing insights into their potential anticancer activity. By comparing treated and untreated cells, we were able to discern distinct cytotoxic and protective effects, highlighting the differential responses of normal and cancerous cells to these agents. The results are shown in Figures 8–12 below.

Figure 8 shows that cells typically exhibit a particularly dark cytoplasm, a regular cell membrane, a barely discernible cell nucleus (Nu), a well-developed rough endoplasmic reticulum (RER), and undamaged mitochondria (mt). It is noteworthy that WEHI-164 cells typically exhibit a minimal number of intracellular vesicles. In comparison, L6 (C and D) cells display a less electron-dense cytoplasm with a predominantly euchromatic nucleus. Additionally, they often contain numerous lipid droplets (LD) and intracellular vesicles (IV), including phagolysosomes and autophagolysosomes with visible lamellar cellular debris.

Figure 9 demonstrates the impact of natural drug exposure on cancer cell morphology. CAPE did not significantly affected cell structure. The general morphology of the cells remains unaltered, and the mitochondria are mostly unaffected. However, there is an slightly increase in the number of intracellular vesicles (IV). Administration of CurE results (Figures 9C, D) in more pronounced alterations. The images demonstrate the presence of numerous intracellular vesicles, a blebbing plasma membrane with intact organelles inside blebs. The presented images suggest the occurrence of early (C) and late (D) apoptotic events, as evidenced by the presence of damaged apoptotic bodies (AB). The exposure of WEHI-164 cells to berberine (Figures 9E, F) resulted in an increased number of visibly damaged mitochondria (mt) and visible distortion of the cell membrane.

As we can observe biochanin A induced an increased number of intracellular vesicles (IV), yet no other significant alterations in mitochondria or cell membrane are observed. Cells cultured with curcumin exhibited a slightly elevated number of intracellular vesicles and, on occasion, lipid droplets. Some mitochondrial damage is evident, though not pervasive.

Figure 11 shows the L6 cells ultrastructure after the exposure to natural drugs. As we can see CAPE induced visible mitochondrial damage, with the presence of numerous lamellized mitochondrial debris. However, there is no evidence of mitophagy or autophagy when cells were treated by CurE. Berberine treatment induced similar alternations.

The exposure of L6 to biochanin A induced comparable events to those observed in Figure 11, with addition to spontaneous mitochondrial damage, and the presence of autophagosomes were observed. These findings suggest that biochanin A induces cellular stress leading to autophagic activity. Curcumin appears to induce

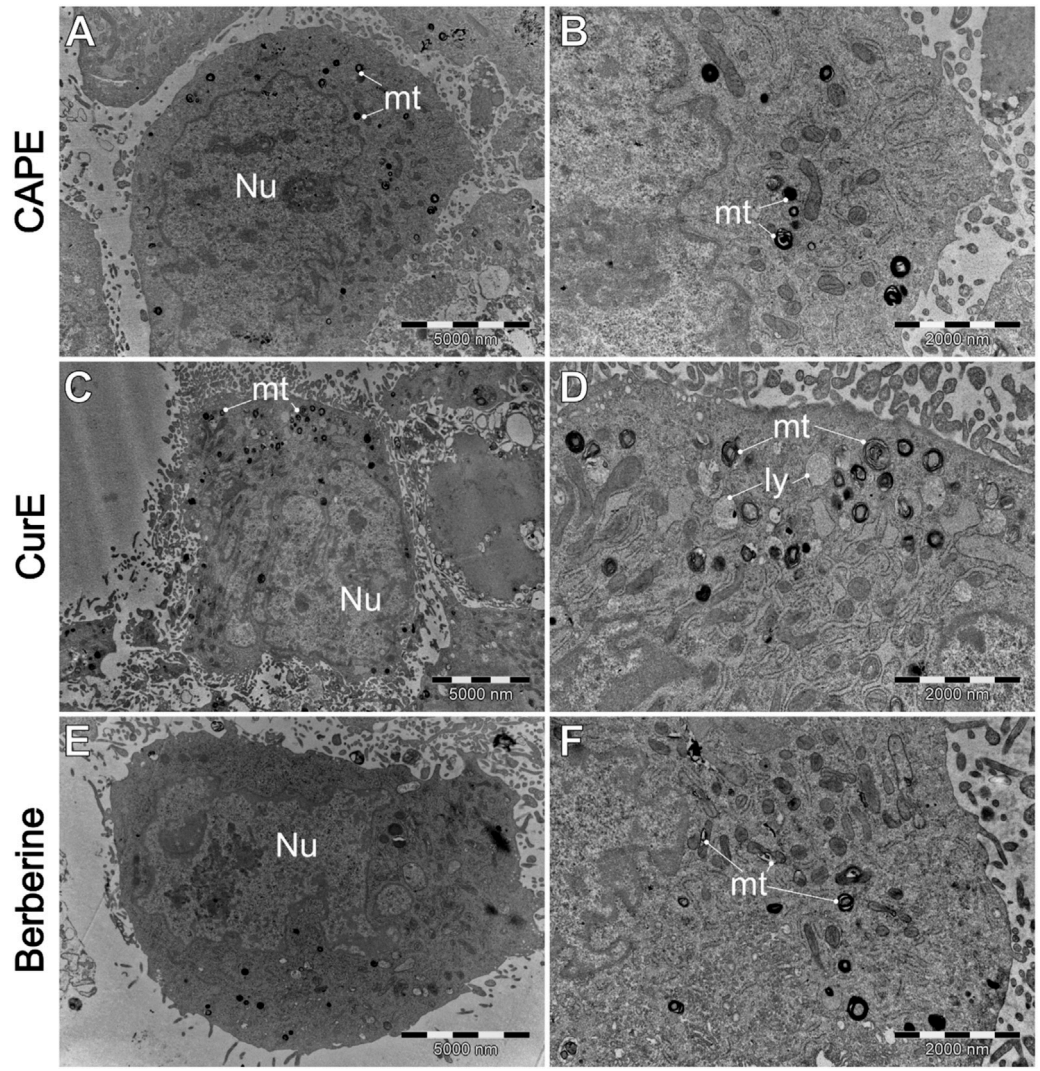

FIGURE 11
A comparison of the ultrastructure o L6 cells, treated by **(A, B)** CAPE (25 μM), **(C, D)** CurE (5 μM) and berberine **(E, F)** (50 μM). IV–intracellular vesicles; LD–lipid droplets; ly–lysosomes. mt–mitochondria; Nu–cell nucleus.

the most pronounced changes, including distortion of the cell membrane (C) and an increased number of cellular debris (D), including evidence of programmed cell death.

We suspect these cellular structures appear to be autophagosomes. Autophagosomes are double-membrane vesicles involved in the degradation and recycling of cellular components through the process of autophagy. These structures are typically seen as spherical or cup-shaped with distinctive membranes, and appear when cells are exposed to stress, e.g., in response to therapy (Yun and Lee, 2018).

Our results indicate that exposure of WEHI-164 cells to berberine (Figures 9E, F) highlighted severe cellular damage, suggesting apoptotic or autophagic processes. The results obtained from TEM analysis revealed differential responses between normal muscle L6 cells and sarcoma WEHI-164 cells to natural anticancer drugs. Biochanin A and berberine induced significant vacuolization and cellular stress in both cell types, with more pronounced effects in cancerous cells. Curcumin appeared to have a more selective impact, causing notable morphological changes in WEHI-164 cells while preserving L6 cell integrity. These findings underscore the potential of these natural compounds in cancer therapy, with varying degrees of cytotoxicity and cellular responses observed under electron microscopy.

3.6 Immunofluorescent visualization of tubulin and zyxin reorganization and FBPase distribution

The distribution of proteins responsible for cytoskeleton organization - zyxin and tubulin, was detected using the immunofluorescence method, and is shown in Figure 13 for normal cells, and Figure 14 for WEHI-164 cells. Control group showed normal distribution and intensity of the tubulin-related (anti-beta tubulin) and zyxin-related fluorescence, indicating

10.3389/fcell.2024.1476007

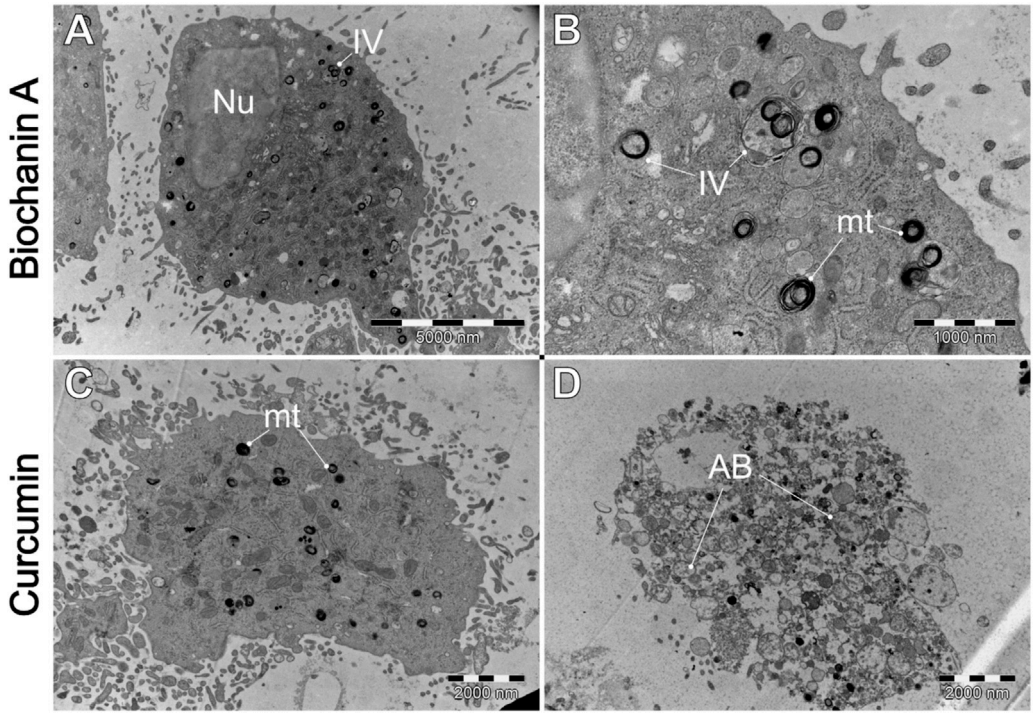

FIGURE 12
Ultrastructural effects of **(A, B)** biochanin A (5 μM) and **(C, D)** curcumin (20 μM) on L6 cells. AB–apoptotic bodies. IV–intracellular vesicles. mt–mitochondria. Nu–cell nucleus.

standard cytoskeletal organization. Curcumin exposure resulted in a noticeable decrease in fluorescence intensity for both tubulin and zyxin, suggesting cytoskeletal disruption. When cells were treated by CurE, a reduction in intensity and some disorganization was noted, though less pronounced as compared to Curcumin. CAPE treatment caused significant reduction in fluorescence intensity, indicating major cytoskeletal disruption. In cells incubated with berberine a lower fluorescence intensity and potential structural changes suggesting cytoskeletal disturbance were observed. Biochanin A incubation induced a reduced intensity and altered distribution of cytoskeletal proteins, indicating reorganization. The obtained results indicate that the treatments with Curcumin, CurE, CAPE, Berberine, and Biochanin A induce disrupt cytoskeletal organization in cancer cells, potentially impairing cell division and motility.

Immunofluorescent analysis of FBPase is demonstrated in Figure 15 A and B.

In the cell L6 line, only in samples incubated with CurE the fluorescence was more intense compared to the control. In the analysis performed on the WEHI-164 cell line, the fluorescence was significantly more intense compared to the control in samples after incubation with CurE, berberine, curcumin and biochanin A (Figure 15 B). Moreover, FBPase localization ceased to be granular, becoming more homogeneous, suggesting that exposure to CurE reduced FBPase interactions with the tubulin cytoskeleton and/or mitochondria. FBPase released from the protein complex is more easily accessible to antibodies. And therefore, the FBPase-related fluorescence is more intense, as it was observed in cancer cells, after CAPE and biochanin.

3.7 Glycogen levels regulation by natural compounds

The evaluation of glycogen levels in L6 (rat myoblast) and WEHI-164 (mouse fibrosarcoma) cells after exposure to natural anticancer drugs may help to understand the metabolic impact of these treatments. Specifically, it enables to investigate whether these drugs disrupt glycogen metabolism, which could lead to reduced glycolytic flux and subsequent energy deprivation in cancer cells. The results of our analysis are shown in Figure 16. These data indicate that L6 cells have higher baseline glycogen levels compared to WEHI-164 cells. This suggests a possible difference in glycogen metabolism or storage capacity between the 2 cell lines. In the case of the drug exposure, all tested compounds reduced glycogen levels in both L6 and WEHI-164 cells, with varying degrees of impact. Berberine and Biochanin A treatment resulted in the most significant reduction in glycogen levels in L6 cells, suggesting a strong inhibitory effect on glycogen storage or synthesis. Curcumin and CAPE moderately reduced glycogen levels in L6 cells. CurE had the least effect on glycogen levels in L6 cells, indicating it may be less effective at altering glycogen metabolism in this cell line. Interestingly, in WEHI-164 cells, all treatments resulted in minor reductions in glycogen levels, but overall the levels remained low compared to L6 cells.

The reduction in glycogen levels may indicate that these compounds inhibit glycogen synthesis or promote glycogen degradation, leading to decreased energy reserves in the cancer cells. This could contribute to the observed cytotoxic effects, as cancer cells are deprived of a crucial energy source, impairing their proliferation and survival.

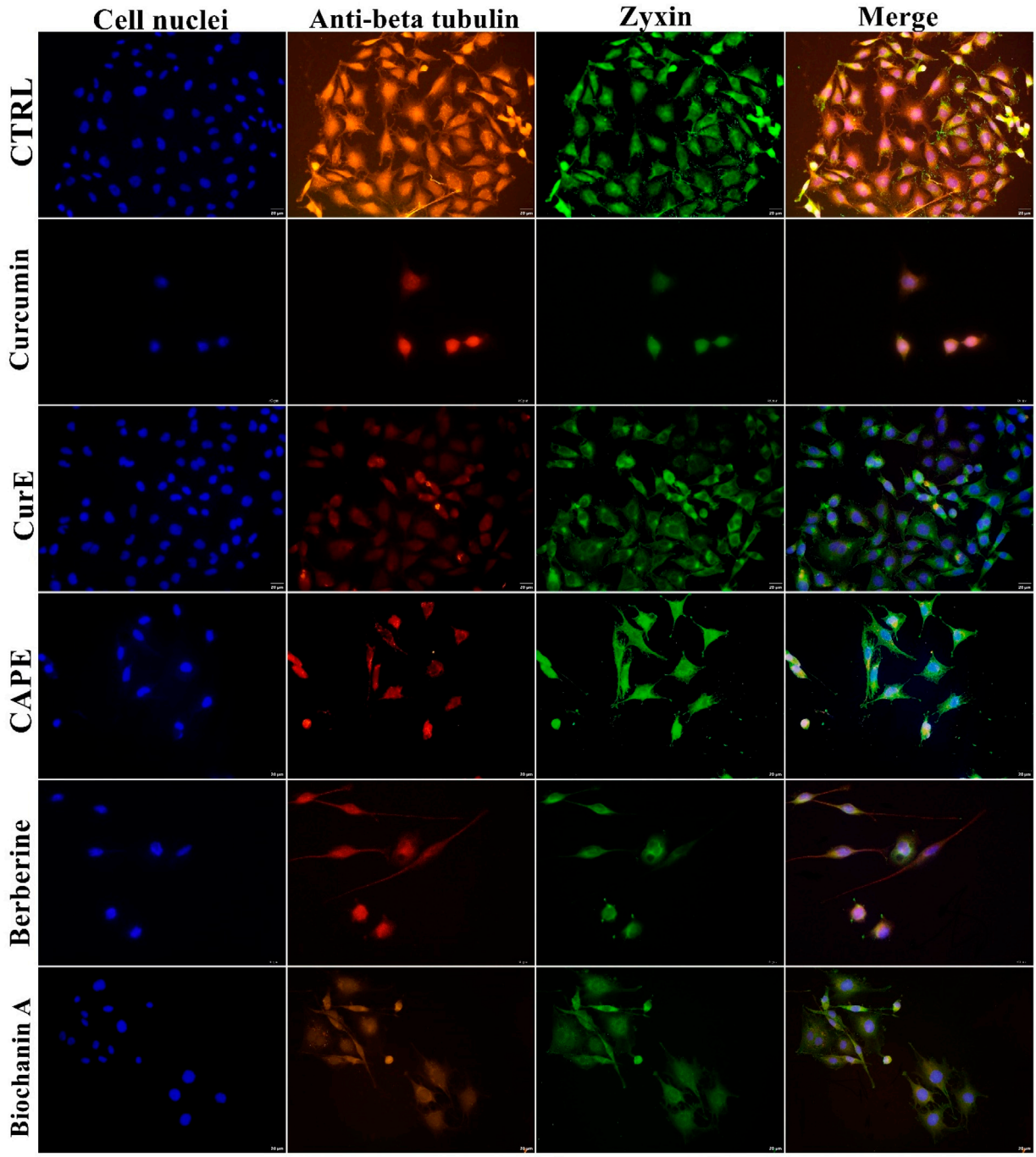

FIGURE 13
Presentation of the effect of curcumin (20 μM), CurE (2.5 μM), CAPE (25 μM), berberine (50 μM) and biochanin A (5 μM) on L6 cells after 24 h of incubation. Nuclei are stained blue with DAPI, zyxin is stained green with AlexaFluor488 and anti-beta tubulin antibody is stained red with AlexaFluor594. Scale bar = 20 μm.

3.8 Branched-chain amino acids levels regulated by natural compounds

Branched-chain amino acids (BCAA), including valine, leucine, and isoleucine, are pivotal amino acids for tumour formation in a range of human malignancies (Xu et al., 2023). A growing body of evidence from scientific studies indicates that there are significant alterations in the metabolism of BCAA and their associated proteins in a number of different cancer phenotypes. This suggests that disturbances in the metabolism of BCAA may become a significant factor in the reprogramming of cancer metabolism (Jung et al., 2021). Elevated levels of branched-chain amino acids (BCAA) have been linked to the suppression of tumour growth, suggesting their potential as anticancer agents (Martin et al., 2020). The findings are

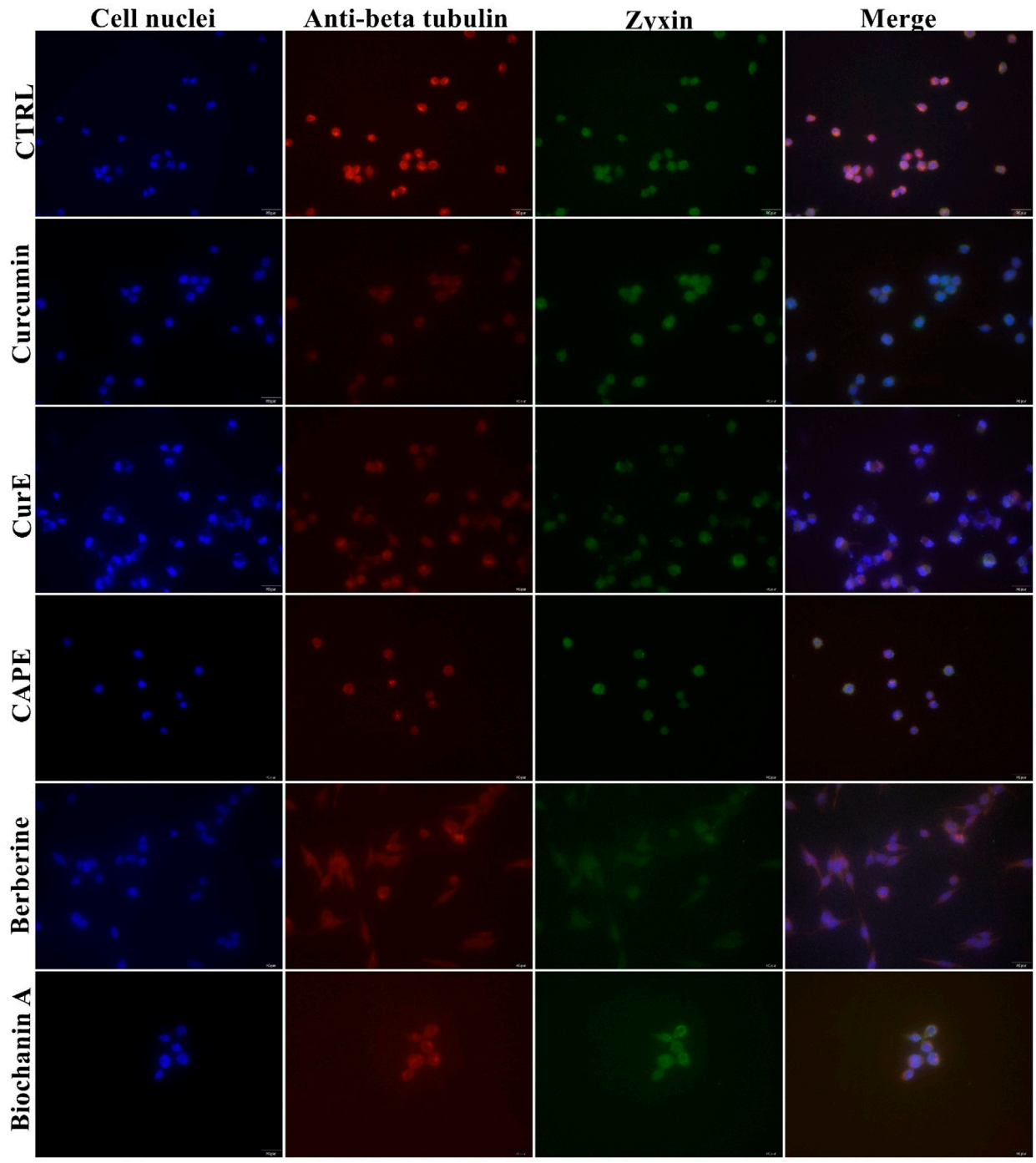

FIGURE 14
Presentation of the effect of curcumin (20 μM), CurE (2.5 μM), CAPE (25 μM), berberine (50 μM) and biochanin A (5 μM) on WEHI-164 cells after 24 h of incubation. Nuclei are stained blue with DAPI, zyxin is stained green with AlexaFluor488 and anti-beta tubulin antibody is stained red with AlexaFluor594. Scale bar = 20 μm.

illustrated in Figure 17. BCAA levels were found to be significantly elevated in cancer cells in comparison to normal muscle cells. The highest concentration of BCAA was observed in WEHI-164 cells following incubation with biochanin A and berberine. The lowest level of BCAA was observed in the cancer cells following incubation with curcumin. In the case of L6 cells, the highest level of luminescence is observed following the use of biochanin A. The remaining compounds demonstrate a lower level of luminescent activity in comparison to biochanin A, which may suggest that this compound exerts the strongest effect on these cells.

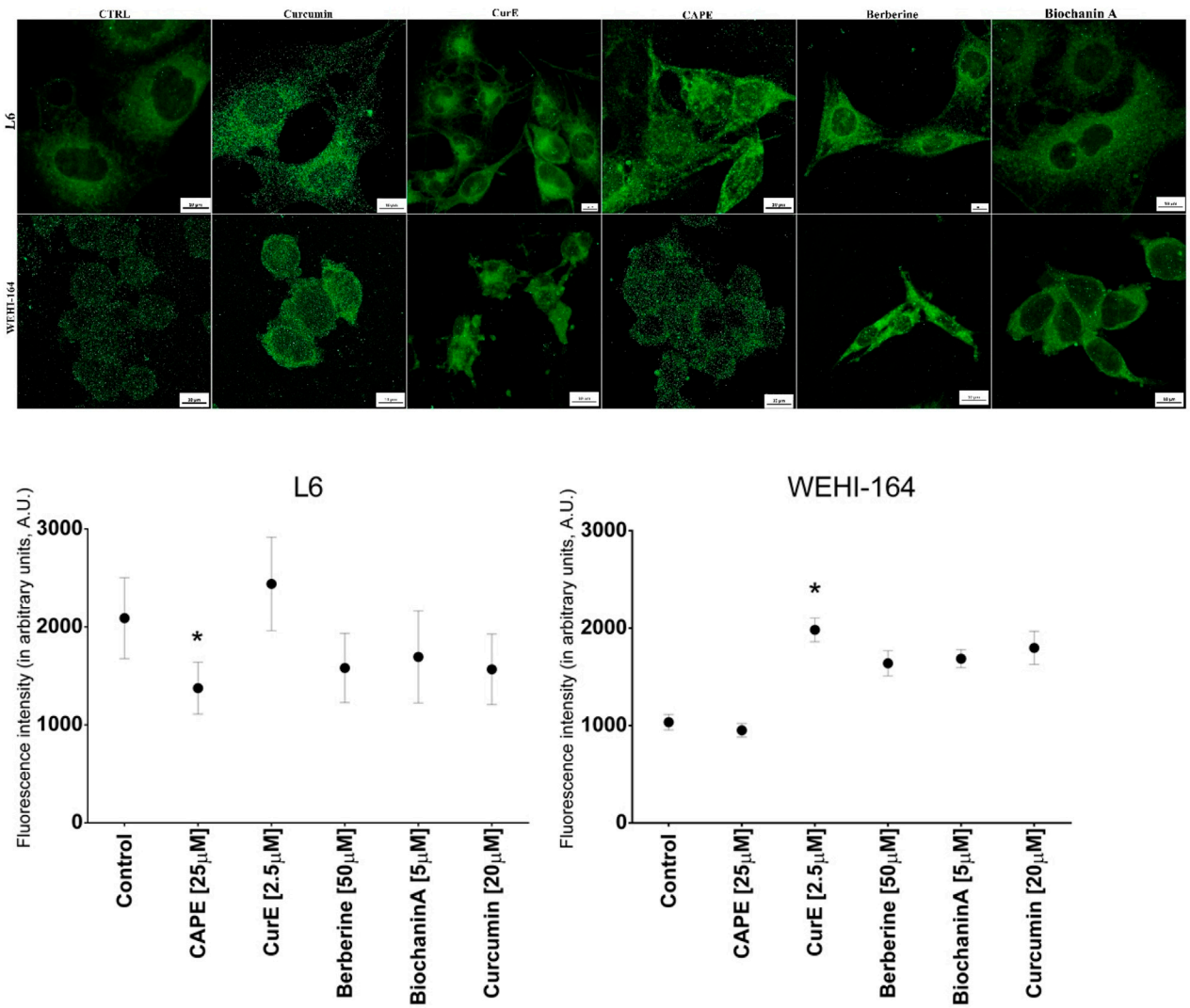

FIGURE 15
Presentation of the effect of curcumin (20 μM), CurE (2.5 μM), CAPE (25 μM), berberine (50 μM) and biochanin A (5 μM) on L6 and WEHI-164 cells after 24 h of incubation using CLSM **(A)**. Muscle FBPase stained green with AlexFluor488. Scale bar = 10 μM. Intensity of fluorescence of AlexaFluor488 (A11029) in L6 and WEHI-164 cells in arbitrary units **(B)**; *$p < 0.05$.

3.9 Wound healing assay

The assay was performed to assess whether berberine (50 μM), CAPE (25 μM), CurE (2.5 μM), curcumin (20 μM) and biochanin A (5 μM) affected the migration of L6 and WEHI-164 cells. Progress in wound healing was analysed after 12, 24, 36 and 48 h with a microscope (magnification ×20). The following photographs show the process of 500 μm cell-free wound gap closure (Figures 18, 19).

Based on the obtained data (Tables 3, 4), it can be concluded that the analysed substances inhibited the closing of the wound gap in cancer cells from the WEHI-164 line. After 48 h of incubation with CurE, the gap was closed by 26.12% compared to the control, which was the lowest result of all the analysed ones. After 48 h of incubation of WEHI-164 cells with curcumin, the gap was closed by 37.12% and after incubation with CAPE by 39.12% compared to the control. The strongest wound closure was observed after 48 h of incubation with biochanin A, where the gap was closed by 72.24%. When the normal L6 cells was incubated substances, the gaps were closed to a very similar extent as in the control case. The results that differed the most from those obtained under control conditions were obtained after 48 h of incubation with berberine, where the gap was closed by 87.12%.

4 Discussion

The present study investigated the effects of several natural NF-κB inhibitors (berberine, curcumin, biochanin A, CurE and CAPE) on fibrosarcoma (WEHI-164) and normal muscle cells (L6). The results showed that these compounds had a stronger cytotoxic effect on cancer cells compared to normal cells, suggesting their potential as effective anti-cancer agents. Moreover, such a selective toxicity is essential to

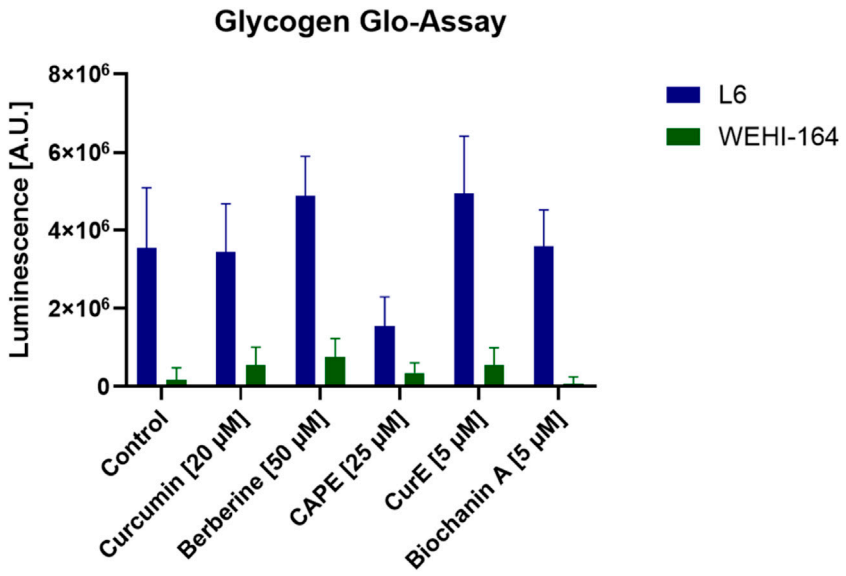

FIGURE 16
Measurement of glycogen levels in L6 and WEHI-164 cells in arbitrary units. Notes: (mean ± SD) N = 3.

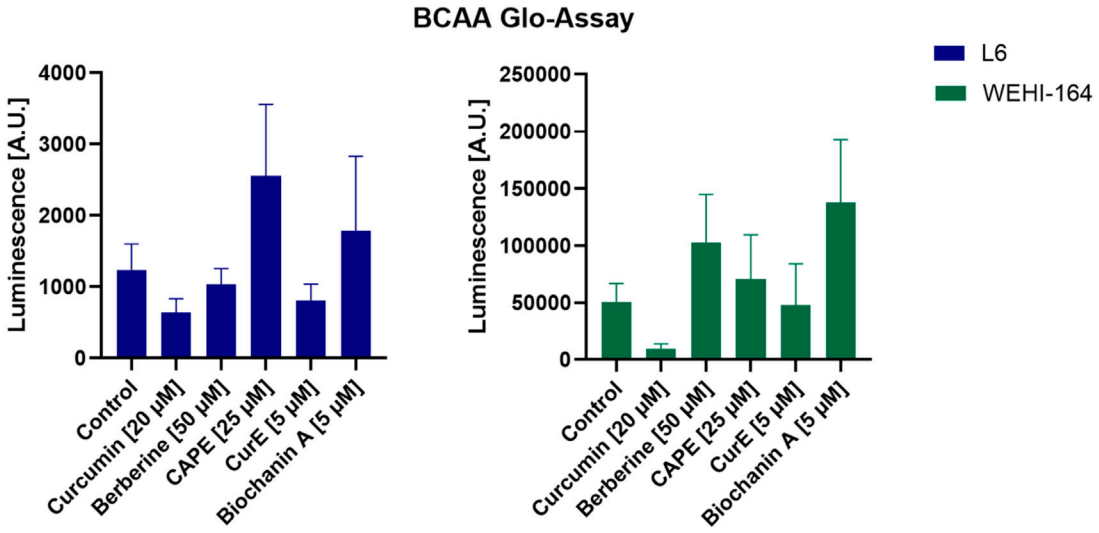

FIGURE 17
Measurement of BCAA levels in L6 and WEHI-164 cells in arbitrary units. Notes: (mean ± SD) N = 3.

minimize side effects in cancer therapy. Apoptosis was induced in WEHI-164 cells by all compounds, with CAPE and curcumin showing significant apoptotic effects after 48 h of incubation. Other studies revealed that curcumin and berberine can inhibit cancer cell migration and invasion by modulating cytoskeletal dynamics and cellular adhesion properties (Pavan et al., 2016). Our results of viability assays confirmed the selective cytotoxicity of these compounds, with cancer cells being more adversely affected than normal muscle cells. Molecular docking revealed that CAPE, biochanin A and CurE inhibited actin polymerization, indicating their potential role in disrupting the cytoskeleton of cancer cells. Berberine's interaction with intracellular kinases, such as AMPK, suggests a unique mechanism where it modulates cellular energy balance and metabolic pathways (Kim et al., 2009). It has been shown that curcumin is able to inhibit actin polymerization and reduce the metastatic potential of cancer cells (Sadeghi et al., 2023). Similarly, CAPE has been shown to interfere with microtubule dynamics, leading to cell cycle arrest and apoptosis in cancer cells (Chuu et al., 2012). Immunocytochemical analysis revealed increased expression of caspase-3 and PARP-1 in WEHI-164 cells after treatment with the tested compounds, supporting the assumption of induction of apoptosis. Transmission electron microscopy revealed cellular stress

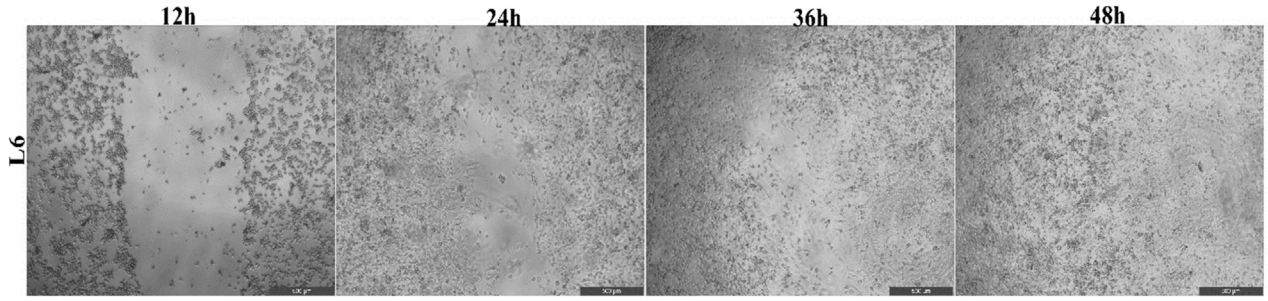

FIGURE 18
Closure of the wound gap in L6 cells after 12, 24, 36 and 48 h after incubation with CurE [2.5 μM].

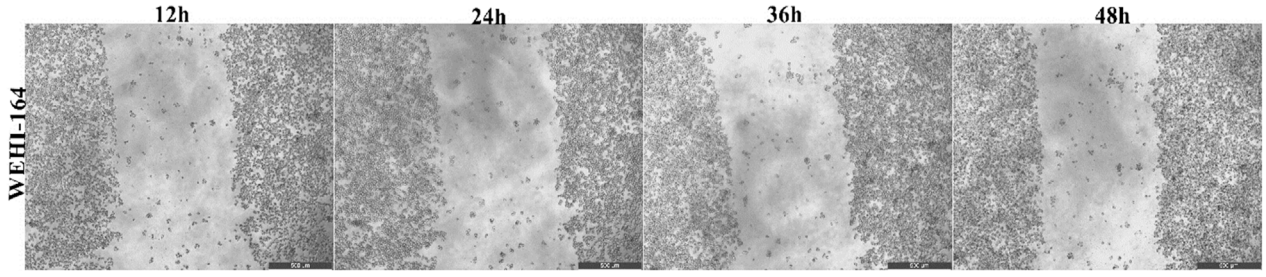

FIGURE 19
Closure of the wound gap in WEHI-164 cells after 12, 24, 36 and 48 h after incubation with CurE [2.5 μM].

TABLE 3 Percentage of L6 cells wound gap closure after incubation of the cells with the analyzed substances.

Concentration	Incubation time			
	12 h	24 h	36 h	48 h
Control	24.32%	47.22%	68.82%	99.24%
Berberine [50 μM]	8.22%	23.34%	51.09%	87.12%
Caffeic acid phenethyl ester (CAPE) [25 μM]	22.98%	41.12%	72.02%	91.14%
Cucurbitacin E (CurE) [2.5 μM]	23.92%	49.12%	87.24%	93.12%
Curcun1in [20 μM]	12.93%	42.12%	74.93%	92.22%
Biochanin A [5 μM]	22.21%	34.12%	64.33%	91.12%

and vacuolization in cancer cells treated with the compounds, with more pronounced effects observed in cancer cells compared to normal cells.

We also verified glycogen and branched-chain amino acids (BCAA) levels. We found that all tested compounds reduced glycogen levels. In cancer cells, glycogen metabolism can support rapid proliferation by providing a quick energy source and intermediates for biosynthetic pathways. It can also impact the Krebs Cycle. The Krebs cycle (TCA cycle) relies on acetyl-CoA derived from glycolysis and other sources. Reducing glycogen levels could reduce glycolytic flux and thereby inhibit the TCA cycle, potentially starving cancer cells of energy and biosynthetic precursors (Halabe Bucay, 2007). Cancer cells often rely on aerobic glycolysis (Warburg effect) rather than oxidative phosphorylation (Pelicano et al., 2006). However, inhibiting glycogen could still stress their metabolism, especially under fluctuating glucose conditions. Compounds that decrease glycogen levels in cancer cells can potentially inhibit their growth by reducing available glucose for glycolysis and the TCA cycle. A decrease in glycogen levels can lead to reduced ATP production, slower proliferation, and increased sensitivity to other metabolic stresses or treatments. Our findings highlight the potential of natural

TABLE 4 Percentage of WEHI-164 cells wound gap closure after incubation of the cells with the analysed substances.

Concentration	Incubation time			
	12 h	24 h	36 h	48 h
Control	20.91%	49.82%	74.23%	99.51%
Berberine [50 μM]	14.31%	36.09%	44.47%	57.72%
Caffeic acid phenethyl ester (CAPE) [25 μM]	10.24%	16.98%	26.12%	39.12%
Cucurbitacin E (CurE) [2.5 μM]	9.24%	17.22%	21.02%	26.12%
Curcumin [20 μM]	7.98%	17.76%	24.98%	37.12%
BiochaninA [5 μM]	14.45%	34.76%	57.12%	72.24%

compounds to disrupt cancer cell metabolism and cytoskeletal organization, contributing to their antiproliferative and cytotoxic effects. For anticancer therapy, targeting glycogen metabolism to decrease glycogen levels in cancer cells could be beneficial (Khan et al., 2020). This approach could (i) starve cancer cells, i.e., reduce energy supply and biosynthetic precursors from glycolysis and the TCA cycle (ii) increase stress and make cancer cells more susceptible to metabolic inhibitors or other treatments. Natural compounds which are potential NF-κB inhibitors can selectively induce apoptosis, disrupt cytoskeletal organization, and impair glycogen metabolism in fibrosarcoma cells while sparing normal muscle cells. These compounds' ability to reduce glycogen levels, inhibit cell migration, and interact with cytoskeletal proteins underscores their potential as multifaceted anti-cancer agents. By targeting both metabolic and structural components of cancer cells, these natural compounds offer a promising approach for cancer therapy, enhancing the effectiveness of existing treatments and reducing side effects.

Berberine has been combined with cisplatin (CPP) (Xiong et al., 2022) or doxorubicin (DOX) (Almatroodi et al., 2022) in studies showing that it enhances the cytotoxicity of cisplatin in cancer cells while protecting normal cells from damage by reducing oxidative stress. This combination has been particularly investigated in lung and ovarian cancers. Similarly CAPE also enhanced anticancer efficacy of DOX (Liang et al., 2023). CAPER revealed promising activity in resistant breast or colon cancers. Other studies showed that curcumin can be used with paclitaxel by inhibiting NF-κB and reducing cancer cell resistance, particularly in breast and ovarian cancer (Aggarwal et al., 2005). Cur was also combined with 5-Fluorouracil (5-FU) demonstrating synergistic effects in colon cancer (Xu et al., 2020). Also CuE was combined with DOX (Si et al., 2019) impaired AKt activation in gastric cancer, or with CPP inhibited the growth of human breast cancer cells *in vitro* (Lan et al., 2013). Thus, these combinations underscore the potential of using natural compounds alongside classical chemotherapeutic agents to improve treatment outcomes, reduce drug resistance, and minimize side effects. Thus, our results contribute to the growing knowledge in the use of natural compounds for cancer treatment. However, future studies should further elucidate the molecular mechanisms involved and explore the synergistic effects of combining these natural inhibitors with conventional chemotherapy and radiotherapy.

5 Conclusion

Results of the study support the hypothesis that natural NF-κB inhibitors can selectively target cancer cells, reducing their viability and inducing apoptosis, while sparing normal cells. This selectivity is critical for the development of safer cancer treatments. The findings provide a rationale for the potential use of these natural compounds in anti-cancer therapy, particularly for fibrosarcoma. Their ability to inhibit key metabolic pathways and induce apoptosis in cancer cells without significantly affecting normal cells positions them as promising candidates for further preclinical and clinical evaluation. Although the *in vitro* results are encouraging, they may not fully reflect the intricate *in vivo* environment. The study is constrained by its exclusive focus on cell lines, consequently, further research involving animal models and clinical trials is required to validate these findings. Further research is required to elucidate the detailed mechanisms of action of these compounds *in vivo*, their pharmacokinetics, and potential synergistic effects with existing chemotherapeutic agents. The findings of this study demonstrate the efficacy of natural NF-κB inhibitors in targeting fibrosarcoma cells, offering a promising direction for the development of more effective and less toxic cancer therapies.

Data availability statement

The raw data supporting the conclusions of this article will be made available by the authors, without undue reservation.

Ethics statement

Ethical approval was not required for the studies on animals in accordance with the local legislation and institutional requirements because only commercially available established cell lines were used.

Author contributions

JR: Conceptualization, Data curation, Formal Analysis, Investigation, Methodology, Validation, Writing–original draft. AG: Formal Analysis, Project administration, Supervision,

Writing–review and editing. MD-Z: Data curation, Investigation, Methodology, Writing–review and editing. KH-L: Data curation, Investigation, Methodology, Writing–review and editing. MK: Data curation, Investigation, Methodology, Writing–review and editing. WS: Data curation, Investigation, Methodology, Software, Writing–review and editing. MP-O: Formal Analysis, Methodology, Writing–review and editing. JK: Conceptualization, Formal Analysis, Funding acquisition, Project administration, Resources, Supervision, Writing–original draft, Writing–review and editing.

Funding

The author(s) declare that financial support was received for the research, authorship, and/or publication of this article. Supported by the funds of Scientific Students Group no. 148 of the Department of Molecular and Cellular Biology, Wroclaw Medical University and by Statutory Funds of Department of Molecular and Cellular Biology, Wroclaw Medical University no. SUBZ.D260.24.076.

Acknowledgments

The authors are thankful to Magda Baran-Pelc for her assistance with the preparation of TEM images.

Conflict of interest

The authors declare that the research was conducted in the absence of any commercial or financial relationships that could be construed as a potential conflict of interest.

Publisher's note

References

Abdel-Latif, M. M. M., Windle, H. J., Homasany, B. S.El, Sabra, K., and Kelleher, D. (2005). Caffeic acid phenethyl ester modulates Helicobacter pylori-induced nuclear factor-kappa B and activator protein-1 expression in gastric epithelial cells. *Br. J. Pharmacol.* 146 (8), 1139–1147. doi:10.1038/sj.bjp.0706421

Aggarwal, B. B., Shishodia, S., Takada, Y., Banerjee, S., Newman, R. A., Bueso-Ramos, C. E., et al. (2005). Curcumin suppresses the paclitaxel-induced nuclear factor-kappaB pathway in breast cancer cells and inhibits lung metastasis of human breast cancer in nude mice. *Clin. Cancer Res. An Official J. Am. Assoc. Cancer Res.* 11 (20), 7490–7498. doi:10.1158/1078-0432.CCR-05-1192

Alakurtti, S., Mäkelä, T., Koskimies, S., and Yli-Kauhaluoma, J. (2006). Pharmacological properties of the ubiquitous natural product betulin. *Eur. J. Pharm. Sci.* 29 (1), 1–13. doi:10.1016/j.ejps.2006.04.006

Almatroodi, S. A., Alsahli, M. A., and Rahmani, A. H. (2022). Berberine: an important emphasis on its anticancer effects through modulation of various cell signaling pathways. *Mol. Basel, Switz.* 27 (18), 5889. doi:10.3390/molecules27185889

Cai, D., Frantz, J. D., Tawa, N. E. J., Melendez, P. A., Oh, B.-C., Lidov, H. G. W., et al. (2004). IKKbeta/NF-kappaB activation causes severe muscle wasting in mice. *Cell* 119 (2), 285–298. doi:10.1016/j.cell.2004.09.027

Chanda, J., Biswas, S., Kar, A., and Mukherjee, P. K. (2020). Determination of cucurbitacin E in some selected herbs of ayurvedic importance through RP-HPLC. *J. Ayurveda Integr. Med.* 11 (3), 287–293. doi:10.1016/j.jaim.2019.01.002

Chuu, C.-P., Lin, H.-P., Ciaccio, M. F., Kokontis, J. M., Hause, R. J. J., Hiipakka, R. A., et al. (2012). Caffeic acid phenethyl ester suppresses the proliferation of human prostate cancer cells through inhibition of p70S6K and Akt signaling networks. *Cancer Prev. Res. Phila. Pa.* 5 (5), 788–797. doi:10.1158/1940-6207.CAPR-12-0004-T

Collins, A. R. (2004). The comet assay for DNA damage and repair: principles, applications, and limitations. *Appl. Biochem. Biotechnol. - Part B Mol. Biotechnol.* 26 (Issue 3), 249–261. doi:10.1385/MB:26:3:249

Colotta, F., Allavena, P., Sica, A., Garlanda, C., and Mantovani, A. (2009). Cancer-related inflammation, the seventh hallmark of cancer: links to genetic instability. *Carcinogenesis* 30 (7), 1073–1081. doi:10.1093/carcin/bgp127

Dalton, M., Holzman, E., Erwin, E., Michelen, S., Rositch, A. F., Kumar, S., et al. (2019). Patient navigation services for cancer care in low-and middle-income countries: a scoping review. *PloS One* 14 (10), e0223537. doi:10.1371/journal.pone.0223537

Dey, P., Kundu, A., Chakraborty, H. J., Kar, B., Choi, W. S., Lee, B. M., et al. (2019). Therapeutic value of steroidal alkaloids in cancer: current trends and future perspectives. *Int. J. Cancer* 145 (7), 1731–1744. doi:10.1002/ijc.31965

Elinav, E., Nowarski, R., Thaiss, C. A., Hu, B., Jin, C., and Flavell, R. A. (2013). Inflammation-induced cancer: crosstalk between tumours, immune cells and microorganisms. *Nat. Rev. Cancer* 13 (11), 759–771. doi:10.1038/NRC3611

Gizak, A., Pirog, M., and Rakus, D. (2012). Muscle FBPase binds to cardiomyocyte mitochondria under glycogen synthase kinase-3 inhibition or elevation of cellular Ca2+ level. *FEBS Lett.* 586 (1), 13–19. doi:10.1016/j.febslet.2011.11.032

Halabe Bucay, A. (2007). The biological significance of cancer: mitochondria as a cause of cancer and the inhibition of glycolysis with citrate as a cancer treatment. *Med. Hypotheses* 69 (4), 826–828. doi:10.1016/j.mehy.2007.02.002

Huang, S., Pettaway, C. A., Uehara, H., Bucana, C. D., and Fidler, I. J. (2001). Blockade of NF-kappaB activity in human prostate cancer cells is associated with suppression of angiogenesis, invasion, and metastasis. *Oncogene* 20 (31), 4188–4197. doi:10.1038/sj.onc.1204535

Huangyang, P., Li, F., Lee, P., Nissim, I., Weljie, A. M., Mancuso, A., et al. (2020). Fructose-1,6-Bisphosphatase 2 inhibits sarcoma progression by restraining mitochondrial biogenesis. *Cell Metab.* 31 (1), 1032–1188.e7. doi:10.1016/j.cmet.2020.04.009

Jia, Q., Cheng, W., Yue, Y., Hu, Y., Zhang, J., Pan, X., et al. (2015). Cucurbitacin E inhibits TNF-α-induced inflammatory cytokine production in human synoviocyte MH7A cells via suppression of PI3K/Akt/NF-κB pathways. *Int. Immunopharmacol.* 29 (2), 884–890. doi:10.1016/j.intimp.2015.08.026

Jin, H., Jin, X., Cao, B., and Wang, W. (2017). Berberine affects osteosarcoma via downregulating the caspase-1/IL-1β signaling axis. *Oncol. Rep.* 37 (2), 729–736. doi:10.3892/or.2016.5327

Jung, M. K., Okekunle, A. P., Lee, J. E., Sung, M. K., and Lim, Y. J. (2021). Role of branched-chain amino acid metabolism in tumor development and progression. *J. Cancer Prev.* 26 (4), 237–243. doi:10.15430/JCP.2021.26.4.237

Khan, T., Sullivan, M. A., Gunter, J. H., Kryza, T., Lyons, N., He, Y., et al. (2020). Revisiting glycogen in cancer: a conspicuous and targetable enabler of malignant transformation. *Front. Oncol.* 10, 592455. doi:10.3389/fonc.2020.592455

Kim, W. S., Lee, Y. S., Cha, S. H., Jeong, H. W., Choe, S. S., Lee, M. R., et al. (2009). Berberine improves lipid dysregulation in obesity by controlling central and peripheral AMPK activity. *Am. J. Physiology - Endocrinol. Metabolism* 296 (4), 812–819. doi:10.1152/ajpendo.90710.2008

Kong, W.-J., Zhang, H., Song, D.-Q., Xue, R., Zhao, W., Wei, J., et al. (2009). Berberine reduces insulin resistance through protein kinase C-dependent up-regulation of insulin receptor expression. *Metabolism Clin. Exp.* 58 (1), 109–119. doi:10.1016/j.metabol.2008.08.013

Kucharczak, J., Simmons, M. J., Fan, Y., and Gélinas, C. (2003). To be, or not to be: NF-kappaB is the answer-role of Rel/NF-kappaB in the regulation of apoptosis. *Oncogene* 22 (56), 8961–8982. doi:10.1038/sj.onc.1207230

Lan, T., Wang, L., Xu, Q., Liu, W., Jin, H., Mao, W., et al. (2013). Growth inhibitory effect of Cucurbitacin E on breast cancer cells. *Int. J. Clin. Exp. Pathology* 6 (9), 1799–1805.

Li, H., Wang, J., Xu, H., Xing, R., Pan, Y., Li, W., et al. (2013). Decreased fructose-1,6-bisphosphatase-2 expression promotes glycolysis and growth in gastric cancer cells. *Mol. Cancer* 12 (1), 110. doi:10.1186/1476-4598-12-110

Li, J., Wang, Y., Li, Q.-G., Xue, J.-J., Wang, Z., Yuan, X., et al. (2016). Downregulation of FBP1 promotes tumor metastasis and indicates poor prognosis in gastric cancer via regulating epithelial-mesenchymal transition. *PloS One* 11 (12), e0167857. doi:10.1371/journal.pone.0167857

Li, Y., Yu, H., Han, F., Wang, M., Luo, Y., and Guo, X. (2018). Biochanin A induces S phase arrest and apoptosis in lung cancer cells. *BioMed Res. Int.* 2018, 3545376. doi:10.1155/2018/3545376

Liang, L.-C., Zhao, L., Yu, B., Hu, H.-X., He, X.-H., and Zhang, Y.-M. (2023). Caffeic acid phenethyl ester reverses doxorubicin resistance in breast cancer cells via lipid metabolism regulation at least partly by suppressing the Akt/mTOR/SREBP1 pathway. *Kaohsiung J. Med. Sci.* 39 (6), 605–615. doi:10.1002/kjm2.12675

Martin, S. B., Reiche, W. S., Fifelski, N. A., Schultz, A. J., Stanford, S. J., Martin, A. A., et al. (2020). Leucine and branched-chain amino acid metabolism contribute to the growth of bone sarcomas by regulating AMPK and mTORC1 signaling. *Biochem. J.* 477 (9), 1579–1599. doi:10.1042/BCJ20190754

Masters, T. A., Kendrick-Jones, J., and Buss, F. (2017). Myosins: domain organisation, motor properties, physiological roles and cellular functions. *Handb. Exp. Pharmacol.* 235, 77–122. doi:10.1007/164_2016_29

Moore-Carrasco, R., Busquets, S., Almendro, V., Palanki, M., López-Soriano, F. J., and Argilés, J. M. (2007). The AP-1/NF-kappaB double inhibitor SP100030 can revert muscle wasting during experimental cancer cachexia. *Int. J. Oncol.* 30 (5), 1239–1245. doi:10.3892/ijo.30.5.1239

Nambiar, R., McConnell, R. E., and Tyska, M. J. (2010). Myosin motor function: the ins and outs of actin-based membrane protrusions. *Cell. Mol. Life Sci. CMLS* 67 (8), 1239–1254. doi:10.1007/s00018-009-0254-5

Neag, M. A., Mocan, A., Echeverría, J., Pop, R. M., Bocsan, C. I., Crişan, G., et al. (2018). Berberine: botanical occurrence, traditional uses, extraction methods, and relevance in cardiovascular, metabolic, hepatic, and renal disorders. *Front. Pharmacol.* 9, 557. doi:10.3389/fphar.2018.00557

Pavan, A. R., Silva, G. D. B. da, Jornada, D. H., Chiba, D. E., Fernandes, G. F. D. S., Man Chin, C., et al. (2016). Unraveling the anticancer effect of curcumin and resveratrol. *Nutrients* 8 (11), 628. doi:10.3390/nu8110628

Pelicano, H., Martin, D. S., Xu, R. H., and Huang, P. (2006). Glycolysis inhibition for anticancer treatment. *Oncogene* 25 (34), 4633–4646. doi:10.1038/sj.onc.1209597

Pietras, Ł., Stefanik, E., Rakus, D., and Gizak, A. (2022). FBP2-A new player in regulation of motility of mitochondria and stability of microtubules in cardiomyocytes. *Cells* 11 (10), 1710. doi:10.3390/cells11101710

Pirog, M., Gizak, A., and Rakus, D. (2014). Changes in quaternary structure of muscle fructose-1,6-bisphosphatase regulate affinity of the enzyme to mitochondria. *Int. J. Biochem. & Cell Biol.* 48, 55–59. doi:10.1016/j.biocel.2013.12.015

Qiao, J., Xu, L., He, J., Ouyang, D., and He, X. (2013). Cucurbitacin E exhibits anti-inflammatory effect in RAW 264.7 cells via suppression of NF-κB nuclear translocation. *Inflamm. Res. Official J. Eur. Histamine Res. Soc.* 62 (5), 461–469. doi:10.1007/s00011-013-0598-z

Radzka, J., Łapińska, Z., Szwedowicz, U., Gajewska-Naryniecka, A., Gizak, A., and Kulbacka, J. (2023). Alternations of NF-κB signaling by natural compounds in muscle-derived cancers. *Int. J. Mol. Sci.* 24 (15), 11900. doi:10.3390/ijms241511900

Reynolds, E. S. (1963). The use of lead citrate at high pH as an electron-opaque stain in electron microscopy. *J. Cell Biol.* 17 (1), 208–212. doi:10.1083/jcb.17.1.208

Sadeghi, M., Dehnavi, S., Asadirad, A., Xu, S., Majeed, M., Jamialahmadi, T., et al. (2023). Curcumin and chemokines: mechanism of action and therapeutic potential in inflammatory diseases. *Inflammopharmacology* 31 (3), 1069–1093. doi:10.1007/s10787-023-01136-w

Si, W., Lyu, J., Liu, Z., Wang, C., Huang, J., Jiang, L., et al. (2019). Cucurbitacin E inhibits cellular proliferation and enhances the chemo-response in gastric cancer by suppressing AKt activation. *J. Cancer* 10 (23), 5843–5851. doi:10.7150/jca.31303

Srivastava, S., Somasagara, R. R., Hegde, M., Nishana, M., Tadi, S. K., Srivastava, M., et al. (2016). Quercetin, a natural flavonoid interacts with DNA, arrests cell cycle and causes tumor regression by activating mitochondrial pathway of apoptosis. *Sci. Rep.* 6 (1), 24049. doi:10.1038/srep24049

Wang, L.-C., Chu, K.-H., Liang, Y.-C., Lin, Y.-L., and Chiang, B.-L. (2010). Caffeic acid phenethyl ester inhibits nuclear factor-kappaB and protein kinase B signalling pathways and induces caspase-3 expression in primary human CD4+ T cells. *Clin. Exp. Immunol.* 160 (2), 223–232. doi:10.1111/j.1365-2249.2009.04067.x

Wang, Z., Zhang, L., Ni, Z., Sun, J., Gao, H., Cheng, Z., et al. (2015). Resveratrol induces AMPK-dependent MDR1 inhibition in colorectal cancer HCT116/L-OHP cells by preventing activation of NF-κB signaling and suppressing cAMP-responsive element transcriptional activity. *Tumour Biol. J. Int. Soc. Oncodevelopmental Biol. Med.* 36 (12), 9499–9510. doi:10.1007/s13277-015-3636-3

Wiśniewski, J., Piróg, M., Hołubowicz, R., Dobryszycki, P., McCubrey, J. A., Rakus, D., et al. (2017). Dimeric and tetrameric forms of muscle fructose-1,6-bisphosphatase play different roles in the cell. *Oncotarget* 8 (70), 115420–115433. doi:10.18632/oncotarget.23271

Wyke, S. M., Russell, S. T., and Tisdale, M. J. (2004). Induction of proteasome expression in skeletal muscle is attenuated by inhibitors of NF-kappaB activation. *Br. J. Cancer* 91 (9), 1742–1750. doi:10.1038/sj.bjc.6602165

Xiong, R.-G., Huang, S.-Y., Wu, S.-X., Zhou, D.-D., Yang, Z.-J., Saimaiti, A., et al. (2022). Anticancer effects and mechanisms of berberine from medicinal herbs: an update review. *Molecules* 27 (Issue 14), 4523. doi:10.3390/molecules27144523

Xu, E., Ji, B., Jin, K., and Chen, Y. (2023). Branched-chain amino acids catabolism and cancer progression: focus on therapeutic interventions. *Front. Oncol.* 13, 1220638. doi:10.3389/fonc.2023.1220638

Xu, T., Guo, P., Pi, C., He, Y., Yang, H., Hou, Y., et al. (2020). Synergistic effects of curcumin and 5-fluorouracil on the hepatocellular carcinoma *in vivo* and vitro through regulating the expression of COX-2 and NF-κB. *J. Cancer* 11 (13), 3955–3964. doi:10.7150/jca.41783

Yu, C., Zhang, P., Lou, L., and Wang, Y. (2019). Perspectives regarding the role of biochanin A in humans. *Front. Pharmacol.* 10, 793. doi:10.3389/fphar.2019.00793

Yun, C. W., and Lee, S. H. (2018). The roles of autophagy in cancer. *Int. J. Mol. Sci.* 19 (11), 3466. doi:10.3390/ijms19113466

frontiers | Frontiers in Cell and Developmental Biology

TYPE Mini Review
PUBLISHED 06 January 2025
DOI 10.3389/fcell.2024.1514898

OPEN ACCESS

EDITED BY
Shoulong Deng,
Chinese Academy of Medical Sciences and Peking Union Medical College, China

REVIEWED BY
Abderrahman Ouban,
Alfaisal University, Saudi Arabia

*CORRESPONDENCE
A. Aartsma-Rus,
a.m.aartsma-rus@lumc.nl

RECEIVED 21 October 2024
ACCEPTED 12 December 2024
PUBLISHED 06 January 2025

CITATION
Aartsma-Rus A (2025) Histone deacetylase inhibition with givinostat: a multi-targeted mode of action with the potential to halt the pathological cascade of Duchenne muscular dystrophy.
Front. Cell Dev. Biol. 12:1514898.
doi: 10.3389/fcell.2024.1514898

Histone deacetylase inhibition with givinostat: a multi-targeted mode of action with the potential to halt the pathological cascade of Duchenne muscular dystrophy

A. Aartsma-Rus*

Department of Human Genetics, Leiden University Medical Center (LUMC), Leiden, Netherlands

Muscle repair and regeneration are complex processes. In Duchenne muscular dystrophy (DMD), these processes are disrupted by the loss of functional dystrophin, a key part of the transmembrane dystrophin-associated glycoprotein complex that stabilizes myofibers, indirectly leading to progressive muscle wasting, subsequent loss of ambulation, respiratory and cardiac insufficiency, and premature death. As part of the DMD pathology, histone deacetylase (HDAC) activity is constitutively increased, leading to epigenetic changes and inhibition of muscle regeneration factors, chronic inflammation, fibrosis, and adipogenesis. HDAC inhibition has consequently been investigated as a therapeutic approach for muscular dystrophies that, significantly, works independently from specific genetic mutations, making it potentially suitable for all patients with DMD. This review discusses how HDAC inhibition addresses DMD pathophysiology in a multi-targeted mode of action and summarizes the recent evidence on the rationale for HDAC inhibition with givinostat, which is now approved by the United States Food and Drug Administration for the treatment of DMD in patients aged 6 years and older.

KEYWORDS

dystrophinopathy, acetylation, muscle repair, myogenesis, inflammation, FAP cells, satellite cells, miRNA

Introduction

In patients with Duchenne muscular dystrophy (DMD), the direct effect of the characteristic lack of dystrophin is the loss of muscle sarcolemma membrane stability, which results in DMD pathology (Mozzetta et al., 2024). DMD is characterized by progressive loss of muscle tissues, leading to loss of ambulation and the need for assisted ventilation, and, eventually, premature death in the 2–4th decade (Ryder et al., 2017; Walter and Reilich, 2017). Indirectly, the loss of dystrophin results in a cascade of pathological events in the muscle cell that include chronic inflammation and failed

Abbreviations: DMD, Duchenne muscular dystrophy; DAPC, dystrophin-associated glycoprotein protein complex; FAP, fibro-adipogenic progenitor; HDAC, histone deacetylase; MHCI, major histocompatibility complex class I; MCHII, major histocompatibility complex class II; miRNA, microribonucleic acid; MPO, myeloperoxidase; MuSC, muscle stem cell; NOS, nitric oxide synthase.

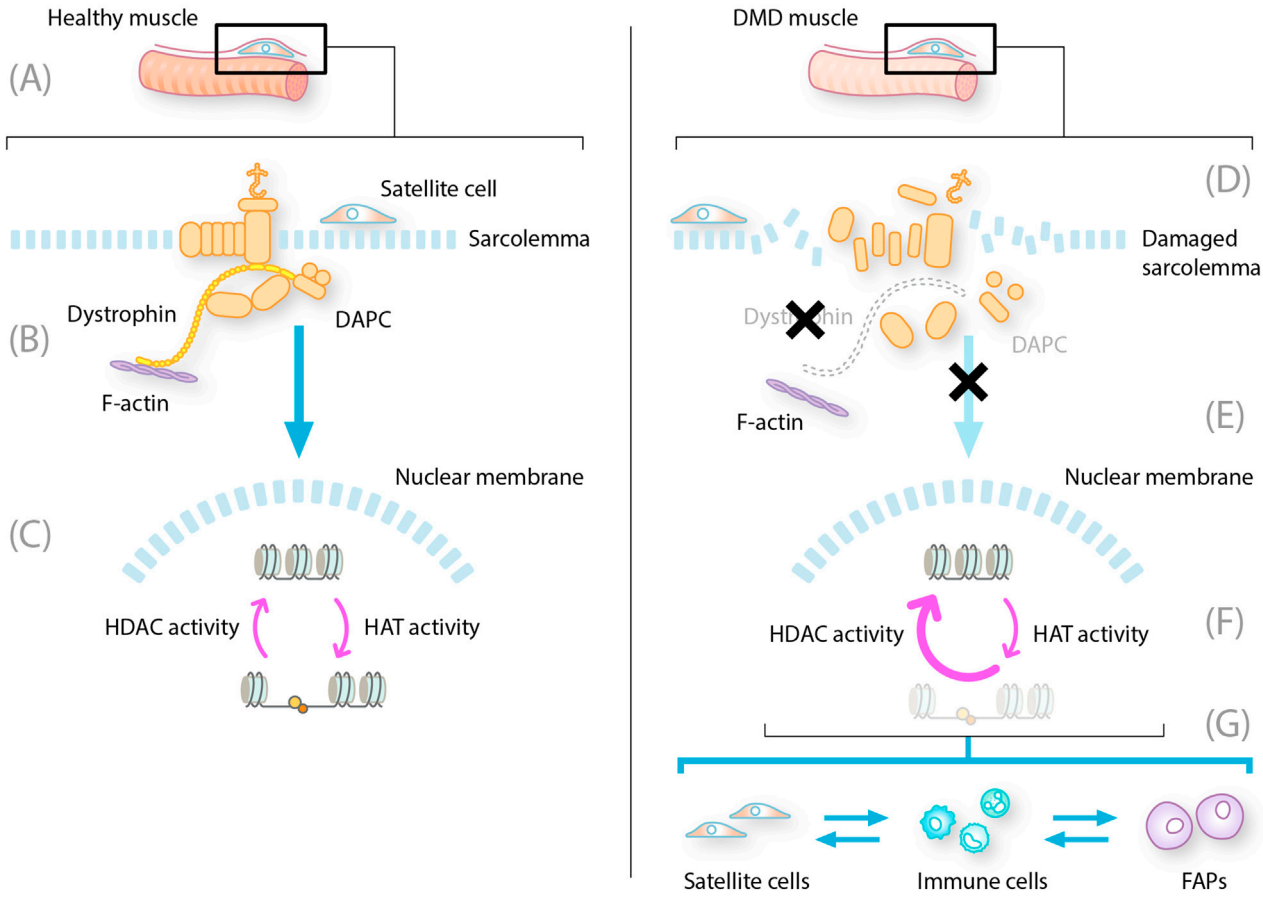

FIGURE 1
Constitutive HDAC activity contributes to dystrophic muscle pathology. DAPC, dystrophin-associated protein complex; DMD, Duchenne muscular dystrophy; FAP, fibro-adipogenic progenitor; HAT, histone acetyltransferase; HDAC, histone deacetylase; MuSC, muscle stem cell; NO, nitrous oxide; NOS, nitric oxide synthase. LEFT: healthy muscle fibers with intact dystrophin and DAPC. **(A)** MuSC and satellite cells reside on the muscle fibers ready to differentiate into new muscle fibers **(B)** Intact DAPC regulates activity of HDAC to allow translation of muscle regeneration factors **(C)** In the nucleus HDAC and HAT work in balance to regulate the expression of muscle regeneration factors RIGHT: DMD muscle with mutated dystrophin and disrupted DAPC **(D)** Absent or mutated dystrophin leads to disruption of the DAPC with multiple consequences for muscle repair **(E)** These consequences include damage to the sarcolemma leading to cytoplasmic leakage displacement of NOS and decreased levels of NO, which, in turn, lead to aberrant constitutive expression of HDACs **(F)** Increased HDAC activity results in repression of translation and transcription of muscle repair regeneration factors **(G)** The absence of gene transcription leads to changes in the production of new myofibres from satellite cells, prolongation of inflammatory phases of repair into a chronic state, and induction of FAP differentiation into fibroblasts and adipocytes.

regeneration (Dowling et al., 2023). One pathological aspect perpetuating the pathological pathways is the increased activity of histone deacetylase (HDAC) enzymes. As such, the global inhibition of HDAC activity has received attention as a therapeutic approach for treating muscular dystrophies (Lamb, 2024). Preclinical and clinical studies have demonstrated positive effects of HDAC inhibition on multiple levels of DMD-related pathogenic events (Mozzetta et al., 2024). Pivotal phase 3 clinical trial data have recently been published for givinostat, an HDAC inhibitor that was investigated in ambulant boys aged 6 years and older with DMD (Mercuri et al., 2024). In this multicenter, randomized trial, givinostat significantly delayed DMD disease progression compared with placebo and had a positive risk/benefit profile. Givinostat has recently been approved by the US Food and Drug Administration for the treatment of DMD in patients aged 6 years and older (Lamb, 2024; United States Food and Drug Administration, 2024), and evaluation by the European Medicines Agency is ongoing (Duchenne UK, 2023). The purpose of this narrative review is to elaborate on how HDAC inhibition addresses DMD pathophysiology in a multi-targeted mode of action and to summarize the recent evidence on the rationale for HDAC inhibition with givinostat.

Dystrophin and DMD

DMD results from mutations in the *DMD* gene encoding dystrophin, the largest known human gene (Aartsma-Rus et al., 2016; Okubo et al., 2017). So far, over 7,000 mutations in the *DMD* gene have been identified (Aartsma-Rus et al., 2016; Bladen et al., 2015). These mutations result in the absence of functional dystrophin (Blake et al., 2002; Hoffman et al., 1987).

Dystrophin has a mechanical, stabilizing function in skeletal muscle fibers by connecting the cytoskeleton—part of the contractile machinery—to the connective tissue surrounding each muscle fiber. Specifically, dystrophin binds to F-actin in the cytoskeleton and to a

part of the transmembrane dystrophin-associated glycoprotein protein complex (DAPC) called beta-dystroglycan, which in turn binds to the connective tissue protein laminin (Mukund and Subramaniam, 2020; Wilson et al., 2022; Campbell and Kahl, 1989; Ervasti and Campbell, 1993; Guiraud et al., 2015).

Normal muscle repair

Muscle contraction and relaxation cause stress to the muscle fibers, and damage can occur during regular activity or trauma. Muscle fibers are postmitotic, and muscle damage repair is orchestrated by satellite cells, quiescent cells that lie on top of muscle fibers, which are activated when there is damage. Upon activation, satellite cells proliferate into muscle stem cells (MuSC), which differentiate into muscle fibers to repair the damage (Figure 1) (Mukund and Subramaniam, 2020). Healthy skeletal muscle has a unique immune-privileged status, with fewer antigen-presenting cells and pro-inflammatory cells present, and no constitutive major histocompatibility complex class I (MHCI) or II (MHCII) expression, resulting in less necrosis and a lower capacity to generate abscesses (Bez Batti Angulski et al., 2023; Sciorati et al., 2016). Contraction can cause membrane damage and leakage of cytoplasmic content into the extracellular compartment. Due to skeletal muscle's unique immune privilege, rapid membrane repair mechanisms, and membrane stability conferred by intact dystrophin, this inflammatory response is limited, controlled, and quickly resolved in healthy muscle (Sciorati et al., 2016).

Myogenesis also depends significantly on the interaction between satellite cells and their microenvironment (Mukund and Subramaniam, 2020). In healthy muscle, injury is repaired by the asymmetric division of satellite cells; the interactions of DAPC subunits are essential for this process (Chang et al., 2018; Duan et al., 2021; Dumont et al., 2015). The activation and migration of satellite cells to the injury site and their proliferation and differentiation into muscle fibers is a synchronized series of stepwise processes. First, upon muscle injury, there is an acute and transient innate immune system response. During this process, the immune system will inhibit the myogenic repair system, enabling inflammatory cells (neutrophils, eosinophils, and macrophages) to be recruited to clear the area of debris. M1 macrophages arrive first and induce a pro-inflammatory phase that, in muscle, causes the secretion of cytokines, promoting myogenic cell proliferation. In the subsequent anti-inflammatory phase, M2 macrophages facilitate myogenic differentiation, stimulating the activation, proliferation, and division of satellite cells (Blau et al., 2015; Rugowska et al., 2021; Ziemkiewicz et al., 2021). Once the damage is cleared, fibro-adipogenic progenitors (FAPs) are activated to repair the extracellular matrix. FAPs are muscle-resident multipotent mesenchymal stem cells that can differentiate into adipocytes, fibroblasts, or osteocytes. Intrinsic and extrinsic regulatory mechanisms control the activation, proliferation, cell fate decision, and clearance of FAPs (Molina et al., 2021). Finally, satellite cells are activated to proliferate and differentiate into mature muscle either by fusing with the remaining muscle fiber or by forming a new fiber within the shell of connective tissue. Many transcription factors are involved in muscle development and repair, and they have a temporal sequence of activation across various stages of myogenesis (Mukund and Subramaniam, 2020). While the differentiation of satellite cells produces new myofibers necessary for muscle repair and regeneration, the self-renewal of satellite cells is crucial for maintaining the stem cell population (Kodippili and Rudnicki, 2023).

Failed muscle repair in DMD

The loss of functional dystrophin in DMD results in the disassembly of DAPC complexes, reduced expression levels of certain DAPC components, and the loss of the interaction between the F-actin cytoskeleton and the extracellular matrix. This leads to wide-ranging consequences, including loss of membrane and myofiber integrity, impaired muscle fiber contractile activity, contraction-induced membrane rupture, and progressive muscle degeneration (Figure 1) (Dowling et al., 2023; Kodippili and Rudnicki, 2023). The membrane leakage leads to continuous release of cytoplasmic content, including damage-associated molecular patterns that are ligands to toll-like receptors, P2RX7, and other pattern recognition receptors on muscle and adaptive immune cells (Bez Batti Angulski et al., 2023; Giordano et al., 2015; Henriques-Pons et al., 2014; Sinadinos et al., 2015). Pattern recognition receptors activate downstream signaling cascades and initiate the innate immune response, and pro-inflammatory cytokines induce the expression of MHCI and MHCII on muscle fibers, removing the immune privilege (Bez Batti Angulski et al., 2023).

Membrane leakage also results in abnormal calcium handling and associated proteolytic degradation of muscle proteins, leading to a cascade of pathological events in the muscle cell and a desynchronization of the repair processes with failure of proper myogenic repair (Dowling et al., 2023).

Compared with the cycling states in normal muscle tissue, the innate and adaptive immune system becomes chronically activated in patients with DMD, inhibiting muscle repair even at locations where the debris has been cleared. The chronic inflammatory response in muscle fibers of patients with DMD is maintained by overlapping pro- and anti-inflammatory signaling, preventing the full resolution of inflammation (Bez Batti Angulski et al., 2023). FAPs are improperly activated and persist at sites of tissue damage. Here, they produce excess connective tissue leading to fibrosis and differentiate into fibroblasts and fat cells that produce fat tissue (adiposis) (Giuliani et al., 2022). The MuSCs maintain a proliferative state, and due to the signals from inflammatory cells and FAPs, they transdifferentiate into FAPs—additionally, increased symmetric satellite cell expansion results in satellite cell hyperplasia. Fewer asymmetric cell divisions lead to low myogenic progenitor cell numbers (Kodippili and Rudnicki, 2023).

Functions of HDACs

HDACs are evolutionarily conserved enzymes that remove acetylated groups from lysine residues in histones. This action leads to a "closed" histone structure and reduced DNA accessibility. The HDAC counterparts, histone acetylases, add

acetyl groups to proteins, leading to an "open" histone structure and increased DNA accessibility for transcription factors (Eslaminejad et al., 2013; Mozzetta et al., 2024).

The combinations of histone modifications determine their overall interaction with DNA, leading to activation and/or inhibition of transcription (Eslaminejad et al., 2013). Many chromatin states are regulated and maintained in a tissue-specific way, ensuring DNA is accessible at specific times and precise locations (Mariño-Ramírez et al., 2005). Specifically, the acetylation and deacetylation of proteins influence important processes in muscle cells (Sandonà et al., 2023).

HDACs have many roles (Molinari et al., 2023; Sandonà et al., 2023); by both directly and indirectly regulating gene expression, they also control key cellular processes through the deacetylation of non-histone proteins and act as effectors in response to physiological and pathological signals (e.g., acetylation of SMADs can dampen TGF-β signaling by reducing SMAD phosphorylation) (Osseni et al., 2022). Genetic and pharmacological manipulations of HDACs in both *in vitro* and *in vivo* settings have emphasized their crucial role in the maintenance and adaptation of skeletal muscle metabolism (Molinari et al., 2023).

Increased levels of HDACs in DMD

A lack of dystrophin results in HDAC hyperactivity, which exacerbates, at least in part, the pathological processes outlined above. Dystrophin, as part of the DAPC, has many other important roles in addition to providing mechanical stability to muscle fibers (Dowling et al., 2023). It is crucial for signal transduction between the internal and external environments of the muscle cell, providing a scaffold responsible for the membrane localization of signaling proteins. In health, the DAPC anchors a variety of signaling molecules to their functional sites at the sarcolemma via the syntrophin protein. One such is the enzyme nitric oxide synthase (NOS), which regulates the intramuscular generation of nitric oxide and microribonucleic acids (miRNAs) required for muscle tissue maintenance and regeneration. This is achieved through the modification of HDACs (Marrone and Shcherbata, 2011). In DMD, dystrophin loss and DAPC disassembly lead to the displacement of muscle-specific NOS. The resultant reduction in nitric oxide generation leads to an aberrant, constitutive hyperactivation of HDACs due to NO-mediated S-nitrosylation (Kodippili and Rudnicki, 2023; Marrone and Shcherbata, 2011; Sandoná et al., 2016).

The consequences of constitutive HDAC activity

Aberrant and constitutive hyperactive HDACs in patients with DMD cause excessive acetyl group removal from histone proteins, preventing transcription of key homeostatic genes (Mozzetta et al., 2024), resulting in a decrease in the levels of myogenic miRNAs (Rugowska et al., 2021).

This has many pathological consequences for muscle damage repair. First, the immune system becomes chronically activated in the muscle (Rosenberg et al., 2015). HDACs appear to have a role in the regulation of the immune response (Licciardi and Karagiannis, 2012; Sweet et al., 2012). In the context of DMD, in which immune cells infiltrate muscles and contribute to disease pathology, the constitutive hyperactivity of HDACs affects the balance between pro-inflammatory and anti-inflammatory immune cell populations, thereby influencing disease progression (Figure 1) (Bez Batti Angulski et al., 2023; Kulthinee et al., 2022; Licciardi and Karagiannis, 2012). Specifically, HDAC hyperactivity has been associated with the suppression of regulatory T cells through the deacetylation of Foxp3 (Beier et al., 2011).

Second, it results in altered FAP activity. The FAPs stall in connective tissue production mode and become fibroblasts and fat cells instead of supporting the satellite cells to differentiate and repair muscle (Figure 2) (Marrone and Shcherbata, 2011; Ren et al., 2024; Rugowska et al., 2021; Saccone et al., 2014; Sandoná et al., 2016). Evidence from a DMD mouse model (*mdx*) has revealed an HDAC-regulated network that consists of myogenic miRNAs and a chromatin remodeling complex that is able to activate the myogenic program in FAPs. HDAC-mediated repression of myogenic miRNAs is reported in dystrophic muscles (Saccone et al., 2014).

Third, activated satellite cells cannot differentiate into new fibers without FAP involvement (Figure 1). Hyperactive HDACs deacetylate faster than HATs (Hyperactive HDACs deacetylate faster than HATs acetylate), thereby reducing the activity of transcription factors and co-factors critical for myogenic differentiation, such as MyoD and MEF2 (Marrone and Shcherbata, 2011; Rugowska et al., 2021) and impairing the differentiation of satellite cells (Marrone and Shcherbata, 2011; Ren et al., 2024). This leads to ineffective muscle repair and regeneration in patients with DMD. Furthermore, the FAPs produce factors causing activated satellite cells to transdifferentiate into fibroblasts and lose muscle repair capability (Molina et al., 2021; Ren et al., 2024).

Proteins other than histones are also regulated by the addition and removal of acetyl groups, which can further exacerbate muscle damage and pathology in DMD. For example, a key regulator of fibrosis, TGF-β, works by triggering the addition of a phosphate group to a protein complex, SMAD, leading to fibrosis (Biernacka et al., 2011). Normally, this process is inhibited by SMAD acetylation (Osseni et al., 2022). However, with HDAC hyperactivity, these acetyl groups are actively removed, reducing the threshold for adding phosphate groups and thus further increasing fibrosis.

HDAC inhibition in dystrophinopathy

The finding that dystrophin deficiency leads to constitutive HDAC activation in muscles has provided a rationale for investigating HDAC inhibitors such as givinostat in DMD (Lamb, 2024): given that multiple muscle damage and repair processes are exacerbated by excessive HDAC activity, inhibiting HDAC activity could improve muscle repair and alleviate DMD pathology. HDAC inhibition is expected to allow immune cells to transition from a pro-inflammatory state to a modulatory state, which would diminish the immune response and reduce the inhibition of muscle repair processes. HDAC inhibition might also direct FAPs to regain their supportive role in muscle repair and prevent their production of fat and connective tissues. Evidence

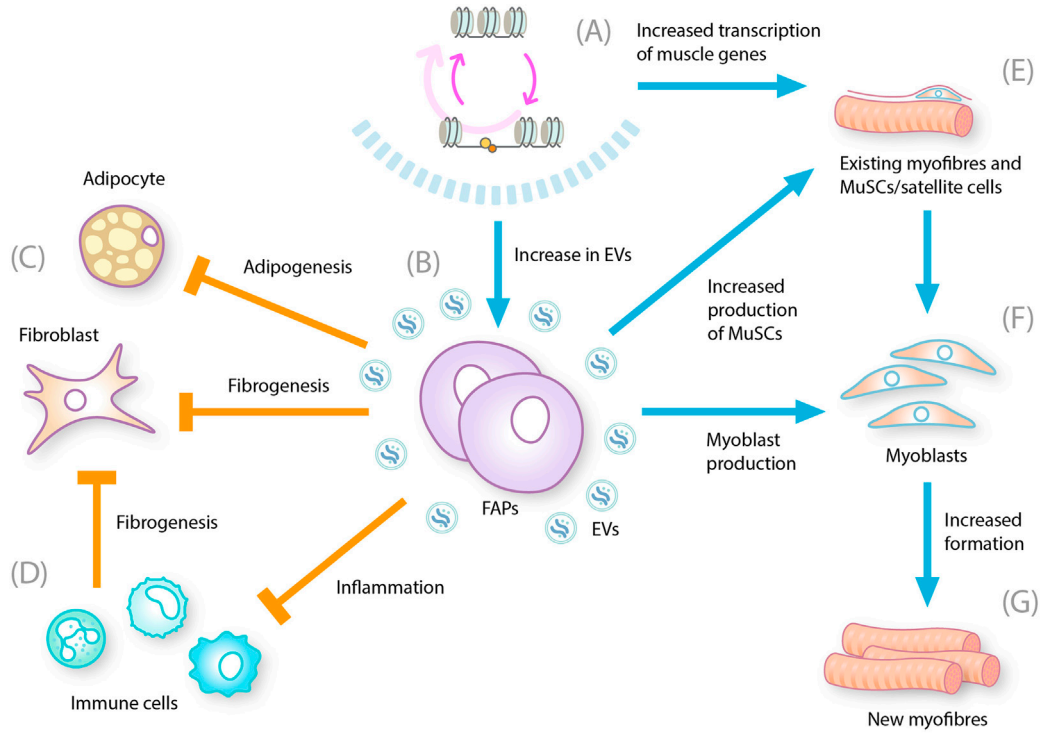

FIGURE 2
Multiple effects of HDAC inhibition on DMD-related pathogenesis. DMD, Duchenne muscular dystrophy; EV, extracellular vesicle; FAP, fibro-adipogenic progenitor; HDACi, histone deacetylase inhibitor, MuSC, muscle stem cell. HDAC inhibition leads to **(A)** Reduction in hyperacetylation of chromatin by HDAC and restoration of gene transcription **(B)** Increase in the number of EVs produced by FAPS that contain microRNAs that influence the biological processes controlling muscle regeneration, fibrogenesis, and inflammation **(C)** Decrease in the differentiation of FAP cells into adipocytes and fibroblasts **(D)** Decrease in chronic inflammation and reduction in inflammatory cytokines, which also reduces fibrosis **(E)** Increases transcription of muscle genes and decreases myofiber membrane leakage and myofiber degeneration/necrosis. Inhibits activation of TGF-β signaling **(F)** Increases fusion of myoblasts into differentiated myotubes **(G)** Increases formation of regenerating, center-nucleated myofibers.

suggests that FAPs exposed to HDAC inhibitors increase the extracellular vesicle levels of a subset of miRNAs that target biological processes such as regeneration, fibrosis, and inflammation (Sandonà et al., 2020). Satellite cells can also be prompted to differentiate into muscle fibers rather than remaining stalled in proliferation mode (Figure 2) (Kodippili and Rudnicki, 2023).

Exposure of *mdx* mice to HDAC inhibitors demonstrated therapeutic effects in dystrophinopathy, including histological improvement in fibrosis and inflammation, as well as enhanced muscle regeneration, decreased membrane permeability, and increased muscle strength and performance (Mozzetta et al., 2024).

Effects of givinostat in DMD

Although HDAC inhibitors have been in development for many years and for many diseases, relatively few have been approved for use in specific indications (Mozzetta et al., 2024). HDAC inhibitors have a narrow therapeutic window; doses above a certain threshold are required for a therapeutic effect, but high doses can be associated with dose-limiting side effects (Sandonà et al., 2023).

Givinostat is an orally bioavailable, potent HDAC inhibitor (Lamb, 2024; United States Food and Drug Administration, 2024) designed to overcome the challenges observed in previous studies (Mozzetta et al., 2024). Unlike other HDAC inhibitors, givinostat has shown efficacy at dosing levels that are generally tolerated (Lamb, 2024; Mercuri et al., 2024).

On a molecular level, HDAC inhibition by givinostat leads to a cascade of changes in gene expression, protein function, and cellular processes. Specifically, one effect of HDAC inhibition by givinostat leads to hyperacetylation of histones, resulting in a more open and relaxed chromatin structure. Consequently, transcription factors and other regulatory proteins can more easily access DNA, enhancing the transcription of genes involved in muscle repair and anti-inflammatory responses. The effects of this inhibition by givinostat have been consistently demonstrated throughout a defined preclinical and clinical program.

Preclinical evidence of givinostat efficacy

The effect of givinostat on myogenic miRNAs has been investigated in *mdx* mice. In untreated *mdx* versus wild-type mice, 120 miRNAs were found to be significantly upregulated and 66 were found to be significantly downregulated (Licandro et al., 2021), and correlations noted with patients with DMD

(Cacchiarelli et al., 2011; Licandro et al., 2021). Furthermore, specific miRNAs have been shown to correlate with DMD pathology. In *mdx* mice, givinostat was shown to induce miRNAs (miR-449a-5p and miR-92b-3p) that are known to be linked to stem cell pluripotency and are reduced in patients with heart failure (Licandro et al., 2021). Both *in vitro* and *ex vivo*, givinostat restored human DMD FAP ability to support MuSC differentiation into multinucleated myotubes, indicating that additional events resulting from DAPC disassembly can be dysregulated in DMD MuSCs (Sandonà et al., 2020). The muscle regeneration factor, miR-206, is repressed in DMD MuSCs (Cacchiarelli et al., 2011); and could be compensated by FAP-derived EVs-miR-206 to restore MuSC ability to regenerate dystrophic muscle (Sandonà et al., 2020).

Histopathological analysis also demonstrated improvements with givinostat treatment. Givinostat significantly reduced fibrosis by up to 30%–40% in *mdx* mice compared with healthy controls and reduced inflammation (Consalvi et al., 2013). In another study, givinostat also reduced fibrosis, necrosis, and fat replacement in skeletal muscle tissue in *mdx* mice (Licandro et al., 2021). Fibrosis, often regarded as the most detrimental consequence of disease progression in DMD mouse models, arises from complex interactions between resident cell types and inflammatory infiltrates. The myeloperoxidase (MPO) enzyme produced by neutrophils, monocytes, and macrophages serves as a marker for quantifying inflammation linked to muscle degeneration in muscular dystrophies. Significantly reduced MPO activity was observed in the muscles of *mdx* mice treated with givinostat compared to those treated with a vehicle control. These results were also supported by functional improvements in *mdx* mice, where givinostat treatment resulted in muscle regeneration. Histological images showed that givinostat increased muscle fiber diameter (measured as myofiber cross-sectional area) in *mdx* mice compared to control (Consalvi et al., 2013). Givinostat treatment resulted in increased muscle strength, demonstrated by dose-dependent improvements in the grip test (Licandro et al., 2021). Improvements were also seen in the treadmill exhaustion test, both in terms of distance covered and time to exhaustion (Consalvi et al., 2013; Licandro et al., 2021).

First-in-human evidence of HDAC inhibition by givinostat

Orally administered givinostat 50 or 100 mg transiently reduced the *in vitro* production of pro-inflammatory cytokines (while not affecting anti-inflammatory cytokines) in a phase 1 trial in healthy males. After seven daily doses of givinostat 200 mg, the reductions in cytokine production were generally similar to those following the initial dose (Furlan et al., 2011).

Clinical evidence of givinostat efficacy

In an open-label, two-part, phase 2 study, the histological effects of givinostat were analyzed in 20 ambulant boys with DMD (Bettica et al., 2016). The histological effect of givinostat treatment was confirmed, with a significant increase in muscle tissue and reductions in fibrosis, tissue necrosis, and fatty replacement.

Givinostat was subsequently shown to slow DMD progression in a placebo-controlled phase 3 trial, in which both groups continued to receive corticosteroids. The results indicated that over 18 months of treatment, givinostat significantly improved muscle function and strength compared with the placebo group. It effectively slowed the progression of muscle degeneration in the participants. The primary endpoint, change in four-stair climb from baseline, was met. All secondary endpoints were in favor of givinostat, including other timed function tests, the North Star Ambulatory Assessment and muscle strength. Givinostat reduced fat infiltration in the vastus lateralis in patients with DMD by 30%. Magnetic resonance spectroscopy evidence suggested less fat infiltration in the vastus lateralis at 72 weeks with givinostat compared to control group (LSM difference in fat fraction −2.92% [−5.64 to −0.20] (Mercuri et al., 2024). These findings are consistent with those observed in the givinostat pre-clinical studies (Consalvi et al., 2013; Licandro et al., 2021) and phase 2 clinical trial (Bettica et al., 2016).

In terms of safety, givinostat was generally well tolerated. The most common side effects were mild to moderate and included monitorable gastrointestinal symptoms such as diarrhea, thrombocytopenia and hypertriglyceridaemia, and were manageable with dose adjustments. No severe or serious adverse events were directly related to the drug or resulted in study withdrawal (Mercuri et al., 2024).

Future considerations for combination treatment

Now that givinostat is approved by the Food and Drug Administration (United States), there is an opportunity for combination with other approved treatments that induce production of partially functional dystrophin. The expectation is that the combination would have added benefit, as the dystrophin-restoring approaches rely on the presence of muscle and muscle quality. The micro-dystrophin gene therapy approach (delandistrogene moxeparvovec) relies on a muscle-specific promotor and thus the transgene will only be expressed in skeletal and cardiac muscle (Hoy, 2023). Furthermore, the micro-dystrophin is only partially functional and will slow down but not stop pathology. As such, a second treatment aiming to slow down muscle pathology should be beneficial. The exon skipping approach (eteplirsen, golodirsen, casimersen and viltolarsen) uses antisense oligonucleotides that target exons during pre-mRNA splicing of dystrophin transcripts (Aartsma-Rus, 2023). These transcripts are only produced in muscle tissue and not in fibrosis or adipose tissues. For exon skipping however, an added benefit of givinostat co-treatment is expected, as it has been shown that dystrophin transcript expression is reduced in patients with DMD due to chromatin remodeling. It is expected that givinostat treatment can increase dystrophin expression *per se*. Without exon skipping, this would not lead to dystrophin protein production; after exon skipping, it would. Indeed, in the *mdx* mouse model, treatment with mouse specific exon skipping compounds and givinostat resulted in increased levels of dystrophin transcripts and protein compared with exon skipping by itself (García-Rodríguez et al., 2020).

Conclusion

DMD pathogenesis is complex and multifaceted. All currently-available dystrophin-restoring treatments restore only partially functional dystrophins that may slow down disease pathology, but the pathophysiological processes remain inevitable. HDACs have been shown to be hyperactive in patients with DMD and contribute to this pathology, therefore HDAC inhibition has arisen as a potential therapeutic option. Through its novel, multi-targeted mode of action, the HDAC inhibitor givinostat has demonstrated the potential to address the pathophysiological cascade of DMD by targeting key pathological events originated by the lack of dystrophin. The reduction of muscle degeneration is achieved by lowering inflammation in the muscle, reverting inhibition of myogenesis, promoting muscle regeneration, and decreasing fibrogenesis and adipogenesis in patients with DMD.

Givinostat is the first nonsteroidal treatment for DMD to be approved for use irrespective of the specific genetic variant underlying the disease and received its first approval for the treatment of DMD in patients ≥6 years old in March 2024 in the United States (Lamb, 2024). Ongoing clinical studies continue to evaluate the potential of HDAC inhibition in DMD and other disorders where elevated HDAC activity plays a role.

Author contributions

AA-R: Writing–original draft, Writing–review and editing.

Funding

The author(s) declare that financial support was received for the research, authorship, and/or publication of this article. This study received funding from Italfarmaco S.p.A who provided funding for writing assistance and covered the open access fee.

Acknowledgments

The author acknowledges Italfarmaco S.p.A., Milan, Italy, for publication coordination and critical review for scientific accuracy, and Paul Wilson, BSc, and Julia Coleman, PhD, of Cognite for medical writing and editorial assistance based on the author's input and direction.

Conflict of interest

Italfarmaco S.p.A had the following involvement in the study: suggestions for manuscripts to include in the review, fact checking and payment for a professional writer to edit the manuscript and draft the figures.

Generative AI statement

The author(s) declare that no Generative AI was used in the creation of this manuscript.

Publisher's note

References

Aartsma-Rus, A. (2023). The future of exon skipping for Duchenne muscular dystrophy. *Hum. Gene Ther.* 34, 372–378. doi:10.1089/hum.2023.026

Aartsma-Rus, A., Ginjaar, I. B., and Bushby, K. (2016). The importance of genetic diagnosis for Duchenne muscular dystrophy. *J. Med. Genet.* 53, 145–151. doi:10.1136/jmedgenet-2015-103387

Beier, U. H., Akimova, T., Liu, Y., Wang, L., and Hancock, W. W. (2011). Histone/protein deacetylases control Foxp3 expression and the heat shock response of T-regulatory cells. *Curr. Opin. Immunol.* 23, 670–678. doi:10.1016/j.coi.2011.07.002

Bettica, P., Petrini, S., D'Oria, V., D'Amico, A., Catteruccia, M., Pane, M., et al. (2016). Histological effects of givinostat in boys with Duchenne muscular dystrophy. *Neuromuscul. Disord.* 26, 643–649. doi:10.1016/j.nmd.2016.07.002

Bez Batti Angulski, A., Hosny, N., Cohen, H., Martin, A. A., Hahn, D., Bauer, J., et al. (2023). Duchenne muscular dystrophy: disease mechanism and therapeutic strategies. *Front. Physiol.* 14, 1183101. doi:10.3389/fphys.2023.1183101

Biernacka, A., Dobaczewski, M., and Frangogiannis, N. G. (2011). TGF-β signaling in fibrosis. *Growth factors.* 29, 196–202. doi:10.3109/08977194.2011.595714

Bladen, C. L., Salgado, D., Monges, S., Foncuberta, M. E., Kekou, K., Kosma, K., et al. (2015). The TREAT-NMD DMD global database: analysis of more than 7,000 Duchenne muscular dystrophy mutations. *Hum. Mutat.* 36, 395–402. doi:10.1002/humu.22758

Blake, D. J., Weir, A., Newey, S. E., and Davies, K. E. (2002). Function and genetics of dystrophin and dystrophin-related proteins in muscle. *Physiol. Rev.* 82, 291–329. doi:10.1152/physrev.00028.2001

Blau, H. M., Cosgrove, B. D., and Ho, A. T. V. (2015). The central role of muscle stem cells in regenerative failure with aging. *Nat. Med.* 21, 854–862. doi:10.1038/nm.3918

Cacchiarelli, D., Legnini, I., Martone, J., Cazzella, V., D'Amico, A., Bertini, E., et al. (2011). miRNAs as serum biomarkers for Duchenne muscular dystrophy. *EMBO Mol. Med.* 3, 258–265. doi:10.1002/emmm.201100133

Campbell, K. P., and Kahl, S. D. (1989). Association of dystrophin and an integral membrane glycoprotein. *Nature* 338, 259–262. doi:10.1038/338259a0

Chang, N. C., Sincennes, M.-C., Chevalier, F. P., Brun, C. E., Lacaria, M., Segalés, J., et al. (2018). The dystrophin glycoprotein complex regulates the epigenetic activation of muscle stem cell commitment. *Cell. Stem Cell.* 22, 755–768.e6. doi:10.1016/j.stem.2018.03.022

Consalvi, S., Mozzetta, C., Bettica, P., Germani, M., Fiorentini, F., Del Bene, F., et al. (2013). Preclinical studies in the mdx mouse model of Duchenne muscular dystrophy with the histone deacetylase inhibitor givinostat. *Mol. Med.* 19, 79–87. doi:10.2119/molmed.2013.00011

Dowling, P., Swandulla, D., and Ohlendieck, K. (2023). Cellular pathogenesis of Duchenne muscular dystrophy: progressive myofibre degeneration, chronic inflammation, reactive myofibrosis and satellite cell dysfunction. *Eur. J. Transl. Myol.* 33, 11856. doi:10.4081/ejtm.2023.11856

Duan, D., Goemans, N., Takeda, S., Mercuri, E., and Aartsma-Rus, A. (2021). Duchenne muscular dystrophy. *Nat. Rev. Dis. Prim.* 7, 13. doi:10.1038/s41572-021-00248-3

Duchenne UK, 2023. DMD treatment Givinostat reaches important stage in European approval process.

Dumont, N. A., Wang, Y. X., von Maltzahn, J., Pasut, A., Bentzinger, C. F., Brun, C. E., et al. (2015). Dystrophin expression in muscle stem cells regulates their polarity and asymmetric division. *Nat. Med.* 21, 1455–1463. doi:10.1038/nm.3990

Ervasti, J., and Campbell, K. (1993). A role for the dystrophin-glycoprotein complex as a transmembrane linker between laminin and actin. *J. Cell. Biol.* 122, 809–823. doi:10.1083/jcb.122.4.809

Eslaminejad, M., Fani, N., and Shahhoseinini, M. (2013). Epigenetic regulation of osteogenic and chondrogenic differentiation of mesenchymal stem cells in culture. *Cell.* 15, 1–10.

Furlan, A., Monzani, V., Reznikov, L. L., Leoni, F., Fossati, G., Modena, D., et al. (2011). Pharmacokinetics, safety and inducible cytokine responses during a phase 1 trial of the oral histone deacetylase inhibitor ITF2357 (givinostat). *Mol. Med.* 17, 353–362. doi:10.2119/molmed.2011.00020

García-Rodríguez, R., Hiller, M., Jiménez-Gracia, L., Van Der Pal, Z., Balog, J., Adamzek, K., et al. (2020). Premature termination codons in the *DMD* gene cause reduced local mRNA synthesis. *Proc. Natl. Acad. Sci. U.S.A.* 117, 16456–16464. doi:10.1073/pnas.1910456117

Giordano, C., Mojumdar, K., Liang, F., Lemaire, C., Li, T., Richardson, J., et al. (2015). Toll-like receptor 4 ablation in mdx mice reveals innate immunity as a therapeutic target in Duchenne muscular dystrophy. *Hum. Mol. Genet.* 24, 2147–2162. doi:10.1093/hmg/ddu735

Giuliani, G., Rosina, M., and Reggio, A. (2022). Signaling pathways regulating the fate of fibro/adipogenic progenitors (FAPs) in skeletal muscle regeneration and disease. *FEBS J.* 289, 6484–6517. doi:10.1111/febs.16080

Guiraud, S., Chen, H., Burns, D. T., and Davies, K. E. (2015). Advances in genetic therapeutic strategies for Duchenne muscular dystrophy. *Exp. Physiol.* 100, 1458–1467. doi:10.1113/EP085308

Henriques-Pons, A., Yu, Q., Rayavarapu, S., Cohen, T. V., Ampong, B., Cha, H. J., et al. (2014). Role of Toll-like receptors in the pathogenesis of dystrophin-deficient skeletal and heart muscle. *Hum. Mol. Genet.* 23, 2604–2617. doi:10.1093/hmg/ddt656

Hoffman, E. P., Brown, R. H., and Kunkel, L. M. (1987). Dystrophin: the protein product of the Duchenne muscular dystrophy locus. *Cell.* 51, 919–928. doi:10.1016/0092-8674(87)90579-4

Hoy, S. M. (2023). Delandistrogene moxeparvovec: first approval. *Drugs* 83, 1323–1329. doi:10.1007/s40265-023-01929-x

Kodippili, K., and Rudnicki, M. A. (2023). Satellite cell contribution to disease pathology in Duchenne muscular dystrophy. *Front. Physiol.* 14, 1180980. doi:10.3389/fphys.2023.1180980

Kulthinee, S., Yano, N., Zhuang, S., Wang, L., and Zhao, T. C. (2022). Critical functions of histone deacetylases (HDACs) in modulating inflammation associated with cardiovascular diseases. *Pathophysiology* 29, 471–485. doi:10.3390/pathophysiology29030038

Lamb, Y. N. (2024). Givinostat: first approval. *Drugs* 84, 849–856. doi:10.1007/s40265-024-02052-1

Licandro, S. A., Crippa, L., Pomarico, R., Perego, R., Fossati, G., Leoni, F., et al. (2021). The pan HDAC inhibitor Givinostat improves muscle function and histological parameters in two Duchenne muscular dystrophy murine models expressing different haplotypes of the LTBP4 gene. *Skelet. Muscle* 11, 19. doi:10.1186/s13395-021-00273-6

Licciardi, P. V., and Karagiannis, T. C. (2012). Regulation of immune responses by histone deacetylase inhibitors. *ISRN Hematol.* 2012, 690901–690910. doi:10.5402/2012/690901

Mariño-Ramírez, L., Kann, M. G., Shoemaker, B. A., and Landsman, D. (2005). Histone structure and nucleosome stability. *Expert Rev. Proteomics* 2, 719–729. doi:10.1586/14789450.2.5.719

Marrone, A. K., and Shcherbata, H. R. (2011). Dystrophin orchestrates the epigenetic profile of muscle cells via miRNAs. *Front. Gene.* 2, 64. doi:10.3389/fgene.2011.00064

Mercuri, E., Vilchez, J. J., Boespflug-Tanguy, O., Zaidman, C. M., Mah, J. K., Goemans, N., et al. (2024). Safety and efficacy of givinostat in boys with Duchenne muscular dystrophy (EPIDYS): a multicentre, randomised, double-blind, placebo-controlled, phase 3 trial. *Lancet Neurology* 23, 393–403. doi:10.1016/S1474-4422(24)00036-X

Molina, T., Fabre, P., and Dumont, N. A. (2021). Fibro-adipogenic progenitors in skeletal muscle homeostasis, regeneration and diseases. *Open Biol.* 11, 210110. doi:10.1098/rsob.210110

Molinari, S., Imbriano, C., Moresi, V., Renzini, A., Belluti, S., Lozanoska-Ochser, B., et al. (2023). Histone deacetylase functions and therapeutic implications for adult skeletal muscle metabolism. *Front. Mol. Biosci.* 10, 1130183. doi:10.3389/fmolb.2023.1130183

Mozzetta, C., Sartorelli, V., and Puri, P. L. (2024). HDAC inhibitors as pharmacological treatment for Duchenne muscular dystrophy: a discovery journey from bench to patients. *Trends Mol. Med.* 30, 278–294. doi:10.1016/j.molmed.2024.01.007

Mukund, K., and Subramaniam, S. (2020). Skeletal muscle: a review of molecular structure and function, in health and disease. *WIREs Mech. Dis.* 12, e1462. doi:10.1002/wsbm.1462

Okubo, M., Goto, K., Komaki, H., Nakamura, H., Mori-Yoshimura, M., Hayashi, Y. K., et al. (2017). Comprehensive analysis for genetic diagnosis of Dystrophinopathies in Japan. *Orphanet J. Rare Dis.* 12, 149. doi:10.1186/s13023-017-0703-4

Osseni, A., Ravel-Chapuis, A., Belotti, E., Scionti, I., Gangloff, Y.-G., Moncollin, V., et al. (2022). Pharmacological inhibition of HDAC6 improves muscle phenotypes in dystrophin-deficient mice by downregulating TGF-β via Smad3 acetylation. *Nat. Commun.* 13, 7108. doi:10.1038/s41467-022-34831-3

Ren, S., Fu, X., Guo, W., Bai, R., Li, S., Zhang, T., et al. (2024). Profound cellular defects attribute to muscular pathogenesis in the rhesus monkey model of Duchenne muscular dystrophy. *Cell.* 187, 6669–6686. doi:10.1016/j.cell.2024.08.041

Rosenberg, A. S., Puig, M., Nagaraju, K., Hoffman, E. P., Villalta, S. A., Rao, V. A., et al. (2015). Immune-mediated pathology in Duchenne muscular dystrophy. *Sci. Transl. Med.* 7, 299rv4. doi:10.1126/scitranslmed.aaa7322

Rugowska, A., Starosta, A., and Konieczny, P. (2021). Epigenetic modifications in muscle regeneration and progression of Duchenne muscular dystrophy. *Clin. Epigenet* 13, 13. doi:10.1186/s13148-021-01001-z

Ryder, S., Leadley, R. M., Armstrong, N., Westwood, M., de Kock, S., Butt, T., et al. (2017). The burden, epidemiology, costs and treatment for Duchenne muscular dystrophy: an evidence review. *Orphanet J. Rare Dis.* 12, 79. doi:10.1186/s13023-017-0631-3

Saccone, V., Consalvi, S., Giordani, L., Mozzetta, C., Barozzi, I., Sandoná, M., et al. (2014). HDAC-regulated myomiRs control BAF60 variant exchange and direct the functional phenotype of fibro-adipogenic progenitors in dystrophic muscles. *Genes. Dev.* 28, 841–857. doi:10.1101/gad.234468.113

Sandonà, M., Cavioli, G., Renzini, A., Cedola, A., Gigli, G., Coletti, D., et al. (2023). Histone deacetylases: molecular mechanisms and therapeutic implications for muscular dystrophies. *IJMS* 24, 4306. doi:10.3390/ijms24054306

Sandonà, M., Consalvi, S., Tucciarone, L., De Bardi, M., Scimeca, M., Angelini, D. F., et al. (2020). HDAC inhibitors tune miRNAs in extracellular vesicles of dystrophic muscle-resident mesenchymal cells. *EMBO Rep.* 21, e50863. doi:10.15252/embr.202050863

Sandoná, M., Consalvi, S., Tucciarone, L., Puri, P. L., and Saccone, V. (2016). HDAC inhibitors for muscular dystrophies: progress and prospects. *Expert Opin. Orphan Drugs* 4, 125–127. doi:10.1517/21678707.2016.1130617

Sciorati, C., Rigamonti, E., Manfredi, A. A., and Rovere-Querini, P. (2016). Cell death, clearance and immunity in the skeletal muscle. *Cell. Death Differ.* 23, 927–937. doi:10.1038/cdd.2015.171

Sinadinos, A., Young, C. N. J., Al-Khalidi, R., Teti, A., Kalinski, P., Mohamad, S., et al. (2015). P2RX7 purinoceptor: a therapeutic target for ameliorating the symptoms of Duchenne muscular dystrophy. *PLOS Med.* 12, e1001888. doi:10.1371/journal.pmed.1001888

Sweet, M. J., Shakespear, M. R., Kamal, N. A., and Fairlie, D. P. (2012). HDAC inhibitors: modulating leukocyte differentiation, survival, proliferation and inflammation. *Immunol. Cell. Biol.* 90, 14–22. doi:10.1038/icb.2011.88

United States Food and Drug Administration, 2024. DUVYZAT (givinostat) oral suspension. *Prescribing Information*. Italfarmaco S.p.A https://www.accessdata.fda.gov/drugsatfda_docs/label/2024/217865Orig1s000lbl.pdf (Accessed December 19, 2024).

Walter, M. C., and Reilich, P. (2017). Recent developments in Duchenne muscular dystrophy: facts and numbers. *J. cachexia sarcopenia muscle* 8, 681–685. doi:10.1002/jcsm.12245

Wilson, D. G. S., Tinker, A., and Iskratsch, T. (2022). The role of the dystrophin glycoprotein complex in muscle cell mechanotransduction. *Commun. Biol.* 5, 1022. doi:10.1038/s42003-022-03980-y

Ziemkiewicz, N., Hilliard, G., Pullen, N. A., and Garg, K. (2021). The role of innate and adaptive immune cells in skeletal muscle regeneration. *Int. J. Mol. Sci.* 22, 3265. doi:10.3390/ijms22063265

frontiers | Frontiers in Medicine

TYPE Systematic Review
PUBLISHED 27 January 2025
DOI 10.3389/fmed.2025.1497538

OPEN ACCESS

EDITED BY
Zhongheng Zhang,
Sir Run Run Shaw Hospital, China

REVIEWED BY
Giovanni Misseri,
Institute Foundation G.Giglio, Italy
Tanya Cully,
University of Otago, New Zealand

*CORRESPONDENCE
Yunzhu Lin
✉ linyunzhu99@scu.edu.cn

RECEIVED 19 September 2024
ACCEPTED 06 January 2025
PUBLISHED 27 January 2025

CITATION
Lian X, Jing Y, Luo T, Guo Y and Lin Y (2025) Pharmacological interventions for the management of anesthesia and sedation in patients with Duchenne muscular dystrophy: a systematic review and meta-analysis.
Front. Med. 12:1497538.
doi: 10.3389/fmed.2025.1497538

Pharmacological interventions for the management of anesthesia and sedation in patients with Duchenne muscular dystrophy: a systematic review and meta-analysis

Xianghong Lian[1,2,3], Yang Jing[1,2,3], Ting Luo[1,2,3], Yixin Guo[1,2,3] and Yunzhu Lin[1,2,3]*

[1]Department of Pharmacy, West China Second University Hospital, Sichuan University, Chengdu, China, [2]Evidence-Based Pharmacy Center, West China Second University Hospital, Sichuan University, Chengdu, China, [3]Key Laboratory of Birth Defects and Related Diseases of Women and Children, Sichuan University, Ministry of Education, Chengdu, China

Background: Patients with duchenne muscular dystrophy (DMD) have an increased risk of complications when they undergo sedation or general anesthesia. However, due to improvements in cardiopulmonary therapies during anesthetic care, patients with DMD are experiencing an unprecedented duration of survival. We performed a systematic analysis to assess the benefits and risks of pharmacological interventions for the management of anesthesia and sedation in DMD patients.

Methods: We included any type of study reporting any drug intervention to manage anesthesia and sedation in participants previously diagnosed with DMD. Our primary outcomes were the onset time, recovery time, and neurodevelopmental disabilities. Seven electronic databases and three clinical trial registry platforms were searched. Data from the eligible studies were combined to calculate pooled risk ratios or standardized mean differences, and some included studies are presented in a narrative synthesis.

Results: Forty studies with 196 DMD participants were included in the analysis. Compared with those of the control group, the sensitivity of patients with DMD to neuromuscular blocking agents (NMBAs) may have resulted in a prolonged onset time [MD = −0.96, 95% CI (0.71, 2.60), I^2 = 33%, P < 0.0001] and recovery time [MD = 2.22, 95% CI (1.14, 3.30), I^2 = 76%, P < 0.0001] from anesthesia. The neuromuscular blocking effects showed a significant age dependence in DMD patients, and the safe use of 2 mg/kg sugammadex to antagonize deep neuromuscular blockade and rapid recovery has been reported. Furthermore, DMD patients are at risk of developing malignant hyperpyrexia with general/inhaled anesthesia, and dantrolene is often used for effective rescue. In addition, general anesthesia and central neuraxial blockade in patients with severe DMD are unsafe because respiratory depression and myocardial complications may occur after the administration of volatile anesthetics and depolarizing muscle relaxants (succinylcholine) during the induction of anesthesia.

Conclusions: Patients with DMD are more sensitive to NMBAs with delayed onset times and prolonged recovery times. Precautions for DMD patients should include quantitative neuromuscular monitoring, electrocardiographic monitoring and rapid airway protection throughout anesthesia. Compared with general anesthesia, regional anesthesia may be a relatively safe option.

KEYWORDS

Duchenne muscular dystrophy, sedative, anesthesia, pharmacological interventions, systematic review, meta-analysis

1 Introduction

Duchenne muscular dystrophy (DMD) is a progressive neuromuscular disease transmitted by X-linked inheritance with an incidence of ∼1 in 3,500 live male births (1, 2). The onset of clinical symptoms usually occurs during early childhood, and progression of the disease leads to a loss of ambulation in late childhood. At present, no cure exists for DMD, and treatment is aimed at minimizing symptoms (3).

Since patients with DMD present a wide range of symptoms, the associated treatment of health concerns is particularly necessary for each individual patient. Thus, patients with DMD often require anesthetic care during muscle biopsy or correction of progressive orthopedic deformities (4). Depending on the type of surgical procedure and the neurocognitive level of the patient, options include general anesthesia, regional anesthesia or procedural sedation (5, 6). However, the potential impacts of DMD on perioperative morbidity and even mortality cannot be ignored, as the literature has suggested a significantly increased risk during anesthetic care in these patients (8, 9). Earlier reports have outlined the potential for perioperative mortality with cardiac arrest and death in 2 of 25 patients requiring anesthetic care (10).

However, more recent reports have shown that with a better understanding of the pathophysiology of the disease, end-organ involvement and improvements in favorable perioperative care outcomes are possible even in this challenging patient population. In a review of 91 DMD patients who underwent 232 orthopedic surgical procedures, Muenster et al. reported no severe anesthesia-related complications and no cases of unexplained fever or rhabdomyolysis (11). Furthermore, in nearly all patients, neuromuscular blockade agents (NMBAs) were used; therefore, the complete spontaneous recovery of neuromuscular blockade (NMB) in DMD patients remains unclear, and the safest anesthetic technique has yet to be established (12–16).

Given the indispensable nature of sedatives and/or analgesia in DMD surgery/diagnosis and the frequency with which medically compromised DMD patients present for treatment, an increased need exists for reliable data that can inform clinical decision-making. Moreover, the relevant question of whether developments and changes in anesthetic techniques in recent years have improved the safety of anesthesia in this special group of DMD patients has gradually attracted widespread attention, but no studies have been published. Thus, the present review aimed to search for current evidence related to the use of analgesedation in the context of both the drugs used and their side effects and to formulate recommendations in this respect. This review is an up-to-date summary of the medical literature concerning this topic and identifies areas in need of future research.

2 Materials and methods

This systematic review and meta-analysis was performed according to the recommendations in the Preferred Reporting Items for Systematic Reviews and Meta Analyses (PRISMA) statement and the guidelines described in the Cochrane Handbook (17).

2.1 Search strategy

Our search comprised three English electronic databases (PubMed, Embase, and Cochrane Library) and four Chinese electronic databases (China National Knowledge Infrastructure, Wan Fang Database, Chinese Biomedical Literature Database, and VIP Database for Chinese Technical Periodicals). Three clinical trial registry platforms were used to identify additional studies, including Clinical Trials.gov, the World Health Organization Clinical Trials Registry Platform and the Cochrane Central Registry of Controlled Trials. The search strategy was specific for each database and included a combination of medical subject headings and free text terms ("DMD" or "Duchenne muscular dystrophy") and ("sedation" or "anesthesia" or "analgosedation"). We looked for additional studies in the reference lists of the selected articles and contacted the authors when the information was unclear. The deadline for the retrieval of all studies was September 2024.

2.2 Inclusion criteria

The following studies were included: (1) studies examining human participants of any age and sex who were previously diagnosed with DMD; (2) any type of drug intervention used for the management of pain and/or sedation; (3) type of study—randomized/non-randomized controlled trials (RCTs), observational studies, case series, and case reports reporting on patients with previously diagnosed DMD; (4) outcomes—the degree and effectiveness of sedation provided by different pharmacological agents, feasibility, and tolerability were assessed, whereas the secondary outcomes included other adverse events.

The exclusion criteria were as follows: (1) studies with incomplete or missing information; (2) studies were not published in Chinese or English; (3) abstracts from conferences and unpublished data; (4) no outcomes related to sedative/narcotic drugs or a lack of a specific sedative/narcotic drug detailed regimen.

2.3 Data extraction

Two authors independently extracted the data using a previously designed data extraction table. The data extracted were the authors, year of publication, country, experimental design, sample size, mean age, intervention measure, dose, type of procedure, and any outcome that met the inclusion criteria.

Two independent reviewers screened all the titles and abstracts to identify potentially eligible articles. They independently applied the eligibility criteria to perform the final selection. When discrepancies occurred between the two reviewers regarding the inclusion of the articles, they discussed and identified the reasons to either include or exclude the articles and then made the final decision. If they could not reach an agreement, the final decision was made by a third reviewer.

2.4 Risk of bias assessment

The Interventions' (MINORS) tool was used to assess the risk of bias in non-randomized studies (18). The quality of case report studies was evaluated using the Joanna Briggs Institute of Australia (JBI) quality assessment tool (19).

2.5 Statistical analysis

The meta-analysis was conducted with RevMan 5.3. The data were pooled and reported as relative risks (RR) or Mean Difference (MD) with 95% confidence interval (CI). Heterogeneity was assessed using *I*-squared (I^2) statistics. A fixed effects model was initially constructed. If significant heterogeneity existed among trials ($I^2 > 50\%$), potential sources of heterogeneity were considered, and where appropriate, a random effects model was used (20, 21). We planned to report outcome data in tables if a meta-analysis was deemed inappropriate, for example, because of clinical or statistical heterogeneity.

3 Results

3.1 Study search and characteristics

The titles and abstracts of a total of 734 studies were screened, of which 670 were deemed irrelevant (Figure 1). The full texts of the remaining 64 studies were read, and 24 were excluded, leaving 40 studies with 196 patients to be included (35 case reports and five non-randomized controlled trials; Tables 1–3) (4, 7, 12–16, 22–54).

All patients needed sedation or anesthesia before surgery or diagnostic procedures, had an American Society of Anesthesiologists (ASA) grade of I–III, and had no history of allergies. Most of the patients were male, whereas three were female and underwent radical mastectomy, cesarean section, and laparoscopic hysterectomy (25, 36, 43). The age ranged from 5 to 58 years. The sample sizes of the included studies varied between 1 and 29. The studies were conducted in Korea ($n = 4$), Iran ($n = 2$), China ($n = 3$), Germany ($n = 2$), America ($n = 9$), Turkey ($n = 2$), the UK ($n = 3$), the Netherlands ($n = 2$), Italy ($n = 1$), Japan ($n = 5$), France ($n = 1$), Brazil ($n = 1$), Belgium ($n = 1$), and India ($n = 4$) from 1995–2019. Some patients with DMD underwent general anesthesia for percutaneous nephrolithotomy, muscle biopsy, corrective orthopedic surgery, laparoscopic cholecystectomy, tumor excision, cholelithiasis, cholecystectomy, etc. Some other patients with DMD underwent local anesthesia for reduction internal fixation, upper extremity amputation, fistulectomy and intercostal nerve blocks. In addition, some patients with DMD underwent general anesthesia supplemented with regional anesthesia for laparoscopic cholecystectomy and traumatic cataract surgery. The duration of most anesthesia operations arranged from 30 min to 2 h.

3.2 Quality assessment (risk of bias assessment)

The quality of case report studies was evaluated using the JBI quality assessment tool. Thirty-five case report studies were included (4, 7, 22–54). The results of the quality evaluation revealed that 82.86% (29/35) of the studies described adverse events and unexpected events, 88.57% (31/35) of the studies clearly described patients' history and the researched intervention and/or treatment measures, 88.57% (31/35) of the studies clearly described patients' demographic characteristics. A total of 91.43% (32/35) of the studies clearly described the health status of the patients after the intervention, and 61.5% (8/13) of the studies described the implications of the study. A total of 85.71% (30/35) of the studies clearly presented the current clinical health problems of the patients. Eighty percent (28/35) of the studies clearly described the diagnosis, assessment method, and outcomes, indicating that the overall quality of case reports was high. The results of quality evaluation of the case reports are shown in Table 4.

A methodological appraisal of the selected non-randomized studies using the MINORS tool is presented in Table 5 (50–54). The assessment scores ranged from 11 to 13, with a maximum global score of 16. Three studies clearly stated the aim of the investigation, reported the prospective collection of data, and properly described the main outcomes. Additionally, no loss of treated subjects during the follow-up period was reported. However, limitations were found in the description of the inclusion of consecutive patients and in the prospective calculation of the study size (50–54). Thus, three studies were classified as "moderate quality" (51, 53, 54) and two studies as "high quality" (50, 52).

3.3 Preoperative evaluation

The cardiac status needs to be carefully considered in the preoperative evaluation of DMD patients. Most of the included

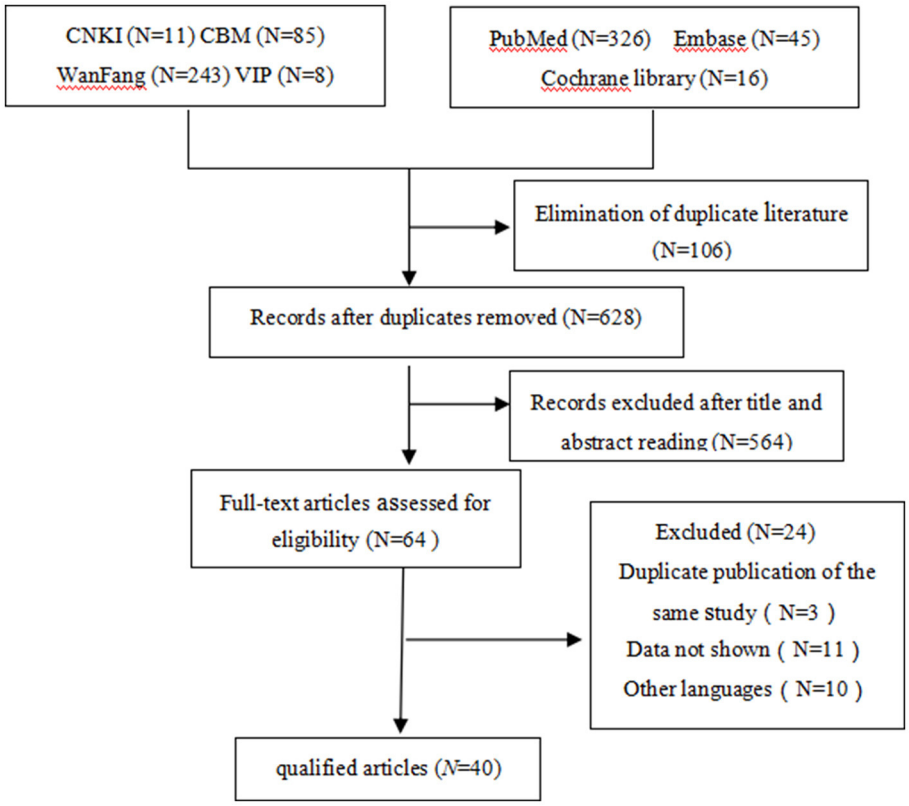

FIGURE 1
Flow diagram of selecting study.

studies performed electrocardiography or pulmonary auscultation before surgery and reported the results. The American Society of Anesthesiologists' physical status of the patients was reported to be I–III (13, 14, 31, 51). The preoperative evaluation should focus on the end-organ involvement of DMD, its evaluation, and the development of an anesthetic drug plan based on these findings. In addition to cardiac involvement, as noted above, respiratory involvement is universally present in patients with DMD. For a full discussion regarding the respiratory concerns of patients with DMD, the reader is referred to the review in the journal written by the pulmonologists who participated in the development of the consensus statement from the American College of Chest Physicians (55).

3.4 Pharmacological interventions

Tables 1, 2 present the drug management strategies used for DMD patients during the induction, maintenance, and recovery periods from anesthesia. Five non-randomized controlled trials compared the DMD group with the control group. Wick et al. (51) determined the onset time and complete spontaneous recovery from neuromuscular blockade after the administration of a standard dose of 0.6 mg/kg rocuronium in patients with advanced DMD compared with controls. Ihmsen et al. (50) compared children with DMD with normal patients to investigate the effects of mivacurium on neuromuscular blockade. Tino Muenster et al. investigated the onset time, peak effect and complete spontaneous recovery from neuromuscular blockade after the administration of a single dose of 0.3 mg/kg rocuronium in DMD patients and compared the data with those of controls (52). Ririe et al. (53) used vecuronium to characterize the neuromuscular blockade of patients with DMD and the response to that of the controls. In addition, Kako et al. (54) evaluated a combination of ketamine with two different doses of dexmedetomidine for sedation during muscle biopsy in patients with DMD.

3.4.1 Main mode of anesthesia

Twenty-six of the included studies involved general anesthesia (4, 12–16, 22–24, 28, 30–32, 37, 39–41, 44, 47–54). Standard intraoperative monitoring, including electrocardiography, automatic blood pressure, and pulse oximetry, was used in the studies. General anesthesia was mostly induced with propofol, fentanyl, pentothal sodium, and midazolam (22–26, 50–52). Rocuronium was administered as a muscle relaxant (14, 15, 24, 32, 39, 48). Anesthesia was mostly maintained with propofol and remifentanil with an oxygen–air mixture (13, 14, 22–25, 28–31). Moreover, a few studies used inhalation induction for general anesthesia with sevoflurane and nitrous oxide (28, 40, 41).

Six studies included regional anesthesia (26, 27, 35, 36, 42, 43). These studies reported local nerve blockade with lidocaine,

TABLE 1 Characteristics of included non-randomized controlled trials.

References	Country	Sample size	Age (year)	Weight (kg)	Group	Main mode of anesthesia	Preoperative evaluation	Anesthesia premedication	Anesthesia induction	Anesthesia maintenance	Operation duration	Postoperative analgesia	Side effects	Onset time (min)	Recovery time (min)
Ihmsen et al. (50)	Iran	8	6.3 ± 1.6	25 ± 8	Control group children	General anesthesia	The plasma cholinesterase activity was within the normal range	Midazolam orally 45 min	2 g/kg fentanyl and 3 mg/kg propofol	8 mg/kg propofol and remifentanil	NA	NA	NA	2.0 (1.3–3.0)	8.5 (6.5–12.0)
		8	13.5 ± 2.6	54 ± 9	Control group adolescents							NA	NA	2.5 (2.0–3.5)	9.1 (7.5–9.8)
		11	7.9 ± 1.2	27 ± 6	DMD group children							NA	NA	2.2 (1.5–4.7)	12 (3.0–21)
		11	13.8 ± 1.5	54 ± 20	DMD group adolescents							NA	NA	4.0 (1.8–7.0)	18 (4.5–45)
Wick et al. (51)	Germany	12	13.3 ± 2.0	49.8 ± 13.6	DMD group	General anesthesia	ASA III	3.75 mg midazolam	2–3 μg/kg fentanyl, 3 mg/kg propofol	8–12 mg/kg propofol, remifentanil	5–7 h	NA	NA	203 (90–420) s	71.0 (39–144)
		12	13.8 ± 3.0	54.5 ± 15.9	Control group		ASA I				2–3 h	NA	NA	90 (60–195) s	16.8 (13–36)
Muenster et al. (52)	Germany	12	13.5 ± 1.7	60.5 ± 9.8	DMD Group	Generalanesthesia	Early left ventricular hypertrophy	3.75 mg midazolam orally 45 min	2–3 μg/kg fentanyl and propofol 3 mg/kg	8–12 mg/kg propofol, remifentanil	5–7 h	NA	NA	315 (120–465) s	72.0 (36–141)
		12	13.7 ± 2.8	53.8 ± 17.8	Control group		NA				2–3 h			195 (75–270) s	13.8 (7–18)
Ririe et al. (53)	USA	8	12 (11–15)	NA	DMD Group	General anesthesia	ASA I	1 mg/kg oral midazolam	10 μg/kg glycopyrrolate,4 mg/kg thiopental, 5–10 μg/kg fentanyl	2–5 μg/kg/h fentanyl, 0.03 mg/kg midazolam	NA	NA	NA	28 (15–43)	36 (13–52)
		8	12 (8–18)	NA	Control group							NA	NA	20 (14–33)	6 (4–9)
Kako et al. (54)	USA	24	9.7 ± 1.4	33.3 ± 7.7	DMD with 1 μg/kg dexmedetomidine	Procedural sedation	ASA nil per os	0.5 mg/kg midazolam, topical lidocaine cream	Dexmedetomidine and 1 mg/kg ketamine	1 μg/kg dexmedetomidine	21 ± 5 min	15 mg/kg acetaminophen	Airway obstruction; vomiting	3.7 ± 2.3	174 ± 58
		29	8.8 ± 1.8	30.2 ± 10.8	DMD with 0.5 μg/kg dexmedetomidine				Dexmedetomidine and 1 mg/kg ketamine	0.5 μg/kg dexmedetomidine	22 ± 7 min		Vomiting	2.8 ± 1.6	146 ± 65

10.3389/fmed.2025.1497538

TABLE 2 Characteristics of included case reports of DMD patients.

References	Country	Sample size	Age (year)	Weight (kg)	Study population	Main mode of anesthesia	Anesthesia premedication	Anesthesia induction	Anesthesia maintenance	Anesthesia reversedation	Operation duration	Postoperative analgesia	Side effects
Kim and Chun (22)	Korea	1	11	53	DMD with percutaneous nephrolithotomy	General anesthesia	Glycopyrrolate 0.2 mg was injected intramuscularly	5 mg/kg opentothal sodium and 5 mg omidazolam	250 mg/kg/min propofol and 0.3 mg/kg/min oremifentanil	2.0 mg/kg sugammadex (106 mg)	90 min	NA	No adverse event
Jung et al. (24)	Korea	1	6	19	DMD with muscle biopsy	General anesthetia	No premedication	Midazolam 1 mg, fentanyl 25 μg, Rocuronium bromide 6 mg	Propofol	4 mg pyridostigmine and 0.16 mg glycopyrrolate	45 min	NA	No complication
Bang et al. (26)	Korea	1	22	47	DMD with a left distal femur fracture and needed to undergo reduction and internal fixation	Peripheral nerve blocks	20 ml of 0.375% ropivacaine	NA	15 and 5 ml of 0.375% ropivacaine into the femoral nerve and the lateral femoral	NA	40 min	NA	NA
Büget et al. (27)	Turkey	1	17	NA	DMD with upper extremity amputation	Regional anesthesia	1% lidocaine	30 ml 0.5% bupivacaine	NA	2 h	NA	Fever of 39°C	
de Boer et al. (12)	Netherlands	1	9	46	DMD with a humerus fracture	General anesthesia	1,000 mg paracetamol	8–12 mg/kg propofol, 0.05–0.20 μg/kg/min remifentanil,1.0 mg/kg rocuronium	4.0 mg/kg sugammadex (184 mg)	35 min	NA	Uneventful	
Wefki Abdelgawwad Shousha et al. (13)	Italy	1	25	NA	DMD with open cholecystectomy	General anesthesia	Ciprofloxacin 2 gm; metronidazole 500 mg; ondansetron 4 mg	Propofol 150 mg, fentanyl 200 mcg, and rocuronium bromide 10 mg	Fentanyl in a total dose of 400 mcg (200–100–100), rocuronium bromide 5 mg repeated every 45 min	150 mg sugammadex	240 min	NA	NA
Obata et al. (28)	Japan	1	11	40 kg	DMD with strabismus	Inhalational induction	NA	Sevoflurane 4%, nitrous oxide 66%	Sevoflurane 1.5–3.0%, nitrous oxide 64%	1 mg/kg dantrolene sodium	51 min	25 mg diclofenac	Rhabdomyolysis

(Continued)

10.3389/fmed.2025.1497538

TABLE 2 (Continued)

References	Country	Sample size	Age (year)	Weight (kg)	Study population	Main mode of anesthesia	Anesthesia premedication	Anesthesia induction	Anesthesia maintenance	Anesthesia reversedation	Operation duration	Postoperative analgesia	Side effects
Obata et al. (28)	Japan	1	11	40 kg	DMD with strabismus	Inhalational induction	NA	Sevoflurane 4%, nitrous oxide 66%	Sevoflurane 1.5–3.0%, nitrous oxide 64%	1 mg/kg dantrolene sodium	51 min	25 mg diclofenac	Rhabdomyolysis
Richa et al. (30)	France	3	11/13/10	31/35/38 kg	DMD wtih posterior spinal surgery	General anesthesia	1 mg/kg of hydroxyzine	1 μg/kg/min remifentanil, propofol 3–5 mg/kg	0.1–0.4 μg/kg/min remifentanil, 3–9 mg/kg/h propofol	NA	345 ± 31 min	Morphine 4 μg/kg, paracetamol 15 mg/kg	No adverse event
Saldanha et al. (31)	Brazil	1	5	20	DMD with tumor excision and cervical emptying	General anesthesia	5 mg midazolam	0.5 μg/kg/min remifentanil, 6 μg/ml propofol	0.3 μg/kg/min Remifentanil and 3 μg/ml propofol	NA	180 min	0.2 mg/kg nalbuphine, 50 mg/kg dipirone	Without intercurrences
		1	24	NA	DMD with cholelithiasis		15 mg propofol, topic lidocaine	2.9 μg/ml propofol, 0.3 μg/kg/min remifentanil	NA	NA	40 min	NA	NA
Kocabas et al. (32)	Turkey	1	5	15	DMD with correction of Fallot's Tetralogy	General anesthesia	NA	6 mg/kg ketamine, 0.02 mg/kg atropine,0.05 mg/kg midazolam and 2 μg/kg fentanyl, Rocuronium 0.6 mg/kg	15 μg/kg fentanyl and 2–5 mg/kg/h ketamine	NA	240 min	15 mg/kg rectal paracetamol, 0.05 mg/kg morphine i.v	NA
Smelt (15)	Netherlands	1	16	60	DMD with scoliosis correction	General anesthesia	NA	1.0 mg alfentanil, 160 mg propofol, 30 mg rocuronium	Piritramide and desflurane?	1.0 mg adrenaline	40 min	NA	Ventricular fibrillation
Irwin and Henderson (16)	Hong Kong	1	14	NA	DMD with posterior spinal fusion	General anesthetic	Temazepam	Propofol and alfentanil supplemented with 65% nitrous oxide, atracurium	Alfentanil with 65% nitrous oxide	Adrenaline 0.5 mg, nitrous oxide	45 min	PCA morphine pump	Asystole

(Continued)

10.3389/fmed.2025.1497538

TABLE 2 (Continued)

References	Country	Sample size	Age (year)	Weight (kg)	Study population	Main mode of anesthesia	Anesthesia premedication	Anesthesia induction	Anesthesia maintenance	Anesthesia reversedation	Operation duration	Postoperative analgesia	Side effects
Rajmala et al. (33)	India	1	9	36	DMD with ophthalmic surgery	General + regional anesthesia	NA	2 mg/kg propofol, 0.05 mg/kg vecuronium,	3 mg/kg propofol oxygen (33%), nitrous oxide (67%), 0.25% bupivacaine	0.05 mg/kg neostigmine, 0.02 mg/kg atropine	NA	NA	Respiratory efforts
Vandepitte et al. (35)	America	1	27	41	DMD with pathologic fracture	Intercostal nerve blocks	NA	4 ml of ropivacaine 0.75% (T7–12)		NA	NA	Paracetamol 500 mg/6 h	NA
Molyneux (36)	UK	1	36 woman	60.3	DMD with a 37 weeks'pregnant woman	Spinal-epidural anesthesia	NA	A total of 2.5 ml of 0.5% hyperbaric bupivacaine with diamorphine		NA	NA	NA	No adverse event
Van Obbergh et al. (37)	Belgium	1	6	16	DMD with bilateral hip osteotomies	General anesthesia	NA	5 mg ketamine, 60 mg thiopentone, 10 mg atracurium,	0.5 μg/kg/min remifentanil	NA	NA	Paracetamol 15 mg/kg	No adverse event
Horikoshi et al. (39)	Japan	1	4	16	DMD with inguinal hernia	General anesthesia	NA	3 mg remimazolam, 100 μg fentanyl, 1.0 mg/kg/min remifentanil, 15 mg/h remimazolam, 10 mg rocuronium	15 mg/h remimazolam, 1.0 mg/kg/min remifentanil	40 mg sugammadex	NA	15 mg flurbiprofen axetil	No complications
Sethna and Rockoff (40)	America	1	5	NA	DMD with muscle biopsy	Inhalation anesthesia	NA	Nitrous oxide, oxygen and halothane by face mask	Dantrole (total dose 9 mg/kg)	NA	NA	Cardiac arrest	
Chalkiadis and Branch (41)	UK	1	8	30.2	DMD with left orchidopexy	Inhalation anesthesia	No premedication	5 mg/kg thiopentone,1.6 μg/kg fentanyl	50% nitrous oxide, oxygen, isoflurane 1.5%	Dantrolene 1 mg/kg	35 min	NA	Cardiac arrest

(Continued)

10.3389/fmed.2025.1497538

TABLE 2 (Continued)

References	Country	Sample size	Age (year)	Weight (kg)	Study population	Main mode of anesthesia	Anesthesia premedication	Anesthesia induction	Anesthesia maintenance	Anesthesia reversedation	Operation duration	Postoperative analgesia	Side effects
Shafy et al. (42)	America	1	36	61.1	DMD with right ischial pressure ulcer	Regional anesthesia	4 mg midazolam	Superficial anesthesia of the skin, subcutaneous tissue was achieved with 1% lidocaine, 3% chloroprocaine	NA	NA	1,000 mg acetaminophen	No adverse event	
Rathi et al. (43)	India	1	34	76	DMD with radical mastectomy	Regional anesthetic	2% lignocaine	0.375% ropivacaine, dexamethasone 4 mg	NA	1 h	1 mg paracetamol	No adverse event	
Kulshrestha et al. (45)	India	1	12	48	DMD with dentigerous cyst	Procedural sedation	0.2 mg glycopyrrolate, 1 μg/kg fentanyl	Dexmedetomidine was administered slowly with a loading dose of 1 μg/kg over 15 min followed by a continuous infusion at 0.5 μg/kg/h		NA	40 min	NA	NA
Raman et al. (46)	America	1	9	45	DMD with esophagogastroduodenoscopy (EGD)	Sedation	15 mg midazolam	1 μg/kg dexmedetomidine, 1 mg/kg ketamine		NA	15 min	NA	NA
Rozmiarek et al. (7)	America	1	21	43	DMD with bone marrow aspiration	Sedation	NA	1 μg/kg Dexmedetomidine, 20 mg Ketamine		NA	NA	NA	NA
Wang and Stanley (47)	America	1	2	15	DMD with silicon implant	General anesthesia	0.2 mg atropine	0.25%−2.75% halothane, 50% nitrous oxide	0.1 mg atropine, 40 mg succinylcholine	15 mg dantrolene	NA	NA	Malignant hyperthermia
		1	3	15	DMD with muscle biopsy	General anesthesia	NA	350 mg methohexitone, 50% nitrous oxide,42 μg fentanyl, 7 mg atracurium	Fentanyl, 50% nitrous oxide	40 mg dantrolene	NA	NA	NA

(Continued)

10.3389/fmed.2025.1497538

TABLE 2 (Continued)

References	Country	Sample size	Age (year)	Weight (kg)	Study population	Main mode of anesthesia	Anesthesia premedication	Anesthesia induction	Anesthesia maintenance	Anesthesia reversedation	Operation duration	Postoperative analgesia	Side effects
Kim et al. (48)	Korea	1	20	39	DMD with LVAD implantation	General anesthesia	NA	4 mcg/ml propofol, 3 ng/ml remifentanil,40 mg rocuronium	2–2.5 mcg/ml propofol, 1–2 ng/ml remifentanil, 2 mcg/kg/min Rocuronium	NA	NA	1,000 mcg fentanyl, 0.3 mg ramosetron	No complications
Frankowski et al. (4)	America	2	10-year-old/9-year-old	54 kg/ 20 kg	DMD with heel cord surgeries	General anesthesia	1.5–2 mg Midazolam	1–2 mg/kg sodium thiopental, 1.5–2.0 mg/kg lidocaine, 2–5 mg/kg fentanyl, 2–4 mg/kg propofol	Propofol and remifentanil infusions at rates of 45–150 μg/kg/min	NA	2.5–3 h	NA	Uneventful

10.3389/fmed.2025.1497538

TABLE 3 Characteristics of included case reports of BMD patients.

References	Country	Sample size	Age (year)	Weight (kg)	Study population	Main mode of anesthesia	Anesthesia premedication	Anesthesia induction	Anesthesia maintenance	Anesthesia reversedation	Operation duration	Postoperative analgesia	Side effects
Parish and Farzin (23)	Iran	1	43	80	BMD with orthopedic surgery	General anesthesia	200 mg hydrocortisone	2 mg midazolam, 250 μg remifentanil and 60 mg lidocaine 2%	75–100 μg/kg/min propofol and 0.05–2 μg/kg/min remifentanil	NA	90 min	NA	No adverse event
Zhou et al. (25)	China	1	56 woman	48	BMD with laparoscopic hysterectomy and bilateral adnexectomy	General anesthesia	NA	2 mg midazolam, 16 mg etomidate, 20 μg sufentanil	75–100 μg /kg/min propofol and 0.05–2 μg/kg/m remifentanil,2% sevoflurane	NA	90 min	5 mg sufentanil and 30 mg ketorolac	No adverse event
Iwata et al. (29)	Japan	1	58	75 kg	BMD with laparoscopic cholecystectomy	General+ regional anesthesia.	NA	4 μg/ml propofol and 0.2 mg fentanyl, and 0.25 μg/kg/min remifentanil	2.5–3 μg/ml propofol; 0.75% ropivacaine, 1% lidocaine 20 ml	NA	NA	Flurbiprofen axetil 50 mg	No adverse event
Shimauchi et al. (14)	Japan	1	54	54	BMD with cholelithiasis	General anesthesia	NA	3 μg/kg fentanyl and 0.6 mg/kg midazolam,0.4 mg/kg Rocuronium	2–4 mg/kg/h propofol, 0.05–0.3 μg/kg/min remifentanil	100 mg sugammadex (2 mg/kg)	92 min	Pethidine (30 mg)	No adverse event
Jain (34)	India	1	34	NA	BMD with fistulectomy under saddle block	General + regional anesthesia	NA	1.8 ml of 0.5% bupivacaine L3–L4; 1.5 mg midazolam; 30 mg propofol.		Propofol was stopped, nebulized salbutamol	NA	NA	Coughing
Peng and Wei (38)	China	1	2	15	BMD with inguinal hernia	General + regional anesthesia	NA	0.15 mg atropine, 0.5 mg midazolam, 45 mg propofol, 30 μg fentanyl, 1 mg cisatracurium besylate. 0.25% ropivacaine 6 ml	2–4 mg/kg/h propofol, 0.05–0.1 μg/kg/min remifentanil	0.2 mg neostigmine, 0.1 mg atropine	20 min	NA	No adverse event

(Continued)

10.3389/fmed.2025.1497538

TABLE 3 (Continued)

References	Country	Sample size	Age (year)	Weight (kg)	Study population	Main mode of anesthesia	Anesthesia premedication	Anesthesia induction	Anesthesia maintenance	Anesthesia reversedation	Operation duration	Postoperative analgesia	Side effects
Kawaai et al. (44)	Japan	1	19	59	BMD with dental treatment	General anesthesia	10 mg Midazolam, 10 mg famotidine	50 mg propofol	6–10 mg/kg propofol, 67% nitrous oxide, 33% oxygen	NA	2 h	NA	No complications
		1	5	11	BMD with dental treatment	General anesthesia	6 mg Diazepam, 2.5 mg famotidin	5% sevoflurane, 67% nitrous oxide, 33% oxygen	6–12 mg/kg propofol, 0.5–1.5% sevoflurane, 67% nitrous oxide, 33% oxygen	NA	2 h 20 min	NA	No complications
Bush and Dubowitz (49)	UK	1	6	NA	BMD with dental treatment	General anesthetic	Diazepam	Nitrous oxide, oxygen and halothane	NA	Calcium chloride, dantrolene	NA	NA	Cardiac arrest

10.3389/fmed.2025.1497538

TABLE 4 Quality evaluation results of case reports.

References	Were patient's demographic characteristics clearly described?	Was the patients history described and presented as a timeline?	Was the current clinical condition of the patient on presentation clearly described?	Were diagnostic tests or assessment methods and the results clearly described?	Was the intervention(s) or treatment procedure(s) clearly described?	Was the post-intervention clinical condition clearly described?	Were adverse events or unanticipated events identified and described?	Does the case report provide takeway lessons?
Kim and Chun (22)	Yes	No	Yes	Yes	Yes	Yes	Yes	Yes
Parish and Farzin (23)	Yes	Yes	Yes	Yes	Yes	Yes	Yes	Yes
Jung et al. (24)	No	No	Yes	Yes	Yes	Yes	No	Yes
Zhou et al. (25)	Yes	Yes	No	Yes	Yes	Yes	Yes	Yes
Bang et al. (26)	Yes	Yes	Yes	Yes	Yes	Yes	Yes	No
Frankowski et al. (4)	Yes	Yes	No	Yes	Yes	No	Yes	Yes
Büget et al. (27)	Yes	Yes	Yes	Yes	Yes	Yes	Yes	Yes
de Boer et al. (12)	Yes	Yes	Yes	Yes	Yes	Yes	Yes	Yes
Wefki Abdelgawwad Shousha et al. (13)	Yes	Yes	Yes	Yes	Yes	Yes	Yes	Yes
Obata et al. (28)	Yes	Yes	Yes	Yes	Yes	Yes	Yes	Yes
Iwata et al. (29)	No	No	Yes	Yes	Yes	Yes	No	Yes
Richa et al. (30)	Yes	Yes	Yes	Yes	Yes	Yes	Yes	Yes
Shimauchi et al. (14)	Yes	Yes	Yes	Yes	Yes	Yes	Yes	Yes
Saldanha et al. (31)	No	No	Yes	No	Yes	Yes	Yes	Yes
Kocabas et al. (32)	Yes	Yes	Yes	Yes	Yes	Yes	No	Yes
Smelt (15)	Yes	Yes	Yes	No	Yes	Yes	Yes	Yes
Irwin and Henderson (16)	Yes	Yes	Yes	Yes	Yes	Yes	Yes	Yes
Rajmala et al. (33)	Yes	Yes	Yes	No	Yes	Yes	Yes	Yes
Jain (34)	Yes	Yes	Yes	Yes	Yes	Yes	Yes	Yes
Vandepitte et al. (35)	Yes	Yes	Yes	Yes	Yes	Yes	No	Yes
Molyneux (36)	Yes	Yes	Yes	Yes	Yes	Yes	Yes	Yes
Van Obbergh et al. (37)	Yes	Yes	Yes	Yes	Yes	Yes	Yes	Yes

(Continued)

10.3389/fmed.2025.1497538

TABLE 4 (Continued)

References	Were patient's demographic characteristics clearly described?	Was the patients history described and presented as a timeline?	Was the current clinical condition of the patient on presentation clearly described?	Were diagnostic tests or assessment methods and the results clearly described?	Was the intervention(s) or treatment procedure(s) clearly described?	Was the post-intervention clinical condition clearly described?	Were adverse events or unanticipated events identified and described?	Does the case report provide takeway lessons?
Peng and Wei (38)	Yes	Yes	Yes	Yes	Yes	Yes	Yes	Yes
Horikoshi et al. (39)	Yes	Yes	No	Yes	Yes	Yes	Yes	Yes
Sethna et al. (8)	No	Yes	Yes	Yes	Yes	Yes	Yes	Yes
Chalkiadis and Branch (41)	Yes	Yes	Yes	Yes	Yes	Yes	Yes	Yes
Shafy et al. (42)	Yes	Yes	Yes	No	Yes	Yes	Yes	Yes
Rathi et al. (43)	Yes	Yes	No	Yes	Yes	Yes	Yes	Yes
Kulshrestha et al. (45)	Yes	Yes	Yes	No	Yes	No	Yes	Yes
Raman et al. (46)	Yes	Yes	Yes	No	Yes	Yes	No	Yes
Rozmiarek et al. (7)	Yes	Yes	Yes	Yes	Yes	No	No	Yes
Wang and Stanley (47)	Yes	Yes	Yes	Yes	Yes	Yes	Yes	Yes
Kim et al. (48)	Yes	Yes	Yes	Yes	Yes	Yes	Yes	Yes
Bush and Dubowitz (49)	Yes	Yes	No	Yes	Yes	Yes	Yes	Yes
Kawaai et al. (44)	Yes	Yes	Yes	No	Yes	Yes	Yes	Yes

10.3389/fmed.2025.1497538

TABLE 5 Quality evaluation results of non-randomized controlled study.

References	A clearly stated aim	Inclusion of consecutive patients	Prospective collection of data	Endpoints appropriate to the aim of study	Unbiased assessment of the study endpoint	Follow-up period appropriate to the aim of the study	Loss to follow up <5%	Prospective calculation of the study size	An adequate control group	Contemporary groups	Baseline equivalence of groups	Adequate statistical analyses
Ihmsen et al. (50)	2	1	1	2	1	0	1	0	1	2	1	1
Wick et al. (51)	2	1	1	2	1	0	1	0	1	1	1	1
Muenster et al. (52)	2	1	1	2	1	0	1	0	1	2	1	1
Ririe et al. (53)	2	1	1	2	1	0	1	0	1	1	1	1
Kako et al. (54)	2	1	1	1	1	0	1	0	1	1	1	1

The total score of MINORS scale was 16 points. 0: the literature has not been reported, 1: the literature has been reported but the information was insufficient, 2: the literature has been reported and sufficient information has been provided, and a total score of ≥13 was classified as high quality literature.

ropivacaine and other drugs. These studies suggested that general anesthesia or central neuraxial blockade in patients with severe DMD is an unsafe approach to anesthesia because of hemodynamic instability and respiratory depression. Peripheral nerve block is the best way to reduce the risk of critical complications and is a safe and feasible approach to anesthesia in patients with severe DMD.

Four of the included studies involved general anesthesia supplemented with regional anesthesia (29, 33, 34, 38). Anesthesia was induced and maintained with propofol, remifentanil, and fentanyl; local nerve block with ropivacaine and lidocaine was performed.

Moreover, four of the included studies involved the use of procedural sedation (7, 45, 46, 54). Procedural sedation was induced and maintained with dexmedetomidine, ketamine and midazolam (7, 45, 46, 54).

3.4.2 Anesthesia premedication

Nineteen studies involved the use of anesthesia drugs as a premedication (4, 12, 13, 16, 22, 23, 30, 31, 42, 44–47, 49–54). The drugs used included midazolam, acetaminophen, morphine, ondansetron, and hydroxyzine. Kim and Chun (22) reported that 0.2 mg of glycopyrrolate was injected intramuscularly for anesthesia premedication. Parish and Farzin (23) reported that a total of 200 mg of hydrocortisone was injected as the stress dose. Some studies have used midazolam as an anesthesia premedication at doses ranging from 1 to 5 mg (4, 50–54).

3.4.3 Anesthesia induction

Twenty-three studies involved the use of anesthesia induction drugs (4, 13–16, 22–25, 28–33, 37–39, 41, 44, 47–49). The drugs used included midazolam, pentothal sodium, rocuronium bromide, sodium thiopental, propofol, and fentanyl. In patients in whom a muscle relaxant is used, monitoring of muscle relaxation was performed via acceleromyography. The agents used for anesthetic induction should be based on the patient's comorbid cardiac condition. Although the effect of etomidate on adrenal function has led to a re-evaluation of its use during endotracheal intubation in critically ill ICU patients, it may still be an appropriate choice for anesthetic induction in patients with diminished myocardial function (56). The depolarizing agent succinylcholine is absolutely contraindicated and should not even be drawn into a syringe. Rocuronium bromide, with its usually short onset time, could be a suitable alternative to succinylcholine in DMD patients when the clinical conditions require rapid muscle relaxation for airway protection. When motor-evoked potentials are used to monitor spinal cord function, a single dose of a non-depolarizing NMBA can be used to facilitate endotracheal intubation. However, in patients with myopathic conditions such as DMD, the duration of blockade is prolonged (57).

Moreover, five non-randomized controlled trials, including a total of 155 patients, compared the DMD group with the control group to determine the onset time and recovery time after the administration of a standard dose of NMBAs in patients (50–54). Compared with the control group, the sensitivity of patients with DMD to NMBAs may result in a prolonged onset time [MD = −0.96, 95% CI (0.71, 2.60), I^2 = 33%, P < 0.0001;

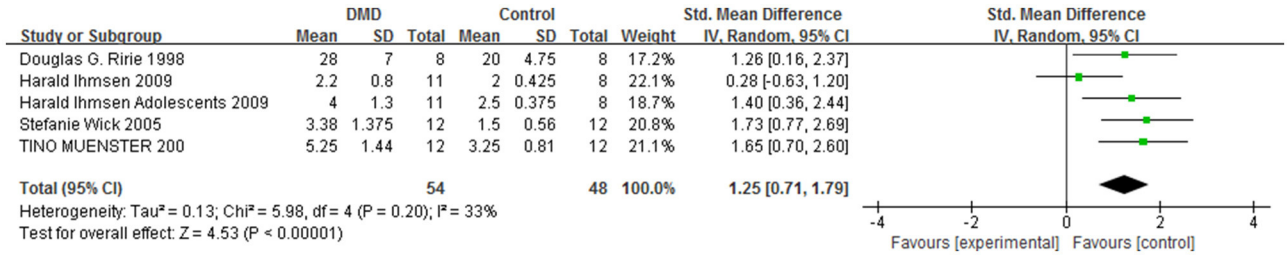

FIGURE 2
Meta-analysis of the onset time (min).

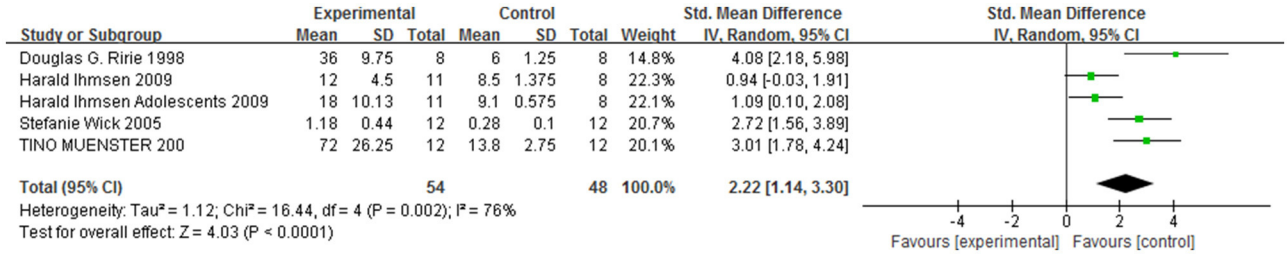

FIGURE 3
Meta-analysis of the recovery time (min).

Figure 2] and recovery time [MD = 2.22, 95% CI (1.14, 3.30), $I^2 = 76\%$, $P < 0.0001$; Figure 3] from anesthesia. Therefore, the anesthetic management of these patients is challenging and may cause serious problems for anesthesiologists. A sensitivity analysis of each comparison revealed no robust changes in significance.

Similarly, Jung et al. (24) documented that the responsiveness of DMD patients administered a standard dosage of non-depolarizing NMBAs differs from that of normal patients. The delayed onset of blockade in DMD patients following the administration of standard-dose rocuronium and prolonged recovery from rocuronium-induced blockade necessitate the need for a careful assessment of neuromuscular function. If rocuronium is administered to patients with DMD, an quantitative assessment of complete neuromuscular recovery, such as acceleromyography, is mandatory.

3.4.4 Anesthesia maintenance

Thirty-two of the included studies involved anesthesia maintenance (4, 7, 12–16, 22–25, 28–34, 37, 39–41, 44–47, 49–54). Intravenous anesthetics such as propofol, fentanyl, remifentanil, ketamine, dexmedetomidine, and rocuronium bromide are reasonable alternatives and are commonly used at variable doses (Table 1). In addition, some studies used inhalation anesthesia with nitrous oxide, oxygen, sevoflurane, isoflurane and halothane to maintain anesthesia (40, 41, 44).

Richa et al. (30) recommended remifentanil for children with DMD. They reported that the combination of propofol and remifentanil infusions with nitrous oxide in oxygen was successful for patients with DMD undergoing spinal surgery. Exaggerated reactions to drugs were not observed. The patient's intraoperative blood pressure and heart rate were stable, and the wake-up test was successful. Alternatively, endotracheal intubation can be accomplished with a combination of propofol and remifentanil to avoid the need for a neuromuscular blocking agent (41).

Moreover, the multidisciplinary panel suggested the use of total intravenous anesthesia (TIVA) to induce and maintain general anesthesia (e.g., propofol and short-acting opioids) (55). Maintenance anesthesia during surgery for scoliosis generally includes TIVA not only due to the abovementioned concerns of rhabdomyolysis related to volatile anesthetic agents but also to facilitate neurophysiological monitoring using motor and somatosensory evoked potentials. Despite the popularity and clinical experience of the use of propofol for TIVA in these patients, recent concerns have been expressed regarding the effect of propofol on mitochondrial oxidative function (10). These concerns have been raised because rhabdomyolysis, which is thought to be secondary to the disruption of mitochondrial fatty acid oxidation, can occur with prolonged propofol infusion in the pediatric ICU setting, and a defect in mitochondrial oxidative capacity is known to occur in patients with muscular dystrophies (58–61). Despite such concerns, TIVA with propofol and a synthetic opioid remains the most commonly chosen anesthetic regimen (11). However, dexmedetomidine may be added to decrease the propofol dose (62, 63). Kako et al. (54) reported that the use of dexmedetomidine (0.5 μg/kg) and ketamine (1 mg/kg) as loading doses followed by continuous infusion of 0.5 kg/kg/h dexmedetomidine achieved the appropriate sedation level with a shorter total recovery time than the higher-dose dexmedetomidine regimen. Therefore, the combination of dexmedetomidine and ketamine is safe and

effective for moderately painful procedures with limited respiratory and cardiovascular effects on high-risk patients.

3.4.5 Adverse events of anesthesia

The sensitivity of patients with DMD to sedative, anesthetic and neuromuscular blocking agents may result in intraoperative and early postoperative cardiovascular and respiratory complications, as well as prolonged recovery from anesthesia. When sedation/anesthetic was excessive, sedation/anesthesia reversal was particularly necessary. Sixteen of the included studies involved the use of anesthesia reversal (12–16, 22, 24, 28, 33, 34, 38–41, 47, 49). Sugammadex, neostigmine and atropine were administered at different doses to reverse cisatracurium besylate-induced neuromuscular blockade (Table 1).

These studies described the efficacy of sugammadex for reversing a prolonged blockade in this setting, but no adverse events were observed (12–14, 22). Jung et al. (24) reported the use of 4 mg of pyridostigmine and 0.16 mg of glycopyrrolate to reverse deep NMB in a child with DMD. Rajmala et al. (33) used 0.05 mg/kg neostigmine and 0.02 mg/kg atropine after the appearance of respiratory efforts, and the postoperative course was uneventful. Similarly, Peng and Wei (38) used 0.2 mg of neostigmine and 0.1 mg of atropine to reverse deep NMB. Treatment with inotropic agents such as milrinone or dobutamine may be necessary to support myocardial function. Close monitoring of cardiac rhythm should be standard, and rhythm abnormalities should be promptly treated (57). Pyridostigmine has been shown to be an effective reversal agent in patients with DMD (24).

Notably, many reports of fatal hyperkalemic cardiac arrest associated with the use of succinylcholine in patients with DMD have raised anesthetists' awareness of this potential complication (16, 28, 40, 41, 47, 49). Therefore, the anesthesia community now commonly accepts that this drug should be strictly avoided in patients with DMD (11). However, rhabdomyolysis may occur in the absence of succinylcholine intraoperatively and during postoperative cardiac arrest as a result of hyperkalemia in patients with DMD (16, 27, 28, 40, 41, 47, 49, 64). The eventual contribution of general anesthetic agents to the cause of the event cannot be ascertained because events occurred during IV and inhaled anesthetic exposure without succinylcholine (16, 28). Moreover, we identified seven cases of rhabdomyolysis and intraoperative cardiac arrest secondary to hyperkalemia during the use of the inhaled anesthetics isoflurane, halothane, and sevoflurane (16, 28, 40, 41, 47, 49). In these patients, a clear precipitant rhythm or event was difficult to discern. Resuscitations persisted in excess of 60 min, with full recoveries obtained in six patients. However, one patient was discharged home with no subjective changes in cerebral function. However, he was paraplegic (sensory level T) (41). Dantrolene is often used empirically after documented concomitant metabolic and respiratory acidosis, with or without modest temperature increases. These cases suggest a predisposition to rhabdomyolysis upon exposure to volatile anesthetics, regardless of surgical stress. The disease is not known to be associated with MH; the components of effective resuscitation are difficult to discern, but a reduction in serum potassium levels is crucial (28, 40, 41, 47, 49).

3.4.6 Postoperative pain control

Appropriate analgesics should be encouraged to provide postoperative analgesia without affecting the patient's normal respiratory function. As in other patients, the analgesic drugs of choice for patients with DMD are opioids. Depending on the duration of the surgical intervention, the choice of opioid should be based on the pharmacological effect and pharmacokinetics. We have administered nearly all clinically used opioids in our series (Tables 1, 2). Six of the included studies investigated postoperative pain control (14, 16, 25, 26, 28–32, 35, 37, 39, 42, 43, 48, 54). Postoperative interventions, such as paracetamol, PCA, morphine pumps, pethidine, nalbuphine, dipirone, flurbiprofen axetil, diclofenac, sufentanil, ketorolac and atropine, were administered at different doses to provide postoperative analgesia (Table 1).

Given the severity of the surgical procedure, several options exist for the provision of postoperative analgesia. In patients undergoing spinal fusion surgery, neuraxial techniques have been used to achieve analgesia through the intermittent or continuous infusion of opioids and/or local anesthetics via epidural catheters, with minimal respiratory side effects (65).

In addition, given their effects on the central control of ventilation and cough effort, options that limit the use of opioids, including adjunct agents or regional anesthesia, should be considered. Preliminary data from the adult population have shown the potential role of the preoperative administration of pregabalin or gabapentin (66). Additionally, postoperative administration of the a2-adrenergic agonist dexmedetomidine and intravenous acetaminophen may play a role. Moreover, caution has been suggested with the use of non-steroidal anti-inflammatory agents given their anecdotal and temporal association with rhabdomyolysis (67, 68).

4 Discussion

Patients with DMD are uniquely vulnerable to the adverse physiological effects of general anesthesia and procedural sedation (55). Tachycardia, ventricular fibrillation and cardiac arrest have been reported during the induction of anesthesia (40, 41, 69–71). In almost all patients assessed in these case reports, DMD was not suspected until a further investigation was prompted by the occurrence of cardiac manifestations. In addition, ventricular fibrillation or cardiac arrest has also been described in patients who are known to have DMD following a return of consciousness while the patient is still in the recovery room (72). Therefore, patients with DMD should receive a detailed preoperative assessment, thoughtful disease-specific intraoperative management and aggressive postoperative monitoring if they are to avoid anesthesia- and surgery-related morbidity and mortality. Moreover, all children presenting for the administration of general anesthesia or sedation should be screened for motor milestones. The inability to walk at an age >18 months or other signs of motor loss or elevated levels of CPK should prompt a suspicion of subclinical myopathy and should warrant a neurological evaluation and genetic testing before elective surgery. Most cases of DMD are detected via genetic testing (55). In addition, timing disease-related major surgical procedures, such as scoliosis surgery, early in a child's life prior to the onset of significant myocardial dysfunction is

recommended to minimize the cardiovascular risk. Finally, surgery for DMD patients should be performed in a hospital equipped to address the unique issues faced by patients with neuromuscular disorders (57).

In addition, because postoperative pulmonary complications might be one of the causes of postoperative complications in DMD patients, before general anesthesia or procedural sedation, the following lung function parameters should be measured to assess the patients' risk of respiratory complications and the need for perioperative and postoperative assisted ventilation or cough. The application of non-invasive ventilation modalities in the preoperative and postoperative setting to limit pulmonary postoperative complications using personalized non-invasive respiratory support is important (55). Options for respiratory support include manual ventilation using a flow-inflated manual resuscitation bag (standard "anesthesia bag") with a full face or nasal mask interface and mechanical support using a conventional or non-invasive positive pressure ventilator via a full face or nasal mask.

Furthermore, these included case studies also revealed that general anesthesia and central neuraxial blockade in patients with severe DMD are unsafe approaches to anesthesia. Peripheral nerve blocks are the best way to reduce the risk of critical complications and are a safe and feasible approach to anesthesia in patients with severe DMD (26, 27, 42, 43). Notably, the general anesthetics that resulted in cardiac complications at induction were succinylcholine and volatile anesthetics. Therefore, the anesthesia community now commonly accepts that anesthetic machines free of volatile agents (including a new disposable breathing circuit) should be used and that succinylcholine is avoided. Monitoring should include a temperature probe, an ECG, and a nerve stimulator (73).

In addition, although general anesthesia may be required for specific procedures, moderately painful procedures such as bone marrow aspiration and biopsy can be performed with procedural sedation and the maintenance of spontaneous ventilation. Given these issues, a need remains for a better agent or agents for procedural sedation. The current evidence suggests the use of a total intravenous anesthesia (TIVA) technique to induce and maintain general anesthesia (e.g., propofol and short-acting opioids) and is advised rather than the use of depolarizing muscle relaxants (48). The authors reported their experience with a combination of ketamine and dexmedetomidine for sedation during bone aspiration and biopsy in an adolescent with DMD (7), which revealed that the application of dexmedetomidine in patients with DMD has the potential to be a promising treatment option in the future.

Moreover, the sensitivity of patients with DMD to NMBAs may result in prolonged onset and recovery times from anesthesia. Muenster et al. speculated that one reason for the prolonged duration of NMB in these patients could be the known degradation of muscle fibers and their replacement by fatty and fibrous tissue with the progression of the disorder. These structural changes are obviously accompanied by a decrease in the total number of neuromuscular junctions and receptors. Consistently, in an experimental study in mdx mice, accelerated degradation of adult nicotinic acetylcholine receptors was observed (74). Such a situation with a reduced number of receptors strongly influences the dose–response relationship of administered non-depolarizing NMBA. Therefore, the wide interpatient variability in the recovery time after the administration of a reduced dose does not allow an estimation of the time needed for complete recovery in a single patient (52). In particular, regarding the prolonged onset time, special attention must be paid to the effect of the relaxant agent used. The use of muscle relaxants is a major concern when performing anesthesia in DMD patients (52). Several prospective investigations have shown that nearly all commonly used non-depolarizing NMBAs can be used in patients with DMD (11). This situation is especially true for rocuronium and mivacurium (11, 52). These reports also revealed that the response to non-depolarizing NMBAs is altered in patients with DMD. The most striking difference is the delayed onset of blockade in DMD patients compared with normal patients. This effect should be considered in situations where rapid airway protection is necessary. Another significant difference is the prolonged duration of recovery from NMB in DMD following standard doses of non-depolarizing NMBAs. Notably, depending on the time of reversal, the duration of residual block after rocuronium may exceed the duration of antagonism by the reversal agent. Therefore, using reversal agents in this situation involves the risk of possible "recurarization" (51). Therefore, even after the administration of a reversal agent, monitoring of muscle strength in the recovery room either quantitatively or clinically should be performed (51). Furthermore, these effects depend on the stage of the disease, with more pronounced effects observed with ongoing progression. This altered response to non-depolarizing NMBAs in patients with DMD makes a quantitative assessment of complete neuromuscular recovery, such as acceleromyography, necessary (11).

In addition, the existing evidence implicates calcium dysregulation as an underlying crucial event in the pathophysiology of DMD (73). In malignant hyperthermia, defective influx and efflux of Ca from the sarcoplasmic reticulum has been observed in mouse models. Since a malignant hyperthermia-like syndrome may occur in DMD patients during anesthesia, maneuvers capable of reducing Ca influx into cells have beneficial effects on these patients DMD; thus, the possibility that a reduction in Ca influx from the sarcoplasmic reticulum by a Ca antagonist, such as dantrolene, may result in additional benefits for patients with DMD (74).

Several limitations of the study should be acknowledged. The strengths of this systematic review include the broad and complete search strategy, the publication of a protocol a priori, and the validated methodology used to assess the included studies, e.g., Cochrane's "Risk of Bias" 2.0 tool and ROBINS-I. We adhered to the protocol to minimize intellectual bias in conducting and reporting the findings. Two authors independently screened studies for inclusion and performed the risk-of-bias assessment. Potential limitations include our broad approach, i.e., for example, we included all studies regardless of the type of drugs, which may have contributed to the high degree of clinical heterogeneity of the included studies. Furthermore, our choice of the definition of outcomes could be discussed. We chose analgesia, sedation and mortality at discharge as the primary outcomes. Unfortunately, a possibility of poorly documented minor complications or minor adverse events caused by anesthetic medication always exists.

Finally, we did not explore the significance of a diagnosis of respiratory or cardiac involvement in the prediction of perioperative complications in DMD patients, and we were not able to perform a retrospective evaluation. No cases of patients requiring postoperative ventilatory support were documented, regardless of whether NMBAs had been used. Follow-up examinations after adverse reactions to general anesthesia are often incomplete, and some patients receive the same type of anesthesia again (75). Whether the negative responses in DMD patients originate during multiple exposures to anesthesia or sedation is unknown, and additional high-quality research is needed to provide more comprehensive information.

Finally, the primary difference between DMD and BMD is the quantity of dystrophin present in skeletal and cardiac muscle. In patients with DMD, dystrophin is almost always absent, whereas partially functional dystrophin is present in patients with BMD and results in a milder form of the disorder and longer survival, which was consistent with the data in Tables 2, 3. However, 2 patients with BMD who were very young were described (23, 49). In addition, compared with patients with BMD, patients with DMD had more comorbid conditions and higher rates of cardiomyopathy and severe restrictive lung disease. However, patients with BMD are present with serious postoperative adverse reactions (49). Postoperatively, DMD and BMD patients must be monitored until cardiorespiratory function returns to the baseline. The current case reports are insufficient for generating definitive conclusions regarding the significant differences between patients with BMD and DMD. Overall, the anesthesia technique must be customized and adjusted for each patient.

5 Conclusions

The results of the included studies confirmed that patients with DMD are more sensitive to NMBAs, which may result in a delayed onset time and prolonged recovery time from anesthesia, and these effects depend on the stage of the disease, with more pronounced effects observed with ongoing progression. Precautions for DMD patients should include quantitative neuromuscular and electrocardiographic monitoring and rapid airway protection throughout anesthesia. The strict avoidance of succinylcholine and volatile anesthetics during anesthesia in patients with DMD can prevent known anesthetic hazards such as rhabdomyolysis or hypercalcemia. Compared with general anesthesia, regional anesthesia can be a relatively safe option (if the surgical site is appropriate for the technique). Dantrolene should be available in the theater and be readily used if events consistent with a malignant hyperpyrexial response to anesthesia occur. However, further prospective clinical trials are needed to determine the most effective interventions for patients with DMD.

Data availability statement

The original contributions presented in the study are included in the article/supplementary material, further inquiries can be directed to the corresponding author.

Author contributions

XL: Writing – original draft, Data curation, Formal analysis. YJ: Data curation, Formal analysis, Methodology, Writing – original draft. TL: Data curation, Formal analysis, Methodology, Writing – original draft. YG: Data curation, Methodology, Writing – original draft. YL: Conceptualization, Writing – review & editing.

Funding

The author(s) declare financial support was received for the research, authorship, and/or publication of this article. This work was supported by Chengdu Pharmaceutical Society pharmaceutical research project (cdyxky5039).

Conflict of interest

The authors declare that the research was conducted in the absence of any commercial or financial relationships that could be construed as a potential conflict of interest.

Publisher's note

References

1. Kunkel LM, Monaco AP, Middlesworth W, Ochs HD, Latt SA. Specific cloning of DNA fragments absent from the DNA of a male patient with an X chromosome deletion. *Proc Natl Acad Sci USA.* (1985) 82:4778–82. doi: 10.1073/pnas.82.14.4778

2. Ray PN, Belfall B, Duff C, Logan C, Kean V, Thompson MW, et al. Cloning of the breakpoint of an X; 21 translocation associated with Duchenne muscular dystrophy. *Nature.* (1985) 318:672–5. doi: 10.1038/318672a0

3. Mah JK. Current and emerging treatment strategies for Duchenne muscular dystrophy. *Neuropsychiatr Dis Treat.* (2016) 12:1795–807. doi: 10.2147/NDT.S93873

4. Frankowski GA, Johnson JO, Tobias JD. Rapacuronium administration to two children with Duchenne's muscular dystrophy. *Anesth Analg.* (2000) 91:27–8. doi: 10.1213/00000539-200007000-00005

5. Caliskan E, Sener M, Kocum A, Aribogan A. Duchenne muscular dystrophy: how I do it? Regional or general anesthesia? *Paediatr Anaesth.* (2010) 19:624–5. doi: 10.1111/j.1460-9592.2009.03020.x

6. Murat I, Esteve C, Montay G, Delleur MM, Gaudiche O, Saint-Maurice C, et al. Pharmacokinetics and cardiovascular effects of bupivacaine during epidural anesthesia in children with Duchenne muscular dystrophy. *Anesthesiology.* (1987) 7:249–52. doi: 10.1097/00000542-198708000-00017

7. Rozmiarek A, Corridore M, Tobias JD. Dexmedetomidine-ketamine sedation during bone marrow aspirate and biopsy in a patient with duchenne muscular dystrophy. *Saudi J Anaesth.* (2011) 5:219–22. doi: 10.4103/1658-354X.82810

8. Sethna NF, Rockoff MA, Worthen HM, Rosnow JM. Anesthesia-related complications in children with Duchenne muscular dystrophy. *Anesthesiology.* (1988) 68:462–5. doi: 10.1097/00000542-198803000-00028

9. Hayes J, Veyckemans F, Bissonnette B. Duchenne muscular dystrophy: an old anesthesia problem revisited. *Paediatr Anaesth.* (2008) 18:100–6. doi: 10.1111/j.1460-9592.2007.02302.x

10. Hopkins PM. Anaesthesia and the sex-linked dystrophies: between a rock and a hard place. *Br J Anaesth.* (2010) 104:397–400. doi: 10.1093/bja/aeq036

11. Muenster T, Mueller C, Forst J, Huber H, Schmitt HJ. Anaesthetic management in patients with Duchenne muscular dystrophy undergoing orthopaedic surgery: a review of 232 cases. *Eur J Anaesthesiol.* (2012) 29:489–94. doi: 10.1097/EJA.0b013e3283566789

12. de Boer HD, van Esmond J, Booij LH, Driessen JJ. Reversal of rocuronium-induced profound neuromuscular block by sugammadex in Duchenne muscular dystrophy. *Paediatr Anaesth.* (2009) 19:1226–8. doi: 10.1111/j.1460-9592.2009.03178.x

13. Wefki Abdelgawwad Shousha AA, Sanfilippo M, Sabba A, Pinchera P. Sugammadex and reversal of neuromuscular block in adult patient with duchenne muscular dystrophy. *Case Rep Anesthesiol.* (2014) 2014:680568. doi: 10.1155/2014/680568

14. Shimauchi T, Yamaura K, Sugibe S, Hoka S. Usefulness of sugammadex in a patient with Becker muscular dystrophy and dilated cardiomyopathy. *Acta Anaesthesiol Taiwan.* (2014) 52:146–8. doi: 10.1016/j.aat.2014.02.005

15. Smelt WL. Cardiac arrest during desflurane anaesthesia in a patient with Duchenne's muscular dystrophy. *Acta Anaesthesiol Scand.* (2005) 49:267–9. doi: 10.1111/j.1399-6576.2004.00596.x

16. Irwin MG, Henderson M. Cardiac arrest during major spinal scoliosis surgery in a patient with Duchenne's muscular dystrophy undergoing intravenous anaesthesia. *Anaesth Intensive Care.* (1995) 23:626–9. doi: 10.1177/0310057X9502300521

17. Higgins J, Thompson SG, Deeks JJ. Cochrane handbook for systematic reviews of interventions version 5.1.0. the cochrane collaboration. *Naunyn Schmiedebergs Arch Exp Pathol Pharmakol.* (2008) 5:S38.

18. Slim K, Nini E, Forestier D, Kwiatkowski F, Panis Y, Chipponi J, et al. Methodological index for non-randomized studies (minors): development and validation of a new instrument. *ANZ J Surg.* (2003) 73:712–6. doi: 10.1046/j.1445-2197.2003.02748.x

19. The Joanna Briggs Instatute. *Joanna Briggs Instatute Reviewers' Manual: 2016 Edition*. Adelaide, SA: The Joanna Bbrigga Institute (2016).

20. Higgins JPT, Thomas J, Chandler J, Cumpston M, Li T, Page MJ, et al. *Cochrane Handbook for Systematic Reviews of Interventions version 6.3 (updated February 2022)*. Cochrane. (2022). Available at: www.training.cochrane.org/handbook

21. DerSimonian R, Laird N. Meta-analysis in clinical trials. *Control Clin Trials.* (1986) 7:177–88. doi: 10.1016/0197-2456(86)90046-2

22. Kim JE, Chun HR. Rocuronium-induced neuromuscular block and sugammadex in pediatric patient with duchenne muscular dystrophy: a case report. *Medicine.* (2017) 96:e6456. doi: 10.1097/MD.0000000000006456

23. Parish M, Farzin H. Adult patient with Becker dystrophy undergoing orthopedic surgery: an anesthesia challenge. *Int Med Case Rep J.* (2018) 11:33–6. doi: 10.2147/IMCRJ.S150037

24. Jung HJ, Kim JB, Im KS, Lee JH, Kim DJ, Cho SA, et al. How should we monitor pediatric patients with Duchenne muscular dystrophy? A case report. *Korean J Anesthesiol.* (2011) 61:159–61. doi: 10.4097/kjae.2011.61.2.159

25. Zhou SY, Wang D, Liu C, Zhang S, Shan BL, Ma HC, et al. Laparoscopic gynecological surgery in an adult woman with Becker muscular dystrophy performed with sevoflurane with cisatracurium anesthesia: a case report. *Medicine.* (2020) 99:e19733. doi: 10.1097/MD.0000000000019733

26. Bang SU, Kim YS, Kwon WJ, Lee SM, Kim SH. Peripheral nerve blocks as the sole anesthetic technique in a patient with severe Duchenne muscular dystrophy. *J Anesth.* (2016) 30:320–3. doi: 10.1007/s00540-015-2127-4

27. Büget MI, Eren I, Küçükay S. Regional anaesthesia in a Duchenne muscular dystrophy patient for upper extremity amputation. *Agri.* (2014) 26:191–5. doi: 10.5505/agri.2014.34713

28. Obata R, Yasumi Y, Suzuki A, Nakajima Y, Sato S. Rhabdomyolysis in association with Duchenne's muscular dystrophy. *Can J Anaesth.* (1999) 46:564–6. doi: 10.1007/BF03013547

29. Iwata M, Kuzumoto N, Akasaki Y, Morioka M, Nakayama K, Matsuzawa N, et al. The ultrasound-guided nerve blocks of abdominal wall contributed to anesthetic management of cholecystectomy in a patient with Becker muscular dystrophy without using muscle relaxants. *JA clinical reports.* (2017) 3:64. doi: 10.1186/s40981-017-0134-1

30. Richa F, Yazigi A, Yazbeck P. Use of remifentanil and propofol without muscle relaxant combined with intrathecal morphine in children with Duchenne's muscular dystrophy undergoing spinal surgery. *J Med Liban.* (2008) 56:181–4.

31. Saldanha RM, Gasparini JR, Silva LS, de Carli RR, de Castilhos VU, das Neves MM, et al. Anesthesia for Duchenne muscular dystrophy patients: case reports. *Rev Bras Anestesiol.* (2005) 55:445–9. doi: 10.1590/S0034-70942005000400009

32. Kocabas S, Yedicocuklu D, Askar F, Atay Y. Anesthetic management of a child with Duchenne muscular dystrophy undergoing correction of Fallot's tetralogy. *Paediatr Anaesth.* (2008) 18:448–50. doi: 10.1111/j.1460-9592.2008.02456.x

33. Rajmala X, Savita S, Kirti K, Nandini X. Intravenous anaesthesia combined with peribulbar block in a child with suspected Duchenne muscular dystrophy. *Acta Anaesthesiol Scand.* (2004) 48:1341. doi: 10.1111/j.1399-6576.2004.00501.x

34. Jain A. Propofol-induced violent coughing in a patient with Becker's muscular dystrophy. *Indian J Pharmacol.* (2011) 43:476–7. doi: 10.4103/0253-7613.83134

35. Vandepitte C, Gautier P, Bellen P, Murata H, Salviz EA, Hadzic A, et al. Use of ultrasound-guided intercostal nerve block as a sole anaesthetic technique in a high-risk patient with Duchenne muscular dystrophy. *Acta Anaesthesiol Belg.* (2013) 64:91—4.

36. Molyneux MK. Anaesthetic management during labour of a manifesting carrier of Duchenne muscular dystrophy. *Int J Obstet Anesth14.* (2005) 58–61. doi: 10.1016/j.ijoa.2004.05.009

37. Van Obbergh LJ, Corteel J, Papadopoulos J, Aunac S. Anesthesia for a child suffering from a deletion in the Xp21 loci resulting in Duchenne disease, glycerol kinase deficiency, and congenital adrenal hypoplasia. *Paediatr Anaesth.* (2011) 21:1085–7. doi: 10.1111/j.1460-9592.2011.03634.x

38. Peng L, Wei W. Anesthesia management in a pediatric patient with Becker muscular dystrophy undergoing laparoscopic surgery: a case report. *World J Clin Cases.* (2021) 9:8852–7. doi: 10.12998/wjcc.v9.i29.8852

39. Horikoshi Y, Kuratani N, Tateno K, Hoshijima H, Nakamura T, Mieda T, et al. Anesthetic management with remimazolam for a pediatric patient with Duchenne muscular dystrophy. *Medicine.* (2021) 100:e28209. doi: 10.1097/MD.0000000000028209

40. Sethna NF, Rockoff MA. Cardiac arrest following inhalation induction of anaesthesia in a child with Duchenne's muscular dystrophy. *Can Anaesth Soc J.* (1986) 33:799–802. doi: 10.1007/BF03027134

41. Chalkiadis GA, Branch KG. Cardiac arrest after isoflurane anaesthesia in a patient with Duchenne's muscular dystrophy. *Anaesthesia.* (1990) 45:22–5. doi: 10.1111/j.1365-2044.1990.tb14497.x

42. Shafy SZ, Hakim M, Villalobos MA, Pearson GD, Veneziano G, Tobias JD, et al. Caudal epidural block instead of general anesthesia in an adult with Duchenne muscular dystrophy. *Local Reg Anesth.* (2018) 11:75–80. doi: 10.2147/LRA.S180867

43. Rathi R, Ramekar A, D'souza N. Combination of regional anaesthetic techniques in a Duchenne Muscular Dystrophy carrier undergoing mastectomy. *Indian J Anaesth.* (2021) 65:260–1. doi: 10.4103/ija.IJA_913_20

44. Kawaai H, Tanaka K, Yamazaki S. Continuous infusion propofol general anesthesia for dental treatment in patients with progressive muscular dystrophy. *Anesth Prog.* (2005) 52:12–6. doi: 10.2344/0003-3006(2005)52[12:CIPGAF]2.0.CO;2

45. Kulshrestha A, Bajwa SJ, Singh A, Kapoor V. Dexmedetomidine and fentanyl combination for procedural sedation in a case of Duchenne muscular dystrophy. *Anesth Essays Res.* (2011) 5:224–6. doi: 10.4103/0259-1162.94788

46. Raman V, Yacob D, Tobias JD. Dexmedetomidine-ketamine sedation during upper gastrointestinal endoscopy and biopsy in a patient with Duchenne muscular dystrophy and egg allergy. *Int J Crit Illn Inj Sci.* (2012) 2:40–3. doi: 10.4103/2229-5151.94899

47. Wang JM, Stanley TH. Duchenne muscular dystrophy and malignant hyperthermia–two case reports. *Can Anaesth Soc J.* (1986) 33:492–7. doi: 10.1007/BF03010977

48. Kim HJ, Kim SY, Ju MH, Lee SY, Byeon GJ, Kim HY, et al. Early extubation after left ventricular assist device implantation in a patient with Duchenne muscular dystrophy: a case report. *J Anesth.* (2021) 35:455–8. doi: 10.1007/s00540-021-02925-9

49. Bush A, Dubowitz V. Fatal rhabdomyolysis complicating general anaesthesia in a child with Becker muscular dystrophy. *Neuromuscul Disord.* (1991) 1:201–4. doi: 10.1016/0960-8966(91)90025-N

50. Ihmsen H, Schmidt J, Schwilden H, Schmitt HJ, Muenster T. Influence of disease progression on the neuromuscular blocking effect of mivacurium in children and adolescents with Duchenne muscular dystrophy. *Anesthesiology.* (2009) 110:1016–9. doi: 10.1097/ALN.0b013e31819daf31

51. Wick S, Muenster T, Schmidt J, Forst J, Schmitt HJ. Onset and duration of rocuronium-induced neuromuscular blockade in patients with Duchenne muscular dystrophy. *Anesthesiology.* (2005) 102:915–9. doi: 10.1097/00000542-200505000-00009

52. Muenster T, Schmidt J, Wick S, Forst J, Schmitt HJ. Rocuronium 0.3 mg x kg-1 (ED95) induces a normal peak effect but an altered time course of neuromuscular block in patients with Duchenne's muscular dystrophy. *Paediatr Anaesth.* (2006) 16:840–5. doi: 10.1111/j.1460-9592.2006.01870.x

53. Ririe DG, Shapiro F, Sethna NF. The response of patients with Duchenne's muscular dystrophy to neuromuscular blockade with vecuronium. *Anesthesiology.* (1998) 88:351–4. doi: 10.1097/00000542-199802000-00013

54. Kako H, Corridore M, Kean J, Mendell JR, Flanigan KM, Tobias JD, et al. Dexmedetomidine and ketamine sedation for muscle biopsies in patients with Duchenne muscular dystrophy. *Paediatr Anaesth.* (2014) 24:851–6. doi: 10.1111/pan.12387

55. Birnkrant DJ, Panitch HB, Benditt JO. American College of Chest Physicians consensus statement on the respiratory and related management of patients with Duchenne muscular dystrophy undergoing anesthesia or sedation. *Chest.* (2007) 132:1977–86. doi: 10.1378/chest.07-0458

56. Scherzer D, Leder M, Tobias JD. Pro-con debate: etomidate or ketamine for rapid sequence intubation in pediatric patients. *J Pediatr Pharmacol Ther.* (2012) 17:142–9. doi: 10.5863/1551-6776-17.2.142

57. Cripe LH, Tobias JD. Cardiac considerations in the operative management of the patient with Duchenne or Becker muscular dystrophy. *Paediatr Anaesth.* (2013) 23:777–84. doi: 10.1111/pan.12229

58. Vasile B, Rasulo F, Candiani A. The pathophysiology of propofol infusion syndrome: a simple name for a complex syndrome. *Intensive Care Med.* (2003) 29:1417–25. doi: 10.1007/s00134-003-1905-x

59. Kuznetsov AV, Winkler K, Wiedemann FR. Impaired mitochondrial oxidative phosphorylation in skeletal muscle of the dystrophin-deficient mdx mouse. *Mol Cell Biochem.* (1998) 183:87–96.

60. Ginns EI, Barranger JA, McClean SW. A juvenile form of glycerol kinase deficiency with episodic vomiting, acidemia, and stupor. *J Pediatr.* (1984) 104:736–9. doi: 10.1016/S0022-3476(84)80956-7

61. Mak TWL, Wong LM, Wong SN. Glycerol kinase deficiency presenting with hypodipsia, osmotic diuresis and severe hy-hypernatremia. *J Inherit Metab Dis.* (2005) 28:1159–61. doi: 10.1007/s10545-005-0101-2

62. Tobias JD, Goble TJ, Bates G. Effects of dexmedetomidine on intraoperative motor and somatosensory evoked potential monitoring during spinal surgery in adolescents. *Pediatr Anesth.* (2008) 18:1082–8. doi: 10.1111/j.1460-9592.2008.02733.x

63. Bala E, Sessler DI, Nair DR. Motor and somatosensory evoked potentials are well maintained in patients given dexmedetomidine during spine surgery. *Anesthesiology.* (2008) 109:417–25. doi: 10.1097/ALN.0b013e318182a467

64. Gurnaney H, Brown A, Litman RS. Malignant hyperthermia and muscular dystrophies. *Anesth Analg.* (2009) 109:1043–8. doi: 10.1213/ane.0b013e3181aa5cf6

65. Tobias JD. A review of intrathecal and epidural analgesia after spinal surgery in children. *Anesth Analg.* (2004) 98:956–65. doi: 10.1213/01.ANE.0000107938.80562.75

66. Rusy LM, Hainsworth KR, Nelson TJ. Gabapentin use in pediatric spinal fusion patients: a randomized, double-blind, controlled controlled trial. *Anesth Analg.* (2010) 110:1393–8. doi: 10.1213/ANE.0b013e3181d41dc2

67. Poole TC, Lim TY, Buck J. Perioperative cardiac arrest in a patient with previously undiagnosed Becker's muscular dystrophy after isoflurane anaesthesia for elective surgery. *Br J Anaesth.* (2010) 104:487–9. doi: 10.1093/bja/aeq035

68. Burke SM, Shorten GD. Perioperative pregabalin improves pain and functional outcomes 3 months after lumbar discectomy. *Anesth Analg.* (2010) 110:1180–5. doi: 10.1213/ANE.0b013e3181cf949a

69. Miller Jr ED, Sanders DB, Rowlingson JC, Berry Jr FA, Sussman MD, Epstein RM, et al. Anesthesia induced rhabdomyolysis in a patient with Duchenne'smuscular dystrophy. *Anesthesiology.* (1978) 48:146–8. doi: 10.1097/00000542-197802000-00012

70. Brownell AKW, Paasuke RT, Elash A. Malignant hypothermia in Duchenne muscular dystrophy. *Anesthesiology.* (1983) 58:180. doi: 10.1097/00000542-198302000-00013

71. Linter SP, Thomas PR, Withington PS, Hall MG. Suxamethonium associated hypertonicity and cardiac arrest in unsuspected pseudohypertrophic muscular dystrophy. *Br J Anaesth.* (1982) 54:1331–2. doi: 10.1093/bja/54.12.1331

72. Boba A. Fatal postanesthetic complications in two muscular dystrophic patients. *J Pediatr Surg.* (1970) 5:71–5. doi: 10.1016/0022-3468(70)90523-3

73. Vallejo-Illarramendi A, Toral-Ojeda I, Aldanondo G, López de Munain A. Dysregulation of calcium homeostasis in muscular dystrophies. *Expert Rev Mol Med.* (2014) 16:e16. doi: 10.1017/erm.2014.17

74. Bertorini TE, Palmieri GM, Griffin J, Igarashi M, Hinton A, Karas JG, et al. Effect of dantrolene in Duchenne muscular dystrophy. *Muscle Nerve.* (1991) 14:503–7. doi: 10.1002/mus.880140603

75. Segura LG, Lorenz JD, Weingarten TN, Scavonetto F, Bojanić K, Selcen D, et al. Anesthesia and Duchenne or Becker muscular dystrophy: review of 117 anesthetic exposures. *Paediatr Anaesth.* (2013) 23:855–64. doi: 10.1111/pan.12248

frontiers | Frontiers in Public Health

TYPE Original Research
PUBLISHED 05 February 2025
DOI 10.3389/fpubh.2025.1410895

OPEN ACCESS

EDITED BY
Shoulong Deng,
Chinese Academy of Medical Sciences and Peking Union Medical College, China

REVIEWED BY
Jagadeesh Uppala,
Medical College of Wisconsin, United States
Yue Zhao,
China Agricultural University, China

*CORRESPONDENCE
Yu Zhao
✉ 862318624@qq.com

†These authors have contributed equally to this work

RECEIVED 17 April 2024
ACCEPTED 13 January 2025
PUBLISHED 05 February 2025

CITATION
Yang J, Chen Z, Dai X, Jiang L, Dai L and Zhao Y (2025) A nomogram to predict sarcopenia in middle-aged and older women: a nationally representative survey in China. *Front. Public Health* 13:1410895. doi: 10.3389/fpubh.2025.1410895

A nomogram to predict sarcopenia in middle-aged and older women: a nationally representative survey in China

Jiayi Yang[1†], Zihao Chen[2†], Xinxin Dai[3], Liyao Jiang[4], Liyan Dai[4] and Yu Zhao[1*]

[1]Department of Gynecology and Obstetrics, The Second Affiliated Hospital of Wenzhou Medical University, Wenzhou, Zhejiang, China, [2]Department of Orthopaedic Surgery, The Second Affiliated Hospital and Yuying Children Hospital of Wenzhou Medical University, Wenzhou, China, [3]Department of Gynecology and Obstetrics, The First Affiliated Hospital of Wenzhou Medical University, Wenzhou, Zhejiang, China, [4]Department of Gynecology and Obstetrics, Lucheng District People's Hospital, Wenzhou, Zhejiang, China

Background: Sarcopenia is a disease characterized by losing muscle mass, strength, and function with age. Studies have shown that sarcopenia is generally higher in women than in men. Therefore, this study used the 2015 China Health and Retirement Longitudinal Study (CHARLS) data to explore further the risk factors associated with sarcopenia in middle-aged and older Chinese women.

Methods: In this study, data from the 2015 CHARLS database were analyzed, comprising 7,805 eligible participants. Participants were categorized into either the sarcopenia group (n = 2,160) or the non-sarcopenia group (n = 5,645) based on the presence or absence of sarcopenia. Through the utilization of logistic regression analysis, multiple risk factors were identified. Additionally, the predictive value of these risk factors was assessed by applying receiver operating characteristic (ROC) curve analysis. Subsequently, a visual nomogram prediction model was developed by incorporating the identified risk factors into R4.1.2 software.

Results: Age, area, education, marriage, waist circumference, stroke, body pain, depression, and region may be closely related to Chinese women with sarcopenia. In addition, this study integrated these sarcopenia-related variables into a comprehensive index, and ROC analysis results showed that the AUC of the composite index was 0.738.

Conclusions: This study found that sarcopenia in Chinese women may be closely related to age, waist, education, marriage, area, stroke, physical pain, depression, and region. In addition, this study constructs a nomogram to help clinicians better screen potential female patients with sarcopenia.

KEYWORDS

women's health, middle and aged women, sarcopenia, nomogram, risk factors

Introduction

Sarcopenia is characterized by the loss of muscle mass, strength, and function that occurs with aging (1). It is a natural part of the aging process, and after middle age, muscle mass typically declines by about 1% per year (2). The consequences of sarcopenia can be significant, including decreased mobility, increased risk of falls and fractures, and decreased quality of life. Moreover, it can also lead to an increased risk of chronic

diseases such as diabetes, obesity, and osteoporosis (3–5). Several factors contribute to the development of sarcopenia, including hormonal changes, decreased physical activity, poor nutrition, and inflammation (3).

Although sarcopenia is common in men and women, Petermann-Rocha et al. found that the prevalence of sarcopenia was higher in women than in men (6). Women generally exhibit lower muscle mass than men, starting from a younger age (7). Consequently, they are at an elevated risk for developing sarcopenia as they age. Hormonal changes during menopause, such as a decrease in estrogen, can further accelerate muscle loss and increase the risk of sarcopenia in women (8). Additionally, certain lifestyle factors may impact sarcopenia risk differently in women. For example, women are more likely to engage in low-impact exercises like walking or yoga, which may not provide enough resistance training to maintain muscle mass. High-impact exercises, such as weightlifting or resistance training, are more effective in preserving muscle mass (9). Hence, it is crucial to prioritize research exploring the connection between sarcopenia and middle-aged and older women.

The China Health and Retirement Longitudinal Study (CHARLS) is a comprehensive research project to gather high-quality microdata representing individuals and families aged 45 and above in China (10). Its primary purpose is to analyze the population aging problem in China and promote interdisciplinary research on this issue. The initial phase of CHARLS, known as the national baseline survey, took place in 2011. It encompassed 150 county- and 450 village-level units and involved ∼17,000 people from around 10,000 households. To ensure the continuity of the study, subsequent surveys will be conducted every 2–3 years, allowing for longitudinal tracking of the participants. The ongoing CHARLS project is valuable, providing comprehensive and periodically updated data on aging and health trends among middle-aged and older individuals in China.

This study used the 2015 CHARLS data to explore further the risk factors associated with sarcopenia in middle-aged and older Chinese women. By analyzing survey data from a large sample, we sought to reveal the prevalence of sarcopenia in middle-aged and older women and possible risk factors in order to provide a scientific basis for prevention and treatment.

Methods

Study design

The study included 7,805 eligible participants from the 2015 CHARLS database. According to the presence or absence of sarcopenia, the patients were divided into the sarcopenia group (n = 2,160) and non-sarcopenia group (n = 5,645) (Figure 1). Age, waist, body mass index (BMI), sleep duration in the past month, education, smoking history, region, region, marriage,

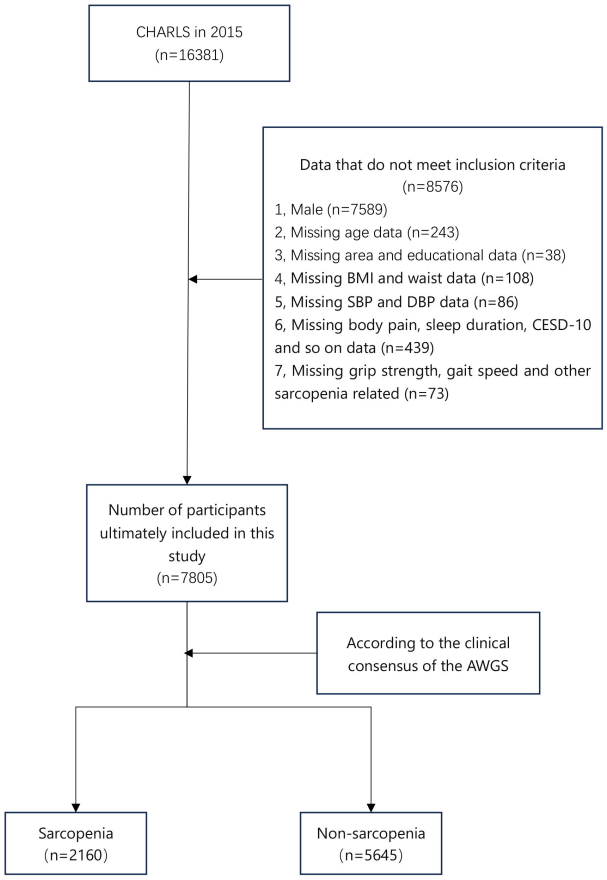

FIGURE 1
Flow chart of participants in the study. CHARLS, China Health and Retirement Longitudinal Study; BMI, body mass index; SBP, systolic blood pressure; DBP, diastolic blood pressure; CESD-10, 10-item Center for Epidemiological Studies Depression Scale; AWGS, Asian Working Group for Sarcopenia.

depression, high blood pressure, dyslipidemia, diabetes or high blood sugar, chronic lung disease, heart disease, stroke, digestive disease, emotional problems, memory-related diseases, arthritis or rheumatism, asthma, frequency of drinking in the past year, body pain, liver disease, and cancer were included in the study.

In addition, this study divides the study population into seven regions based on geographical, economic, and cultural considerations. Northeast (Heilongjiang, Jilin, and Liaoning provinces), East (Anhui, Fujian, Jiangsu, Jiangxi, Zhejiang, Shandong, and Shanghai), North (Hebei, Shanxi, Inner Mongolia Autonomous Region, Tianjin, and Beijing), Central (Hubei, Hunan and Henan provinces), South (Guangdong and Guangxi provinces), Southwest (Yunnan, Guizhou, Sichuan and Chongqing) and Northwest China (Qinghai, Shaanxi, Gansu and Xinjiang Autonomous Region). The survey did not include Hainan Province, Taiwan Province, Ningxia Autonomous Region, Tibet Autonomous Region, Hong Kong Special Administrative Region, and Macao Special Administrative Region.

Self-reports were used to determine whether participants had hypertension, dyslipidemia, diabetes or high blood sugar, cancer, chronic lung disease, liver disease, heart disease, stroke,

Abbreviations: CHARLS, China Health and Retirement Longitudinal Study; BMI, body mass index; SBP, systolic blood pressure; DBP, diastolic blood pressure; CESD-10, 10-item Center for Epidemiological Studies Depression Scale; AWGS, Asian Working Group for Sarcopenia; ROC, receiver operating characteristic; AUC, area under the curve.

kidney disease, digestive disease, emotional problems, arthritis or rheumatism, memory-related diseases, and asthma. For example, participants were asked, "Has a doctor ever told you that you have dyslipidemia?" If the participant answered "Yes" to this question, the participant was considered to have dyslipidemia. In addition, according to Chinese clinical guidelines, participants are also considered to have high blood pressure when their average systolic blood pressure (SBP) is greater than or equal to 140 mmHg or their average diastolic blood pressure (DBP) is greater than or equal to 90 mmHg.

Depression was evaluated using the 10-item Center for Epidemiological Studies Depression Scale (11) (CESD-10) in the CHARLS questionnaire. Participants with a CESD-10 score of 10 or higher were categorized as having depressive symptoms.

The definition of sarcopenia

According to the consensus of the 2019 version of the Asian Working Group for Sarcopenia (AWGS) (12), sarcopenia is defined as "age-related loss of muscle mass coupled with low muscle strength and/or low physical performance." Low muscle strength is primarily defined as a grip strength greater than 28 kg for men and less than 18 kg for women. Low physical performance was defined as a 6-meter walk of less than 1.0 m/s or five chair standing tests greater than or equal to 12 s.

This study divided participants into sarcopenia and non-sarcopenia groups based on whether they met diagnostic criteria for low muscular strength or low physical performance.

Inclusion and exclusion criteria

The inclusion criteria were: (1) Female, (2) The diagnostic criteria of sarcopenia conform to the consensus of the 2019 version of the AWGS. The exclusion criteria were: (1) Clinical baseline characteristics were missing, such as education, BMI, etc. (2) Male.

Statistics

Data distribution was assessed using the Shapiro-Wilk test. Patient characteristics were described using median (interquartile range [IQR]) or frequency and percentage, as appropriate. A non-parametric test (Mann-Whitney *U*-test or Kruskal-Wallis test) was employed for data with non-normal distribution or heterogeneity of variances. Categorical variables were presented as percentages and analyzed using the Pearson Chi-squared test. Relevant risk factors ($P < 0.05$) were identified through multivariate logistic regression analysis and integrated into a composite index. The predictive performance of this composite index was evaluated using the receiver operating characteristic (ROC) curve. All statistical analyses were conducted using SPSS software (version 26.0; SPSS et al., USA).

Furthermore, the final risk factors were integrated into the R4.1.2 software (R Foundation for Statistical Computing, Vienna, Austria) to establish a nomogram prediction model. The effectiveness of the model's predictions was assessed using the consistency index (C-index), with a range of 0.5–1.0. Accuracy was positively associated with the C-index value. The calibration curve, which included an image comparison of predicted and actual risks, was used to evaluate the prediction consistency. The conformity of the model was determined by how closely the predicted risk aligned with the standard curve.

Results

A total of 7,805 female participants were included in the study, of whom 2,160 had sarcopenia, and 5,645 did not. There were significant differences in age, waist, BMI, sleep duration over the past month, education, smoking history, region, area, marriage, depression, hypertension, dyslipidemia, diabetes or high blood sugar, chronic lung disease, heart disease, stroke, digestive diseases, emotional problems, memory-related diseases, arthritis or rheumatism, asthma, and body pain (all *P* values < 0.05). There were no significant differences in the frequency of drinking in the past year, liver disease, and cancer (Table 1).

A binary multi-factor logistics regression analysis was used to analyze the above-related variables, and it was finally found that age, area, education, marriage, waist, stroke, body pain, depression, and region were risk factors for female sarcopenia (*P* values were all < 0.05) (Table 2). In addition, these risk factors were integrated into a composite index (age + area + education + marriage + waist + stroke + body pain + depression + region).

ROC curve analysis showed that the area under the curve (AUC) of the composite indicator for predicting sarcopenia was 0.738 (95% CI 0.725–0.750 $p < 0.001$) (Figure 2). In addition, this study established a nomogram to visually screen Chinese female patients with sarcopenia by screening relevant risk factors (Figure 3). After 1,000 repetitions of bootstrap self-sampling, the C-index of the model is 0.738, indicating that the agreement between the predicted value and the actual observed value meets the standard. Moreover, Figure 4 shows that the calibration curve is well-fitted.

Discussion

A series of variables, such as age, BMI, and educational background, were included in this study. It was finally found through logistics regression analysis and other related analysis methods that age, area, education background, marriage, waist, stroke, body pain, depression, and region may be closely related to female sarcopenia patients. In this study, these sarcopenia-related variables were integrated into a composite indicator, and ROC analysis was used to evaluate the efficacy of this composite indicator in predicting female sarcopenia patients. The results of the ROC analysis showed that the AUC of this composite index was 0.738, which was effective in evaluating sarcopenia. In addition, this study created a nomogram of the risks associated with sarcopenia to help clinicians better screen women with sarcopenia.

Long-term living environment is also closely related to the prevalence of sarcopenia. In this study, similar to previous studies, the prevalence of sarcopenia was generally higher in rural

10.3389/fpubh.2025.1410895

TABLE 1 Comparison of clinical baseline features between the two groups.

Variables	Non-sarcopenia (n = 5,645)	Sarcopenia (n = 2,160)	P value
Age (years)	58 (52–65)	66 (59–74)	<0.001
Waist (cm)	86.0 (79.0–92.6)	86.6 (79.0–94.6)	0.003
BMI (kg/m^2)	24.20 (21.93–26.61)	23.71 (21.13–26.57)	<0.001
Sleep duration over the past month (hours)	6.0 (5.0–8.0)	6.0 (4.5–8.0)	<0.001
Education, *n* (%)			<0.001
No formal education	4672 (82.8)	1902 (88.1)	
Elementary school	276 (11.3)	184 (8.5)	
Middle school	193 (3.4)	46 (2.1)	
High school or higher	232 (4.1)	28 (1.3)	
Smoking history, *n* (%)			<0.001
Never smoked	5,232 (92.6)	1,894 (87.7)	
Have smoked	419 (7.4)	267 (12.3)	
Frequency of drinking in the past year, *n* (%)			0.069
No drinking	4,762 (84.3)	1,863 (86.1)	
Drink but less than once a month	423 (7.5)	120 (5.5)	
Drink more than once a month	467 (8.3)	181 (8.4)	
Region, *n* (%)			<0.001
Northeast	431 (7.6)	183 (8.5)	
East	1,840 (32.6)	660 (30.6)	
North	634 (11.2)	317 (14.7)	
Central	915 (16.2)	273 (12.6)	
South	494 (8.8)	139 (6.4)	
Southwest	966 (17.1)	352 (16.3)	
Northwest	365 (6.5)	236 (10.9)	
Area, *n* (%)			<0.001
Urban	1,372 (24.3)	397 (18.4)	
Rural	4,273 (75.7)	1,763 (81.6)	
Marriage, *n* (%)			<0.001
Unmarried	611 (10.8)	542 (25.1)	
Married	5,034 (89.2)	1,618 (74.9)	
Depression, *n* (%)	2,415 (42.8)	1,095 (50.7)	<0.001
Hypertension, *n* (%)	2,067 (36.6)	1,066 (49.4)	<0.001
Dyslipidemia, *n* (%)	498 (8.8)	233 (10.8)	0.008
Diabetes or high blood sugar, *n* (%)	298 (5.3)	167 (7.7)	<0.001
Cancer, *n* (%)	71 (1.3)	35 (1.6)	0.217
Chronic lung diseases, *n* (%)	408 (7.2)	251 (11.6)	<0.001
Liver disease, *n* (%)	203 (3.6)	83 (3.8)	0.607
Heart disease, *n* (%)	614 (10.9)	365 (16.9)	<0.001
Stroke, *n* (%)	68 (1.2)	66 (3.1)	<0.001
Kidney disease, *n* (%)	303 (5.4)	151 (7.0)	0.006
Digestive disease, *n* (%)	1,322 (23.4)	618 (28.6)	<0.001

(Continued)

TABLE 1 (Continued)

Variables	Non-sarcopenia (n = 5,645)	Sarcopenia (n = 2,160)	P value
Emotional problems, n (%)	65 (1.2)	43 (2.0)	0.005
Memory-related disease, n (%)	51 (0.9)	39 (1.8)	0.001
Arthritis or rheumatism, n (%)	1,883 (33.3)	949 (43.9)	<0.001
Asthma, n (%)	140 (2.5)	100 (4.6)	<0.001
Body pain, n (%)	1,834 (32.5)	1,023 (47.4)	<0.001

BMI, body mass index.

TABLE 2 Logistic regression analysis of female sarcopenia related factors.

Variables	P	OR	95% CI
Age (years)	<0.001	1.079	1.072–1.086
Area	<0.001	1.514	1.317–1.740
Education	0.039	0.903	0.820–0.995
Marriage	<0.001	0.759	0.654–0.881
Waist	0.026	1.005	1.001–1.009
Stroke	0.002	1.773	1.225–2.566
Body pain	<0.001	1.634	1.4456–1.834
Depression	0.040	1.127	1.006–1.262
Region	<0.001		
East	0.001	0.651	0.502–0.845
North	<0.001	0.472	0.384–0.579
Central	0.015	0.752	0.597–0.947
South	<0.001	0.407	0.323–0.513
Southwest	<0.001	0.338	0.258–0.444
Northwest	<0.001	0.447	0.357–0.559

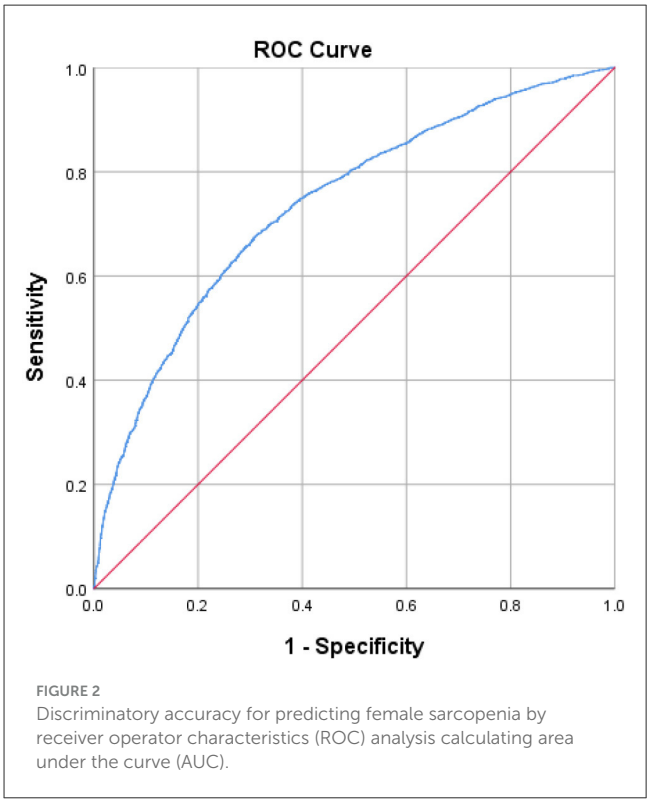

FIGURE 2
Discriminatory accuracy for predicting female sarcopenia by receiver operator characteristics (ROC) analysis calculating area under the curve (AUC).

areas than in urban areas (13). The prevalence of sarcopenia is generally higher in rural areas, possibly due to a series of reasons such as poor environment and lower education level in rural areas. In China, seven regions are divided according to economic and geographical characteristics, including Northeast, North, East, Central, South, Southwest, and Northwest. Various factors, including environmental factors, genetic background, and medical resources, may influence the differences in the prevalence of sarcopenia between different regions. In this study, sarcopenia patients were mainly found in southern China. As the most economically active region in China, the southern region has attracted many people to migrate and settle here. Sarcopenia is a genetic disorder that is passed on through genetic mutations. Due to the large population in the southern region, the susceptibility to genetic mutations is relatively high, which may partly explain the results of this study.

Numerous risk factors were linked to sarcopenia in recent research. Zhang et al. found that imbalances in protein metabolism (protein degradation over protein synthesis), which lead to severe reductions in muscle strength and motor capacity, are associated with regulation of the ubiquitin-proteasome system, oxidation reactions, and autophagy, as well as potential novel mechanisms, including altered miRNA profiles and gut microbiota (14). At the same time, sarcopenia is closely related to glucose metabolism, and studies have found that sarcopenia is related to hypoglycemia treatment in skeletal muscle, Inflammation, insulin resistance, and impaired intramuscular blood flow regulation significantly affect how skeletal muscles process glucose (15). Aging, type 2 diabetes, and obesity are all associated with changes in the metabolism of fatty acids (FAs); lipid buildup inside muscle cells is a major cause of muscle insulin resistance and ceramide formation. One of the main indicators of sarcopenia is muscular fat infiltration (16). In addition, gynecological cancer patients are at risk of sarcopenia, Cancer-related malnutrition has a complicated etiology that includes metabolic abnormalities, such as lipolysis and proteolysis, and a systemic pro-inflammatory state of malignancy (17, 18).

The relationship between age and sarcopenia is a complex one. Sarcopenia is commonly associated with aging and is often seen in older adults (19). As we age, several physiological

changes contribute to the development of sarcopenia. These include hormonal changes, decreased physical activity, inadequate nutrition, and chronic inflammation (20, 21). These factors can lead to a progressive loss of muscle mass, strength, and function. Similar to the above study, age is also an essential factor in female sarcopenia patients in this study.

While age is a significant risk factor for developing sarcopenia, it is not the sole determinant. Lifestyle factors such as physical activity level, dietary habits, and overall health also play a role (22). This study found that female sarcopenia patients were generally less educated and unmarried. Highly educated people and married people tend to devote their spare time to exercise and nutrition intake to maintain a healthy state, which prevents the occurrence of sarcopenia to a certain extent (23, 24). In addition, similar to the findings of Sousa-Santos et al. (25), this study found that marriage and high education were negatively correlated with the occurrence of sarcopenia.

In this study, the waist of female patients with sarcopenia was significantly higher than that of non-sarcopenia patients. Waist circumference is frequently utilized as an indicator of abdominal obesity. There is growing evidence of a link between sarcopenia and abdominal obesity (26, 27). The findings of Kim et al. (28) also support the conclusion of this study that obesity is significantly related to the occurrence of sarcopenia. There are a few mechanisms through which abdominal obesity may contribute to sarcopenia. Chronic inflammation and insulin resistance, often in people with abdominal obesity, can negatively affect muscle protein synthesis and promote muscle breakdown (26). Additionally, adipose tissue produces various substances called adipokines that can harm muscle function and metabolism (29).

As an aging, degenerative disease, sarcopenia is closely related to many chronic diseases, such as depression, stroke, and body

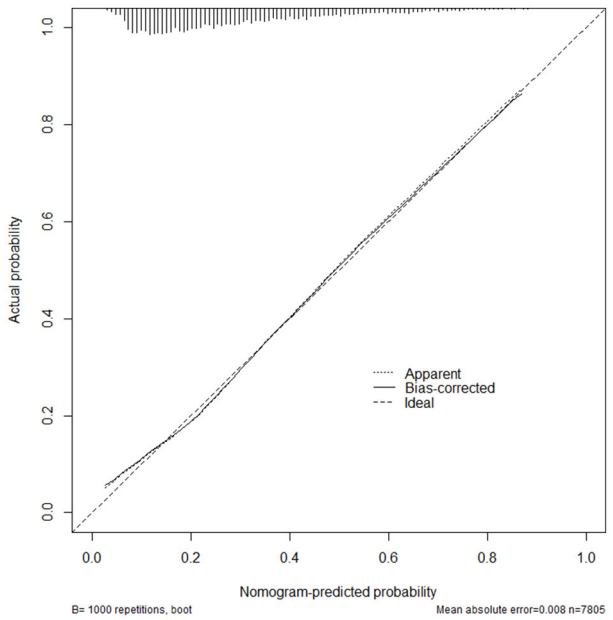

FIGURE 4
Calibration curve for nomogram prediction of female sarcopenia.

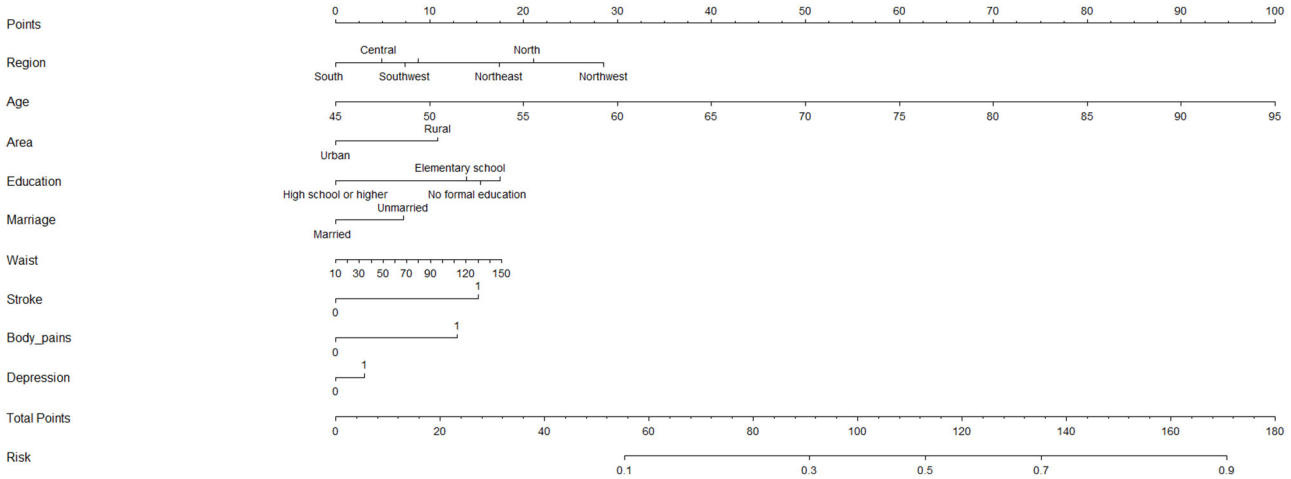

FIGURE 3
A nomogram was established to predict the female sarcopenia. Identify the individual characteristics: For each characteristic (e.g., Region, Age, Area, etc.), locate the corresponding value for the individual. Draw a vertical line from the value to the "Points" scale at the top to determine the score for that characteristic. Calculate the total score: Add up all the points from the individual characteristics to calculate the "Total Points." Estimate the risk: Match the total score to the "Risk" scale at the bottom of the chart to obtain the estimated probability of the risk. Variable Descriptions: Region: The geographic region where the individual resides (South, Southwest, Northeast, Northwest, or Central). Age: The individual's age, ranging from 45 to 95 years. Area: Indicates whether the individual lives in an urban or rural area. Education: The highest level of education attained: High school or higher; Elementary school; No formal education; Marriage: Whether the individual is married or unmarried. Waist: Waist circumference in centimeters, ranging from 10 to 150. Stroke: Indicates whether the individual has a history of stroke (0 = No, 1 = Yes). Body_pains: Indicates whether the individual experiences body pains (0 = No, 1 = Yes). Depression: Indicates whether the individual has symptoms of depression (0 = No, 1 = Yes). Risk Scale: The risk scale at the bottom translates the total score into a probability value (ranging from 0.1 to 0.9). This value represents the likelihood of the outcome being assessed (e.g., a health condition or disease).

pain. People with depression may experience reduced physical activity, lack of motivation, and interest, which can lead to a loss of muscle mass. In addition, because people with depression may suffer from distress and distress, they may neglect or abandon proper eating and exercise habits in terms of self-care, which can also lead to further declines in muscle function and mass (30, 31). Because strokes damage the neural pathways between the brain and muscles, patients can experience muscle atrophy, decreased muscle strength, and dysfunction after a stroke. In addition, patients often require a long rehabilitation and recovery process after a stroke, which can lead to chronic inactivity and loss of physical function, further exacerbating the extent of sarcopenia (32, 33). There are some correlations between body pain and sarcopenia. Although body pain is not a direct symptom of sarcopenia, there can be an interaction between the two. Individuals with sarcopenia often encounter a decline in muscle mass and strength, which can result in abnormal loads and imbalances in the body. Consequently, this can provoke muscle and joint pain. However, pain can lead to movement restrictions that prevent the muscles from being adequately stimulated and used. This lack of movement and activity may promote muscle atrophy and decreased function, worsening sarcopenia (34, 35).

However, there are several limitations to this study. First of all, this study is a cross-sectional study, so there are difficult to control confounding factors, recall bias, and other limitations. Second, due to the significant absence of certain sarcopenia-related variables, such as participants' daily activity levels, this study did not include them. Finally, due to the absence of some biomarker data in the 2018 CHARLS data, the 2015 CHARLS data were included in this study. These studies may lead to some bias in the results of this study.

Conclusion

This study found that sarcopenia in Chinese women may be closely related to age, waist, education, marriage, area, stroke, physical pain, depression, and region. In addition, this study constructs a nomogram to help clinicians better screen potential female patients with sarcopenia.

Data availability statement

The datasets presented in this study can be found in online repositories. The names of the repository/repositories and accession number(s) can be found in the article/supplementary material.

Ethics statement

The studies involving humans were approved by Biomedical Ethics Committee of Peking University. The studies were conducted in accordance with the local legislation and institutional requirements. The participants provided their written informed consent to participate in this study. The animal study was approved by Biomedical Ethics Committee of Peking University. The study was conducted in accordance with the local legislation and institutional requirements. Written informed consent was obtained from the individual(s) for the publication of any potentially identifiable images or data included in this article.

Author contributions

JY: Conceptualization, Data curation, Formal analysis, Funding acquisition, Investigation, Methodology, Project administration, Resources, Software, Supervision, Validation, Visualization, Writing – original draft, Writing – review & editing. ZC: Conceptualization, Data curation, Formal analysis, Funding acquisition, Investigation, Methodology, Project administration, Resources, Software, Supervision, Validation, Visualization, Writing – original draft, Writing – review & editing. XD: Conceptualization, Data curation, Formal analysis, Funding acquisition, Investigation, Methodology, Project administration, Resources, Software, Supervision, Validation, Visualization, Writing – original draft, Writing – review & editing. LJ: Conceptualization, Data curation, Formal analysis, Funding acquisition, Investigation, Methodology, Project administration, Resources, Software, Supervision, Validation, Visualization, Writing – original draft, Writing – review & editing. LD: Conceptualization, Data curation, Formal analysis, Funding acquisition, Investigation, Methodology, Project administration, Resources, Software, Supervision, Validation, Visualization, Writing – original draft, Writing – review & editing. YZ: Conceptualization, Data curation, Formal analysis, Funding acquisition, Investigation, Methodology, Project administration, Resources, Software, Supervision, Validation, Visualization, Writing – original draft, Writing – review & editing.

Funding

The author(s) declare that no financial support was received for the research, authorship, and/or publication of this article.

Acknowledgments

We want to express our sincere gratitude to the CHARLS research and field team and to every respondent who participated in this study for their invaluable contributions.

Conflict of interest

The authors declare that the research was conducted in the absence of any commercial or financial relationships that could be construed as a potential conflict of interest.

Publisher's note

All claims expressed in this article are solely those of the authors and do not necessarily represent those of their affiliated

organizations, or those of the publisher, the editors and the reviewers. Any product that may be evaluated in this article, or claim that may be made by its manufacturer, is not guaranteed or endorsed by the publisher.

References

1. Cruz-Jentoft AJ, Bahat G, Bauer J, Boirie Y, Bruyère O, Cederholm T, et al. Sarcopenia: revised European consensus on definition and diagnosis. *Age Ageing.* (2019) 48:16–31. doi: 10.1093/ageing/afz046

2. Wilkinson DJ, Piasecki M, Atherton PJ. The age-related loss of skeletal muscle mass and function: measurement and physiology of muscle fibre atrophy and muscle fibre loss in humans. *Ageing Res Rev.* (2018) 47:123–32. doi: 10.1016/j.arr.2018.07.005

3. Yuan S, Larsson SC. Epidemiology of sarcopenia: prevalence, risk factors, and consequences. *Metabolism.* (2023) 144:155533. doi: 10.1016/j.metabol.2023.155533

4. Inoue T, Maeda K, Nagano A, Shimizu A, Ueshima J, Murotani K, et al. Undernutrition, sarcopenia, and frailty in fragility hip fracture: advanced strategies for improving clinical outcomes. *Nutrients.* (2020) 12:23743. doi: 10.3390/nu12123743

5. Huang CB, Hu JS, Tan K, Zhang W, Xu TH, Yang L. Application of machine learning model to predict osteoporosis based on abdominal computed tomography images of the psoas muscle: a retrospective study. *BMC Geriatr.* (2022) 22:796. doi: 10.1186/s12877-022-03502-9

6. Petermann-Rocha F, Chen M, Gray SR, Ho FK, Pell JP, Celis-Morales C. Factors associated with sarcopenia: a cross-sectional analysis using UK Biobank. *Maturitas.* (2020) 133:60–7. doi: 10.1016/j.maturitas.2020.01.004

7. Bahat G, Turkmen BO, Aliyev S, Catikkas NM, Bakir B, Karan MA. Cut-off values of skeletal muscle index and psoas muscle index at L3 vertebra level by computerized tomography to assess low muscle mass. *Clin Nutr.* (2021) 40:4360–5. doi: 10.1016/j.clnu.2021.01.010

8. Geraci A, Calvani R, Ferri E, Marzetti E, Arosio B, Cesari M. Sarcopenia and menopause: the role of estradiol. *Front Endocrinol (Lausanne).* (2021) 12:682012. doi: 10.3389/fendo.2021.682012

9. Fyfe JJ, Hamilton DL, Daly RM. Minimal-dose resistance training for improving muscle mass, strength, and function: a narrative review of current evidence and practical considerations. *Sports Med.* (2022) 52:463–79. doi: 10.1007/s40279-021-01605-8

10. Zhao Y, Hu Y, Smith JP, Strauss J, Yang G. Cohort profile: the China health and retirement longitudinal study (CHARLS). *Int J Epidemiol.* (2014) 43:61–8. doi: 10.1093/ije/dys203

11. Demirchyan A, Petrosyan V, Thompson ME. Psychometric value of the Center for Epidemiologic Studies Depression (CES-D) scale for screening of depressive symptoms in Armenian population. *J Affect Disord.* (2011) 133:489–98. doi: 10.1016/j.jad.2011.04.042

12. Chen L-K, Woo J, Assantachai P, Auyeung T-W, Chou M-Y, Iijima K, et al. Asian working group for sarcopenia: 2019 consensus update on sarcopenia diagnosis and treatment. *J Am Med Direct Assoc.* (2020) 21:300–7.e302. doi: 10.1016/j.jamda.2019.12.012

13. Moon SW, Kim KJ, Lee HS, Yun YM, Kim JE, Chun YJ, et al. Low muscle mass, low muscle function, and sarcopenia in the urban and rural elderly. *Sci Rep.* (2022) 12:14314. doi: 10.1038/s41598-022-18167-y

14. Zhang J, Yu Y, Wang J. Protein nutritional support: the classical and potential new mechanisms in the prevention and therapy of sarcopenia. *J Agric Food Chem.* (2020) 68:4098–108. doi: 10.1021/acs.jafc.0c00688

15. Lisco G, Disoteo OE, De Tullio A, De Geronimo V, Giagulli VA, Monzani F, et al. Sarcopenia and diabetes: a detrimental liaison of advancing age. *Nutrients.* (2023) 16:10063. doi: 10.3390/nu16010063

16. Al Saedi A, Debruin DA, Hayes A, Hamrick M. Lipid metabolism in sarcopenia. *Bone.* (2022) 164:116539. doi: 10.1016/j.bone.2022.116539

17. Morton M, Patterson J, Sciuva J, Perni J, Backes F, Nagel C, et al. Malnutrition, sarcopenia, and cancer cachexia in gynecologic cancer. *Gynecol Oncol.* (2023) 175:142–55. doi: 10.1016/j.ygyno.2023.06.015

18. Zhang FM, Wu HF, Shi HP Yu Z, Zhuang CL. Sarcopenia and malignancies: epidemiology, clinical classification and implications. *Ageing Res Rev.* (2023) 91:102057. doi: 10.1016/j.arr.2023.102057

19. Cruz-Jentoft AJ, Sayer AA. Sarcopenia. *Lancet.* (2019) 393:2636–46. doi: 10.1016/S0140-6736(19)31138-9

20. Livshits G, Kalinkovich A, A. cross-talk between sestrins, chronic inflammation and cellular senescence governs the development of age-associated sarcopenia and obesity. *Ageing Res Rev.* (2023) 86:101852. doi: 10.1016/j.arr.2023.101852

21. Gungor O, Ulu S, Hasbal NB, Anker SD, Kalantar-Zadeh K. Effects of hormonal changes on sarcopenia in chronic kidney disease: where are we now and what can we do? *J Cachexia Sarcopenia Muscle.* (2021) 12:1380–92. doi: 10.1002/jcsm.12839

22. Papadopoulou SK, Papadimitriou K, Voulgaridou G, Georgaki E, Tsotidou E, Zantidou O, Papandreou D. Exercise and nutrition impact on osteoporosis and sarcopenia-the incidence of osteosarcopenia: a narrative review. *Nutrients.* (2021) 13:4499. doi: 10.3390/nu13124499

23. Saadeh M, Prinelli F, Vetrano DL, Xu W, Welmer AK, Dekhtyar S, et al. Mobility and muscle strength trajectories in old age: the beneficial effect of Mediterranean diet in combination with physical activity and social support. *Int J Behav Nutr Phys Act.* (2021) 18:120. doi: 10.1186/s12966-021-01192-x

24. Chang BK. Differences in self-rated health and physical activity due to education level among Koreans: understanding implications of physical education. *Iran J Public Health.* (2021) 50:1983–992. doi: 10.18502/ijph.v50i10.7498

25. Sousa-Santos AR, Afonso C, Borges N, Santos A, Padrão P, Moreira P. T FA. Sarcopenia, physical frailty, undernutrition and obesity cooccurrence among Portuguese community-dwelling older adults: results from Nutrition UP 65 cross-sectional study. *BMJ Open.* (2020) 10:e033661. doi: 10.1136/bmjopen-2019-033661

26. Li CW Yu K, Shyh-Chang N, Jiang Z, Liu T, Ma S, et al. Pathogenesis of sarcopenia and the relationship with fat mass: descriptive review. *J Cachexia Sarcopenia Muscle.* (2022) 13:781–94. doi: 10.1002/jcsm.12901

27. Bosello O, Vanzo A. Obesity paradox and aging. *Eat Weight Disord.* (2021) 26:27–35. doi: 10.1007/s40519-019-00815-4

28. Kim SH, Jeong JB, Kang J, Ahn DW, Kim JW, Kim BG, et al. Association between sarcopenia level and metabolic syndrome. *PLoS ONE.* (2021) 16:e0248856. doi: 10.1371/journal.pone.0248856

29. Gonzalez-Gil AM, Elizondo-Montemayor L. The role of exercise in the interplay between myokines, hepatokines, osteokines, adipokines, and modulation of inflammation for energy substrate redistribution and fat mass loss: a review. *Nutrients.* (2020) 12:1899. doi: 10.3390/nu12061899

30. Li Z, Tong X, Ma Y, Bao T, Yue J. Prevalence of depression in patients with sarcopenia and correlation between the two diseases: systematic review and meta-analysis. *J Cachexia Sarcopenia Muscle.* (2022) 13:128–44. doi: 10.1002/jcsm.12908

31. Brooks JM, Titus AJ, Bruce ML, Orzechowski NM, Mackenzie TA, Bartels SJ, et al. Depression and handgrip strength among U.S. adults aged 60 years and older from NHANES 2011-2014. *J Nutr Health Aging.* (2018) 22:938–43. doi: 10.1007/s12603-018-1041-5

32. Su Y, Yuki M, Otsuki M. Prevalence of stroke-related sarcopenia: A systematic review and meta-analysis. *J Stroke Cerebrovasc Dis.* (2020) 29:105092. doi: 10.1016/j.jstrokecerebrovasdis.2020.105092

33. Li W, Yue T, Liu Y. New understanding of the pathogenesis and treatment of stroke-related sarcopenia. *Biomed Pharmacother.* (2020) 131:110721. doi: 10.1016/j.biopha.2020.110721

34. Lin T, Dai M, Xu P, Sun L, Shu X, Xia X, Zhao Y, Song Q, Guo D, Deng C, Yue J. Prevalence of sarcopenia in pain patients and correlation between the two conditions: a systematic review and meta-analysis. *J Am Med Dir Assoc.* (2022) 23:902.e901–2.e920. doi: 10.1016/j.jamda.2022.02.005

35. Kim HI, Ahn SH, Kim Y, Lee JE, Choi E, Seo SK. Effects of sarcopenia and sarcopenic obesity on joint pain and degenerative osteoarthritis in postmenopausal women. *Sci Rep.* (2022) 12:13543. doi: 10.1038/s41598-022-17451-1

frontiers | Frontiers in Public Health

TYPE Original Research
PUBLISHED 03 April 2025
DOI 10.3389/fpubh.2025.1521736

OPEN ACCESS

EDITED BY
Kunihiro Tsuchida,
Fujita Health University, Japan

REVIEWED BY
Natalia Sharashkina,
Pirogov Russian National Research Medical University, Russia
Mario Salazar-Paramo,
University of Guadalajara, Mexico

*CORRESPONDENCE
Haiyan Wang
✉ 430140465@qq.com

RECEIVED 02 November 2024
ACCEPTED 24 March 2025
PUBLISHED 03 April 2025

CITATION
Qiao M, Wang H, Qin M, Xing T and Li Y (2025) Development and validation of a predictive model for the risk of possible sarcopenia in middle-aged and older adult diabetes mellitus in China.
Front. Public Health 13:1521736.
doi: 10.3389/fpubh.2025.1521736

Development and validation of a predictive model for the risk of possible sarcopenia in middle-aged and older adult diabetes mellitus in China

Mengyuan Qiao[1], Haiyan Wang[2]*, Mengzhen Qin[2], Taohong Xing[3] and Yingyang Li[4]

[1]School of Nursing, Henan University of Science and Technology, Luoyang, China, [2]Xinjiang Emergency Center, People's Hospital of Xinjiang Uygur Autonomous Region, Ürümqi, China, [3]Endoscopy Centre, The First Affiliated Hospital of Henan University of Science and Technology, Luoyang, China, [4]Department of Critical Care Surgery, The First Affiliated Hospital of Henan University of Science and Technology, Luoyang, China

Background: People with diabetes mellitus (DM) have a significantly increased risk of sarcopenia. A cross-sectional analysis was performed using nationally representative data to evaluate possible sarcopenia in middle-aged and older adults with diabetes mellitus, and to develop and validate a prediction model suitable for possible sarcopenia in middle-aged and older adults with diabetes mellitus in the Chinese community.

Methods: Data from the China Health and Retirement Longitudinal Study (CHARLS), which focuses on people 45 years of age or older, served as the basis for the prediction model. CHARLS 2015 participants were used in the study, which examined 53 factors. In order to guarantee model reliability, the study participants were split into two groups at random: 70% for training and 30% for validation. Ten-fold cross-validation and Least Absolute Shrinkage and Selection Operator (LASSO) regression analyses were used to determine the best predictors for the model. The factors associated with sarcopenia in DM were researched using logistic regression models. Nomogram were constructed to develop the predictive model. The performance of the model was assessed using area under the curve (*AUC*), calibration curves and decision curve analysis (*DCA*).

Results: A total of 2,131 participants from the CHARLS database collected in 2015 passed the final analysis, and the prevalence of sarcopenia was 28.9% (616/2131). Eight factors were subsequently chosen as predictive models by LASSO logistic regression: age, residence, body mass index, diastolic blood pressure, cognitive function, activities of daily living, peak expiratory flow and hemoglobin. These factors were used in the nomogram predictive model, which showed good accuracy and agreement. The *AUC* values for the training and validation sets were 0.867 (95%CI: 0.847~0.887) and 0.849 (95%CI: 0.816~0.883). Calibration curves and DCA indicated that the nomogram model exhibited good predictive performance.

Conclusion: The nomogram predictive model constructed in this study can be used to evaluate the probability of sarcopenia in middle-aged and older adult DM, which is helpful for early identification and intervention of high-risk groups.

KEYWORDS

diabetes mellitus, middle-aged and older adults, sarcopenia, prediction model, nomogram

1 Introduction

Diabetes mellitus (DM) is a metabolic disease that is hyperglycemia caused by defective insulin secretion or action. The prevalence of DM is high, with one in eleven people worldwide currently diagnosed with DM (1). According to the statistics of the International Diabetes Federation (IDF), as of 2021, the global DM patients have reached 537 million cases, of which 6.3 million died of DM, and it is expected that by 2045, the global DM patients will reach nearly 784 million, of which China leads the world in diabetes cases with 140 million diabetics in 2021 and has the fastest growing diabetes incidence in the world (2). Notably, the prevalence is highest in the middle-aged and older adult population (3). With the progression of DM, a series of complications occur when the function of organs such as kidneys, blood vessels, nervous system and eyes of the body are affected (1). In recent years, sarcopenia has been recognized as the third type of complication in diabetic patients, presenting a reversible character (4).

The European Working Group on Sarcopenia (EWGSOP) was the first to publish a consensus on sarcopenia, defining sarcopenia as a geriatric syndrome with loss of muscle mass, loss of muscle strength and/or reduced somatic function associated with ageing (5). It has been reported that the number of patients with muscle wasting disorders will reach 200 million worldwide in 2050 (6). As muscle mass declines, it increases the risk of falls, disability, re-hospitalisation and death in patients, leading to an increase in adverse clinical events and placing a significant strain and economic burden on healthcare systems and society (7).

DM and sarcopenia are mutually reinforcing, they share common risk factors and age-related trends (5). Therapeutic strategies for DM limit energy intake, accelerating the loss of muscle strength and muscle mass in patients, further increasing the incidence of sarcopenia (8). The risk of sarcopenia in diabetic mellitus patients is 1.5–3 times higher than that in the non-diabetic people (9, 10). Significantly, patients with sarcopenia also exacerbate glucose metabolism disorders due to their decreased muscle mass and function (11), and the two disorders contribute to each other.

The prevalence and related variables of sarcopenia in older persons are currently the subject of increased research, whereas fewer studies have developed risk prediction models for the risk of sarcopenia in DM. A predictive model for sarcopenia in the Chinese older adult population has been developed by based on the CHARLS database (12), but the study was conducted only in the older adult, and was not applicable to the specific population of middle-aged and older adult DM. To improve the prognosis of the DM population, it is crucial to construct a predictive model appropriate for the risk of sarcopenia in middle-aged and older DM patients.

2 Methods

2.1 Study participants

The data used for this article were obtained from the CHARLS investigators and are publicly available at http://charls.pku.edu.cn. The CHARLS is an ongoing longitudinal survey that provides high-quality microdata on households and individuals aged 45 years and older in China With the aim of analyzing population ageing issues and promoting interdisciplinary research on ageing. The project received approval from the Biomedical Ethics Committee (IRB00001052-11015) of Peking University in Beijing, China, and our study strictly adhered to the principles outlined in the Declaration of Helsinki; informed consent was obtained from all participants. For this study, we used data from the 2015 CHARLS to extract demographic background, general health status, disease history, and biochemical parameters. The inclusion criteria were as follows: (a) age $\geq$ 45 years; (b) having diabetes mellitus; (c) answering the questions about sarcopenia. Data missing by more than 20% were excluded. Finally, a total of 2,131 respondents participated in the study. The data filtering process is shown in Figure 1.

2.2 Assessment of diabetes

During blood collection for the CHARLS data, we asked participants to fast the night before. Blood collection was performed by medical professionals. If participants were unable to meet the fasting requirement, blood samples were still collected and blood glucose values were analyzed as higher random plasma glucose (RPG). Participants with incident DM were identified based on the following criteria (13): previously diagnosed with diabetes; higher hemoglobin A1c (HbA1c) level ($\geq$6.5%); higher fasting plasma glucose (FPG) level ($\geq$126 mg/dL); and/or RPG level ($\geq$200 mg/dL).

2.3 Assessment of sarcopenia

In this study, we adopted the Asian Working Group for Sarcopenia (AWGS) 2019 standard to define and evaluate sarcopenia using three indexes: muscle strength, physical function and appendicular skeletal muscle mass (ASM) (14), specific assessment of sarcopenia can be found in Supplementary material.

2.3.1 Muscle strength

Muscle strength was measured using a grip strength meter, and values below 28 kg for males and below 18 kg for females indicate decreased muscle strength.

2.3.2 Physical function

Physical function included the gait speed, the five-time chair stand test, and the short physical performance battery (SPPB). The total score of SPPB was 12 points with 4 points for each test. According to the AWGS 2019 recommendations, low physical performance was defined as 6-m walking speed <1 m/s or 5-times chair stand test time $\geq$ 12 s, or SPPB score $\leq$ 9 points.

2.3.3 Appendicular skeletal mass (ASM)

In our article, we used an anthropometric equation to estimate the muscle mass, which has previously been validated in Chinese individuals, and the ASM equation model showed a high level of agreement with DXA (15, 16).

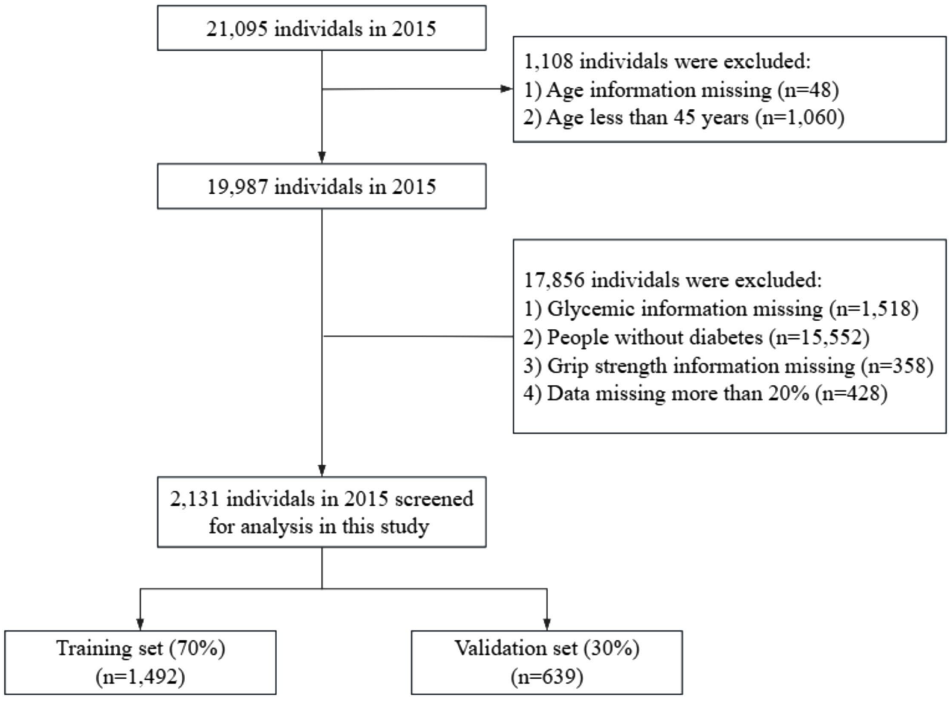

FIGURE 1
Flowchart of the study.

$$\mathrm{ASM} = 0.193 \times \mathrm{weight}\,(\mathrm{kg}) + 0.107 \times \mathrm{height}\,(\mathrm{cm}) - 4.157 \times \mathrm{gender}\,(\mathrm{male} = 1, \mathrm{female} = 2) - 0.037 \times \mathrm{age} - 2.631$$

Height-adjusted muscle mass was calculated as ASM/Ht^2 = ASM/height (m)^2. The cut-off point for low muscle mass was based on the lowest 20% percentile of ASM/Ht^2 in the study population. Since our data are derived from the 2015 CHARLS data, we refer to the criteria of Wu et al. (17). Therefore, the ASM/Ht^2 cut-off for female was <5.08 kg/m^2, and the ASM/Ht^2 cut-off for male was <6.88 kg/m^2.

2.4 Predictors

2.4.1 Demographic characteristics

Demographic characteristics include age, body mass index, sex, marital status, residence, education, pension insurance, and health insurance.

2.4.2 Vital signs

Vital signs including temperature, pulse, respiratory rate, systolic blood pressure (SBP) and diastolic blood pressure (DBP) at the first records after admission.

2.4.3 Health status and behavior

Health status and behaviors include smoking, drinking, history of disease (chronic disease, hypertension, cancer, lung disease, heart disease, stroke, arthritis, dyslipidaemia, liver disease, kidney disease, stomach disease, asthma), fall down, sleep duration, myopia, hyperopia, hearing, self-reported health status, peak expiratory flow (PEF), activities of daily living (ADL) and social participation.

(1) The CHARLS assesses the respondents' ability to perform activities of daily living using the Basic Activities of Daily Living (BADL) and Instrumental Activities of Daily Living (IADL), with six items selected for the BADL: dressing, bathing, eating, getting in and out of bed, going to the toilet, and controlling urine and faeces; and six items for the IADL: doing household chores, cooking, shopping on one's own, making a phone call, taking medication, and controlling money. In both BADL and IADL, completing all 6 items without difficulty was considered to be functionally intact, and completing any one of them without difficulty was defined as functionally impaired (18, 19).

(2) The data on participation in social activities were obtained from the CHARLS questionnaire, 'Did you do any of the following activities in the past month (multiple answers allowed)', with the following answers: (a)visiting the home, socializing with friends; (b) playing mahjong, chess, cards, going to the community room; (c) providing help to your relatives, friends or neighbors who do not live with you, without any compensation, friends or neighbors; (d) going to parks or other places to dance, work out, practice qigong; (e) taking part in community organizations; (f) volunteering or charitable activities; (g) taking care of sick people or people with disabilities you do not live with free of charge; (h) going to school or attending training courses; (i) speculating on stocks (funds and other financial securities); (j) surfing the internet; (k) others; (l) none of the above. For the above 12

options, if you choose any one of (a) to (l), you are considered to have participated in activities, and it is marked as '1', while if you choose (l), you are considered to have not participated in social activities, and it is marked as '0' (20, 21).

2.4.4 Mental health parameters

Mental health parameters included self-reported depression and cognitive function.

(1) Depression was assessed by the 10-item score of the Centre for Epidemiological Studies Depression Scale (CESD-10) from the CHARLS data. It was divided into 4 levels according to scores of 0, 1, 2, and 3, and the 10-item scores ranged from 0–30, with >10 defined as having a tendency to be depressed (22, 23).
(2) Measurement of cognitive function included two dimensions, situational memory and mental state, with overall cognitive function scores ranging from 0 to 21, with higher scores indicating better cognitive function. (a) Situational memory: a total score of 10 points, divided into instantaneous memory and delayed recall. Instantaneous memory was measured by asking the respondents to immediately recall the 10 words just read to them by the investigator; delayed recall required the respondents to recall the same 10 words again after 4 to 10 min. One point was awarded for each correctly recalled word, and the average of the two tests was taken as the total situational memory score. (b) Mental state: The total score is 11 points, divided into time orientation, calculation ability and drawing ability. Time orientation requires respondents to answer the day of the year, month, day, season and day of the week, answer 1 correctly scored 1 point, a total of 5 points. Computing ability requires respondents to carry out five calculations (answer 100 minus 7 equals how much, the answer to the value of the value of the answer and then subtracted from the 7, repeat 4 times), if the respondent calculations are wrong, but the results of the next calculation is equal to the last error value minus 7, can still be scored one point, a total of five points. Drawing ability requires respondents were asked to draw a picture of two overlapping pentagrams displayed by the investigator, and one point was awarded to those who drew the picture (24).

2.4.5 Biochemical parameters

After the home interview, 8 mL of fasting venous blood was collected by professional staff and the samples were sent to the laboratory of the Chinese Center for Disease Control and Prevention (CDC) in Beijing, China, where they were stored at −80°C. Hemoglobin (Hb), white blood cell (WBC), c-reactive protein (CRP), Hematocrit (HCT), mean corpuscular volume (MCV), Platelets (PLT), total cholesterol (TC), triglyceride (TG), high-density lipoprotein cholesterol (HDL-c), low-density lipoprotein cholesterol (LDL-c), Blood Urea Nitrogen (BUN), Creatinine, Uric acid and Cystatin C were collected by a professional staff.

2.5 Statistical analyses

Statistical analyses were performed using R 4.3.0. The CHARLS data were randomly divided into a training set and an internal validation set in a ratio of 7:3.

(1) Statistical description: quantitative data conforming to normal distribution were expressed as means ± standard deviations, and the *t*-test was used for inter-group comparisons. Non-normally distributed data were expressed as medians and tertile range, and the rank sum test was used for inter-group comparisons.
(2) Predictor variable screening: model over-fitting was prevented by LASSO regression, penalties on coefficients prevented the problem of covariance, and logistic regression was subsequently performed to determine the independent risk factors for sarcopenia in middle-aged and older adult diabetic populations. All tests were two-sided, and $p < 0.05$ was considered a statistically significant difference.
(3) Nomogram predictive model construction: logistic regression was used to construct the predictive model, and the 'rms' package was used to construct the nomogram predictive model for sarcopenia.
(4) Evaluation of the model: the C_index of the sarcopenia nomogram predictive model was calculated to assess the discriminatory ability of the model, and the calibration curve of the sarcopenia predictive model was produced to determine the degree of agreement between the predicted probability and the observed results. Clinical validity was assessed by decision curve analysis (*DCA*).
(5) Model validation: *AUC*, calibration curves and *DCA* were used to validate the predictive performance of the nomogram model.

3 Results

3.1 Participants characteristics

Our study included 2,131 middle aged and older adult diabetic patients. The mean age was 63.32 ± 8.90 years, of which 1,227 (57.6%) were male and 904 (42.4%) were female. The prevalence of sarcopenia in middle-aged and older adult diabetic patients was 28.9% (616/2,131). Baseline characteristics are shown in Supplementary Table 1. Among middle-aged and older adult diabetic patients, 1,492 (70%) and 639 (30%) were randomly assigned to the training and validation sets, respectively. The results in Supplementary Table 2 show that there was no significant difference ($p > 0.05$) between the predictors of the training and validation date sets and the baselines were comparable. The baseline characteristics of the training set participants are shown in Table 1.

3.2 LASSO and logistic regression

Using whether or not sarcopenia occurred in middle-aged or older adult diabetic participants as the outcome variable, all candidate predictor variables were included in LASSO regression, and the independent variable screening and cross-validation process of LASSO regression are shown in Figures 2A,B, respectively. Non-zero coefficients were selected as potential predictors of sarcopenia. In order to ensure that the model is both efficient and concise, and considering the simplicity and operability in the process of practical clinical application, the Lambda.lse value (Lambda = 0.02787465) with the cross-validation error within the range of plus or minus one

10.3389/fpubh.2025.1521736

TABLE 1 Baseline characteristics of the training set participants.

Variables	Overall (*n* = 1,492)	No sarcopenia (*n* = 1,063)	Possible sarcopenia (*n* = 429)	*p*-value
Demographic characteristics				
Age, Median (IQR)	63.0 (57.00,69.00)	61.00 (55.00,67.00)	69.00 (62.00,75.00)	<0.001
BMI (kg/m^2)	25.03 (22.62,27.65)	25.81 (23.96,28.28)	22.08 (19.72,24.89)	<0.001
Sex (%)				<0.001
Male	650 (43.6)	512 (48.2)	138 (32.2)	
Female	842 (56.4)	551 (51.8)	291 (67.8)	
Education (%)				<0.001
Primary school or below	704 (47.2)	434 (40.8)	270 (62.7)	
Junior high school/ technical secondary school	610 (40.9)	479 (45.1)	131 (30.5)	
High school and above	178 (11.9)	150 (14.1)	28 (6.5)	
Marital status (%)				<0.001
Married	1,258 (84.3)	938 (88.2)	320 (74.6)	
Unmarried	234 (15.7)	125 (11.8)	109 (25.4)	
Residence (%)				<0.001
Urban	622 (41.7)	470 (44.8)	146 (34.0)	
Rural	870 (58.3)	587 (55.2)	283 (66.0)	
Medical insurance (%)				0.016
No	108 (7.2)	66 (6.2)	42 (9.8)	
Yes	1,384 (92.8)	997 (93.8)	387 (90.2)	
Endowment insurance (%)				0.001
No	541 (36.3)	457 (43.0)	84 (19.6)	
Yes	951 (63.7)	606 (57.0)	345 (80.4)	
Vital signs				
Temperature (°C)	36.7 (36.6, 37.0)	36.7 (36.6, 37.0)	36.6 (36.5; 37.0)	0.615
Pulse (times/min)	75.50 (68.00,83.00)	75.00 (67.50,82.50)	76.50 (69.00,84.50)	0.014
Respiratory rate (times/min)	20.0 (20.0, 20.0)	20.0 (20.0, 20.0)	19.0 (19.0, 20.0)	0.471
SBP (mmHg)	130.00 (118.13,145.38)	130.00 (119.50,145.50)	130.50 (114.50,145.00)	0.276
DBP (mmHg)	75.50 (68.00,83.50)	76.50 (69.00,84.00)	71.50 (65.50,80.25)	<0.001
Health status and behavior				
Smoking (%)				<0.001
No	860 (57.6)	575 (54.1)	285 (66.4)	
Yes	632 (42.4)	488 (45.9)	144 (33.6)	
Drinking (%)				0.006
No	835 (56.0)	571 (53.7)	264 (61.5)	
Yes	657 (44.0)	492 (46.3)	165 (38.5)	
Chronic diseases (%)				0.670
No	129 (8.6)	94 (8.8)	35 (8.2)	
Yes	1,363 (91.4)	969 (91.2)	394 (91.8)	
Hypertension (%)				0.673
No	684 (45.8)	491 (46.2)	193 (45.0)	
Yes	808 (54.2)	572 (53.8)	236 (55.0)	
Cancer (%)				0.743
No	1,465 (98.2)	1,043 (98.1)	422 (98.4)	
Yes	27 (1.8)	20 (1.9)	7 (1.6)	

(Continued)

10.3389/fpubh.2025.1521736

TABLE 1 (Continued)

Variables	Overall (*n* = 1,492)	No sarcopenia (*n* = 1,063)	Possible sarcopenia (*n* = 429)	*p*-value
Chronic lung disease (%)				0.001
No	1,270 (85.1)	925 (87.0)	345 (80.4)	
Yes	222 (14.9)	138 (13.0)	84 (19.6)	
Heart disease (%)				0.173
No	1,077 (72.2)	778 (73.2)	299 (69.7)	
Yes	415 (27.8)	285 (26.8)	285 (26.8)	
Stroke (%)				0.012
No	1,397 (93.6)	1,006 (94.6)	391 (91.1)	
Yes	95 (6.4)	57 (5.4)	38 (8.9)	
Arthritis (%)				<0.001
No	787 (52.7)	607 (57.1)	180 (42.0)	
Yes	705 (47.3)	456 (42.9)	249 (58.0)	
Dyslipidemia (%)				<0.001
No	930 (62.3)	617 (58.0)	313 (73.0)	
Yes	562 (37.7)	446 (42.0)	116 (27.0)	
Liver disease (%)				0.347
No	1,350 (90.5)	957 (90.0)	393 (91.6)	
Yes	142 (9.5)	106 (10.0)	36 (8.4)	
Kidney disease (%)				0.290
No	1,311 (87.9)	928 (87.3)	383 (89.3)	
Yes	181 (12.1)	135 (12.7)	46 (10.7)	
Stomach disease (%)				0.019
No	1,016 (68.1)	743 (69.9)	273 (63.6)	
Yes	476 (31.9)	320 (30.1)	156 (36.4)	
Asthma (%)				<0.001
No	1,375 (92.2)	1,003 (94.4)	372 (86.7)	
Yes	117 (7.8)	60 (5.6)	57 (13.3)	
Fall down (%)				0.002
No	1,187 (79.6)	868 (81.7)	319 (74.4)	
Yes	305 (20.4)	195 (18.3)	110 (25.6)	
Tap water (%)				0.001
No	368 (24.7)	238 (22.4)	130 (30.3)	
Yes	1,124 (75.3)	825 (77.6)	299 (69.7)	
ADL (%)				<0.001
Non-disability	938 (62.9)	727 (68.4)	211 (49.2)	
Disability	554 (37.1)	336 (31.6)	218 (50.8)	
Social participation (%)				<0.001
No	664 (44.5)	423 (39.8)	241 (56.2)	
Yes	828 (55.5)	640 (60.2)	188 (43.8)	
Hyperopia (%)				<0.001
Good	409 (27.4)	248 (23.3)	161 (37.5)	
Fair	723 (48.5)	530 (49.9)	193 (45.0)	
Poor	360 (24.1)	285 (26.8)	75 (17.5)	

(Continued)

TABLE 1 (Continued)

Variables	Overall (n = 1,492)	No sarcopenia (n = 1,063)	Possible sarcopenia (n = 429)	p-value
Myopia (%)				0.002
Good	354 (23.7)	229 (21.5)	125 (29.1)	
Fair	766 (51.3)	550 (51.7)	216 (50.3)	
Poor	372 (24.9)	284 (26.7)	88 (20.5)	
Hearing (%)				<0.001
Good	251 (16.8)	153 (14.4)	98 (22.8)	
Fair	798 (53.5)	580 (54.6)	218 (50.8)	
Poor	443 (29.7)	330 (31.0)	113 (26.3)	
Self-assessed health status (%)				<0.001
Good	507 (34.0)	321 (30.2)	186 (43.4)	
Fair	747 (50.1)	561 (52.8)	186 (43.4)	
Poor	238 (16.0)	181 (17.0)	57 (13.3)	
Sleep time (h)	6.00 (5.00,8.00)	6.00 (5.00,8.00)	6.00 (5.00,8.00)	0.297
PEF (L/min)	300.00 (220.00,380.00)	329.00 (250.00,400.00)	240.00 (170.00,310.00)	<0.001
Mental health parameters				
Depression (scores)	8.00 (4.00,13.00)	7.00 (3.00,12.00)	10.00 (5.00,16.00)	<0.001
Cognitive function (scores)	11.50 (8.50,14.00)	12.00 (9.50,14.50)	9.50 (6.50,12.35)	<0.001
Biochemical parameters				
Hb (g/dL)	13.70 (12.60,14.80)	13.90 (12.80,15.00)	13.00 (12.00,14.10)	<0.001
WBC (1,000)	6.10 (5.10,7.32)	6.13 (5.19,7.33)	5.84 (4.93,7.30)	0.021
CRP (mg/L)	2.00 (1.00,3.57)	2.10 (1.10,3.50)	1.80 (0.90,5.60)	0.084
HCT (%)	41.35 (38.00,44.60)	42.00 (38.70,45.10)	39.70 (36.45,43.25)	<0.001
MCV (fl)	91.20 (87.10,94.80)	91.20 (87.30,94.60)	91.60 (87.05,95.35)	0.289
PLT (10^9/L)	203.00 (159.00,246.00)	204.00 (162.00,246.00)	201.00 (154.00,246.00)	0.295
TC (mg/dl)	187.64 (163.03,213.13)	187.64 (162.93,212.74)	186.87 (163.32,213.32)	0.879
TG (mg/dL)	143.36 (98.23,209.73)	150.44 (104.42,221.24)	122.12 (85.84,177.88)	<0.001
HDL-c (mg/dL)	47.49 (40.93,54.83)	46.33 (40.15,53.28)	49.81 (42.66,59.46)	<0.001
LDL-c (mg/dL)	102.32 (84.17,122.78)	103.09 (84.56,122.78)	101.16 (83.01,123.55)	0.666
BUN (mg/dL)	15.13 (12.61,18.21)	15.13 (12.61,18.21)	15.13 (12.61,18.49)	0.823
Creatinine (mg/dL)	0.74 (0.63,0.89)	0.75 (0.64,0.88)	0.72 (0.63,0.90)	0.489
Uric acid (mg/dL)	4.90 (4.10,6.00)	5.00 (4.20,6.00)	4.90 (3.90,5.80)	0.025
Cystatin C (mg/L)	0.86 (0.74,0.98)	0.83 (0.72,0.95)	0.93 (0.78,1.06)	<0.001

BMI, body mass index; SBP, systolic blood pressure; DBP, diastolic blood pressure; ADL, activities of daily living; PEF, peak expiratory flow; Hb, hemoglobin; WBC, white blood cell; CRP, c-reactive protein; HCT, hematocrit; MCV, mean corpuscular volume; PLT, platelets; TC, total cholesterol; TG, triglyceride; HDL-c, high-density lipoprotein cholesterol; LDL-c, low-density lipoprotein cholesterol; BUN, blood urea nitrogen.

standard error of the minimum error was selected as the optimal penalty coefficient in our study, at which time the model contained 13 variables, including age, gender, BMI, residence, smoking, arthritis, cognitive function, depression, social participation, ADL, PEF, DBP, and Hb. These factors were then included in the logistic regression model. It was ultimately found that, Age ($p < 0.001$), Residence ($p = 0.003$), BMI ($p < 0.001$), Cognitive function ($p = 0.003$), ADL ($p < 0.001$), DBP ($p = 0.019$), Breathing ($p < 0.001$) and Hb ($p < 0.001$) were found to be associated with the development of sarcopenia in middle-aged and older adult diabetic mellitus (Table 2).

3.3 Developing predictive models

Logistic regression was used to establish the predictive model. Variance inflation factor (*VIF*) test was performed and the VIF values for all variables were in the range of 1.09 to 1.54, with *VIF* values below five. The model was well fitted with no covariance. A predictive model was presented using nomogram, which allowed for a quantitative possible predictive of sarcopenia in middle-aged and older adult diabetic patients (Figure 3). Individual scores for each predictor variable in the nomogram model ranged from 0 to 100, and total scores ranged from 420 to 600. When using the nomogram

10.3389/fpubh.2025.1521736

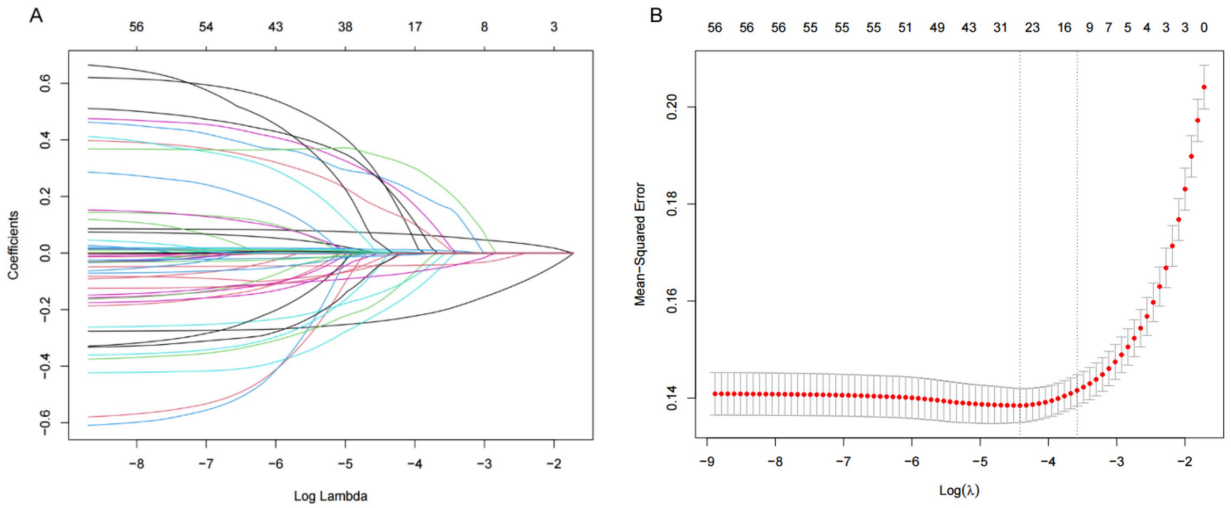

FIGURE 2
Demographic and clinical feature selection using the LASSO regression model. **(A)** According to the logarithmic (lambda) sequence, a coefficient profile was generated, and non-zero coefficients were produced by the optimal lambda. **(B)** The optimal parameter (lambda) in the LASSO model was selected via tenfold cross-validation using minimum criteria. The partial likelihood deviation (binomial deviation) curve relative to log (lambda) was plotted. A virtual vertical line at the optimal value was drawn using one SE of minimum criterion (the 1-SE criterion).

TABLE 2 The prediction model with multivariate logistic regression.

Variables	OR	95%CI	*p*-value
Residence			0.003
Urban	Reference		
Rural	1.575	[1.163,2.133]	
ADL			<0.001
Non-disability	Reference		
Disability	1.874	[1.392,2.522]	
Cognitive function	0.927	[0.888,0.967]	<0.001
Age	1.079	[1.060,1.100]	<0.001
BMI	0.759	[0.725,0.795]	<0.001
DBP	0.984	[0.970,0.997]	0.019
PEF	0.995	[0.993,0.996]	<0.001
Hb	0.860	[0.795,0.931]	<0.001

BMI, body mass index; ADL, Activities of daily living; DBP, mean diastolic blood pressure; Hb, Hemoglobin; OR, odds ratio; CI, confidence interval.

predictive model, the corresponding scores of each independent influencing factor were projected onto the first row, and then the scores of the eight influencing factors were cumulatively summed to obtain the total score, based on which the probability of the occurrence of sarcopenia in middle-aged and older adult diabetic patients was judged to be high or low.

3.4 Predictive model validation

As shown in Figure 4A, the *AUC* value for the predictive model was 0.867 (95%CI: 0.847~0.887), and the optimal threshold was 0.279, sensitivity was 0.797 and specificity was 0.778. The calibration curve indicated a good model fit ($\chi^2 = 13.483$, $df = 8$, $p = 0.097$), $p > 0.05$, the difference was not statistically significant, suggesting that the predictive ability of the predictive model was more consistent with the actual incidence rate, and the Brier score was 0.009, indicating that the model was well calibrated (Figure 5A). The clinical validity of the model was assessed using a *DCA* curve, which showed that the training set exceeded the extremes, indicating that the nomogram predictive model provided superior net benefit and predictive accuracy (Figure 6A). Validation of the predictive model using the validation set showed an *AUC* value of 0.849 (95%CI: 0.816~0.883) for the validation set (Figure 4B), and the calibration curve indicated a good fit of the model ($\chi^2 = 14.327$, $df = 8$, $p = 0.074$) (Figure 5B). The *DCA* curves demonstrate the clinical validity of the model (Figure 6B).

4 Discussion

The results of this study indicated that the prevalence of sarcopenia in middle-aged and older adult diabetic patients in China was 28.9%, higher than the findings of Li et al. (25) (18.86%), and the reason for analysis was mainly related to the different ages of the included population, with the prevalence of sarcopenia gradually increasing with age, and middle-aged and older adult population as a priority group (26). Sarcopenia has been considered as the third type of complication in diabetic patients, as a new diabetic complication, presenting reversible characteristics, so the early identification of diabetic patients with the presence of sarcopenia in the high-risk group, and the prevention in advance, can delay or even reverse the occurrence of sarcopenia.

In this study, age was found to be a risk factor for the development of sarcopenia in diabetic mellitus. Older adult patients are already a high prevalence group for sarcopenia, and the prevalence of sarcopenia has been as high as 6.8% to 18.5% in the Chinese community's older adult population, and even higher in the middle-aged and older adult population with associated chronic diseases (27). The decline in muscle mass and muscle strength with age is greater in

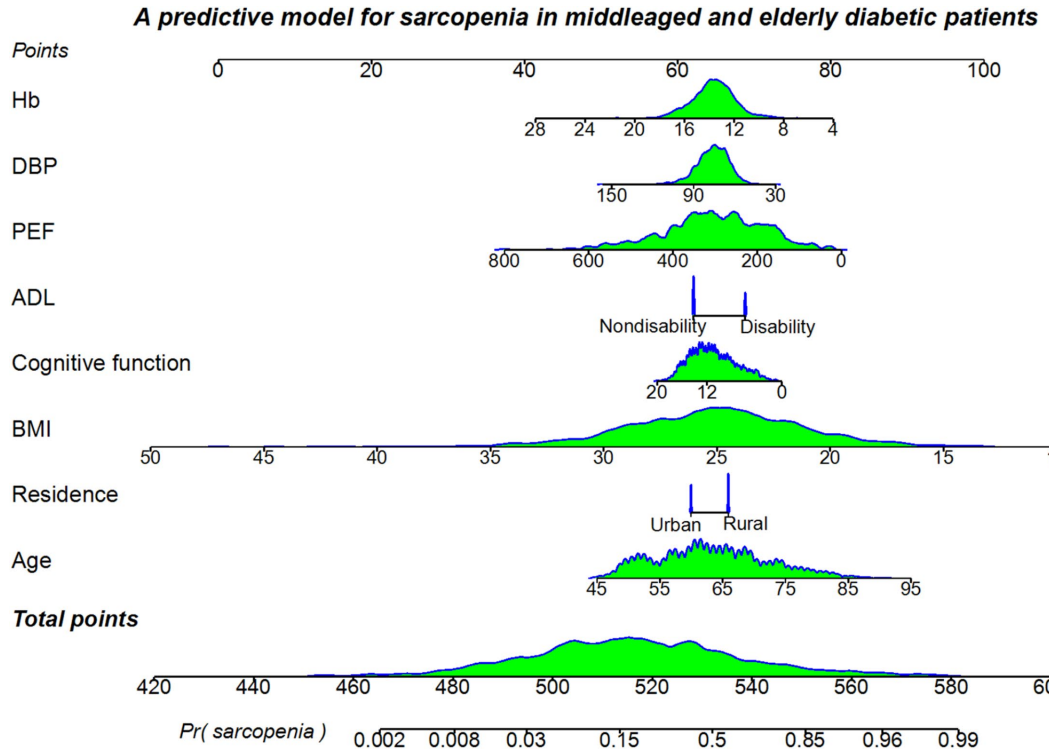

FIGURE 3
A nomogram predictive model for sarcopenia in middle-aged and older adult diabetic patients in China.

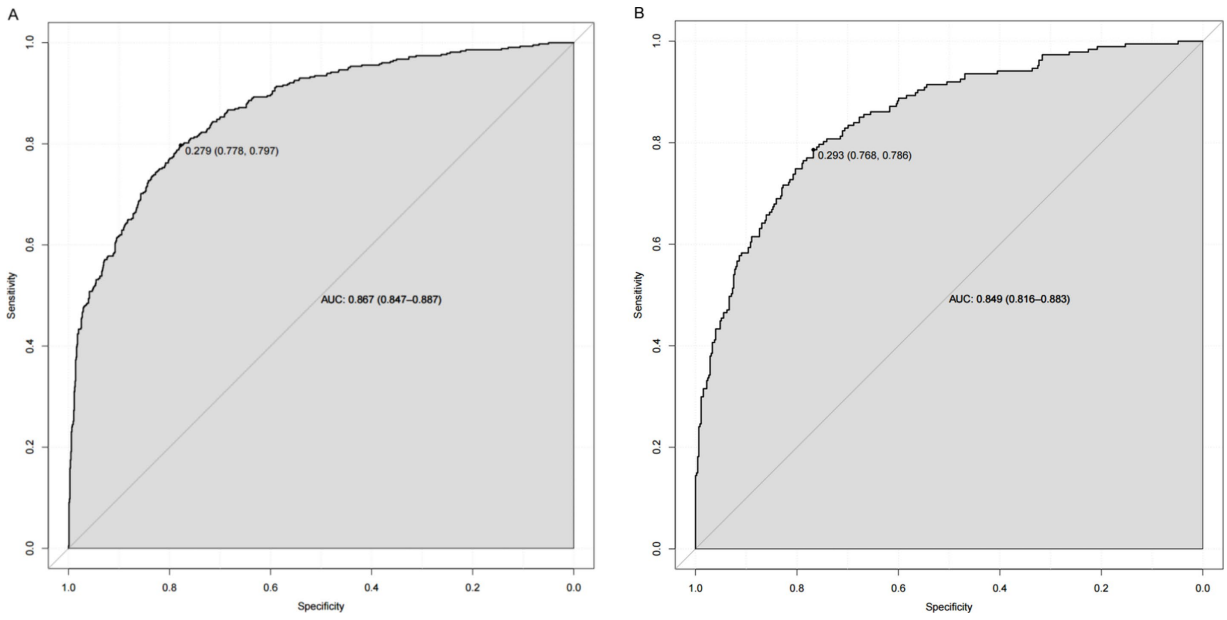

FIGURE 4
(A) Nomogram *ROC* curves generated from the training data set. **(B)** Nomogram *ROC* curves generated using the validation data set.

diabetic patients than in non-diabetic patients (5, 28, 29). After the age of 50 years, muscle mass decreases by approximately 1 to 2% per year, accompanied by a progressive loss of muscle mass, strength and function due to a decrease in the number and size of type II muscle fibres (30, 31). Therefore, muscle mass in the older adult diabetic population needs to be taken care of.

The results of the present study showed that lower BMI increased the risk of developing sarcopenia, similar to the findings of Chen et al.

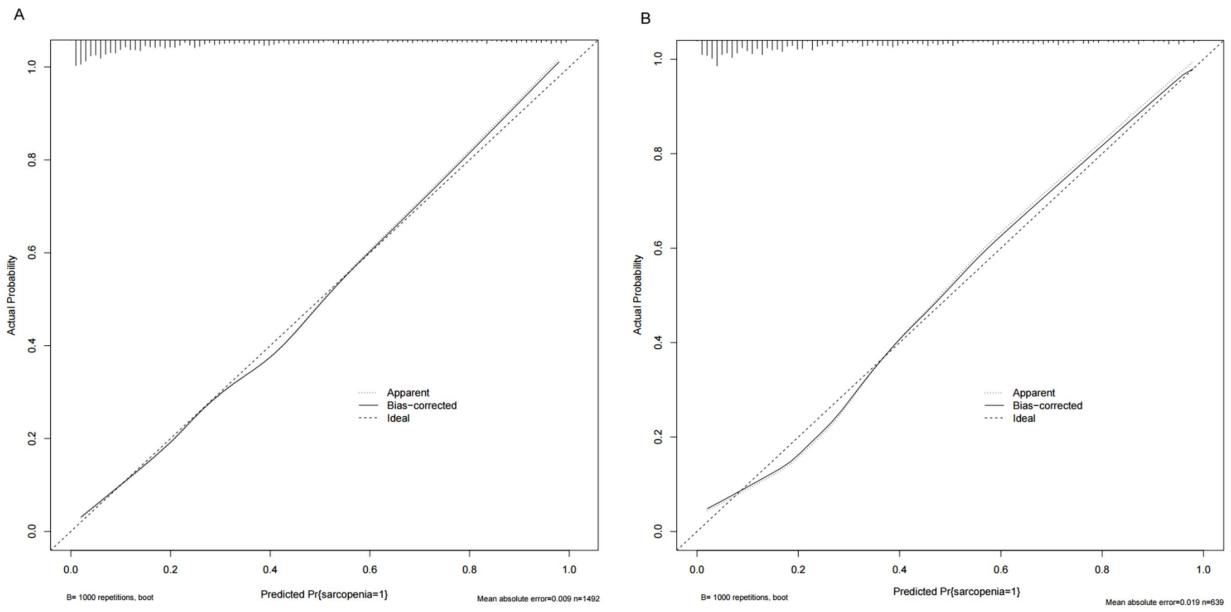

FIGURE 5
(A) Calibration plots for training data set. **(B)** Calibration plots for validation data set.

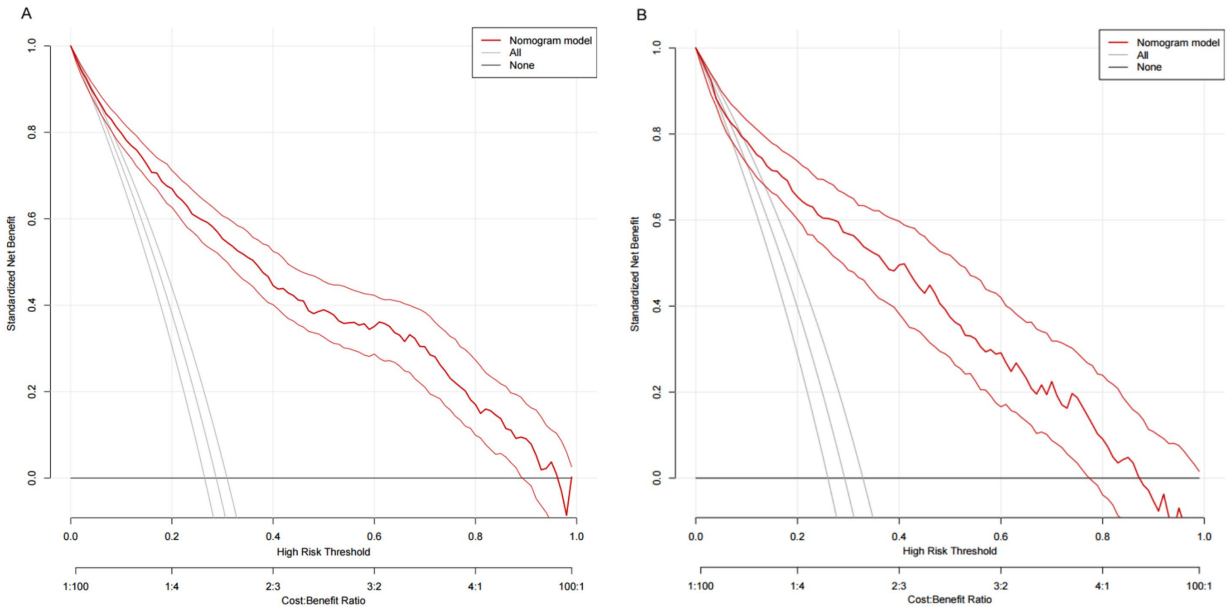

FIGURE 6
(A) DCA curves for training data set. **(B)** DCA curves for validation data set.

(32). Decrease in BMI was associated with low muscle mass, and lower BMI was considered as a dietary tendency to choose a lower protein content for intake. However, Dai et al. (33) found that the risk of developing sarcopenia was about 6.12 times higher when the BMI was ≥30 kg/m^2. Middle-aged and older adult diabetic patients with high body fat may be more likely to develop sarcopenia, considered as infiltration of adipose tissue in muscle and bone tissue stimulates sarcopenia (34). Adipose tissue can also cause chronic inflammation, leading to adipose-secreted cytokines that inhibit muscle protein synthesis, osteoblast differentiation and production, resulting in abnormal bone tissue and muscle function (35). Therefore, in addition to diabetes patients with low BMI, obese individuals should also be the focus of attention when evaluating for community sarcopenia groups.

The results of this study also showed that decreased Hb is a risk factor for sarcopenia, and decreased Hb responds to conditions such as anaemia and malnutrition in the organism (36, 37). In diabetic mellitus patients, the normal energy intake of the organism is affected due to long-term dietary control and medication. If energy intake is

low and cannot match the level of energy expenditure, it leads to weight loss and muscle mass loss in the older adult, and loss of muscle mass and function is the main feature of sarcopenia (5). As a result, a diabetic diet can be customized based on the patient's BMI and Hb test results. Maintaining a healthy nutritional status is crucial for blood glucose control and preventing sarcopenia.

The results of the study showed that the prevalence of sarcopenia was higher in middle-aged and older adult diabetic patients living in rural areas compared to those living in urban areas. For middle-aged and older adult diabetic patients living in urban areas, early diagnosis and prevention of the illness are simpler, and information is easier to obtain (38). At the same time, some activities and exercise venues and equipment are more available in the city. Therefore, in the future, middle-aged and older adult people living in rural areas should pay more attention to muscle exercise and DM health education.

Our study revealed that the risk of sarcopenia increases with poorer cognitive function. DM patients are prone to cognitive dysfunction due to thickening of the basement membrane of the brain and increased permeability of the blood–brain barrier, where proteins and other plasma constituents penetrate into the perivascular compartments and damage neurons (39, 40). In individuals with diabetes, cognitive impairment may be a contributing factor to a decrease in physical activity duration and an increase in the frequency and length of periods of inactivity and lying down. Secondly, low cognitive function can lead to difficulties with dietary intake and reduced eating, and diabetics themselves require long-term dietary control due to disease factors, all of which accelerate sarcopenia. Notably, hyperglycaemia may also lead to oxidative stress and inflammatory responses, which are common mechanisms for both cognitive impairment and sarcopenia (28). Focusing on muscle function is therefore much more crucial for people with DM who also have cognitive problems.

The results of this study showed that disability is a risk factor for sarcopenia in diabetic patients. Chronic disruptions in glucose metabolism can result in a number of consequences, including cardiovascular disease, nephropathy, and neuropathy. These conditions can make it more difficult for the patient to take care of themselves and raise the risk of incapacitation (41). Disability most directly leads to decreased mobility and increased prevalence of sarcopenia. Sarcopenia should therefore be considered while screening for disabilities.

Peak expiratory flow (PEF) is a simple screening tool for lung function and is defined as the instantaneous velocity at the fastest expiratory flow during exertion spirometry, reflecting the strength of the respiratory muscles (42). In this study, PEF was found to be a risk factor for the development of sarcopenia in middle-aged and older adult DM patients. The hyperglycaemic state of the body in diabetic patients affects lung physiology, inflammation and bacterial infections, which may lead to a loss of respiratory muscle mass and strength, and/or a decrease in lung function, which is known as sarcopenia (43). According to the 2010 consensus of the European Working Group on Sarcopenia in the older adult, PEF is determined by respiratory muscle strength in people without lung disease (5), and it can be used as an indicator of respiratory sarcopenia (44). Consequently, middle-aged and older diabetes patients with pulmonary dysfunction must actively manage their blood glucose levels. Lip-contraction belly breathing training is one way to strengthen the respiratory muscles and lessen respiratory sarcopenia.

Also, this study found that low diastolic blood pressure is strongly associated with the development of sarcopenia. Diastolic blood pressure is the pressure generated by the elastic retraction of arterial blood vessels when the heart is in diastole, and low diastolic blood pressure may indicate that the heart is not pumping enough blood to the body during diastole, which may also affect the supply of nutrients to the muscles (44). Low diastolic blood pressure may be a sign of declining fitness in the older adult, which is closely associated with sarcopenia. Therefore, in the future, patients with DM combined with hypertension should be concerned about muscle loss in addition to cardiac, cerebral, and renal complications.

The nomogram prediction model constructed in our study has a good prediction performance. First, the area under the ROC curve of the model is 0.867, which is greater than 0.800, indicating that the model has a good degree of discrimination. Second, the calibration curve of the model is close to the standard curve (45-degree line), indicating a high degree of agreement between the predicted probabilities and the observations. Finally, the DCA curve is within the probability threshold interval and above the reference line, indicating that the model has some clinical application value. Our study compares with the study by Zhang et al. (45) on sarcopenia in the older adult, where BMI and DBP were common predictors in both studies, but the *AUC* in our study was 0.867 (95%CI: 0.847~0.887) much higher than the latter (0.77, 95%CI: 0.75~0.79). And the results of the present study were more applicable to DM population. As shown in the nomogram predictive model, BMI was relatively more important, followed by PEF, age, Hb, DBP, cognitive function, ADL, and residence. The nomogram predictive model is simple and easy to use and the eight predictors are easily accessible. Community workers can assign values to each predictor and calculate the total score, and differentiate between high- and low-risk groups according to the optimal threshold value of 0.279, which not only reduces the computational burden of the users, but also saves the time of the assessment effectively.

The predictive model we constructed had good discrimination and accuracy, and the results of internal validation were found to be a valuable tool for assessing sarcopenia in DM patients. However, this study also has some limitations. Firstly, only data from 2015 in the CHARLS database were selected for this study, which was retrospective. Second, this study was only internally validated without external validation, and the study population was from China, which limits its generalization. Finally, the survey method of this study is self-report, the results of the questions will be affected by the subjective consciousness of the patients, and this study selected the middle-aged and older adult population, some of them will have memory bias, and the accuracy of the results may be affected to some extent. Large-sample, multi-center studies should be carried out in the future to investigate causality and validate the results.

5 Conclusion

Our study constructed a risk predictive model for sarcopenia in middle-aged and older adult DM patients with good predictive efficacy, which screened 8 predictors, including age, gender, residence, PEF, Hb, DBP, cognitive function, and ADL. The predictive model was built by combining the above 8 independent risk factors for sarcopenia in diabetic patients, which transformed the complex equation into a

visual model. This novel screening tool is accurate, specific, and cost-effective, highlighting its potential value in clinical applications.

Data availability statement

The original contributions presented in the study are included in the article/Supplementary material, further inquiries can be directed to the corresponding author.

Ethics statement

The studies involving human participants were reviewed and approved by Ethics approval for the CHARLS study was obtained from the Institutional Review Board (IRB) at Peking University. The IRB approval number for the main household survey was IRB00001052-11015 and for the biomarker collection was IRB00001052-11014. The patients/participants provided their written informed consent to participate in this study.

Author contributions

MYQ: Data curation, Formal analysis, Investigation, Writing – original draft. HW: Data curation, Methodology, Writing – review & editing. MZQ: Investigation, Methodology, Writing – original draft. TX: Conceptualization, Software, Writing – review & editing. YL: Supervision, Validation, Writing – original draft.

Funding

The author(s) declare that financial support was received for the research and/or publication of this article. This study was supported by the project of 'Tianshan Yingcai' High-level Training Programme for Medicine and Health (TSYC202301A085).

Acknowledgments

We thank the staff and participants of CHARLS.

Conflict of interest

The authors declare that the research was conducted in the absence of any commercial or financial relationships that could be construed as a potential conflict of interest.

Generative AI statement

The authors declare that no Gen AI was used in the creation of this manuscript.

Publisher's note

Supplementary material

The Supplementary material for this article can be found online at: https://www.frontiersin.org/articles/10.3389/fpubh.2025.1521736/full#supplementary-material

References

1. Khan MAB, Hashim MJ, King JK, Govender RD, Mustafa H, Al KJ. Epidemiology of type 2 diabetes – global burden of disease and forecasted frends. *J Epidemiol Glob Health*. (2020) 10:107–11. doi: 10.2991/jegh.k.191028.001

2. Sun H, Saeedi P, Karuranga S, Pinkepank M, Ogurtsova K, Duncan BB, et al. IDF diabetes atlas: global, regional and country-level diabetes prevalence estimates for 2021 and projections for 2045. *Diabetes Res Clin Pract*. (2022) 183:109119. doi: 10.1016/j.diabres.2021.109119

3. Saeedi P, Petersohn I, Salpea P, Malanda B, Karuranga S, Unwin N, et al. Global and regional diabetes prevalence estimates for 2019 and projections for 2030 and 2045: results from the international diabetes federation diabetes atlas, 9th edition. *Diabetes Res Clin Pract*. (2019) 157:107843. doi: 10.1016/j.diabres.2019.107843

4. Yan Y, Wu T, Zhang M, Li C, Liu Q, Li F. Prevalence, awareness and control of type 2 diabetes mellitus and risk factors in Chinese elderly population. *BMC Public Health*. (2022) 22:1382. doi: 10.1186/s12889-022-13759-9

5. Cruz-Jentoft AJ, Baeyens JP, Bauer JM, Boirie Y, Cederholm T, Landi F, et al. Sarcopenia: European consensus on definition and diagnosis: report of the European working group on sarcopenia in older people. *Age Ageing*. (2010) 39:412–23. doi: 10.1093/ageing/afq034

6. Wang T. Searching for the link between inflammaging and sarcopenia. *Ageing Res Rev*. (2022) 77:101611. doi: 10.1016/j.arr.2022.101611

7. Beaudart C, Demonceau C, Reginster JY, Locquet M, Cesari M, Cruz Jentoft AJ, et al. Sarcopenia and health-related quality of life: a systematic review and meta-analysis. *J Cachexia Sarcopenia Muscle*. (2023) 14:1228–43. doi: 10.1002/jcsm.13243

8. Mesinovic J, Fyfe JJ, Talevski J, Wheeler MJ, Leung GKW, George ES, et al. Type 2 diabetes mellitus and sarcopenia as comorbid chronic diseases in older adults: established and emerging treatments and therapies. *Diabetes Metab J*. (2023) 47:719–42. doi: 10.4093/dmj.2023.0112

9. Wang T, Feng X, Zhou J, Gong H, Xia S, Wei Q, et al. Type 2 diabetes mellitus is associated with increased risks of sarcopenia and pre-sarcopenia in Chinese elderly. *Sci Rep*. (2016) 6:38937. doi: 10.1038/srep38937

10. Yeung SSY, Reijnierse EM, Pham VK, Trappenburg MC, Lim WK, Meskers CGM, et al. Sarcopenia and its association with falls and fractures in older adults: a systematic review and meta-analysis. *J Cachexia Sarcopenia Muscle*. (2019) 10:485–500. doi: 10.1002/jcsm.12411

11. Qiao YS, Chai YH, Gong HJ, Zhuldyz Z, Stehouwer CDA, Zhou JB, et al. The association between diabetes mellitus and risk of sarcopenia: accumulated evidences from observational studies. *Front Endocrinol*. (2021) 12:782391. doi: 10.3389/fendo.2021.782391

12. Li Q, Cheng H, Cen W, Yang T, Tao S. Development and validation of a predictive model for the risk of sarcopenia in the older adults in China. *Eur J Med Res*. (2024) 29:278. doi: 10.1186/s40001-024-01873-w

13. American Diabetes Association Professional Practice Committee. Classification and Diagnosis of Diabetes: Standards of medical care in diabetes-2022. *Diabetes Care*. (2022) 45:S17–s38. doi: 10.2337/dc22-S002

14. Chen LK, Woo J, Assantachai P, Auyeung TW, Chou MY, Iijima K, et al. Asian working group for sarcopenia: 2019 consensus update on sarcopenia diagnosis and treatment. *J Am Med Dir Assoc*. (2020) 21:300–7.e2. doi: 10.1016/j.jamda.2019.12.012

15. Yang M, Hu X, Wang H, Zhang L, Hao Q, Dong B. Sarcopenia predicts readmission and mortality in elderly patients in acute care wards: a prospective study. *J Cachexia Sarcopenia Muscle*. (2017) 8:251–8. doi: 10.1002/jcsm.12163

16. Wen X, Wang M, Jiang CM, Zhang YM. Anthropometric equation for estimation of appendicular skeletal muscle mass in Chinese adults. *Asia Pac J Clin Nutr*. (2011) 20:551–6.

17. Wu X, Li X, Xu M, Zhang Z, He L, Li Y. Sarcopenia prevalence and associated factors among older Chinese population: findings from the China health and retirement longitudinal study. *PLoS One*. (2021) 16:e247617. doi: 10.1371/journal.pone.0247617

18. Jin X, He J, Liang Y, Sun X, Yan S, Wu Y, et al. Associations between household solid fuel use and activities of daily living trajectories: a nationwide longitudinal study of middle and older adults in China. *Environ Int*. (2022) 170:107605. doi: 10.1016/j.envint.2022.107605

19. Yuan M, Qin F, Zhou Z, Fang Y. Gender-specific effects of adverse childhood experiences on incidence of activities of daily life disability in middle-age and elderly Chinese population. *Child Abuse Negl*. (2021) 117:105079. doi: 10.1016/j.chiabu.2021.105079

20. Ning H, Zhang H, Xie Z, Jiang W, Xie S. Relationship of hearing impairment, social participation and depressive symptoms to the incidence of frailty in a community cohort. *J Am Geriatr Soc*. (2023) 71:1167–76. doi: 10.1111/jgs.18164

21. Feng Z, Cramm JM, Jin C, Twisk J, Nieboer AP. The longitudinal relationship between income and social participation among Chinese older people. *SSM-Popul Health*. (2020) 11:100636. doi: 10.1016/j.ssmph.2020.100636

22. Boey KW. Cross-validation of a short form of the CES-D in Chinese elderly. *Int J Geriatr Psychiatry*. (1999) 14:608–17. doi: 10.1002/(SICI)1099-1166(199908)14:8<608::AID-GPS991>3.0.CO;2-Z

23. Zhang W, Ding Z, Peng Y, Wang H, Sun Y, Ke H, et al. LUTS/BPH increases the risk of depressive symptoms among elderly adults: a 5-year longitudinal evidence from CHARLS. *J Affect Disord*. (2024) 367:210–8. doi: 10.1016/j.jad.2024.08.205

24. Lei X, Liu H. Gender difference in the impact of retirement on cognitive abilities: evidence from urban China. *J Comp Econ*. (2018) 46:1425–46. doi: 10.1016/j.jce.2018.01.005

25. Li R, Lin S, Tu J, Chen Y, Cheng B, Mo X, et al. Establishment and evaluation of a novel practical tool for the diagnosis of pre-sarcopenia in young people with diabetes mellitus. *J Transl Med*. (2023) 21:393. doi: 10.1186/s12967-023-04261-w

26. Koo BK, Roh E, Yang YS, Moon MK. Difference between old and young adults in contribution of β-cell function and sarcopenia in developing diabetes mellitus. *J Diabetes Investig*. (2015) 7:233–40. doi: 10.1111/jdi.12392

27. Yang LJ, Wu GH, Yang YL, Wu YH, Zhang L, Wang MH. Nutrition, physical exercise, and the prevalence of sarcopenia in elderly residents in nursing homes in China. *Med Sci Monit*. (2019) 25:4390–9. doi: 10.12659/MSM.914031

28. Shatila H, Ghazal N, Bukshaisha G, Al-Zeyara S, Khoury CFE, Bassil M. Risk and determinants of sarcopenia in people with diabetes: a case-control study from Qatar biobank cohort. *BMC Endocr Disord*. (2024) 24:205. doi: 10.1186/s12902-024-01722-1

29. Chen H, Huang X, Dong M, Wen S, Zhou L, Yuan X. The association between sarcopenia and diabetes: from pathophysiology mechanism to therapeutic strategy. *Diabetes Metab Syndr Obes*. (2023) 16:1541–54. doi: 10.2147/DMSO.S410834

30. Sieber CC. Malnutrition and sarcopenia. *Aging Clin Exp Res*. (2019) 31:793–8. doi: 10.1007/s40520-019-01170-1

31. Mathewson SL, Azevedo PS, Gordon AL, Phillips BE, Greig CA. Overcoming protein-energy malnutrition in older adults in the residential care setting: a narrative review of causes and interventions. *Ageing Res Rev*. (2021) 70:101401. doi: 10.1016/j.arr.2021.101401

32. Chen F, Xu S, Wang Y, Chen F, Cao L, Liu T, et al. Risk factors for sarcopenia in the elderly with type 2 diabetes mellitus and the effect of metformin. *J Diabetes Res*. (2020) 2020:3950404. doi: 10.1155/2020/3950404

33. Dai S, Shu D, Meng F, Chen Y, Wang J, Liu X, et al. Higher risk of sarcopenia in older adults with type 2 diabetes: NHANES 1999-2018. *Obes Facts*. (2023) 16:237–48. doi: 10.1159/000530241

34. Merchant RA, Seetharaman S, Au L, Wong MWK, Wong BLL, Tan LF, et al. Relationship of fat mass index and fat free mass index with body mass index and association with function, cognition and sarcopenia in pre-frail older adults. *Front Endocrinol (Lausanne)*. (2021) 12:765415. doi: 10.3389/fendo.2021.765415

35. Walsh JS, Vilaca T. Obesity, type 2 diabetes and bone in adults. *Calcified Tissue Int*. (2017) 100:528–35. doi: 10.1007/s00223-016-0229-0

36. Avila JC, Samper-Ternent R, Wong R. Malnutrition risk among older Mexican adults in the Mexican health and aging study. *Nutrients*. (2021) 13:1615. doi: 10.3390/nu13051615

37. Zhang Z, Pereira SL, Luo M, Matheson EM. Evaluation of blood biomarkers associated with risk of malnutrition in older adults: a systematic review and meta-analysis. *Nutrients*. (2017) 9:829. doi: 10.3390/nu9080829

38. Sauliune S, Mesceriakova-Veliuliene O, Kalediene R. Inequalities in life expectancy by place of residence and its changes in Lithuania during 1990-2018. *Eur J Pub Health*. (2024) 30:30. doi: 10.1093/eurpub/ckaa165.450

39. Han F, Kong X, Lv W, Li S, Sun Y, Wu Y. Association of diabetes mellitus with gait and falls in community-dwelling older adults: serial mediation of vision and cognition. *Arch Gerontol Geriat*. (2022) 104:104827. doi: 10.1016/j.archger.2022.104827

40. Callisaya ML, Beare R, Moran C, Phan T, Wang W, Srikanth VK. Type 2 diabetes mellitus, brain atrophy and cognitive decline in older people: a longitudinal study. *Diabetologia*. (2018) 62:448–58. doi: 10.1007/s00125-018-4778-9

41. Joshi SA, Patel VD, Eapen C, Hariharan K. Proportion and distribution of upper extremity musculoskeletal disorders and its association with disability in type 2 diabetes mellitus. *J Hand Ther*. (2021) 35:597–604. doi: 10.1016/j.jht.2021.04.013

42. Fragoso CAV, Gill TM. Respiratory impairment and the aging lung: a novel paradigm for assessing pulmonary function. *J Gerontol A Biol Sci Med Sci*. (2012) 67:264–75. doi: 10.1093/gerona/glr198

43. Nagano A, Wakabayashi H, Maeda K, Kokura Y, Miyazaki S, Mori T, et al. Respiratory sarcopenia and sarcopenic respiratory disability: concepts, diagnosis, and treatment. *J Nutr Health Aging*. (2021) 25:507–15. doi: 10.1007/s12603-021-1587-5

44. Kera T, Kawai H, Hirano H, Kojima M, Watanabe Y, Motokawa K, et al. Definition of respiratory sarcopenia with peak expiratory flow rate. *J Am Med Dir Assoc*. (2019) 20:1021–5. doi: 10.1016/j.jamda.2018.12.013

45. Zhang XZ, Xie WQ, Chen L, Xu GD, Wu L, Li YS, et al. Blood flow restriction training for the intervention of sarcopenia: current stage and future perspective. *Front Med (Lausanne)*. (2022) 9:894996. doi: 10.3389/fmed.2022.89499

frontiers | Frontiers in Pediatrics

TYPE Case Report
PUBLISHED 29 April 2025
DOI 10.3389/fped.2025.1508565

OPEN ACCESS

EDITED BY
Shoulong Deng,
Chinese Academy of Medical Sciences and Peking Union Medical College, China

REVIEWED BY
Lorenzo Pavone,
University of Catania, Italy
Elvio Della Giustina,
University Hospital of Modena, Italy

*CORRESPONDENCE
Wenbin Dong
✉ dongwenbin2000@163.com

†These authors have contributed equally to this work and share first authorship

RECEIVED 09 October 2024
ACCEPTED 17 April 2025
PUBLISHED 29 April 2025

CITATION
Jieda X, Yang C, Wu Y, Zhang R, Xu W and Dong W (2025) Neonatal spinal muscular atrophy with brain magnetic resonance imaging hypersignal: a case report.
Front. Pediatr. 13:1508565.
doi: 10.3389/fped.2025.1508565

Neonatal spinal muscular atrophy with brain magnetic resonance imaging hypersignal: a case report

Xiaolin Jieda[1,2†], Chaoge Yang[2,3†], Yue Wu[1,2], Rong Zhang[1], Wanting Xu[1,2] and Wenbin Dong[1*]

[1]Department of Neonatology, Children's Medical Center, The Affiliated Hospital of Southwest Medical University, Luzhou, Sichuan, China, [2]Department of Pediatrics, Southwest Medical University, Luzhou, China, [3]Department of Neurosurgery, The Affiliated Hospital of Southwest Medical University, Luzhou, China

Spinal muscular atrophy (SMA) is an autosomal recessive genetic disorder marked by progressive, symmetrical muscle weakness and atrophy. While only a limited number of studies on human SMA have demonstrated brain involvement, there are also few reports detailing early brain MRI changes in SMA patients. In this paper, we present the case of a child whose initial symptom was limb hypotonia. The child's brain MRI revealed abnormal signal changes and genetic testing ultimately confirmed the diagnosis of SMA. By reviewing relevant literature, we aim to summarize the brain MRI signal changes observed in SMA patients and explore their possible mechanisms, with the goal of enhancing clinicians' ability to identify and treat neonatal SMA at an early stage.

KEYWORDS

neonatal, spinal muscular atrophy (SMA), SMN, brain MRI, case report

Introduction

SMA is a degenerative neuromuscular disease affecting lower motor neurons in the anterior horn of the spinal cord, primarily caused by a homozygous deletion of SMN1 on chromosome 5q13 (1, 2). Its incidence ranges from 1/6,000 to 1/10,000, with a carrier frequency of 1/40 to 1/60 (1, 2). This case initially presented with decreased muscle tone in the extremities. Although some structures of the brain MRI showed abnormal signal changes similar to bilirubin encephalopathy, clinical manifestations and additional examinations did not support this diagnosis, leading to a final diagnosis of SMA through genetic testing. Characteristic brain imaging findings in neonatal SMA are rarely reported and are often confused with conditions like bilirubin encephalopathy, hypoxic-ischemic encephalopathy, and hypoglycemic encephalopathy, making diagnosis challenging. Further research is needed to clarify the diagnostic value of brain imaging changes in SMA.

Case report

We report a neonate presenting with hypotonia one day after birth. Born at 40^{+5} weeks with Apgar scores of 1–5–10 min are all rated at 10 and a weight of 2,700 g, the child showed no abnormalities in the amniotic fluid, umbilical cord, or placenta, nor signs of

intrauterine distress or premature rupture of membranes. The child did not show any decrease in fetal movement or fetal heart rate during pregnancy. The mother's gestational age was 32 years. His parents had no history of smoking, alcohol, drug use, or inherited metabolic diseases. The child exhibited good development, alertness, and mild jaundice. Physical examination showed no abnormalities in the heart, lungs, or abdomen and no barrel chest or paradoxical breathing exercises. The child's upper limbs could move horizontally but could not be lifted off the bed, both lower limbs could be lifted slightly off the bed but could not resist resistance, the limbs were floppy and could not be flexed naturally in the supine position, and they were in a "frog position" in the prone position. None of the tendon reflexes were elicited, the feeding and sucking reflex could be elicited, whereas the grip and hug reflexes were markedly diminished. He had difficulty in erecting his head, and he had no myoclonus, tongue spasms, or finger contractures. The "Medical Research Council Scale for Muscle Strength" suggests grade 2 muscle strength in the upper limbs and grade 3 in the lower limbs. Upon admission, blood glucose was 3.4 mmol/L, serum total bilirubin was 9.5 mg/dl, and blood gas analysis was normal. During hospitalization, results for NSE (35 ng/ml), blood cell analysis + CRP, urine analysis, stool routine, liver and kidney function tests, electrolytes, blood culture, TORCH tests, procalcitonin, pre-blood transfusion, and Epstein–Barr virus tests were all normal. A spine MRI was unremarkable, while a brain MRI on postnatal day 3 showed symmetrical patchy T1W1 hyperintensity in the bilateral basal ganglia, thalamus, periventricular area, and brainstem (Figure 1). We did genetic testing, which showed a homozygous deletion of exon 7 of the SMN1 gene, with a heterozygous deletion in both parents, confirming a diagnosis of spinal muscular atrophy. Sadly, the child's parents withdrew treatment, and he died of respiratory failure a week later.

Discussion

In this case, the child was admitted to the hospital with reduced muscle tone as the primary symptom. His brain MRI showed high signal changes in multiple regions on T1WI. Neonatal brain MRI signal changes can have various causes, we excluded the diagnosis of bilirubin encephalopathy and the fact that the child had no postnatal hypoxic-ischemic events, such as asphyxia, intrauterine distress, severe hypoglycemia, or significant infections, making the origin of the MRI changes unclear. Ultimately, a diagnosis of SMA was confirmed through genetic testing.

SMA is the second most common fatal autosomal recessive disease in infancy and is classified into five types based on symptom onset and highest motor milestones achieved (2, 3). Patients with type 0, I, and II are more severe, and they mostly die from respiratory failure, while type III and IV life expectancy are generally not affected (1). Two SMA-related genes, SMN1 and SMN2, are located on chromosome 5, differing by a single nucleotide (C-to-T transition in exon 7); SMN1 produces SMN protein normally, whereas SMN2 produces only 10% of the total SMN protein (1). When a homozygous deletion of SMN1 exon 7 occurs on 5q13, SMN2 alone produces insufficient SMN protein, leading to SMA. Therefore, its severity and prognosis are closely linked to the number of SMN2 copies, with fewer copies indicating a more severe disease.

SMN protein levels in the brain have been found to decrease during development, especially in the fetal and postnatal stages (4), suggesting a critical role for SMN protein in the early stages of brain development. Neuropathological data show that severe forms of SMA affect the brain (5), and reduced brain structural size is observed in mouse models of severe SMA, especially in regions associated with high SMN protein levels, suggesting that high SMN protein levels are required for brain development (6). We speculate that the brain MRI changes may be related to SMA, although few studies have explored this. To further explore the characteristics of MRI changes in the brain of SMA, we reviewed the previously published English literature. Three case-control studies showed abnormal gray matter changes in patients with SMA, and seven individual studies reported a total of 16 patients with different types of SMA. They mention the presence of symmetrical high signal in the white matter, putamen and thalamus in patients with SMA type 0 (7); periventricular posterior horn of the lateral ventricle and bilateral anterolateral thalamus high-signal-intensity lesions in children with SMA type I (8); periventricular high intensity around the posterior horns of lateral ventricles and delayed myelin formation in patients with SMA type II (9) (Table 1).

Further exploration of the pathogenesis suggests that there is a modifier gene for SMA, the zinc finger protein (ZPR1) gene (10). It can interact with SMN sites to induce neuronal differentiation, stimulate axon growth in motor neuron-like cells, and increase SMN levels (10, 11). We hypothesized that previously reported cerebral atrophy may be related to chronic hypoxia in the brain (12), because defects in ZPR1 in critically ill SMA patients contribute to phrenic nerve axonal loss of function and myelin proliferation, leading to defects in diaphragmatic respiratory function causing respiratory muscle weakness, which ultimately can lead to chronic hypoxia in the brain (10), Hypoxia can cause brain MRI signal changes, and abnormal signals may appear in the basal ganglia, thalamus and surrounding cortex (13). Moreover, the low SMN levels in SMA can lead to motor neuron degeneration, potentially causing insufficient myelin maturation. This could explain white matter atrophy and high-signal intensity in the lateral ventricle and thalamus, which may reflect unmyelinated regions or abnormal myelin development (14). Obviously, these brain MRI changes are unusual, and the brain MRI changes in SMA patients are diverse, and we cannot conclude that the brain MRI changes in SMA patients are specific. The mechanism of brain MRI changes in patients with SMA is not fully understood, and the evidence that ZPR1 deficiency allows hypoxic episodes and reduced SMN protein levels to cause brain MRI signal alterations remains insufficient. However, abnormal MRI signal may indicate the presence of SMA, and clinicians should be alert to the occurrence of such diseases. This paper reports abnormal MRI signal changes in a patient with SMA, suggesting a possible connection to the disease. A limitation of this case is that the child did not undergo SMN2 gene copy number testing, but in combination with the time of onset of the disease and the characteristics of the child, we made a clinical diagnosis of SMN type 0.

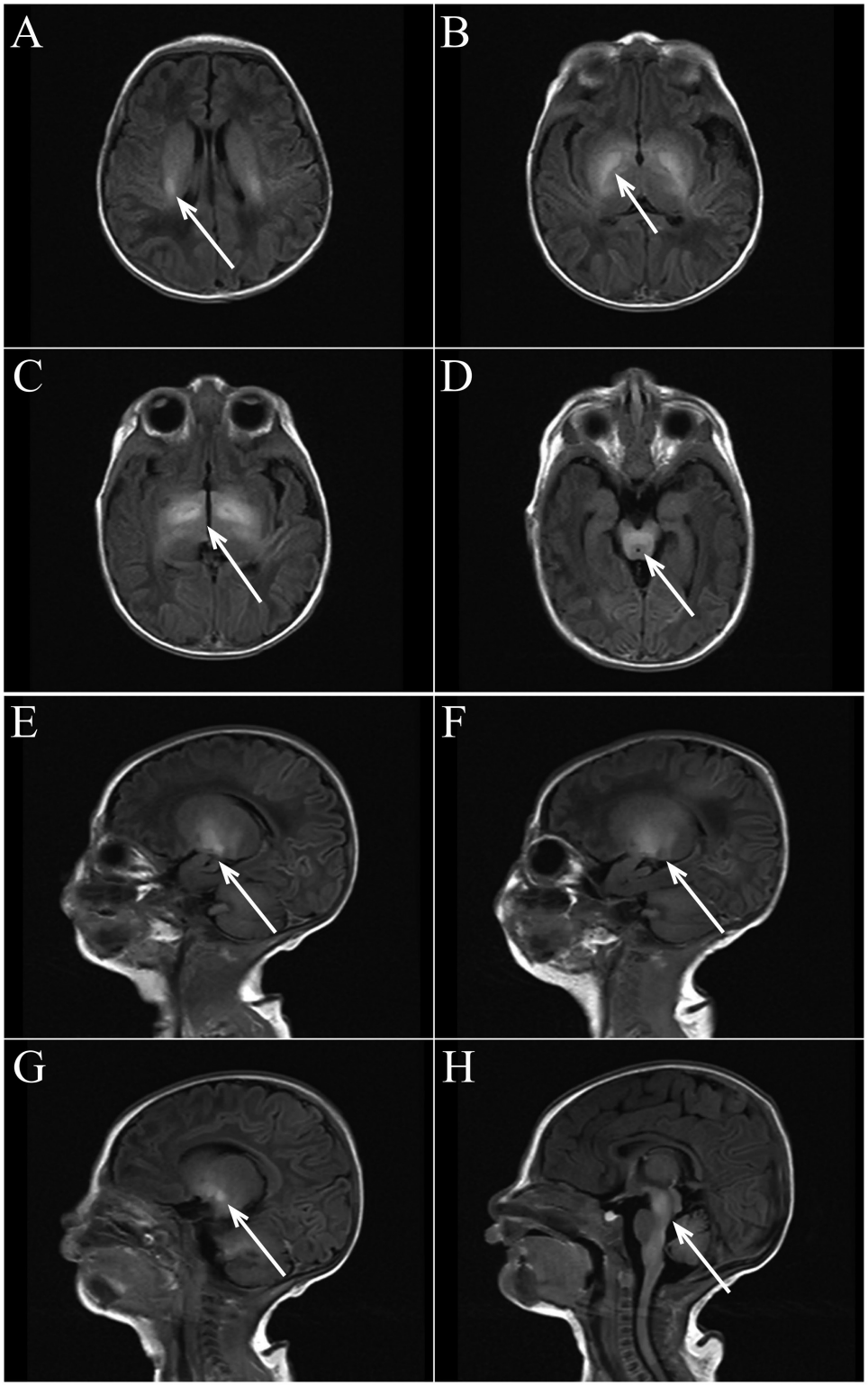

FIGURE 1
(A–D axial view) bilateral basal ganglia, thalamus, lateral ventricle, brain stem symmetrical patchy T1WI high signal shadow. (E–H sagittal view) Bilateral basal ganglia, thalamus, lateral ventricle, brain stem symmetrical patchy T1WI high signal shadow.

SMN1 deletion and SMN2 copy number can be detected by a variety of techniques, with genetic testing serving as the gold standard for diagnosing SMA. Although brain MRI is not required for diagnosis, it can reveal structural brain changes and is a widely available, non-invasive tool that may assist in the diagnostic process. Early treatment has been shown to prevent

TABLE 1 Review the literature on brain MRI signal changes in SMA patients.

No.	Ref.	Year	Classification of type/ number of cases	The main imaging findings
1	Shen et al. (16)	2024	II/22 III/21	Children with type 2 and type 3 SMA have extensive, multifocal, symmetric gray and white matter changes.
2	Losito et al. (9)	2021	II/1	T1W1: There was an area of high intensity around the posterior horn of the lateral ventricle, delayed myelination, and dysplasia of the corpus callosum
3	de Borba et al. (17)	2020	III/19 lV/6	The cerebellar volume of SMA patients was significantly smaller and lobular gray matter was significantly reduced. (T1-weighted image)
4	Maeda K et al. (7)	2019	0/1	Progressive atrophy was observed in the cerebral cortex, subcortical white matter, thalamus, and basal ganglia, and symmetrical hyperintensities were observed in the white matter, putamen, and thalamus.
5	Mendonca et al. (12)	2019	0/3	There was supratentorial atrophy, thinning of the corpus callosum, widening of the sulci and ventricles, severe reduction of white matter (3/3), and severe atrophy of the hippocampus. In two patients, the putamen and thalamus (lateral and occipital) were detected symmetrically hyperintense on T2-weighted images and FLAIR sequences, with ventricular dilatation.
6	Querin G et al. (18)	2019	III/19 lV/6	Patients with SMA have increased gray matter density in motor and extra-motor areas. (T1-weighted image)
7	Ito et al. (8)	2004	I/1	T2-weighted and FLAIR images showed high signal intensity lesions around the posterior horn of the lateral ventricle and bilateral anterolateral thalamus.
8	Oka et al. (19)	1995	I/1	T1w1-weighted images diffuse brain atrophy with more prominent white matter, with agenesis of the corpus callosum, enlargement of the third ventricle and lateral ventricle, and T2-weighted sequences showed areas of hyperintensity around the posterior horn of the lateral ventricle.
9	Cneude et al. (20)	1999	I/1	Central nervous system (thalamus, cerebellum) lesions, Severe cortical dysplasia.
10	Yohannan et al. (21)	1991	I/8	Seven cases showed generalized cortical atrophy, and one case showed hypoattenuated, non-enhancing areas in the white matter involving both frontal lobes.

the most severe forms of SMA, with its effectiveness highly dependent on early administration. Presymptomatic treatment can result in normal or mildly subnormal motor development that would otherwise progress to severe disease. Currently, several approaches are available for early treatment of SMA (15), which are based on the general principle of increasing SMN protein expression. Pharmacological or gene therapies that increase SMN2 expression, antisense oligonucleotide (ASO) -based therapies, and virus-mediated therapies are included (1). ZPR1 upregulates SMN2 protein transcription and promotes SMN protein activation for myelin regeneration, and upregulation of ZPR1 expression to increase SMN levels is a viable therapeutic target for the development of new approaches to SMA treatment (10, 11).

Conclusion

Brain MRI signal changes of SMA are rare, with high mortality and poor prognosis. So far, SMA can only delay the progression of the disease rather than completely cure it (1), which highlights the difficulty and importance of differential diagnosis of this disease. Genetic testing is the key to the diagnosis of SMA, and cranial MRI may be helpful for the diagnosis. Prenatal diagnosis and newborn screening are the most important prevention options, and early identification and treatment can help improve the prognosis of SMA patients.

Data availability statement

The original contributions presented in the study are included in the article/Supplementary Material, further inquiries can be directed to the corresponding author.

Ethics statement

Written informed consent was obtained from the minor(s)' legal guardian/next of kin for the publication of any potentially identifiable images or data included in this article.

Author contributions

XJ: Writing – original draft. CY: Writing – original draft. YW: Writing – original draft. RZ: Writing – review & editing. WX: Writing – review & editing. WD: Writing – review & editing.

Funding

The author(s) declare that no financial support was received for the research and/or publication of this article.

Conflict of interest

The authors declare that the research was conducted in the absence of any commercial or financial relationships that could be construed as a potential conflict of interest.

Generative AI statement

The author(s) declare that no Generative AI was used in the creation of this manuscript.

Publisher's note

References

1. Kolb SJ, Kissel JT. Spinal muscular atrophy. *Neurol Clin*. (2015) 33:831–46. doi: 10.1016/j.ncl.2015.07.004

2. Burr P, Reddivari AKR. *Spinal Muscle Atrophy, StatPearls, StatPearls Publishing Copyright © 2024*. Treasure Island (FL): StatPearls Publishing LLC (2024). Ineligible companies. Disclosure: Anil Kumarch Reddy Reddivari declares no relevant financial relationships with ineligible companies.

3. Ojala KS, Reedich EJ, DiDonato CJ, Meriney SD. In search of a cure: the development of therapeutics to alter the progression of spinal muscular atrophy. *Brain Sci*. (2021) 11(2):194. doi: 10.3390/brainsci11020194

4. Ramos DM, d'Ydewalle C, Gabbeta V, Dakka A, Klein SK, Norris DA, et al. Age-dependent SMN expression in disease-relevant tissue and implications for SMA treatment. *J Clin Invest*. (2019) 129:4817–31. doi: 10.1172/JCI124120

5. Masson R, Brusa C, Scoto M, Baranello G. Brain, cognition, and language development in spinal muscular atrophy type 1: a scoping review. *Dev Med Child Neurol*. (2021) 63:527–36. doi: 10.1111/dmcn.14798

6. Wishart TM, Huang JP, Murray LM, Lamont DJ, Mutsaers CA, Ross J, et al. SMN Deficiency disrupts brain development in a mouse model of severe spinal muscular atrophy. *Hum Mol Genet*. (2010) 19:4216–28. doi: 10.1093/hmg/ddq340

7. Maeda K, Chong PF, Yamashita F, Akamine S, Kawakami S, Saito K, et al. Global central nervous system atrophy in spinal muscular atrophy type 0. *Ann Neurol*. (2019) 86:801–2. doi: 10.1002/ana.25596

8. Ito Y, Kumada S, Uchiyama A, Saito K, Osawa M, Yagishita A, et al. Thalamic lesions in a long-surviving child with spinal muscular atrophy type I: MRI and EEG findings. *Brain Dev*. (2004) 26:53–6. doi: 10.1016/S0387-7604(03)00075-5

9. Losito L, Gennaro L, Lucarelli E, Trabacca A. Brain MRI abnormalities in a child with spinal muscular atrophy type II. *Acta Neurol Belg*. (2021) 121:1883–5. doi: 10.1007/s13760-020-01524-x

10. Ahmad S, Wang Y, Shaik GM, Burghes AH, Gangwani L. The zinc finger protein ZPR1 is a potential modifier of spinal muscular atrophy. *Hum Mol Genet*. (2012) 21:2745–58. doi: 10.1093/hmg/dds102

11. Kannan A, Jiang X, He L, Ahmad S, Gangwani L. ZPR1 Prevents R-loop accumulation, upregulates SMN2 expression and rescues spinal muscular atrophy. *Brain*. (2020) 143:69–93. doi: 10.1093/brain/awz373

12. Mendonça RH, Rocha AJ, Lozano-Arango A, Diaz AB, Castiglioni C, Silva AMS, et al. Severe brain involvement in 5q spinal muscular atrophy type 0. *Ann Neurol*. (2019) 86:458–62. doi: 10.1002/ana.25549

13. Parmentier CEJ, de Vries LS, Groenendaal F. Magnetic resonance imaging in (Near-)term infants with hypoxic-ischemic encephalopathy. *Diagnostics*. (2022) 12:645. doi: 10.3390/diagnostics12030645

14. Mugisha N, Oliveira-Carneiro A, Behlim T, Oskoui M. Brain magnetic resonance imaging (MRI) in spinal muscular atrophy: a scoping review. *J Neuromuscul Dis*. (2023) 10:493–503. doi: 10.3233/JND-221567

15. De Siqueira Carvalho AA, Tychon C, Servais L. Newborn screening for spinal muscular atrophy—what have we learned? *Expert Rev Neurother*. (2023) 23:1005–12. doi: 10.1080/14737175.2023.2252179

16. Shen W, Yan Z, Su S, Xiang P, Zhou Q, Zou M, et al. Gray and white matter abnormalities in children with type 2 and 3 SMA: a morphological assessment. *Eur J Pediatr*. (2024) 183:1381–8. doi: 10.1007/s00431-023-05397-z

17. de Borba FC, Querin G, França MC Jr., Pradat PF. Cerebellar degeneration in adult spinal muscular atrophy patients. *J Neurol*. (2020) 267:2625–31. doi: 10.1007/s00415-020-09875-4

18. Querin G, El Mendili MM, Lenglet T, Behin A, Stojkovic T, Salachas F, et al. The spinal and cerebral profile of adult spinal-muscular atrophy: a multimodal imaging study. *Neuroimage Clin*. (2019) 21:101618. doi: 10.1016/j.nicl.2018.101618

19. Oka A, Matsushita Y, Sakakihara Y, Momose T, Yanaginasawa M. Spinal muscular atrophy with oculomotor palsy, epilepsy, and cerebellar hypoperfusion. *Pediatr Neurol*. (1995) 12:365–9. doi: 10.1016/0887-8994(95)00058-N

20. Cneude F, Sukno S, Boidein F, Dehouck MB, Bourlet A, Vittu G. Cerebral agyria-pachygyria in a child with Werdnig-Hoffmann disease. *Rev Neurol*. (1999) 155:589–91.

21. Yohannan M, Patel P, Kolawole T, Malabarey T, Mahdi A. Brain atrophy in Werdnig-Hoffmann disease. *Acta Neurol Scand*. (1991) 84:426–8. doi: 10.1111/j.1600-0404.1991.tb04982.x

Frontiers in
Cell and Developmental Biology

Explores the fundamental biological processes of life, covering intracellular and extracellular dynamics.

The world's most cited developmental biology journal, advancing our understanding of the fundamental processes of life. It explores a wide spectrum of cell and developmental biology, covering intracellular and extracellular dynamics.

Discover the latest Research Topics

See more →

Frontiers

Avenue du Tribunal-Fédéral 34
1005 Lausanne, Switzerland
frontiersin.org

Contact us

+41 (0)21 510 17 00
frontiersin.org/about/contact